University of Nottingham
UK | CHINA | MALAYSIA

Investigating Serum Biomarkers, Disease Pathways and Vitamin D in Association with Cardiovascular Disease in Great Apes

By
Rachel Jarvis

Thesis submitted to
The School of Veterinary Medicine and Science
University of Nottingham

For the degree of
Doctor of Philosophy
Submitted January 2025

Supervised by

Professor Kate White
University of Nottingham
Professor Matyas Liptovszky
University of Nottingham
Professor Peter Graham
University of Nottingham

Dr Melissa Grant
University of Birmingham
Dr Kerstin Baiker
Veterinary Pathology Group
Phillipa Dobbs
Twycross Zoo

ABSTRACT

Great apes (bonobos, chimpanzees, gorillas and orangutans) in zoological collections play an important role in conservation, and a better understanding of the health challenges they face is crucial. Cardiovascular disease (CVD) is a leading cause of morbidity and mortality, with particular concern arising from a prevalent and poorly understood phenotype: idiopathic myocardial fibrosis (IMF). This thesis investigates diagnostic biomarkers, disease pathways, and vitamin D status as a possible risk factor in CVD, particularly IMF, to address critical knowledge gaps and inform best practice for the management of great apes in human care. The literature review establishes the context for this work by exploring the prevalence and potential aetiopathogeneses of CVD in great apes, highlighting the pressing need for research into IMF. Chapter 1 identifies three potential serum biomarkers of IMF, with one marker in particular showing promise as a novel diagnostic tool, although further validation is required. Chapter 2 assesses the cardiac tissue proteome associated with IMF, showing significant alterations in proteins associated with calcium regulation, mitochondrial and contractile function, and extracellular matrix (ECM) remodelling, revealing key biological pathways involved in IMF progression for the first time. In chapter 3, myocardial gene expression is explored, targeting markers that have been implicated in fibrosis elsewhere. Key pre-analytical and methodological challenges are highlighted, which should be considered in any future work investigating the molecular drivers of IMF. Chapter 4 shifts focus to vitamin D, a potential modifiable risk factor for IMF, revealing widespread low vitamin D status in a large number of great apes in European zoos. UVB exposure, diet, and outdoor access are significant factors influencing vitamin D status in these animals, emphasising the importance of husbandry practices in mitigating potential health risks, though further species-specific investigation is needed. Together, the findings of this thesis advance our understanding of IMF in great apes considerably, and may contribute to the development of evidence-based strategies to improve their health and welfare. Future research should focus on validating novel diagnostic biomarkers and investigating disease pathways in a larger cohort, as well as exploring likely risk factors in conjunction with CVD outcomes more directly, in order to inform interventions to improve health outcomes for these endangered species in human care.

ACKNOWLEDGEMENTS

I would like to thank the following people, whose support has made the completion of this thesis possible:

All of my supervisors, from whom I have learned so much – not least how to be a better (and more confident!) scientist. Your expertise in your range of fields brought so much balance and perspective to this project. Despite the many ups and downs during my PhD journey, I have truly felt so well-supported, listened to, and encouraged. I consider myself extremely lucky to have had such a wonderful supervisory team.

The Twycross Zoo vet team (Liz Hanson, Jo Rudd, Ed Green, Sam Ashfield, Phillipa Dobbs, Sophie Moittié, Pip Bucknell), research team (Lisa Gillespie, Dalma Zsalako), and great ape keeper team – who facilitated my research with the Ape Heart Project and helped countless times with the many incoming and outgoing samples, technical questions, behind-the-scenes animal observations, and generally making me feel so welcome within the TZ community. It was extra special, being able to connect in person with the species and real-world contexts behind my research, putting the whole thing into perspective and making it feel even more worthwhile.

Christopher Reeves (Manchester University NHS FT), Juliana Andrea Berner and Christina Hvilsom (Copenhagen Zoo/EAZA Biobank), and Antonia Morey Matamalas, Marta Nobre de Castro Pereira, Emma Pritchard, and Ceri Staley (UoN SVMS/pathology service) – who all truly went above and beyond to facilitate and participate in the research, despite the many obstacles and sometimes peculiarities involved in obtaining and working with great ape samples.

The Great Ape TAG, EEP members and committees – for their invaluable advice, help, and support within the zoo community.

My friends from the UoB labs: Lisa Shriane (who also helped as a technician), Ben Hewitt (who also helped with one of the studies), Maria Muchova, Dario Balacco, Sandeep Shirgill, Olga Yevlashevskaya, Lea Wood, Peter Smith, Veksina Raman, Jiwon Choi, Luciana Solera Sales, Lauter Pelenpenko, and Alex Robinson. I will always be so thankful for the friendship, moral support, fits of laughter, crosswords,

pub trips, karaoke mishaps, and espressos. We laughed, we cried, and we muddled through PhD life together.

The friends I met at Twycross Zoo while collecting data during lockdown but who, years later, are still a big part of my life – Sara de Vittoris, Elizabeth Warren, Sadie Tenpas – for the happiness (and endless great ape knowledge!) you brought to my life, then and now. You made the pandemic years bearable, and my PhD journey was infinitely better because you were part of it.

My lovely netball friends (Ashby Netball Club, Sweaty Netties, and now Ballasalla Netball Club) – for helping me stay (mostly) sane and healthy.

My 'timeless' friends, Isobel, Katie, Maddie, and Mel – for always being there when I need you and for cheering me on from the sidelines, even when we lived far apart and you probably had very little clue what my project was even about ("something about ape hearts?").

My sister, brother, mum, and dad – it is because of you I have had the freedom to explore my passions in life and go this far in my academic journey, and it is because of you I have felt a forcefield of strength, pride, resilience and love keeping me going, no matter what life has thrown our way.

My husband, Connor (and dog, Rozy) – you are my rock, and my home, wherever we go. In the last four years we have seen the brightest and darkest times of our lives so far. Your unwavering support has quite literally carried me through, and I'll never be able to fully express my gratitude. I suppose I'm also thankful that you have a good surname – 'Dr Martin' has a nice ring to it, for some reason…

Table of Contents

ABSTRACT 2

ACKNOWLEDGEMENTS 3

LIST OF FIGURES 7

LIST OF TABLES 9

LIST OF APPENDICES 11

LIST OF PUBLICATIONS 12

LIST OF ABBREVIATIONS 13

ETHICAL STATEMENT 17

LITERATURE REVIEW 18

I. The Great Apes: Ecology, Morbidity and Mortality 18

II. Cardiovascular Disease (CVD) in Great Apes 22

III. Diagnostic Tools for CVD in Great Apes 26

IV. Possible Aetiopathogeneses of Idiopathic Myocardial Fibrosis (IMF) in Great Apes 30

V. Vitamin D: Importance and Potential Role in IMF in Great Apes 34

VI. Conclusions and Thesis Aims 39

1. DISCOVERY AND VALIDATION OF NOVEL SERUM BIOMARKERS OF IMF IN CHIMPANZEES 40

1.1 Introduction 40

1.2 Materials and methods 43

1.3 Results 53

1.4 Discussion 65

2. THE CARDIAC TISSUE PROTEOME ASSOCIATED WITH IMF IN CHIMPANZEES 73

2.1 Introduction 73

2.2 Materials and methods 75

2.3 Results 80
2.4 Discussion 86
3. TARGETED INVESTIGATION OF MYOCARDIAL GENE EXPRESSION IN CHIMPANZEES 92
3.1 Introduction 92
3.2 Materials and methods 95
3.3 Results 111
3.4 Discussion 118
4. EXPLORATION OF VITAMIN D STATUS IN EUROPEAN ZOO-HOUSED GREAT APES 122
4.1 Introduction 122
4.2 Materials and methods 126
4.3 Results 131
4.4 Discussion 152
THESIS CONCLUSIONS 160
LITERATURE CITED 163
APPENDICES 212
Appendix A 212
Appendix B 232
Appendix C 233

LIST OF FIGURES

Figure 1.1: Volcano plot showing differences in protein expression (NPX) between chimpanzees affected by IMF (n=6) and healthy controls (n=4)..... 54
Figure 1.2: Normalised Protein eXpression (NPX) of proteins in chimpanzees affected by IMF (n=6) versus healthy controls (n=4), as tested with Proximity Extension Assay (Olink® Target 96 Cardiovascular Panel III, v.6112), which corresponds to relative protein concentrations within the sample on a log 2 scale. 57
Figure 1.3: Range-finding results showing the dilution effect on the measurement of ICAM-2, AXL, and PECAM-1 concentrations in serum..... 60
Figure 1.4: Spike-and-recovery performance of ELISA kits for ICAM-2, AXL, and PECAM-1 using spiked serum samples (a known amount of analyte added to the sample matrix) and a control spike (a known amount of analyte added to the standard diluent). 61
Figure 1.5: [A]: Expression (ng/mL) of ICAM-2, AXL and PECAM-1 as tested by ELISA in the subset of 10 chimpanzees from Study A. [B]: Expression (ng/mL) of ICAM-2, AXL and PECAM-1 as tested by ELISA in all 26 chimpanzees (excluding outliers where applicable) from Study B. 63
Figure 2.1: Volcano plot showing the -log10(p value) and log2(fold change) of relative abundance of 514 proteins discovered by mass spectrometry in chimpanzees affected by IMF (n=6) versus healthy controls (n=4)..... 81
Figure 2.2: Interaction network for proteins differentially expressed in chimpanzees affected by IMF (n=6) compared with healthy controls (n=4), as discovered by mass spectrometry. 84
Figure 3.1: Difference in RNA concentration (µg/mL) and purity (260nm/280nm) between two sample preservation methods: FFPE and RNAlater..... 115
Figure 3.2: Expression of target genes (n=13) in myocardial tissue from chimpanzees affected by IMF (n=9) versus healthy controls (n=4). 117
Figure 4.1: Map depicting global annual mean UVB (J/m^2) with corresponding colours ranging from 939 J/m^2 (blue) to 6160 J/m^2 (red), with four sub-maps showing geographic origins of samples from [A]: Bonobos (n=49 samples from 5 zoos); [B]: Chimpanzees (n=251 samples from 34 zoos); [C]: Gorillas (n=106 samples from 23 zoos); [D]: Orangutans (n=58 samples from 17 zoos)..... 133

Figure 4.2: Total 25-OHD concentrations (nmol/L) across all species. 135
Figure 4.3: Distribution of total 25-OHD concentration categories across species. 136
Figure 4.4: Scatterplots showing the relationship between sample storage time (months) and total 25-OHD (nmol/L) for bonobos (n=49), chimpanzees (n=251), gorillas (n=106), and orangutans (n=58). 138
Figure 4.5: Total 25-OHD concentrations (nmol/L) for two sample types, serum and plasma..... 139
Figure 4.6: Total 25-OHD concentrations (nmol/L) by health status..... 141
Figure 4.7: Total 25-OHD concentrations (nmol/L) by coat quality. 142
Figure 4.8: Total 25-OHD concentrations (nmol/L) by sex, age group, body condition score, contraception status, pregnancy status, and lactation status. 143
Figure 4.9: Seasonal variation in total 25-OHD concentrations (nmol/L) for each species. 145
Figure 4.10: Frequency distribution of UVB irradiance (W/m²) across all samples. 146
Figure 4.11: Relationship between UVB irradiance and total 25-OHD concentrations for each species. 147
Figure 4.12: Total 25-OHD concentrations (nmol/L) by outdoor access. 149
Figure 4.13: Total 25-OHD concentrations (nmol/L) by presence of pellets in the diet. 150
Figure 4.14: Total 25-OHD concentrations (nmol/L) by presence of supplementation in diet (left), and presence of artificial UV lighting or UV-permeable materials in enclosures (right)..... 151

LIST OF TABLES

Table 1.1: Study subjects: chimpanzees with a known cardiac phenotype, as confirmed histologically, categorised as Control (healthy) vs. Affected (diseased). . 45
Table 1.2: Results of one-tailed Welch's t test for independent samples and Area Under Curve (AUC) analysis for proteins (as detected with Olink® Target 96 Cardiovascular Panel III, v.6112). 55
Table 1.3: Assay performances for ICAM-2, AXL and PECAM-1 as tested via commercially available human ELISA kits. 59
Table 1.4: Diagnostic performance metrics for ICAM-2 based on ELISA data. 64
Table 2.1: Study subjects: chimpanzees with a known cardiac phenotype (n=10), as confirmed histologically, categorised as Affected (diseased) or Control (healthy).... 75
Table 2.2: Data column headings and descriptions as found in the original Excel spreadsheet of protein abundance data from mass spectrometry readout..... 78
Table 2.3: Proteins of interest (n=13) from proteomic exploration by mass spectrometry in chimpanzees (*Pan troglodytes*) affected by IMF (n=6) and healthy controls (n=4). 82
Table 2.4: Overrepresented biological functions implicated by networks involving proteins of interest (n=11) as discovered by mass spectrometry of myocardial tissue samples from chimpanzees affected by IMF (n=6) and healthy controls (n=4). 85
Table 3.1: Study subjects: chimpanzees with a known cardiac phenotype (n=13), as confirmed histologically, categorised as Affected (diseased) or Control (healthy).... 96
Table 3.2: Mass (g) of tissue samples used for the extraction and purification of total RNA from myocardial tissue stored in RNAlater (n=14). 102
Table 3.3: Primer sequences of selected reference genes (n=8): ACTB, B2M, GAPDH, LDHA, RPS12, RPS20, RPL27, YWHAZ; and target genes (n=15): CCN2, COL1A1, COL3A1, FN1, GAL-3, IL-6, IL-11, MMP-2, MMP-9, SPP1, TGF-β1, TIMP-1, VDR-01, VDR-02, VEGF..... 106
Table 3.4: Concentration (µg/mL) and purity (260nm/280nm) of RNA extracted from FFPE myocardial tissue from two chimpanzees (*Pan troglodytes*) as assessed by a NanoDrop® instrument..... 112

Table 3.5: RNA concentration (µg/mL), purity (260nm/280nm), and sample storage time (months) of myocardial tissue samples from chimpanzees affected by IMF (n=9) and healthy controls (n=4). 114
Table 4.1: Reference ranges used for the interpretation of vitamin D status (total 25-OHD, nmol/L) of zoo-housed great apes, as adapted from known human ranges. 127
Table 4.2: Questionnaire sent to zoos of origin in order to gather additional data regarding vitamin D status of great apes. 130
Table 4.3: Demographics of study animals from which 25-OHD was measured. ... 132
Table 4.4: Mean 25-OHD concentrations (nmol/L) and the proportion (%) of samples from each species that fell within the defined human reference range categories: Deficient (<25 nmol/L), Insufficient (25–50 nmol/L), Adequate (51–75 nmol/L), and Optimal (>75 nmol/L). 134

LIST OF APPENDICES

Appendix A: An overview of post-mortem cardiac examinations carried out between October 2020 and August 2023. 212
Appendix B: Example layout used for 96-well microplates for RT-qPCR. 232
Appendix C: Moittié, S., Jarvis, R., Bandelow, S., et al. (2022) Vitamin D status in chimpanzees in human care: a Europe wide study. Scientific Reports, 12: 17625. doi:10.1038/s41598-022-21211-6. 233

LIST OF PUBLICATIONS

Moittié, S., **Jarvis, R.**, Bandelow, S., et al. (2022) Vitamin D status in chimpanzees in human care: a Europe wide study. *Scientific Reports*, 12: 17625. doi:10.1038/s41598-022-21211-6.

LIST OF ABBREVIATIONS

25-OHD	25-hydroxyvitamin D
ACM	Arrhythmogenic Cardiomyopathy
ACTB	Actin Beta
AHP	Ape Heart Project
AMSF	Advanced Mass Spectrometry Facility
APHA	Animal and Plant Health Agency
ARVC	Arrhythmogenic Right Ventricular Cardiomyopathy
ATP	Adenosine Triphosphate
AUC	Area Under the Curve
AXL	Receptor Protein-Tyrosine Kinase
B2M	Beta-2-Microglobulin
BMI	Body Mass Index
BNP	Brain-type Natriuretic Peptide
BSA	Bovine Serum Albumin
CBS	Citrate-Buffered Saline
cDNA	Complementary Deoxyribonucleic Acid
CITES	Convention on International Trade in Endangered Species of Wild Fauna and Flora
CK	Creatinine Kinase
cm	Centimetres
CNRQ	Calibrated Normalised Relative Quantity
COL1A1	Collagen Type I Alpha 1 Chain
COL3A1	Collagen Type III Alpha 1 Chain
COX	Cytochrome c Oxidase
Cq	Quantification Cycle
CRP	C-Reactive Protein
CTGF/CCN2	Connective Tissue Growth Factor / Cellular Communication Network Factor 2
cTnI	Cardiac Troponin I
cTnT	Cardiac Troponin T
CVD	Cardiovascular Disease

DCM	Dilated Cardiomyopathy
DNA	Deoxyribonucleic Acid
EAZA	European Association of Zoos and Aquaria
ECG	Electrocardiogram
ECM	Extracellular Matrix
ELISA	Enzyme Linked Immunosorbent Assay
EU	European Union
FASP	Filter-Aided Sample Preparation
FFPE	Formalin-Fixed-Paraffin-Embedded
FN1	Fibronectin 1
g	Grams
GAL-3	Galectin-3
GAPDH	Glyceraldehyde-3-Phosphate Dehydrogenase
H&E	Haematoxylin and Eosin
HRP	Horseradish-Peroxidase
ICAM-2	Intercellular Adhesion Molecule 2
ICTP	Initial Carboxyl-terminal Telopeptide
IF	Interstitial Fibrosis
IL-6	Interleukin 6
IL-11	Interleukin 11
IMF	Idiopathic Myocardial Fibrosis
IQR	Interquartile Range
IVC	Inferior Vena Cava
IVS	Inter-ventricular Septum
LC-MS/MS	Liquid Chromatography and Tandem Mass Spectrometry
LDHA	Lactate Dehydrogenase A
LOD	Limit of Detection
LVFW	Left Ventricular Free Wall
LVOT	Left Ventricular Outflow Tract
MIQE	Minimum Information for Publication of Quantitative Real-Time PCR Experiments
MMP-1	Matrix Metalloproteinase 1
MMP-2	Matrix Metalloproteinase 2

MMP-9	Matrix Metalloproteinase 9
MRI	Magnetic Resonance Imaging
mRNA	Messenger Ribonucleic Acid
MS	Mass Spectrometry
NHP	Non-Human Primate
NPV	Negative Predictive Value
NPX	Normalised Protein Expression
NT-proBNP	N-Terminal pro-Brain-type Natriuretic Peptide
OD	Optical Density
PBS	Phosphate Buffered Saline
PCA	Principal Component Analysis
PCR	Polymerase Chain Reaction
PEA	Proximity Extension Assay
PECAM-1	Platelet Endothelial Cell Adhesion Molecule 1
PIIINP	Procollagen III N-terminal protein
PINP	Procollagen I N-terminal protein
PMI	Post-Mortem Interval
PPE	Personal Protective Equipment
PPV	Positive Predictive Value
qPCR	Quantitative Polymerase Chain Reaction
RAA	Right Atrial Appendage
RAAS	Renin-Angiotensin-Aldosterone System
RF	Replacement Fibrosis
RNA	Ribonucleic Acid
ROC	Receiver Operating Characteristic
ROS	Reactive Oxygen Species
RPL27	Ribosomal Protein L27
RPS12	Ribosomal Protein S12
RPS20	Ribosomal Protein S20
RSV	Respiratory Syncytial Virus
RT-qPCR	Reverse Transcription Quantitative Polymerase Chain Reaction
RVFW	Right Ventricular Free Wall
RVOT	Right Ventricular Outflow Tract
SD	Standard Deviation

SPP1/OPN	Secreted Phosphoprotein 1 / Osteopontin
STRING	Search Tool for the Retrieval of Interacting Genes/Proteins
SVMS	School of Veterinary Medicine and Science
TBS	Tris-Buffered Saline
TGF-β1	Transforming Growth Factor Beta 1
TIMP-1	Tissue Inhibitor of Metalloproteinase 1
TMT	Tandem Mass Tag
UK	United Kingdom of Great Britain and Northern Ireland
UVB	Ultraviolet B
VEGF	Vascular Endothelial Growth Factor
VDR	Vitamin D Receptor
VSA	Veterinary Surgeons Act
YWHAZ	Tyrosine 3-Monooxygenase / Tryptophan 5-Monooxygenase Activation Protein Zeta

ETHICAL STATEMENT

Full ethical approval was obtained via the Committee for Animals and Research Ethics at the School of Veterinary Medicine and Science, University of Nottingham, UK (approval number SVMS 3064 200106 and 2253 18322 Non ASPA VSA). This research used scientific samples from zoo-housed great apes, including post-mortem (i.e., hearts) and ante-mortem (i.e., serum) samples taken opportunistically while animals were anaesthetised. Convention on International Trade of Endangered Species (CITES) permits were obtained from the relevant authorities prior to international movement of samples.

LITERATURE REVIEW

I. The Great Apes: Ecology, Morbidity and Mortality

The great apes (*Hominidae*) represent a taxonomic family of primates comprising *Pan paniscus* (bonobos), *Pan troglodytes* (chimpanzees), *Gorilla gorilla* (Western gorillas), *Gorilla beringei* (Eastern gorillas), *Pongo pygmaeus* (Bornean orangutans), *Pongo abelii* (Sumatran orangutans), *Pongo tapanuliensis* (Tapanuli orangutans), and *Homo sapiens* (humans). Populations of all non-human great apes are in decline, and are at risk of extinction in the wild. All species are classified as either Endangered or Critically Endangered by the International Union for Conservation of Nature (IUCN) due to habitat destruction, poaching, infectious diseases, and human-wildlife conflict (Maisels et al., 2018; Humle et al., 2016; Fruth et al., 2016; Ancrenaz et al., 2016; Singleton et al., 2017; Plumptre et al., 2019; Nowak et al., 2017).

Given this threat to the survival of these species, managed care settings such as zoos and sanctuaries play a key role in conservation by providing safe environments, supporting breeding programs, and serving as genetic reservoirs (Rabb, 1994; Ballou et al., 2010). Animals in these settings serve as ambassadors for their species, encouraging public connection and support for their conservation and environmental initiatives (Kruger and Viljoen, 2023; Pearson et al., 2014). Additionally, given the high genetic and physiological similarity, studying health and diseases in great apes can provide models for understanding similar conditions in humans (and vice versa), as demonstrated in comparative medicine and “One Health” approaches (Lowenstine et al., 2016; Videan et al., 2009; Moresco et al., 2022). However, the responsibility of ensuring species survival in captivity also brings with it important considerations for their welfare. Animal welfare encompasses the physical, mental, and behavioural well-being of animals, and is an ever-evolving science (Tallo-Parra et al., 2023; Freire and Nicol, 2019). Animal welfare is increasingly central to zoos' ethical responsibilities, conservation efforts, and educational missions, since it plays a key role in maintaining public trust and demonstrating zoos' commitment to the animals under their care (Fourage et al., 2023; Tallo-Parra et al., 2023). Continuous monitoring and modern, data-driven approaches (e.g., through behavioural observations and machine

learning) are considered crucial for identifying and addressing welfare concerns (Liptovszky, 2024; Brookes et al., 2022). Species with complex cognitive and foraging needs, such as great apes, are particularly vulnerable to poor welfare (Mellor et al., 2021; Clark, 2011), and states of prolonged stress, also known as allostatic overload, are known to contribute to the onset of diseases (Golbidi et al., 2015; Edes, 2020; Edes et al., 2020c). The relationship between health and welfare in zoo animals is intricate, as improvements in veterinary care, husbandry practices, and nutrition can improve overall health and longevity, but this increased longevity also leads to a higher risk of age-related diseases and welfare challenges (Krebs et al., 2018; Ross et al., 2022; Strong et al., 2017). The various health challenges faced by great apes will now be explored, beginning with non-cardiovascular conditions. Available information on wild populations is included for consideration and comparison.

Detailed morbidity and mortality data in wild great apes remain limited due to the difficulty of ante-mortem diagnostics, as wild animals often hide clinical signs of disease to avoid predation and social conflicts or exclusion (Wobeser, 2006). Additionally, the vast and remote habitats of great apes complicate the retrieval of deceased individuals for post-mortem analysis, further restricting our understanding of their health and mortality (Terio et al., 2011; Leendertz et al., 2006; Wobeser, 2006). Most available information comes from habituated groups under long-term study. In reports from Gombe National Park in Tanzania, ‘illness’ accounted for 58% of deaths, with respiratory disease responsible for 48% and polio 12% (Williams et al., 2008), with parasitic infestations and degenerative joint disease notably common in older individuals (Terio et al., 2011). Simian immunodeficiency virus (SIV) was identified in 4 of 11 chimpanzees that died over 6 years, with AIDS-like disease implicated in two cases (Terio et al., 2011). Similarly, disease was reported to have caused 48% of deaths at Mahale Mountains National Park in Tanzania (Nishida et al., 2003). Outbreaks of *Bacillus anthracis*, influenza, conjunctivitis, Ebola, and monkeypox have also been reported (Leendertz et al., 2004; Boesch and Boesch-Achermann, 2000). Respiratory disease outbreaks, particularly in habituated populations, are frequently linked to human-animal transmission (Kaur et al., 2008; Nishida et al., 2003; Leendertz et al., 2006; Hanamura et al., 2008). Conspecific aggression and trauma are also significant causes of mortality. At Mahale, 16% of deaths were attributed to aggression (Nishida et al., 2003). At Gombe, conspecific aggression accounted for 20% of deaths

(Williams et al., 2008), and in a later report, trauma was the leading cause of death over a 6-year period (Terio et al., 2011). In Taï National Park in Côte d'Ivoire, intra-group aggression caused injuries in 30 individuals over 17 years, with inter-group aggression responsible for one case (Boesch and Boesch-Achermann, 2000). A large-scale review of mortality across five chimpanzee communities – Gombe, Taï, Kibale (Uganda), Mahale, and Bossou (Guinea) – found males had higher overall mortality across all age groups, with only 27% reaching 15 years compared to 41% of females (Hill et al., 2001).

In human care, captive great apes experience a variety of diseases, with changes in the leading causes of mortality over time likely reflecting improvements in husbandry practices. In earlier studies, gastrointestinal (GI) diseases were reported as a major cause of mortality in chimpanzees (Schmidt, 1978). GI parasitism and bacterial infections were important problems for orangutans, while arthritis and GI issues predominated in gorillas (Munson and Montali, 1990). A 22-year mortality review of a chimpanzee colony highlighted respiratory, GI, and trauma as major causes of death (Hubbard et al., 1991). Another review found infectious diseases to be the primary cause of death in captive chimpanzees prior to 1991, when improved husbandry likely reduced their prevalence (Varki et al., 2009). In aged (≥35 years old) great apes, reproductive and renal disorders were reported as significant chronic health issues, alongside obesity and type II diabetes (Nunamaker et al., 2012; Lowenstine et al., 2016).

Previous work within our wider research group included a systematic review of the literature surrounding captive great ape morbidity and mortality (Strong et al., 2016). This highlighted the diversity of health challenges faced by captive great apes, as well as great disparity between species in the number of publications – for example, 40% of the identified literature pertained to chimpanzees, while only 2% for bonobos. As reported, chimpanzees appeared susceptible to respiratory infections, often linked to respiratory syncytial virus (RSV), and GI diseases were a concern across all species. Orangutans were reported to be affected by zoonotic diseases such as RSV and varicella virus, reflecting their sensitivity to human-transmitted pathogens. Gorillas showed a higher reported prevalence of degenerative conditions, including arthritis and spondylosis. In a further review, specifically of gorilla mortality (Strong et al., 2017), GI diseases (23%) and trauma (15%) were identified as major causes of death.

Trauma-related fatalities were most prevalent among younger apes, often due to conspecific aggression or maternal neglect. Moreover, the review noted an increased prevalence of chronic, age-related conditions that affect overall health and quality of life. In addition to the findings listed, the literature has increasingly highlighted the prominence of cardiovascular disease (CVD) in particular, which will now be addressed in more detail.

II. Cardiovascular Disease (CVD) in Great Apes

Although CVD is reported relatively infrequently in wild great apes, it has been identified in some instances. Congestive heart failure was documented as the cause of death in an adult female chimpanzee in the Taï Forest (Leendertz et al., 2006). A mortality review from Gombe found cardiomyofibre changes and mild to moderate myocardial fibrosis in adult chimpanzees, though CVD was not deemed to be the cause of death (Terio et al., 2011). In one case of sudden death, post-mortem autolysis prevented a definitive diagnosis, but CVD could not be ruled out (Terio et al., 2011). CVD was diagnosed in two semi-wild bonobos from the Democratic Republic of Congo (DRC), where encephalomyocarditis virus (EMCV) was associated with cardiomegaly and myocardial fibrosis (Jones et al., 2005, 2011). A conference abstract noted CVD in six of eight necropsied wild Eastern lowland gorillas (*Gorilla beringei graueri*) over four years in the DRC (Kambale et al., 2014). For orangutans, evidence is sparse, with one report documenting a female with a systolic heart murmur during relocation (Kilbourn et al., 2003). Though it is likely that CVD in wild great apes is underreported, and true prevalence therefore unknown, there is currently no evidence to suggest that CVD is a prominent cause of morbidity and mortality in wild populations.

In captive populations, CVD is commonly reported as a leading cause of mortality. Early studies identified congenital malformations, degenerative changes, inflammatory conditions, and vascular diseases as notable forms of CVD in chimpanzees (Schmidt, 1978). Another report documented cardiac amyloidosis and arrhythmias in a chimpanzee, and cardiac fibrosis in orangutans (Munson and Montali, 1990). Cardiomyopathy resembling human familial arrhythmogenic right ventricular cardiomyopathy (ARVC) was also identified in young chimpanzees, as characterised by fibrofatty infiltration and ventricular wall thickening (Tong et al., 2014). Other work has shown an association between renal and cardiac disease in older chimpanzees, as characterised by concurrent myocardial fibrosis and glomerulosclerosis (Chilton et al., 2016).

In the aforementioned work by Strong et al. (2016, 2017), CVD was identified as a prominent cause of death in zoo-housed great apes. A more detailed review of CVD epidemiology and pathology in great apes over a 10-year period provided additional

insights (Strong et al., 2018b). Cardiomyopathy was identified as the most common CVD phenotype, responsible for 54% of cardiovascular deaths overall. The term cardiomyopathy refers to refers to a group of diseases that affect the muscle tissue of the heart, often leading to structural and functional abnormalities. This can result in the heart becoming enlarged, thickened, or stiffened, impairing its ability to function effectively. There are various types, including dilated, hypertrophic, and restrictive cardiomyopathies, each with distinct pathophysiological features and clinical implications (Towbin and Jefferies, 2017).

Chimpanzees appeared to exhibit a higher susceptibility to CVD at a younger age, with 19% of cases occurring before 20 years of age (Strong et al., 2018b). Chimpanzees also had the highest proportion of deaths due to cardiomyopathies, particularly among males. In gorillas, cardiomyopathies accounted for 47% of CVD-related deaths, followed by arterial diseases such as aortic dissection (20%). Male gorillas were significantly more affected, with a risk of CVD mortality over eight times higher than that of females. Similarly, cardiomyopathies were a leading cause of CVD deaths in bonobos (54%), though arterial disorders were more prevalent in bonobos compared to other species. Orangutans exhibited the lowest proportion of CVD-related deaths (16%), with cardiomyopathies being relatively rare, comprising only 17% of their CVD mortalities. Among the cardiomyopathies, myocardial fibrosis was the most frequently reported, often associated with sudden death (42% of CVD-related deaths), peri-anaesthetic complications, and heart failure. Sudden death was observed across all species, underscoring the urgent need for proactive screening to identify at-risk individuals before the disease progresses to its terminal stages (Strong et al., 2018b).

The aetiology of myocardial fibrosis in captive great apes is often unclear, and as such it has been suitably named idiopathic myocardial fibrosis (IMF) in much of the literature. Myocardial fibrosis is characterised by the progressive infiltration and replacement of normal myocardial tissue with excessive fibrous tissue, with resultant conduction abnormalities and arrhythmias eventually leading to sudden cardiac death (Lammey et al., 2008b, 2008a). This is in contrast to the most common forms of CVD in humans, which often involves coronary artery atherosclerosis and ischaemia (Varki et al., 2009). In one study, IMF was implicated in 52% of chimpanzee deaths, though diagnostic limitations were noted (Seiler et al., 2009; Sleeper, 2009). Similarities with human ARVC have been observed in some cases, further complicating diagnosis and

classification (Tong et al., 2014). Continued further investigations from within our research group identified IMF in 91% (30/33) of European zoo-housed, but 0% (0/25) of African sanctuary-housed, chimpanzees (Strong et al., 2020). IMF in these cases (and the cases used in the research chapters of this thesis) was characterised by two distinct histopathological patterns: interstitial fibrosis, marked by fibrous tissue deposition between intact myocardial cells (indicative of earlier disease stages), and replacement fibrosis, where cardiomyocytes were extensively replaced with dense fibrous tissue, often disrupting myocardial architecture (reflecting advanced disease stages). IMF was frequently associated with sudden death, contributing to a significant portion of cardiovascular-related deaths, as well as peri-anaesthetic deaths and heart failure. Other clinical and post-mortem findings of IMF often included cardiomegaly, ventricular thickening, and fibrofatty replacement, with histopathological evidence of myofibroblast activity contributing to excessive fibrosis (Strong et al., 2020).

Due to a growing interest in CVD in zoo-housed great apes, several key research groups have been formed. The USA-based Great Ape Heart Project, established in 2010, focuses on addressing CVD in great apes through a centralised cardiac clinical diagnostic database. The UK-based International Primate Heart Project aims to establish cardiac health reference values and investigate the causes of CVD, enhancing diagnostic accuracy and understanding disease mechanisms. This PhD, however, is part of the Ape Heart Project (AHP) research group, building on previous work to improve our overall understanding of CVD, particularly IMF, in great apes. The AHP was formed over a decade ago at Twycross Zoo and its biggest strength is the consistent, detailed post-mortem examinations, including histopathology, carried out by a board-certified veterinary pathologist on a large number of great apes (now over 100 animals examined). This, along with other clinical and pathology-based work, has contributed collaboratively to a growing body of important findings (Strong et al., 2016, 2017, 2018a; Baiker et al., 2018; Strong et al., 2018b, 2018c; Moittié et al., 2020a; Strong et al., 2020; Moittié et al., 2020c; Baiker et al., 2020; Raindi et al., 2022; Drane et al., 2019, 2020; Moittié et al., 2022, 2020b; Bucknell et al., 2023).

However, IMF still presents a major challenge for the health of captive great apes due to its high prevalence and strong association with sudden cardiac death. Its progressive nature and unclear aetiology underline the continued need for focused research to improve diagnostics, uncover its pathogenesis, and identify key risk

factors. Such efforts are essential to inform targeted management strategies and improve long-term health outcomes for these endangered species in human care.

III. Diagnostic Tools for CVD in Great Apes

Post-mortem cardiac examinations, including histopathology, can be considered the most accurate and widely used diagnostic tool for CVD, particularly IMF, in great apes (Strong et al., 2020). Historically, post-mortem examinations in zoos lacked standardisation, with inconsistent reporting of pathological lesions complicating efforts to assess disease prevalence over time (Strong et al., 2016, 2017). The AHP addressed this issue by introducing standardised post-mortem protocols for macroscopic and histopathologic evaluations (Strong et al., 2018c), and continues to gather the largest pathological dataset for captive great apes through the systematic examination of formalin-fixed whole hearts. To date, the project has analysed the hearts of 59 chimpanzees, 29 gorillas, 20 orangutans, and 11 bonobos (total n=119). Previous doctoral theses and publications have extensively detailed the morphology of many of these hearts (Strong, 2017; Moittié, 2021; Strong et al., 2020; Moittié et al., 2020a, 2020c). While the continued characterisation of cardiac phenotypes was not within the novel research focus of this thesis, Appendix A summarises the findings from recent cases examined during this PhD, undertaken by the author of this thesis in collaboration with the AHP's board-certified veterinary pathology team. This information is included for interest, and to complement and further contextualise the main research chapters within the wider AHP framework.

However, while post-mortem evaluation is highly accurate and useful in characterising CVD phenotypes, the overarching goal is to be able to improve health outcomes in these species. Reliable ante-mortem diagnostic tools are essential for early detection, clinical management and improved understanding of CVD, particularly IMF. Clinical diagnostic techniques such as blood pressure monitoring, implantable loop recorders (ILRs), electrocardiograms (ECGs), and echocardiograms are used to diagnose CVD in great apes, though their feasibility may be restricted in the zoo setting, with limited comparative data available from wild counterparts (Drane et al., 2019, 2020; Magden et al., 2016; Moittié, 2021). Blood pressure reference intervals for chimpanzees have been established, but depend on the anaesthetic agent used during data collection (Ely et al., 2011b, 2013). ILRs are rarely implemented due to cost and implantation complexities, while ECGs and echocardiograms normally require anaesthesia, which can confound results (Strong et al., 2018a; Bucknell et al., 2023). Modern approaches

for obtaining ECG readings on conscious animals are becoming more common, but can be less accurate due to movement artifacts and stress-induced variations (Olds et al., 2023; Cloutier Barbour et al., 2020). Additionally, arrhythmias detected due to IMF may indicate advanced disease stages, limiting its effectiveness as an intervention strategy. Other work has reported that diagnostic imaging accuracy varies due to differences in protocols, study duration, and the expertise of those interpreting the data (Shave et al., 2014; Boyd et al., 2019).

While other forms of CVD may be detectable by the methods outlined, the ability to detect IMF ante-mortem is inherently more challenging. According to the literature, traditional diagnostic tools such as echocardiography are limited in detecting myocardial fibrosis due to its histological nature (Zhu et al., 2022; Ravassa et al., 2023a). Advanced techniques like strain analysis and mechanical dispersion may offer indirect assessments but lack specificity and are operator-dependent (Zhu et al., 2022; Ravassa et al., 2023a). Cardiac MRI is the gold standard for non-invasive fibrosis detection in humans, with techniques like late gadolinium enhancement and T1 mapping enabling precise assessment of replacement and interstitial fibrosis (Zhu et al., 2022; Shaw et al., 2016). However, its cost and technical requirements make it widely impractical for zoo-housed great apes (Zhu et al., 2022). Another method, endomyocardial biopsy (EMB), would provide histological confirmation, but its invasiveness and logistical constraints hinders its use in the zoo setting. Overall, this highlights the need for non-invasive, cost-effective diagnostic methods tailored to zoo-housed great apes.

Blood-based biomarkers present a promising alternative, as blood sampling is routine in zoo veterinary care, either under anaesthesia or through behavioural training for conscious sampling (Rivera and Leach, 2023). Biomarkers (biological markers) are measurable indicators of normal physiological or pathological processes and are widely used alongside other diagnostic tools in human and veterinary medicine (Myers et al., 2017). Their role in diagnosing CVD in humans and other species has been extensively explored, yet their utility in great apes, particularly for detecting IMF, remains an area of active investigation.

The most commonly used cardiac biomarkers are cardiac troponins I and T (CTnI and CTnT) and N-terminal pro-brain-type natriuretic peptide (NT-proBNP). These

biomarkers have proven efficacy in diagnosing ischaemic heart disease and heart failure in other species (Oyama, 2013). Cardiac troponins are intracellular proteins associated with actin filaments in cardiomyocytes. When myocardial injury occurs, such as during prolonged ischaemia, troponins are released into the circulation (Antman et al., 2000). However, in great apes, their diagnostic application is limited due to the lack of validated reference intervals and differences in common disease presentations (Ely et al., 2011a; Varki et al., 2009). For instance, in one study, CTnI was elevated in a chimpanzee prior to sudden cardiac death, but the assay used was not species-validated (Feltrer et al., 2016). In other primates, CTnI levels rose in response to medical testing procedures that increased heart rate and blood pressure, suggesting that non-cardiac factors may influence biomarker levels (Reagan et al., 2017). NT-proBNP is a marker of myocardial stretching and stress, released by the myocardium in response to increased cardiac wall tension (Tang et al., 2007). It is preferred over brain-type natriuretic protein (BNP) due to its greater stability and longer half-life in circulation (Oyama, 2013). Elevated NT-proBNP levels have been correlated with left ventricular dysfunction and heart failure in captive gorillas, though false positives occurred in cases of renal dysfunction (Murray et al., 2019). Similarly, a young male chimpanzee diagnosed post-mortem with arrhythmogenic cardiomyopathy had rising NT-proBNP levels in the two years prior to death (Flach et al., 2010; Tong et al., 2014). In another study, elevated NT-proBNP was observed in two chimpanzees who eventually succumbed to CVD (Raindi et al., 2022). Overall, though these commonly used markers are useful, they may not be specific enough to particular CVD phenotypes, such as IMF.

Other biomarkers have been evaluated with varying success. For example, inflammatory markers such as C-reactive protein (CRP) and interleukin-6 (IL-6) have shown limited utility. Elevated CRP levels were useful in diagnosing and managing CVD in a female chimpanzee, facilitating treatment and return to clinical normality (Van Zijll Langhout et al., 2017). However, CRP and IL-6 did not significantly predict CVD or mortality in captive gorillas (Edes and Crews, 2019; Edes and Brand, 2021). Recent advances have evaluated biomarkers such as cortisol, IL-6, tumour necrosis factor-alpha (TNF-α), albumin, and lipid profiles for their potential in predicting mortality and chronic disease risks in gorillas (Edes et al., 2020a, 2022), but species-specific differences in cytokine profiles highlighted the need for tailored diagnostic reference

ranges. Markers of oxidative stress and lipid profiles (e.g., cholesterol, triglycerides, HDL/LDL ratios) were successfully used to assess chimpanzees' susceptibility to oxidative stress and CVD compared to humans (Videan et al., 2009). Markers of fibrosis, such as ICTP and PIIINP, have also demonstrated some promise. ICTP detected CVD in chimpanzees with concurrent renal disease, while PIIINP successfully detected trends in CVD severity (Ely et al., 2010). This demonstrates that the use of pathophysiology-specific markers, as well as longitudinal trend monitoring to account for inter-individual variability, is important.

Given the wide scope and variability of potential biomarkers of CVD, modern techniques such as mass spectrometry and high-throughput immunoassays can be utilised to identify novel biomarkers or biomarker signatures, that are sensitive and specific to a particular disease, in a particular species (Fu and Van Eyk, 2006; Geyer et al., 2017; Petrera et al., 2021; Shing et al., 2023). There are no published studies of this kind in great apes, but a proteomic investigation in other primates identified three serum proteins (SAA, A1AGP, Apo A1) as significantly altered in animals with cardiac injury (Song et al., 2014), while no alteration in cardiac troponins was found. In humans, multiplex immunoassays frequently identify novel disease biomarkers, and are growing in popularity (Assarsson et al., 2014a; Skau et al., 2023; Sonnenschein et al., 2021; Braadt et al., 2023; Shaw et al., 2016).

By leveraging advances in biomarker discovery, it may become possible to detect incipient CVD in great apes before clinical signs appear, enabling timely therapeutic interventions. Ultimately, tailored biomarker signatures that reflect the unique pathophysiology of IMF, but that are practical for real-time monitoring in zoo-housed great apes, hold the greatest promise for improving clinical outlook in these species.

IV. Possible Aetiopathogeneses of Idiopathic Myocardial Fibrosis (IMF) in Great Apes

As one of the leading causes of mortality in zoo-housed great apes, understanding the possible risk factors and molecular mechanisms underpinning IMF is vital for developing targeted prevention and intervention strategies. This section explores the potential aetiopathogeneses of IMF, incorporating insights from humans and other species where necessary, since very little is currently known about this in great apes.

Age is a well-known risk factor for the development of CVD, with older individuals more commonly affected (Strong et al., 2016, 2017; Edes and Brand, 2021). Ageing is known to exacerbate CVD risk factors such as hypertension and cardiorenal disease (Ely et al., 2013; Chilton et al., 2016). Fibrosis is also considered to be part of the normal ageing process, as the myocardium adapts to long-term mechanical stress (Lakatta, 1993). However, IMF as observed in great apes does not appear to align with normal age-related changes, in that it is more severe, and younger individuals are also affected (Strong et al., 2020). Captive chimpanzees in particular have been reported to die of CVD at young ages (Strong et al., 2016), including in other cases linked to genetic conditions like ARVC (Flach et al., 2010; Tong et al., 2014).

Males appear more at risk of severe CVD, and an earlier onset of CVD, than females (Strong et al., 2016, 2017, 2018b). This sex disparity may result from factors such as higher systolic blood pressure, hormonal influences (discussed in more detail below), and genetic traits linked to the Y chromosome (Seiler et al., 2009; Lammey et al., 2008a; Strong et al., 2018b; Dennis et al., 2019). Male chimpanzees, in particular, also experience elevated metabolic and psychosocial stress, increasing their vulnerability to sudden cardiac events (Lammey et al., 2008a; Sleeper et al., 2005; Wittig et al., 2015).

Hormonal pathways, particularly involving aldosterone and cortisol, contribute to blood pressure regulation and may promote cardiac fibrosis by activating fibroblasts and increasing collagen synthesis (Meredith et al., 2015). Chronic stress, which alters adrenal hormone production, may exacerbate these effects in zoo-housed great apes (Videan et al., 2009). Stress has well-documented effects on cardiovascular health in

humans and animal models, increasing sympathetic activity and promoting pro-fibrotic pathways (Golbidi et al., 2015; Ramzan et al., 2020).

Hypertension is a well-documented condition in captive great apes, particularly chimpanzees, and it likely contributes to IMF through pressure overload mechanisms. In chimpanzees, hypertension has been identified as a risk factor for cardiac disease, including myocardial fibrosis and sudden cardiac death, with studies reporting systemic hypertension in affected individuals (Lammey et al., 2008a; Seiler et al., 2009). Cardiac arrhythmias and myocardial fibrosis has also been observed in chimpanzees, with systemic hypertension implicated as a key driver of these conditions (Lammey et al., 2008a; Ely et al., 2013). Chronic hypertension can result in left ventricular hypertrophy and eventual cardiac dysfunction, driven by mechanical stress-induced activation of fibroblasts and extracellular matrix (ECM) deposition via angiotensin II and endothelin-1 signalling pathways (Wynn, 2008; González et al., 2002; Barallobre-Barreiro et al., 2016b; Shaw et al., 2016). Evidence from gorillas further highlights the risks associated with untreated hypertension, with chronic systemic hypertension in a Western lowland gorilla linked to myocardial fibrosis and eventual heart failure (Miller et al., 1999). The accumulation of collagen in the ECM, particularly types I and III, is a hallmark of IMF and contributes to cardiac stiffness and impaired contractility (Wynn, 2008; Lammey et al., 2008a). Proteomic studies in humans have demonstrated changes in the phosphorylation states of sarcomeric proteins as biomarkers of cardiac injury, suggesting that similar approaches in non-human primates could elucidate the molecular adaptations associated with mechanical stress in IMF (Paola Gómez-Mendoza et al., 2021).

As above, ECM dysregulation is a hallmark of myocardial fibrosis, characterised by excessive deposition of collagens and other structural proteins (Wynn, 2008; Varki et al., 2009). Dysregulation of ECM turnover, driven by imbalances between matrix metalloproteinases (MMPs) and their inhibitors (TIMPs), has been reported as central to fibrosis progression (Wynn, 2008). Comparative studies have revealed increased myocardial collagen in chimpanzees compared to humans, even in clinically healthy individuals, highlighting the increased risk for the onset of IMF (Varki et al., 2009). Histopathological evaluations of IMF cases have demonstrated excessive interstitial collagen deposition and fibrosis-associated ECM remodelling, with evidence of both interstitial and replacement fibrosis (Strong et al., 2020; Baldessari et al., 2013;

Lammey et al., 2008a; Seiler et al., 2009). The involvement of connective tissue growth factor (CTGF) in enhancing collagen synthesis and ECM remodelling has been highlighted, which further underscores the role of ECM-specific molecular mediators in IMF pathogenesis (Koitabashi et al., 2007). Transforming growth factor-β1 (TGF-β1) is likely another key mediator, by regulating ECM protein synthesis and inhibiting protease activity to prevent ECM degradation (Lijnen et al., 2000). An increased ratio of type I to type III collagen and cross-linking of collagen fibres is known to exacerbate ECM rigidity, contributing to impaired diastolic function and left ventricular stiffness (Ravassa et al., 2023a; Henderson et al., 2020).

Chronic inflammation and oxidative stress may also be involved in IMF. Cytokines such as interleukin-6 (IL-6) and galectin-3 (GAL-3) act as both biomarkers and mediators of fibrosis in human CVD (Van Linthout and Tschöpe, 2017; Lok et al., 2010). TGF-β1 not only promotes fibroblast activation but also mediates downstream effectors like IL-11, further amplifying inflammatory and fibrotic responses (Schafer et al., 2017). IMF cases in great apes often exhibit mild to moderate inflammatory cell infiltration, including macrophages and T-cells, suggesting a role for inflammation in disease progression (Strong et al., 2020; Seiler et al., 2009). Elevated levels of allostatic load biomarkers, including cortisol and interleukin-6, support the link between stress-induced inflammation and CVD in great apes (Edes et al., 2020b, 2020c; Edes, 2020; Edes et al., 2020a). Additionally. reactive oxygen species (ROS) may exacerbate IMF by promoting oxidative damage, impairing mitochondrial function, and activating profibrotic signalling pathways such as TGF-β1 and nuclear factor-κB (NF-κB) (Dietl and Maack, 2017; Mongirdienė et al., 2022). Elevated oxidative stress biomarkers have highlighted the susceptibility of chimpanzees to oxidative damage and premature CVD compared to humans (Videan et al., 2007a, 2007b). Further studies also suggest a role for inflammatory markers such as cardiotrophin-1 and its interaction with galectin-3 in worsening fibrosis through profibrotic pathways (Martínez-Martínez et al., 2019).

Nutritional factors may also play an important role, especially in the zoo context. Zoo diets, often high in energy-dense foods like cultivated fruits and primate kibble, contrast sharply with wild diets by being lower in fibre and higher in sodium and carbohydrates (Cabana et al., 2018; Van Mulders et al., 2024). A recent review by Van Mulders et al. (2024) highlighted that great ape zoo diets that are high in sodium and

low in fibre contribute significantly to risk factors for IMF by promoting hypertension, metabolic disturbances, and oxidative stress. They noted that excessive sugar intake leads to hyperglycaemia and glycation, impairing vascular function and promoting inflammation, while imbalanced omega-3 to omega-6 ratios in the diet also increase chronic inflammation (Van Mulders et al., 2024). Elsewhere, obesity and excess dietary sodium have been specifically linked to hypertension in chimpanzees (Ely et al., 2013; Elliott et al., 2007). Moreover, higher body mass index (BMI) has been correlated with increased inflammatory biomarkers in chimpanzees, similar to findings in humans, and further linking nutritional factors to CVD risk (Obanda et al., 2014). Another study demonstrated that low-sugar, high-fibre diets can improve oxidative stress markers and reduce behavioural abnormalities like regurgitation and reingestion, while also reversing prediabetic states in great apes (Cabana et al., 2018).

Finally, vitamin D deficiency has emerged as a possible important factor in IMF aetiopathogenesis. In humans, vitamin D plays a cardioprotective and regulatory role in myocardial fibrosis by inhibiting TGF-β1-mediated myofibroblast activation, reducing collagen synthesis and fibrosis (Meredith et al., 2015). Vitamin D has also been shown to regulate the renin-angiotensin-aldosterone system (RAAS), reducing angiotensin II activity and mitigating hypertension, a key risk factor for myocardial fibrosis as described above (González et al., 2002; Jia et al., 2014; Rostand, 1997; Pilz et al., 2009). Environmental considerations that increase vitamin D synthesis, alongside reducing dietary sugars and increasing fibre, could provide systemic benefits by reducing oxidative stress, regulating blood pressure, and mitigating profibrotic pathways (Cabana et al., 2018). In zoo-housed great apes, lower serum vitamin D concentrations have been specifically linked to IMF, with levels correlating to seasonal variations in UV exposure (Strong et al., 2020; Van Mulders et al., 2024).

Although literature points towards IMF being a complex condition influenced by many factors (age, sex, hormonal imbalances, ECM dysregulation, chronic stress, hypertension, inflammation, diet and environment), the exact aetiopathogeneses remain unclear and require investigation. Explorations of proteomic and molecular signatures in the IMF phenotype would provide important insights. Vitamin D and its potential role in IMF will now be explored in greater detail.

V. Vitamin D: Importance and Potential Role in IMF in Great Apes

Vitamin D comprises a collection of fat-soluble secosteroids, and its main source in humans and animals is dependent on direct, unfiltered sunlight. Cholecalciferol (vitamin D_3) is synthesised when UVB radiation from the sun interacts with 7-dehydrocholesterol in the skin (Holick et al., 1980). Ergocalciferol (vitamin D_2) is synthesised by plants and fungi, and obtained by humans and animals from dietary sources (Holick et al., 1980). Both vitamin D_2 and D_3 are inactive forms that are hydroxylated by the liver and converted into the major circulating metabolite: calcifediol. Otherwise known as 25-hydroxyvitamin D (25-OHD), calcifediol is the biomarker used to measure vitamin D status and is relatively stable with a half-life of 2-3 weeks (Jones et al., 1998; Lund et al., 1980). Finally, 25-OHD is converted by the kidneys into the active form of vitamin D – calcitriol ($1,25[OH]_2D$).This active form interacts with cells by binding to the vitamin D receptor (VDR) in the cytoplasm, which then translocates to the nucleus, , and is thought to directly regulate over 200 genes (DeLuca, 2004; Kongsbak et al., 2013).

Vitamin D primarily impacts the musculoskeletal system by facilitating intestinal absorption of essential minerals like calcium, magnesium, and phosphorus, which are crucial for healthy bone function (Jones et al., 1998; Holick, 2004a). Severe vitamin D deficiency can cause osteoporosis, osteomalacia, and rickets (Holick, 2004a). Beyond this, vitamin D plays a role in immunomodulation, with deficiencies linked to autoimmune diseases such as rheumatoid arthritis and multiple sclerosis (Szodoray et al., 2008), and higher intake associated with reduced incidence of influenza, periodontal disease, and post-operative infections (Schwalfenberg, 2011). It may also influence other aspects of health, with potential links to schizophrenia, Parkinson's disease, type 1 diabetes, and certain cancers, though these associations remain largely correlational and require further randomised control trials (Holick, 2004a, 2004b; Deluca et al., 2013; Jorde and Grimnes, 2015). Conversely, excessive vitamin D can lead to hypercalcaemia, causing soft tissue calcification and renal toxicity (The Scientific Advisory Committee on Nutrition, 2016). Despite growing knowledge about the importance of vitamin D in overall health, establishing universal vitamin D intake recommendations is challenging, due to large individual variations in synthesis and metabolism (The Scientific Advisory Committee on Nutrition, 2016).

Vitamin D's cardioprotective role is well-documented, including its involvement in regulating hypertension via the RAAS, improving endothelial function, and reducing vascular inflammation, all of which are implicated in CVD (Rostand, 1997; Pilz et al., 2009). Epidemiological studies in humans have highlighted the association between vitamin D deficiency and increased CVD risk. For instance, blood cholesterol and blood pressure tend to be higher in winter and at higher latitudes, mirroring patterns of vitamin D deficiency (Grimes et al., 1996; Rostand, 1997). Another large patient analysis found that vitamin D deficiency was significantly associated with risk factors such as diabetes and hypertension, as well as outcomes including myocardial infarction and stroke (Anderson et al., 2010). Similarly, a meta-analysis of multiple studies reported an inverse relationship between vitamin D status and CVD risk, although causality remains uncertain (Wang et al., 2012). In animal studies, VDR knockout mice developed cardiac hypertrophy and hypertension (Bouillon et al., 2008), and vitamin D supplementation in rats reduced oxidative stress and inflammatory markers linked to CVD (Farhangi et al., 2017).

In chimpanzees, the potential role of vitamin D deficiency in IMF has been highlighted. Zoo-housed chimpanzees with IMF were found to have lower serum vitamin D levels, particularly during periods of low UV exposure, and three individuals with IMF had notably lower levels at or before the time of death compared to those without IMF (Strong et al., 2020). A recent review further supported the hypothesis that vitamin D deficiency may contribute to IMF development in great apes, particularly those housed in northern regions with limited UV exposure (Van Mulders et al., 2024). Overall, these findings align with the hypothesis that vitamin D deficiency exacerbates collagen deposition, oxidative stress, inflammation, mitochondrial dysfunction, and calcium dysregulation; molecular pathways that have the potential to be implicated in IMF (Wimalawansa, 2019; Srinivasan and Avadhani, 2012; Meredith et al., 2015). Despite this, very little is currently known about 'normal' vitamin D status in great apes, and the factors that may affect it.

In humans, vitamin D deficiency is a global public health concern influenced by UVB exposure and a range of physiological factors (Lips, 2010; Prentice, 2008; British Association of Dermatologists et al., 2010). Sunlight exposure is the primary determinant of vitamin D synthesis, and low UVB availability, particularly at latitudes above 37°N in winter, can lead to deficiency (Webb et al., 1988; Holick et al., 1981).

Additionally, sunlight exposure is more effective than dietary supplementation at raising serum 25-OHD concentrations (Bogh et al., 2012; Ala-Houhala et al., 2012). Sun avoidance behaviours like seeking shade or wearing sun-protective clothing further increase deficiency risk, even in healthy individuals (Tangpricha et al., 2002; Linos et al., 2012; Hoegh et al., 1999). There may also be physiological reasons behind vitamin D deficiency. For instance, people with darker skin pigmentation synthesise less vitamin D_3 due to melanin's protective role in regulating UVB absorption, necessitating greater UVB exposure to achieve adequate 25-OHD levels (Webb et al., 2018; Clemens et al., 1982; Hall et al., 2010; Jablonski and Chaplin, 2010). Obesity also contributes to deficiency, as vitamin D is stored in adipose tissue, which influences its bioavailability (Wortsman et al., 2000). Ageing also reduces vitamin D synthesis due to lower skin 7-dehydrocholesterol levels, which can be further compounded by reduced outdoor activity, particularly in institutionalised elderly individuals (MacLaughlin and Holick, 1985; Parfitt et al., 1982). Overall, considering what we know to affect vitamin D status in humans, it can be hypothesised that great apes in European zoos are at risk of vitamin D deficiency due to their dark skin pigmentation, body hair coverage and exposure to lower average UVB levels than they would otherwise experience in their native geographic ranges.

Relatively few studies have examined vitamin D in non-human great apes, despite their genetic similarity to humans and their large numbers in human care. Early research found that zoo-housed gorillas and orangutans had markedly lower vitamin D compared to three other Old-World primate species (Crissey et al., 1998). In another study, chimpanzees, gorillas and orangutans had significantly lower 25-OHD status than six other primate species studied, with chimpanzees showing the lowest concentrations despite dietary intakes exceeding established recommendations (Crissey et al., 1999). Severe vitamin-D-deficiency rickets was diagnosed in three juvenile chimpanzees who were exclusively breastfed and had no unfiltered sunlight exposure (Junge et al., 2000). A juvenile gorilla diagnosed with severe hypocalcaemia was found to also have a serum 25-OHD level below the commonly accepted human threshold for sufficient serum vitamin D (≤50 nmol/L) (Chatfield et al., 2012). Outdoor access has been shown to significantly improve vitamin D levels, with captive chimpanzees and gorillas housed outdoors having higher concentrations compared to those kept indoors (Videan et al., 2007b; Bartlett et al., 2017). These findings suggest

that dietary intake alone may be insufficient for maintaining optimal vitamin D levels in great apes, and highlight the importance of outdoor access in zoo husbandry practices.

More recently, large-scale studies have shed light on vitamin D status in chimpanzees in human care in a larger sample population. A multi-zoo analysis conducted by our research group examined 245 serum samples from 140 chimpanzees, making it the largest study on vitamin D status in non-human great apes to date (Moittié et al., 2022). The study identified a 33% prevalence of vitamin D insufficiency (according to human reference ranges), as well as several significant predictors of vitamin D status, as reported by the participating zoos in sampling questionnaires. For instance, the provision of unlimited outdoor access was associated with significantly higher 25-OHD levels, whereas an abnormal health status was linked with lower levels. Seasonal variation was also a strong predictor of vitamin D status, with summer levels being the highest and winter the lowest. This further highlights the importance of UVB exposure, and a review of husbandry practices in light of the findings was recommended.

Additionally, a pilot study examined serum 25-OHD in 127 chimpanzees housed in two sanctuaries in West Africa, providing the first dataset of this size for chimpanzees living in their range countries (Feltrer-Rambaud et al., 2023). The study identified sex, age, and sun exposure as significant predictors of vitamin D status. Females had higher serum 25-OHD levels than males, while infants exhibited significantly lower levels than juveniles and adults. Habitat type, reflecting varying degrees of sun exposure, was also a key factor, with chimpanzees in more open habitats exhibiting higher concentrations. Despite year-round access to outdoor habitats in equatorial regions, median serum 25-OHD levels were below the human threshold for adequate vitamin D. While this may represent ‘normal’ vitamin D levels and requirements in this species, it must be noted that the two studies (Moittié et al., 2022; Feltrer-Rambaud et al., 2023) differed in their analytical method, which is known to cause great variability in results and hinders comparability of results between studies (Ferrari et al., 2017; Holmes et al., 2013; Moittié et al., 2020b). To highlight this further, a previous validation study measuring 25-OHD in dried blood spot (DBS) cards and serum demonstrated significant analytical variability in vitamin D measurement in chimpanzees, even when using the ‘gold standard’ technique; Liquid Chromatography and Tandem Mass Spectrometry (LC-MS/MS) (Moittié et al., 2020b). This emphasises the need for

standardised methods in vitamin D measurement, as well as species-specific reference ranges to assess vitamin D status accurately and evaluate its clinical implications (Friedrichs et al., 2012). Overall, these large-scale studies indicate the multifactorial nature of vitamin D status in chimpanzees, demonstrating the interplay of environmental, physiological, and management factors.

Despite this, the relationship between vitamin D deficiency and CVD in great apes, particularly IMF, remains poorly understood. Additionally, the lack of data on bonobos, gorillas and orangutans, as well as inconsistencies in vitamin D measurement methods across studies, further reveals important knowledge gaps. There is therefore a need to explore vitamin D status in a wider population of great apes, in a standardised way, and to further investigate the factors affecting vitamin D status in zoo settings in light of its potential importance in IMF.

VI. Conclusions and Thesis Aims

Great apes face considerable threats in the wild, but even in managed care settings, they encounter distinct health challenges. CVD is a major cause of death in captive great apes, with IMF being particularly prevalent and poorly understood. Current diagnostic tools for CVD in great apes, and particularly IMF, may be inadequate. Post-mortem histopathology examination remains the current gold standard in this context, but is retrospective and therefore cannot aid in early intervention. Minimally-invasive ante-mortem diagnostics, such as circulating biomarkers, show promise but are relatively underexplored in these species. There is a need to develop reliable, yet accessible and realistic, diagnostic methods tailored to the unique physiology and management contexts of great apes. The pathogenesis of IMF is likely multifactorial and complex, and while the involvement of processes such as oxidative stress and ECM dysregulation seem likely, the precise molecular mechanisms remain unclear. Additionally, the role of likely risk factors, such as chronic stress, hypertension and zoo-specific dietary or environmental conditions in exacerbating the risk of IMF is not well characterised, though vitamin D deficiency is increasingly recognised as having potential involvement. However, there is limited understanding of what constitutes ‘normal’ vitamin D status in great apes, and inconsistencies in measurement methods further complicate comparisons across studies. Addressing these issues is essential to establish effective husbandry practices and evaluate the possible role of vitamin D as a modifiable risk factor for IMF. Building on the knowledge gaps identified in the literature, this thesis aims to:

1. Investigate potential biomarkers for the early detection of IMF, using advanced techniques to identify sensitive and specific markers in chimpanzee serum.
2. Explore the cardiac tissue proteome in chimpanzees affected by IMF, to identify biological pathways involved in disease progression.
3. Quantify the expression of genes that are likely involved in IMF, to better understand its molecular pathways and identify potential therapeutic targets.
4. Assess vitamin D status and its determinants in the European zoo population of great apes, in light of its importance in overall health and potential role in IMF.

1. DISCOVERY AND VALIDATION OF NOVEL SERUM BIOMARKERS OF IMF IN CHIMPANZEES

1.1 Introduction

While understanding the possible aetiopathogeneses of IMF is key to establishing appropriate treatment pathways, the ability to detect incipient IMF is essential for the effective application of such treatments. At present, there is no fully reliable way to diagnose IMF ante-mortem in great apes. Cardiac ultrasound, though an informative tool for assessing structural and functional changes, cannot always visualise fibrosis, which is a histological alteration (Zhu et al., 2022; Ravassa et al., 2023b). As a result, IMF diagnosis via echocardiography is often limited to advanced stages of disease when functional changes become evident, corresponding to end-stage heart failure (Ravassa et al., 2023b). Furthermore, cardiac ultrasound generally requires general anaesthesia, which itself alters cardiac function and introduces variability depending on the specific anaesthetic protocol and timing (Shave et al., 2014; Loushin, 2005; Strong et al., 2018a; Bucknell et al., 2023). In humans, the gold standard for diagnosing cardiac fibrosis ante-mortem is endomyocardial biopsy, often complemented by advanced imaging techniques such as cardiac MRI (Ravassa et al., 2023b; Zhu et al., 2022). However, these methods are not commonly used in veterinary medicine, and are impractical for widespread use in zoo-housed great apes, since most zoos lack the funding, time, equipment or expertise necessary to conduct such detailed investigations. Thus, in great apes, IMF is most commonly diagnosed post-mortem through histological examination of cardiac tissue (Strong et al., 2018c).

The discovery of effective ante-mortem diagnostic tests would allow earlier detection, facilitate longitudinal studies, and support research into disease progression and potential interventions. In zoological institutions that perform veterinary procedures under anaesthesia, blood sampling is common practice. Conscious blood sampling, though requiring behavioural training, is also increasingly favoured due to being less invasive and having fewer health risks than general anaesthesia (Rivera and Leach, 2023). Therefore, diagnostic tests that require blood derivatives such as serum or plasma are feasible and appropriate in the context of zoo-housed species.

Blood-based biomarkers are increasingly utilised to assess the health status of zoo-housed species, facilitating informed management decisions. In pre-movement testing, biomarkers can ensure that individuals with compromised health are not transferred to other zoos, thereby preventing potential exacerbation of their condition or leading to unnecessary stress (Edes et al., 2023; Brown et al., 2016). Similarly, pre-breeding testing employs biomarkers to detect heritable diseases, guiding breeding decisions to avoid propagation of such conditions (Ghosal et al., 2023; Brown et al., 2016). Furthermore, biomarkers assist in euthanasia decisions by providing objective data on disease progression, particularly in cases where quality of life is compromised (Chapman et al., 2023).

Biomarkers have long been used for the diagnosis of CVD in human and veterinary patients. Although well-established markers such as cardiac troponin I (cTnI) and N-terminal pro-brain-type natriuretic peptide (NT-proBNP) are highly useful, their appropriateness varies considerably between species, analytical methods, and CVD phenotypes, and reference intervals in non-human great apes are lacking (Joblon et al., 2022; Feltrer et al., 2016; Zabka et al., 2009; Ely et al., 2011a; Oyama, 2013; Van Zijll Langhout et al., 2017). Thus, while cTnI and NT-proBNP are primarily used for diagnosing myocardial infarction and heart failure, these markers may not be representative of other disease processes such as IMF in chimpanzees.

Few studies have explored circulating biomarkers for ante-mortem diagnosis of CVD in chimpanzees. In a pilot study on 20 chimpanzees of varying cardiac phenotypes (as assessed clinically ante-mortem), five known biomarkers of fibrogenesis, MMP1, TIMP1, PINP, ICTP and PIIINP, were screened for prognostic value. Of these, ICTP and PIIINP were of interest (Ely et al., 2010). In a further study, Ely et al. (2011) then tested four other markers in a group of 85 chimpanzees and found that BNP was a significant predictor of CVD status, while complete lipid panel, C-reactive protein (CRP) and cTnI were not. In another study, creatinine kinase (CK), cardiac troponin T (cTnT) and CRP, but not NT-proBNP, were indicative of myocarditis in a female chimpanzee (Van Zijll Langhout et al., 2017).

To our knowledge, ours is the first study on circulating biomarkers of CVD in chimpanzees that uses available post-mortem histopathological data to confirm the corresponding cardiac phenotype of its study animals. This is the only accurate way

to determine whether any circulating biomarkers are reliable predictors of cardiovascular morbidity (Institute of Medicine, 2010), and the accumulation of histopathological data acquired by the Ape Heart Project (Twycross Zoo, UK) over the years is therefore an important advantage. Our chosen method of biomarker candidate selection (Olink® Proximity Extension Assay) demonstrates a modern and systematic approach to screen for biomarkers that are sensitive and specific to a particular disease (Morrow and De Lemos, 2007). This targeted proteomics discovery method has a biological basis for selection by using a fixed panel of relevant analytes, and was primarily designed for human applications. However, this study leverages the cross-reactivity of the assay with the genomes of non-human great apes, allowing us to extend its use to chimpanzees. Additionally, the use of combinations of markers, or biomarker 'signatures', are known to be more desirable than single markers alone since they attain a higher disease specificity (Fu and Van Eyk, 2006; Geyer et al., 2017; Petrera et al., 2021; Ravassa et al., 2023b).

While initial high-content analysis (such as that used by Olink) is important for biomarker discovery, it is useful to then consider other methods, such as Enzyme Linked Immunosorbent Assay (ELISA), for routine clinical monitoring of the biomarkers that were discovered. Moreover, the development of ELISAs to test for particular analytes, if not already commercially available, can lead to other real-time applications such as antibody-based rapid diagnostics at point of care.

The initial biomarker discovery with Olink was performed prior to the commencement of this PhD. The subsequent ELISA testing took place four years afterwards, and was carried out between 2021 and 2022. All data analysis was performed during the PhD, by the author of this thesis. The aim of this study was to:

1. Identify candidate biomarkers that have the potential to be routinely measured in serum for the diagnosis of IMF in chimpanzees.

1.2 Materials and methods

Study subjects

Serum samples from 26 zoo-housed chimpanzees (*Pan troglodytes*) with a known cardiac phenotype were included in this study. Individuals were categorised as such according to the findings of standardised cardiac post-mortem examinations carried out by a board-certified veterinary pathologist in association with the 'Ape Heart Project' (Twycross Zoo, UK) (Strong et al., 2018c). Individuals were classed as Affected (diseased) if they showed moderate to marked chronic cardiovascular lesions that were consistent with IMF, or classed as Control (healthy) if they showed no or minimal cardiovascular changes that could be indicative of IMF. In all cases, the clinical history, circumstances of death, and whole-body post-mortem findings (as provided by the zoos of origin), were used to support and finalise the cardiac phenotyping.

A subset of samples (Study A, n=10 chimpanzees) was used for the initial biomarker discovery, with a further 16 samples (Study B, n=26 chimpanzees) included in the later validation of potential diagnostic assays. Study A consisted of 7 males and 3 females, with ages at death ranging from 18 to 62 years (median = 35 years). Among these, 6 individuals were categorised as Affected and 4 as Control. The time between serum sampling and death for all individuals in Study A ranged from 0 to 35 months (median = 0 months). For the Affected individuals in Study A, the time between serum sampling and death ranged from 0 to 14 months (median = 0.5 months), and from 0 to 35 months (median = 4.5 months) for the Control group.

Study B included 11 males and 15 females, with ages at death ranging from 9 to 62 years (median = 38 years). Of these, 18 were categorised as Affected and 8 as Control. The time between serum sampling and death for all individuals in Study B ranged from 0 to 215 months (median = 0 months). For the Affected individuals in Study B, the time between serum sampling and death ranged from 0 to 215 months (median = 4 months), and from 0 to 35 months (median = 0 months) for the Control group. A summary of information regarding all study subjects and their disease classifications can be found in Table 1.1.

All serum samples were collected opportunistically by veterinarians according to the Veterinary Surgeons' Act (VSA) or international equivalent, and spun down and separated before being stored frozen at -20°C or below. All appropriate permits and licenses were obtained before samples were transported from the zoos of origin (n=15 zoos) with freezer packs as coolant. Long-term storage of all samples was at -80°C.

Table 1.1: Study subjects: chimpanzees with a known cardiac phenotype, as confirmed histologically, categorised as Control (healthy) vs. Affected (diseased). Study A (n=10) was used for initial biomarker screening via Proximity Extension Assay (Olink® Target 96 Cardiovascular Panel III, v.6112). Study B (n=26) included all individuals from Study A with an additional 16 chimpanzees, and was used for subsequent ELISA testing.

Study group		Study ID	Age at death (years)	Sex	Time between serum sample and death (months)	Disease phenotype
Study A (n=10)	Study B (n=26)	C2	37	Male	12	Affected
		C3	33	Male	1	Affected
		C4	33	Male	0	Affected
		C15	46	Female	0	Affected
		C18	18	Male	0	Affected
		C30	21	Male	14	Affected
		C9	32	Female	35	Control
		C31	62	Female	9	Control
		C20	21	Male	0	Control
		C26	28	Male	0	Control
		C8	39	Male	50	Affected
		C10	24	Female	7	Affected
		C17	45	Male	27	Affected
		C24	46	Female	0	Affected
		C29	44	Female	0	Affected
		C34	42	Female	215	Affected
		C35	39	Female	19	Affected
		C41	43	Female	0	Affected
		C42	42	Female	0	Affected
		C44	32	Male	12	Affected
		C46	49	Female	26	Affected
		C47	47	Female	0	Affected
		C1	9	Male	0	Control
		C11	42	Female	0	Control
		C25	21	Female	0	Control
		C36	10	Female	0	Control

Olink biomarker discovery (Study A)

Prior to the commencement of this PhD, serum samples from Study A (250 µL per sample, n=10) were sent on dry ice to a commercial laboratory (Olink Proteomics, Uppsala, Sweden). 1 µL per sample was required for analysis using the high-performance Proximity Extension Assay (PEA) with a targeted panel of 92 protein biomarkers (Olink® Target 96 Cardiovascular Panel III, v.6112) to determine whether any proteins were significantly altered in chimpanzees affected by IMF (n=6) versus healthy controls (n=4). PEA readout values were in the form of Normalised Protein eXpression (NPX) on a log 2 scale, which corresponds to relative protein concentrations within the sample.

The Olink panel uses internal and external controls to ensure data accuracy. Internal controls such as Incubation Control 1 and 2 (non-human antigens), Extension Control (an antibody with unique DNA-tags), and Detection Control (a double-stranded DNA amplicon) monitor immunoreaction, extension, and amplification/detection steps, ensuring consistency across samples (Olink, 2021a). External controls include the Inter-Plate Control (IPC), a synthetic pool of 92 antibodies with unique DNA-tags, used to normalise data across plates and runs. Negative controls (buffer only) set the background noise for each assay. A pooled plasma sample is recommended as a sample control to assess variation within and between plates through inter- and intra-assay CVs. Olink's proprietary software uses these controls to normalise NPX values and reduce technical variation. This ensures that observed protein changes reflect disease-induced variations, minimising non-disease-related variability such as sample processing differences.

ELISA validation (Study B)

During the course of this PhD, ELISAs were used as subsequent protein measurements to further explore the biomarkers identified from the Olink screening in serum samples from Study B (n=26). The following ELISA kits, containing the basic components necessary for the development of sandwich ELISAs, were assessed for use with chimpanzee serum: Human Axl DuoSet and Human CD31/PECAM-1 DuoSet (catalog numbers DY154, DY806) (R&D Systems Inc., Minneapolis, USA), and Human ICAM-2 Matched Antibody Pair Set (catalog number SEK10332) (Sino Biological Inc.,

Eschborn, Germany). All assays were carried out at room temperature at University of Birmingham's School of Dentistry, Institute of Clinical Sciences (5 Mill Pool Way, Birmingham, UK). 96-well plates with a Nunc MaxiSorp surface treatment were used (catalog number 442404, Thermo Scientific™). An automatic plate washer was used for all wash steps, and a 2N solution of sulphuric acid (H_2SO_4) was used to stop the reactions at the final stage, prior to determining the optical density (OD) using a microplate reader at 450nm and 570nm to allow for wavelength correction. The strength of the colour changes of the samples corresponded to the concentration of the analyte, and each plate included a seven-point standard curve using two-fold serial dilutions of the high standard received in each kit. The substrate solution used in all cases was a 1:1 mixture containing two colour reagents: Phosphate-Citrate Buffer with Urea Hydrogen Peroxide, and 3,3',5,5'-Tetramethylbenzidine Dihydrochloride (catalog numbers P4560 and T3405, Merck Life Science UK Ltd) dissolved in 10 mL deionised water. All solutions and buffers were freshly made up prior to the commencement of ELISAs.

OD readout data from the assays were processed and transformed using Microsoft Excel. The final OD value for each sample was obtained by subtracting the 570nm reading from the 450nm reading. This correction ensures that only specific signals related to the analyte of interest are considered, minimising any background absorbance signal. A seven-point standard curve using known concentrations from serial dilutions of the standards was plotted on a logarithmic scale. Using the line of best fit regression equation from the standard curve ($y = mx + c$), OD data of the test samples were converted into analyte concentrations with any dilution factors then accounted for.

The ICAM-2 kit was stored at -20°C, and contained the following reagents: rabbit anti-ICAM-2 capture antibody, rabbit anti-ICAM-2 detection antibody conjugated to horseradish-peroxidase (HRP), and a recombinant human protein standard. The standard was reconstituted with a detection antibody dilution buffer (0.5% bovine serum albumin [BSA] and 0.05% Tween20 in Tris-buffered saline [TBS]), and the other kit reagents were diluted to a working concentration using citrate-buffered saline (CBS) or detection antibody dilution buffer, as per the manufacturer's instructions. Plates were first coated with 100 µL capture antibody per well and incubated overnight at +4°C. The following day, the plates were washed six times using 400 µL wash buffer

(0.05% Tween20 in TBS) per well. Plates were blocked by adding 300 µL of blocking buffer (2% BSA and 0.05% Tween20 in TBS) per well and incubated for a minimum of one hour at room temperature prior to washing again. Standards diluted with sample dilution buffer (0.1% BSA and 0.05% Tween20 in TBS) and samples (100 µL per well) were added to the plate in duplicate and incubated for two hours at room temperature prior to washing. 100 µL of the detection antibody was added to each well and incubated for one hour at room temperature. After a final wash step, 200 µL of the substrate solution was added to the wells and incubated at room temperature away from light for 20 minutes, or until the standards on the plate showed a defined colour change gradient. To stop the reactions, 50 µL of the stop solution (2N H_2SO_4) was added prior to measuring the OD.

The AXL and PECAM-1 kits were from the same manufacturer and therefore the overarching protocols were the same. Both kits were stored at +4°C and contained mouse anti-human capture antibody, biotinylated goat or sheep anti-human detection antibody, streptavidin conjugated to HRP, and a recombinant human protein standard. All components were initially reconstituted, and later diluted to their working concentrations, with either neat phosphate-buffered saline (PBS) or PBS with added carrier protein (reagent diluent, 1% BSA in PBS), as per the manufacturer's instructions. Plates were first coated with 100 µL capture antibody and incubated overnight at room temperature. The following day, the plates were washed six times using 400 µL wash buffer (0.05% Tween20 in PBS) per well. Plates were blocked by adding 300 µL of reagent diluent per well and incubated for a minimum of one hour at room temperature prior to washing again. Standards and samples (100 µL per well) diluted in the chosen reagent diluent were added to the plate in duplicate and incubated for two hours at room temperature prior to washing. 100 µL of the detection antibody was added to each well and incubated for two hours at room temperature. After washing, 100 µL of streptavidin-HRP was added to each well and incubated for 20 minutes at room temperature away from light. After a final wash step, 100 µL of the substrate solution was added to the wells and incubated at room temperature away from light for 20 minutes, or until the standards on the plate showed a defined colour change gradient. To stop the reactions, 50 µL of the stop solution was added before measuring the OD.

Quality control and optimisation

Prior to using up the valuable chimpanzee serum samples for final analyte measurements (in some cases, less than 1 mL of serum remained for an individual), it was necessary to verify and optimise the performance of the assays. Optimisation of commercially available ELISA kits is often necessary to account for specific sample matrices, such as chimpanzee serum, which may introduce unique variables affecting assay performance. This practice is common to ensure accuracy and reliability in diverse research contexts (Minic and Zivkovic, 2020; Jaedicke et al., 2012). Using pooled human serum (ethics approval: 19/SW/0198 Dental Research Tissue Bank at University of Birmingham's School of Dentistry) as well as serum from one chimpanzee (study ID: C47) from whom there was a large volume of serum remaining, quality control tests including inter- and intra-assay variation, limit of detection (analytical sensitivity), range-finding, and spike-and-recovery were carried out for each ELISA kit (Thermo Scientific, 2007; Jaedicke et al., 2012).

Inter-assay variation measures consistency between separate runs of the same assay, while intra-assay variation assesses consistency within replicates of a single run. When sample replicates were n=3 or above, both factors were calculated as the coefficient of variation (CV%), derived from the standard deviation divided by the mean, multiplied by 100 (Jaedicke et al., 2012; Minic and Zivkovic, 2020). Analytical sensitivity (limit of detection) is the minimum detectable concentration of the analyte. It was calculated by adding two standard deviations to the mean OD obtained from 30 replicates of the zero standard (reagent diluent with no added sample).

The range-finding exercise was conducted in order to assess at what dilution factor, if any, the analyte concentration measurement was stable and within the mid-range of the standard curve (Minic and Zivkovic, 2020). By plotting analyte concentration (adjusted for dilution factor) against the dilution factor, the point at which dilution had little effect on measured concentrations (indicated by a plateau) was identified.

Then, a spike-and-recovery assay was performed using the sample dilution factor, where applicable, as determined by the range-finding exercise. For this, a known amount of analyte was added (spiked) into the test sample matrix and compared to an identical spike in the standard diluent. Where sample dilution was necessary, two different reagent diluents were tested for recovery: PBS with carrier protein (1% BSA)

or without. This approach evaluates whether components in the sample matrix (e.g., serum) affect assay response differently than the standard diluent, aiming to maximise the signal-to-noise ratio and ensure consistent responses for the same analyte concentration in both matrices, allowing for reliable test sample measurement from the standard curve (Thermo Scientific, 2007). If the average recovery falls within 80–120%, it indicates that the matrices have minimal impact on the assay's accuracy. The recovery (%) was calculated using the following equation (Jaedicke et al., 2012):

$$\frac{(Assay\ result\ for\ spiked\ sample) - (Assay\ result\ for\ neat\ sample)}{Amount\ spiked} * 100$$

After these quality control and assay performance verifications, optimisation of the sample dilution factor and reagent diluent used was carried out prior to final sample measurements (Minic and Zivkovic, 2020). When final desired assay conditions were reached, all chimpanzees (Study B, n=26) were tested for the three analytes ICAM-2, AXL and PECAM-1.

Data analysis

All data were analysed using GraphPad Prism desktop software v10.3.0 (https://www.graphpad.com/scientific-software/prism/). The significance threshold was set to $p<0.05$ in all cases. All data were checked for normality using a Shapiro-Wilk test, which is appropriate for sample sizes <50 (Mishra et al., 2019). Where data were not normally distributed, non-parametric Mann-Whitney tests were used. Where data were normally distributed, parametric Welch's t tests for independent samples were used to test for significant differences between chimpanzees affected by IMF and healthy controls. One-tailed tests were selected based on the hypothesis that analytes in the Olink cardiovascular panel would be raised in the diseased individuals, allowing for increased statistical power by focusing on the direction of expected change (Cho and Abe, 2013). A volcano plot was also created for the benefit of visualising the distribution of the data, though it should be noted that this plot function on GraphPad Prism is only able to perform two-tailed t-tests, therefore the statistical significance shown on the volcano plot differs slightly from the one-tailed p values reported.

The data from Study A were in the form of NPX values and were already normalised on a log2 scale, meeting the assumptions of parametric tests. The Area Under the Curve (AUC) value for corresponding Receiver Operating Characteristic (ROC) curves was assessed for all 92 assay proteins. ROC curves are used to assess how well a diagnostic test can accurately distinguish between two conditions (e.g., affected vs. control), and the AUC is a numerical way to summarise the ROC curve's performance (Pepe, 2003; Hanley and McNeil, 1982).

The data from Study B were in the form of protein concentration in ng/mL. Data were inspected in conjunction with each individual assay's limit of detection, and assessed for outliers using GraphPad Prism's built-in outlier analysis. Any values that fell below the assay's limit of detection, or that were identified as outliers, were excluded from subsequent analysis. ELISA data from Study B were evaluated for all 26 chimpanzees, as well as only the subset of 10 chimpanzees from Study A for a more direct comparison between the Olink and ELISA results.

Diagnostic value

Where statistical significance was reached with ELISA, the diagnostic value of a protein biomarker was assessed by calculating Youden's Index (*J*) from ROC curve data, where:

$$J = Sensitivity + Specificity - 1$$

Sensitivity and specificity values were obtained for various cut-off thresholds using GraphPad Prism's ROC analysis, and Youden's Index was calculated for each threshold (Youden, 1950; Ruopp et al., 2008). The Positive Predictive Value (PPV) and Negative Predictive Value (NPV) were then calculated to assess the diagnostic utility at the optimal cut-off, as determined from the ROC and Youden's Index analysis. PPV was defined as the proportion of true positives among all positive test results:

$$PPV\ (\%) = \frac{True\ Positives}{True\ Positives + False\ Positives} * 100$$

while NPV was defined as the proportion of true negatives among all negative test results:

$$NPV\ (\%) = \frac{True\ Negatives}{True\ Negatives + False\ Negatives} * 100$$

Post-hoc sample size calculation

Where statistical significance was reached with ELISA, a post-hoc sample size calculation was conducted. First, the pooled standard deviation (SD_{pooled}) was calculated using the formula:

$$SD_{pooled} = \sqrt{\frac{(n_1 - 1){SD_1}^2 + (n_2 - 1){SD_2}^2}{n_1 + n_2 - 2}}$$

where n_1 and n_2 represent the sample sizes, and SD_1 and SD_2 the standard deviations, of the diseased and control groups (Borenstein et al., 2009; Goulet-Pelletier and Cousineau, 2018). Then, the effect size (Cohen's *d*) was calculated as:

$$d = \frac{M_1 - M_2}{SD_{pooled}}$$

where M_1 and M_2 are the group means of the diseased and control groups. As continuous, normally distributed, and independent grouped data, most requirements for Cohen's *d* were met (Cohen, 1988; Borenstein et al., 2009; Goulet-Pelletier and Cousineau, 2018). However, due to unequal variances between the groups, and the small ($n < 16$) sample sizes in each group, a Hedges' *g* correction factor (*J*) was applied (Hedges, 1981; Borenstein et al., 2009; Goulet-Pelletier and Cousineau, 2018). The correction factor (*J*) was calculated as:

$$J = 1 - \frac{3}{4(n_1 + n_2 - 2) - 1}$$

Then, Hedges' *g* was calculated as:

$$g = d * J$$

Finally, using the calculated effect size (Hedges' *g*), a sample size calculation was performed in G*Power (v3.1.9.7) for a one-tailed t-test with an alpha level of 0.05, power of 95% ($1 - \beta$), and an allocation ratio (n_2 / n_1) of 0.5 to account for the unequal group sizes (Faul et al., 2009).

1.3 Results

Olink biomarker discovery (Study A)

All of the 92 analytes tested in the serum screening were detectable in all samples, confirming cross-reactivity with the analytes in the assay panel. Figure 1.1 shows a volcano plot for the benefit of visualising the significance and direction of changes in all 92 proteins. Proteins with an AUC value of >0.7 (n=28) were selected for further investigation. An AUC value of >0.7 is widely considered to be acceptable, and in this case, it denotes that a biomarker is sensitive and specific enough to correctly classify these chimpanzees as 'affected by IMF' or 'healthy control'. Parametric one-tailed Welch's t tests for independent samples were used to assess whether any of the 28 proteins were significantly altered in chimpanzees affected by IMF (n=6) compared with healthy controls (n=4). Among the 28 proteins of interest that were identified (Area Under Curve >0.7), three proteins, which are involved in fibrosis and inflammation, were markedly different in diseased chimpanzees compared with controls: Intercellular Adhesion Molecule 2 (ICAM-2), Receptor Protein-Tyrosine Kinase (AXL), and Platelet Endothelial Cell Adhesion Molecule 1 (PECAM-1). Expression of all three markers was significantly increased in the diseased group. For ICAM-2, the mean ± SD expression was 6.31 ± 0.42 NPX in the Affected group (n=6) and 5.50 ± 0.12 NPX in the Control group (n=4; p=0.002). For AXL, the mean ± SD expression was 10.69 ± 0.36 NPX in the Affected group and 9.79 ± 0.50 NPX in the Control group (p=0.013). For PECAM-1, the mean ± SD expression was 4.73 ± 0.55 NPX in the Affected group and 4.14 ± 0.37 NPX in the Control group (p=0.039, one-tailed Welch's t-test for independent samples). Table 1.2 shows the AUC and Welch's t test values for the 28 proteins of interest, in order of p value significance, and a visual representation of the differences in expression between the affected and control groups can be found Figure 1.3.

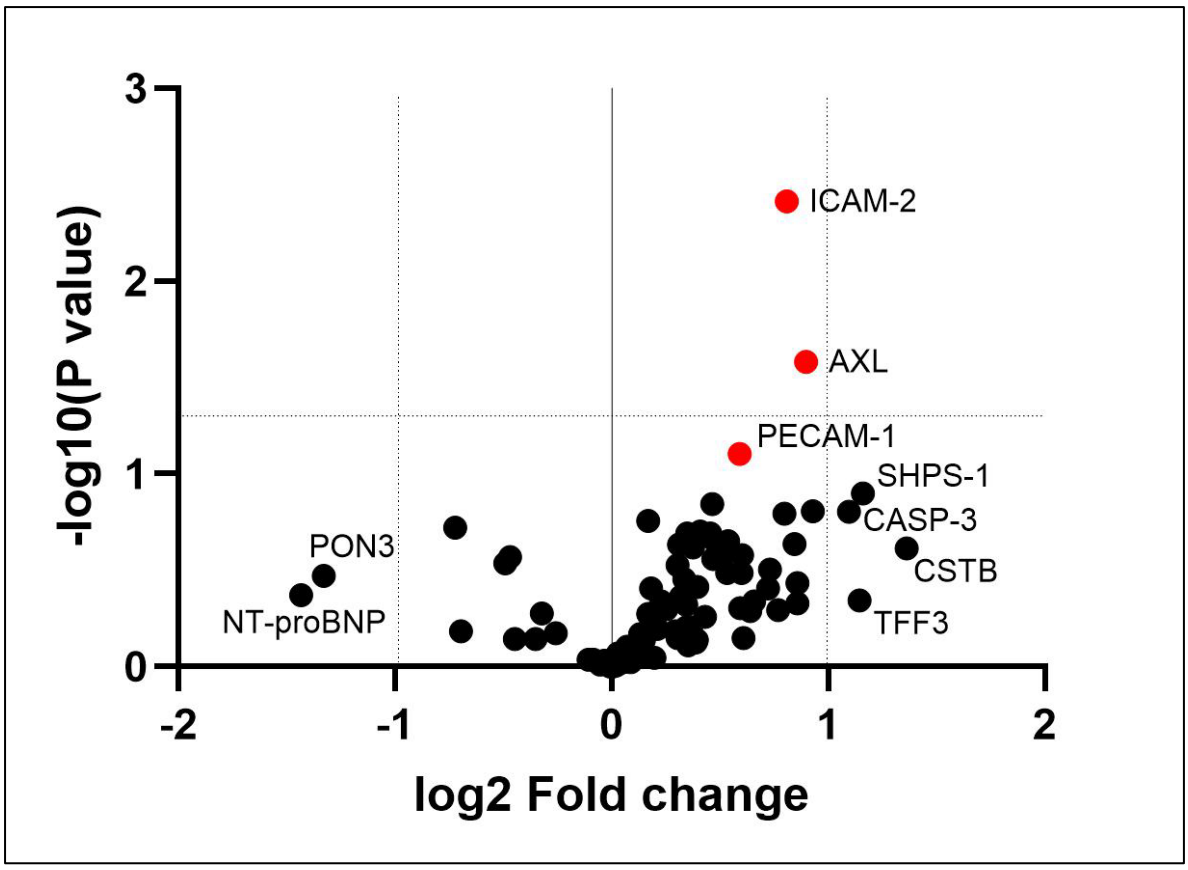

Figure 1.1: Volcano plot showing differences in protein expression (NPX) between chimpanzees affected by IMF (n=6) and healthy controls (n=4).
The plot displays the -log10(p-value) (two-tailed Welch's t tests) versus log2 fold change for 92 proteins (Olink® Target 96 Cardiovascular Panel III, v.6112). Proteins in red (ICAM-2, AXL, and PECAM-1) represent those selected for further exploration using ELISA, based on their significant differential expression as identified elsewhere in one-tailed Welch's t tests. Dotted lines indicate thresholds for statistical significance (-log10[p value] > 1.3) and log2 fold change > 1 or < -1. Positive log2 fold change indicates upregulation in the diseased group, while negative values indicate downregulation.

Table 1.2: Results of one-tailed Welch's t test for independent samples and Area Under Curve (AUC) analysis for proteins (as detected with Olink® Target 96 Cardiovascular Panel III, v.6112).
Only proteins with an AUC value of >0.7 are included (n=28). Asterisks denote a significant difference (** = p<0.01, * = p<0.05) in protein expression (NPX) between chimpanzees affected by IMF (n=6) and healthy controls (n=4).

Protein	p-value	AUC value
ICAM-2	0.002 **	1.000
AXL	0.013 *	0.917
PECAM-1	0.039 *	0.833
SHPS-1	0.063	0.875
CCL16	0.072	0.792
TNFRSF14	0.078	0.750
CASP-3	0.078	0.750
SELP	0.081	0.708
COL1A1	0.088	0.792
TIMP4	0.095	0.792
IL-17RA	0.099	0.792
ALCAM	0.102	0.750
RARRES2	0.102	0.708
PCSK9	0.111	0.792
JAM-A	0.115	0.708
CD93	0.116	0.708
ITGB2	0.121	0.708
CSTB	0.122	0.708
EPHB4	0.133	0.750
CXCL16	0.138	0.750
Vwf	0.146	0.708
AP-N	0.149	0.750
Ep-CAM	0.157	0.792
CDH5	0.176	0.750
SELE	0.184	0.708
MMP-2	0.193	0.708
IGFBP-2	0.197	0.708
TNF-R1	0.257	0.708

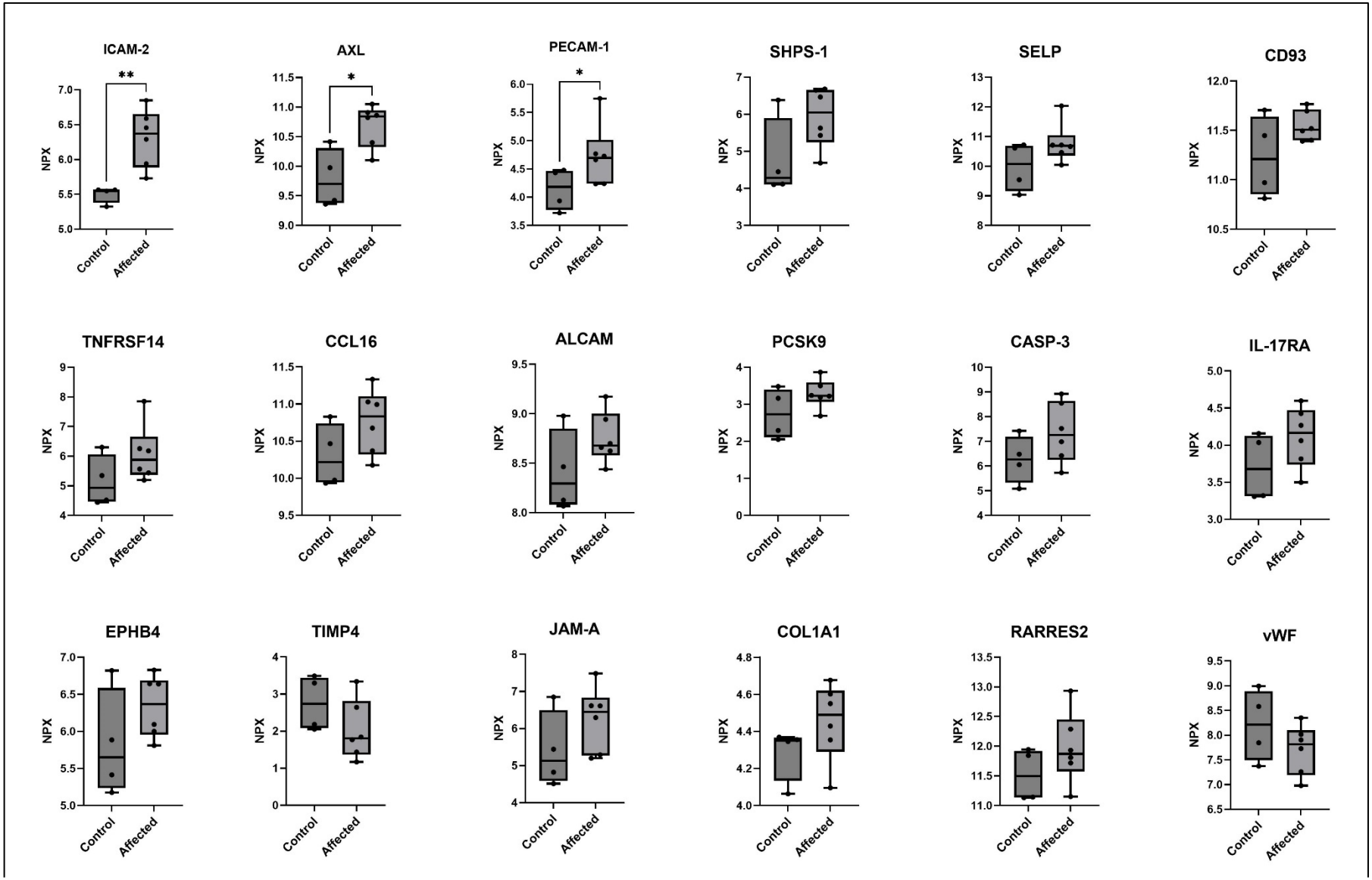
ICAM-2
**
AXL
*
PECAM-1
*
SHPS-1
SELP
CD93
TNFRSF14
CCL16
ALCAM
PCSK9
CASP-3
IL-17RA
EPHB4
TIMP4
JAM-A
COL1A1
RARRES2
vWF
NPX
Control
Affected

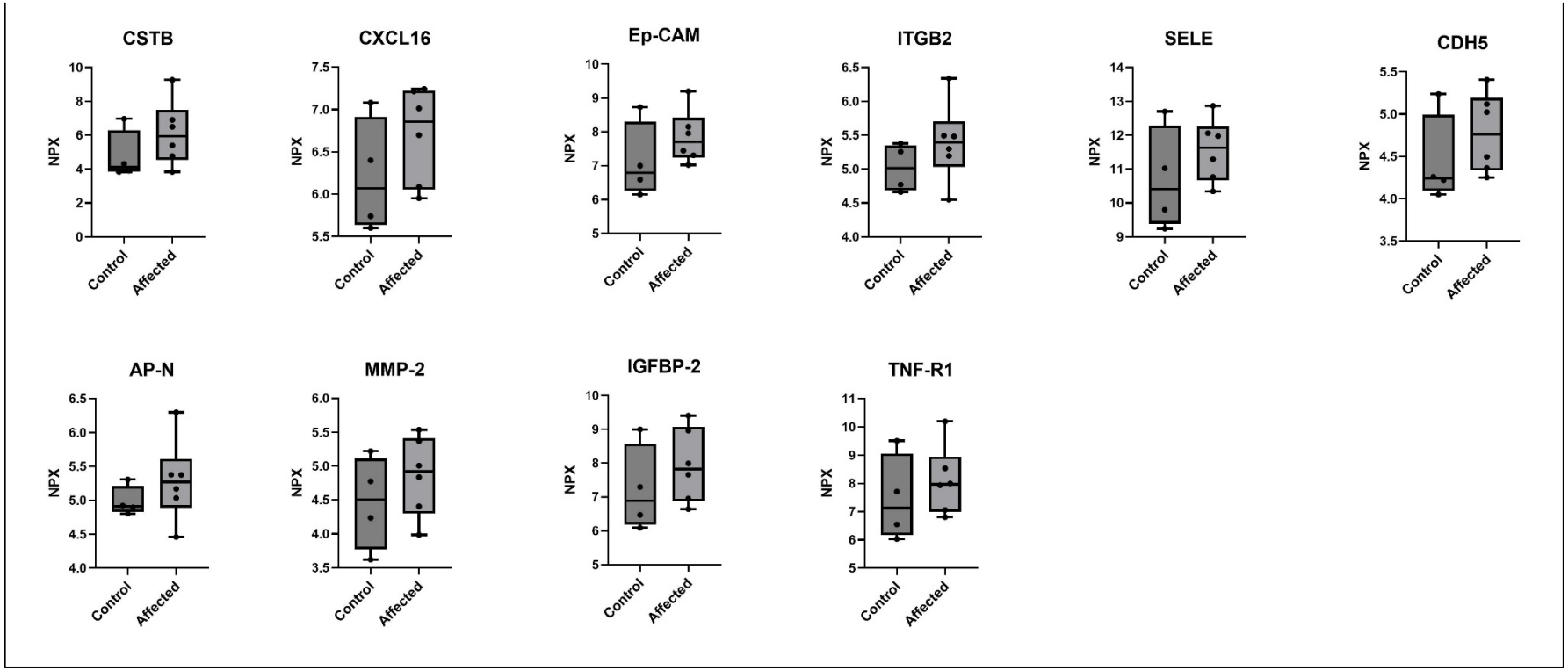

Figure 1.2: Normalised Protein eXpression (NPX) of proteins in chimpanzees affected by IMF (n=6) versus healthy controls (n=4), as tested with Proximity Extension Assay (Olink® Target 96 Cardiovascular Panel III, v.6112), which corresponds to relative protein concentrations within the sample on a log 2 scale.
The 28 proteins with the highest Area Under Curve (>0.7) out of 92 proteins tested in the assay are shown. Pairwise comparisons are displayed above each box-and-whisker plot where statistical significance is reached (one-tailed Welch's t tests, ** = $p<0.01$, * = $p<0.05$).

ELISA validation (Study B)

Quality control and optimisation

The ICAM-2 Matched Antibody Pair Set ELISA kit (Sino Biological, Eschborn, Germany) performed with an inter-assay variation (CV%) of 17%, and intra-assay variation of 7%. The analytical sensitivity was 0.191 ng/mL, which fell within the range of the standard curve stated by the manufacturer (0.0469–3 ng/mL). The range-finding assay revealed that no dilution of serum samples was needed. ICAM-2 showed a mean recovery (%) of 91% overall, with 100% recovery in the control spike (a known amount of analyte added to the standard diluent), and 86% recovery in serum (a known amount of analyte added to undiluted human and chimpanzee serum).

The AXL DuoSet ELISA kit (R&D Systems, Abingdon, UK) performed with inter- and intra-assay variations (CV%) of 10% and 4% respectively. The analytical sensitivity was 0.033 ng/mL, which was below the lowest point of the standard curve range as stated by the manufacturer (0.0625–4 ng/mL). A 1:120 dilution in was found to be effective at ensuring the concentration of AXL in serum fell within the mid-range of the standard curve, while ensuring no adverse dilution effect. Overall, AXL showed a mean recovery (%) of 106%. When using PBS (without BSA) as the reagent diluent, there was a 110% AXL recovery in serum and 113% AXL recovery in the control spike. For this reason, as well as the fact that it is recommended elsewhere to use a sample diluent with no carrier protein for the dilution of complex sample matrices such as serum (Thermo Scientific, 2007), PBS was chosen as the reagent diluent for the 1:120 sample preparations.

The PECAM-1 DuoSet ELISA kit (R&D Systems, Abingdon, UK) performed with inter- and intra-assay variations (CV%) were 10% and 3% respectively. The analytical sensitivity was 0.140 ng/mL, which was below the lowest point of the standard curve range as stated by the manufacturer (0.156–10 ng/mL). A 10-fold dilution (1:10) was found to be appropriate for PECAM-1, which showed a mean recovery of 106% overall. Again, PBS (without BSA) was chosen as the optimal sample diluent, as it gave a PECAM-1 recovery of 101% in 1:10 preparations of serum.

Table 1.3 shows a summary of assay performance results. The dilution effect and spike-and-recovery performances for all three proteins can be found in Figure 1.4 and Figure 1.5.

Table 1.3: Assay performances for ICAM-2, AXL and PECAM-1 as tested via commercially available human ELISA kits.

The standard curve range is as stated by the kit manufacturers. Analytical sensitivity (limit of detection) was calculated by adding 2 standard deviations to the mean optical density obtained from assaying 30 replicates of the zero standard. The % Recovery is the mean spike-and-recovery from a control spike (a known amount of analyte added to the standard diluent) and spiked serum (a known amount of analyte added to the sample matrix).

	ICAM-2	**AXL**	**PECAM-1**
Range (standard curve)	0.0469–3 ng/mL	0.0625–4 ng/mL	0.156–10 ng/mL
Inter-assay CV%	17%	10%	10%
Intra-assay CV%	7%	4%	3%
Analytical sensitivity	< 0.191 ng/mL	< 0.033 ng/mL	< 0.140 ng/mL
Dilution factor	Undiluted	1:120	1:10
% Recovery	91%	106%	106%
Reagent diluent	N/A	PBS	PBS

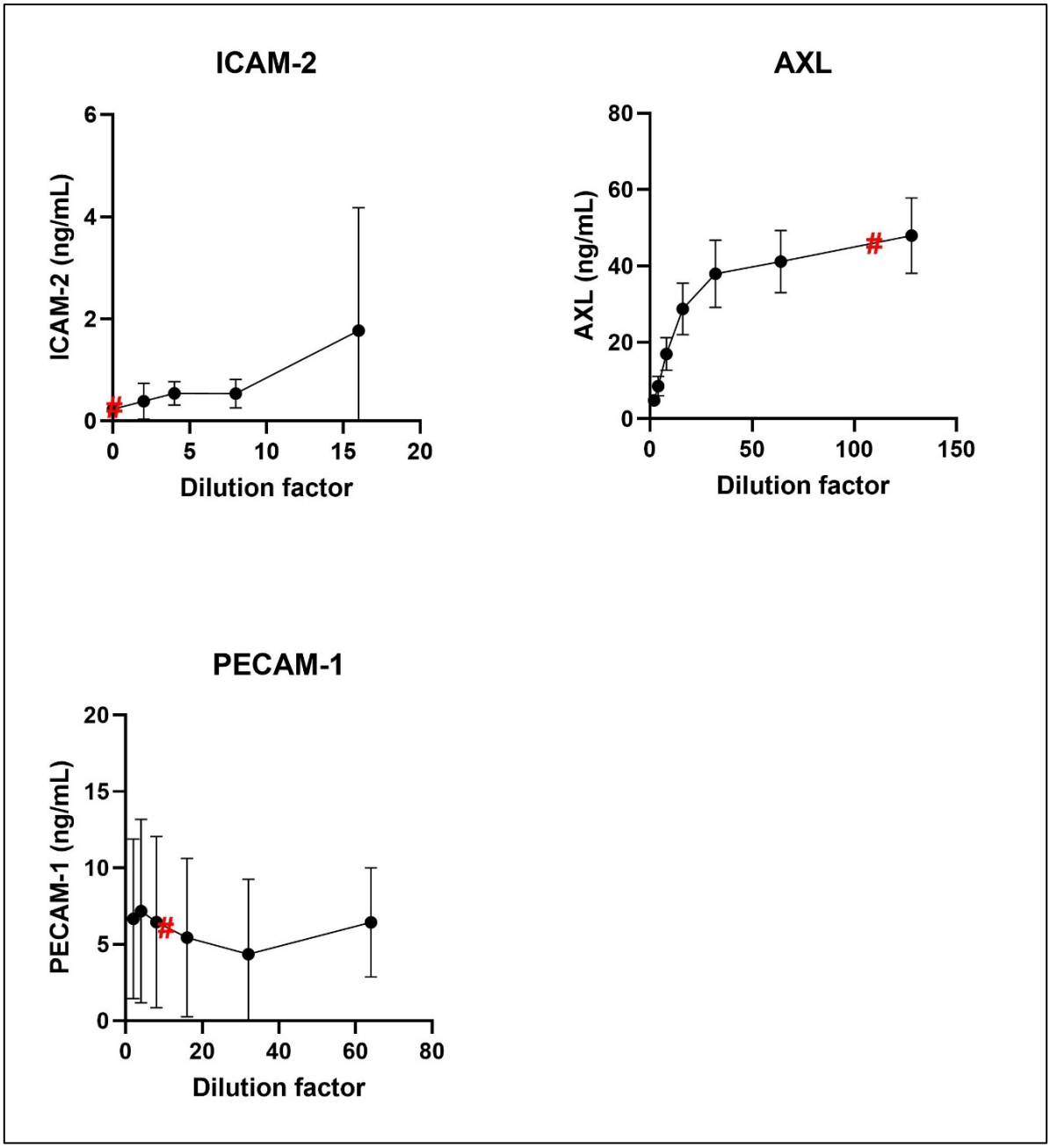

Figure 1.3: Range-finding results showing the dilution effect on the measurement of ICAM-2, AXL, and PECAM-1 concentrations in serum.

The y-axis represents the concentration of each protein (ng/mL), adjusted for the dilution factor, and the x-axis represents the dilution factor. The red hash symbol (#) indicates the chosen dilution factor for subsequent ELISA testing: 0 (undiluted) for ICAM-2, 120 for AXL, and 10 for PECAM-1. Error bars represent the standard deviation of the mean from repeated measurements of both human and chimpanzee serum.

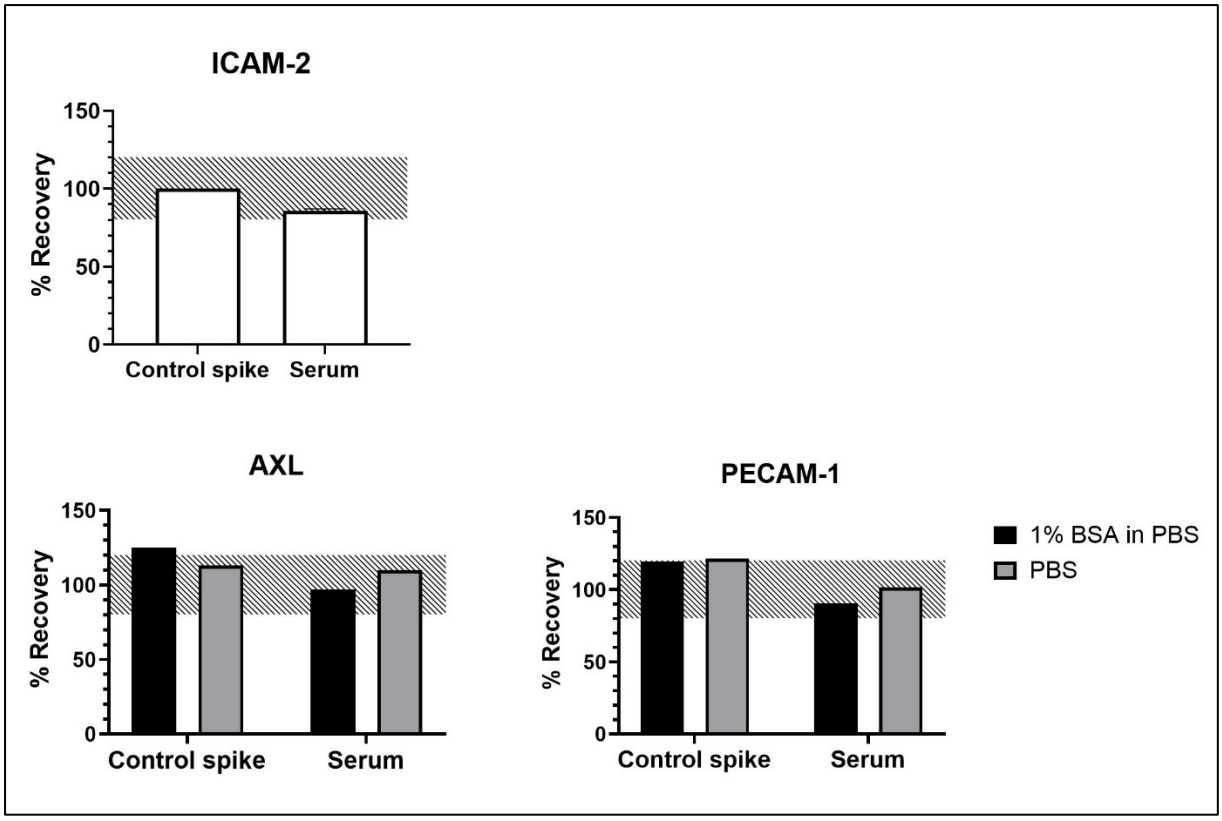

Figure 1.4: Spike-and-recovery performance of ELISA kits for ICAM-2, AXL, and PECAM-1 using spiked serum samples (a known amount of analyte added to the sample matrix) and a control spike (a known amount of analyte added to the standard diluent).

For the assays requiring sample dilution, AXL (1:120) and PECAM-1 (1:10), two reagent diluents were tested: PBS with 1% BSA (black bars) and PBS without carrier protein (grey bars). The shaded area represents the optimal recovery range of 80–120%.

Protein expression

For ICAM-2, seven samples fell below the limit of detection (n=1 Control, n=6 Affected), and one was identified as an outlier (n=1 Control), and were subsequently removed from analysis. The diseased group showed significantly higher concentrations of ICAM-2 (n=6, mean ± SD = 2.62 ± 1.99 ng/mL) than healthy controls (n=12, mean ± SD = 0.58 ± 0.55 ng/mL) (Welch's t test p = 0.003). AXL concentrations were not significantly different between diseased chimpanzees (n=18, mean ± SD = 48.79 ± 20.99 ng/mL) and healthy controls (n=8, mean ± SD = 48.75 ± 32.47 ng/mL) (Welch's t test p = 0.499). No samples were excluded based on limit of detection or outlier identification for AXL. With PECAM-1, three samples were identified as outliers (n=1 Control, n=2 Affected) and subsequently removed from analysis. PECAM-1 did not differ significantly between diseased chimpanzees (n=16, mean ± SD = 2.93 ± 1.37 ng/mL) and healthy controls (n=7, mean ± SD = 3.33 ± 1.18 ng/mL) (Mann-Whitney test p = 0.188).

When considering only the ELISA data from the initial subset of 10 chimpanzees (the same individuals from Study A) in isolation, no statistically significant differences were found for any of the three proteins, though ICAM-2 approached significance: ICAM-2 (Mann-Whitney test p = 0.057), AXL (Welch's t test p = 0.341) and PECAM-1 (Welch's t test p = 0.387). Figure 1.6 shows the protein expression as measured by ELISA in the initial subset of chimpanzees (n=10) as well as the larger group used in Study B.

Diagnostic value

For ICAM-2, the only protein showing a significant difference between diseased and healthy chimpanzees, the highest Youden's Index (J = 0.667) was observed at a cut-off value of >1.536 ng/mL. At this threshold, ICAM-2 demonstrated a diagnostic sensitivity of 66.67% (correctly identifying eight out of 12 diseased individuals) and a specificity of 100% (correctly excluding all healthy controls), as shown in Table 1.4. At this cut-off value of >1.536 ng/mL, the PPV was 100% and the NPV was 60%.

Post-hoc sample size calculation

A post-hoc sample size calculation for ICAM-2, as measured with ELISA, indicated that 38 samples (n=13 Control, n=25 Affected) would be required to achieve 95% statistical power with the current effect size of 1.16 (Hedges' g).

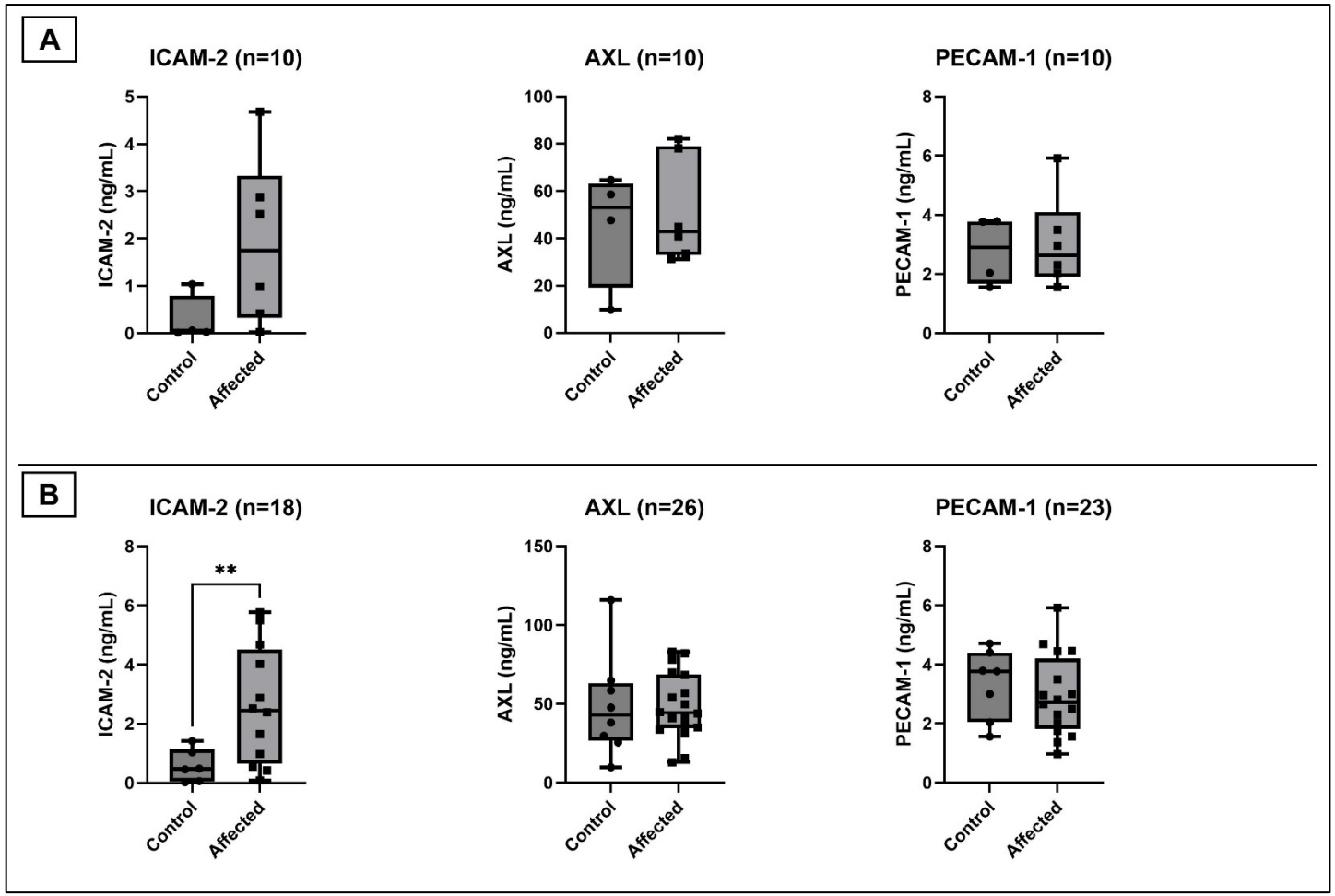

Figure 1.5: [A]: Expression (ng/mL) of ICAM-2, AXL and PECAM-1 as tested by ELISA in the subset of 10 chimpanzees from Study A. [B]: Expression (ng/mL) of ICAM-2, AXL and PECAM-1 as tested by ELISA in all 26 chimpanzees (excluding outliers where applicable) from Study B.
Pairwise comparisons are displayed above each box-and-whisker plot where statistical significance is reached (parametric one-tailed Welch's t test, or non-parametric one-tailed Mann-Whitney test: ** = $p<0.01$).

Table 1.4: Diagnostic performance metrics for ICAM-2 based on ELISA data.
Sensitivity, specificity, and Youden's Index (*J*) were calculated for various cut-off values of ICAM-2 concentrations (ng/mL). Sensitivity represents the percentage of diseased individuals correctly identified, while specificity represents the percentage of healthy individuals correctly identified. Youden's Index identifies the cut-off value that provides the optimal balance between sensitivity and specificity. The optimal cut-off, >1.536 ng/mL, maximises Youden's Index (*J*=0.6667).

Cut-off (ng/mL)	Sensitivity (%)	Specificity (%)	Youden's Index (*J*)
> 0.04117	100	16.67	0.1667
> 0.07595	100	33.33	0.3333
> 0.2557	91.67	33.33	0.25
> 0.4382	83.33	33.33	0.1666
> 0.4709	83.33	50	0.3333
> 0.5163	83.33	66.67	0.5
> 0.7657	75	66.67	0.4167
> 1.011	66.67	66.67	0.3334
> 1.229	66.67	83.33	0.5
> 1.536	66.67	100	0.6667
> 2.021	58.33	100	0.5833
> 2.453	50	100	0.5
> 2.698	41.67	100	0.4167
> 3.450	33.33	100	0.3333
> 4.352	25	100	0.25
> 5.094	16.67	100	0.1667
> 5.637	8.333	100	0.08333

1.4 Discussion

Olink findings

Olink's PEA was chosen as a biomarker discovery tool due to its high sensitivity, specificity, and multiplexing capabilities, along with its robustness, reproducibility, and ease of use (Assarsson et al., 2014b; Petrera et al., 2021). In the initial Olink discovery, three protein biomarkers were identified as being significantly increased in serum in diseased chimpanzees with IMF (as confirmed histologically) compared with their healthy counterparts. Though the Olink screening used a panel of 92 proteins that are generally involved in human CVD, the three resultant candidates ICAM-2, AXL and PECAM-1 have been indicated more specifically in inflammatory and fibrotic diseases in the wider literature. This observation aligns with the notion that IMF is predominantly an inflammatory and fibrotic heart disease rather than the typical forms of CVD observed in most other animal species, such as atherosclerosis (Strong et al., 2020, 2018b).

ICAM-2 is present on the surface of platelets and is an essential ligand in antigen-specific immune responses including the migration of immune cells during inflammation and thrombosis (Diacovo et al., 1994; Lyck and Enzmann, 2015; Amsellem et al., 2014). The diagnostic utility of ICAM-2 as a biomarker has been explored in various diseases, having been shown to be upregulated during inflammatory lung diseases such as cystic fibrosis and idiopathic pulmonary fibrosis (Chong et al., 2021; Tsoutsou et al., 2004). It has also been implicated in vascular diseases and endothelial dysfunction during chronic heart failure (Bouwens et al., 2020; Głogowska-Ligus et al., 2013).

AXL is a transmembrane tyrosine kinase receptor expressed ubiquitously in mammalian tissues with importance in cell adhesion, inflammatory responses, and coagulation (Linger et al., 2008; Hafizi and Dahlbäck, 2006). Overexpression of AXL has been indicated in various morbidities, including coagulopathy, autoimmune disease, and cancers (Pidkovka and Belkhiri, 2023; Linger et al., 2008). Notably, AXL is also directly involved in fibrotic diseases of the kidney, intestines, liver and lungs (Nilsson et al., 2021; Steiner et al., 2021; Staufer et al., 2017; Yang et al., 2021), and

can play a maladaptive role in cardiac remodelling and inflammation during CVD (DeBerge et al., 2021; Batlle et al., 2014; Caldentey et al., 2019; Batlle et al., 2019).

PECAM-1 is an endothelial adhesion molecule within the immunoglobulin superfamily that, similarly to ICAM-2, regulates thrombosis, cardiomyocyte contractility, transendothelial immune cell migration and endothelial cell function (McCormick et al., 2015; Newman et al., 1990). PECAM-1 expression is linked with myocardial damage following ischaemic events, and its genetic polymorphisms are linked directly with diseases of the coronary vasculature and acute cardiac events in humans (Ronghai et al., 2019; Reschner et al., 2009; Serebruany et al., 1999). Moreover, PECAM-1 has been directly indicated in the disease progression of liver fibrosis (Raskopf et al., 2014).

The widely used cardiac biomarker NT-proBNP was not significantly altered in this group of diseased chimpanzees. NT-proBNP is primarily a valuable marker for cardiac wall stress and subsequent heart failure (Zile et al., 2016). Its use as a marker of myocardial fibrosis in humans and other species has produced mixed results (Zhang et al., 2016; Chevalier et al., 2022), and its lack of upregulation in the diseased group in this study indicates that it may not be an appropriate biomarker of IMF in chimpanzees. Another widely used marker, cardiac troponin (cTnI or cTnT), was not part of Olink's protein assay panel and was therefore not tested. Cardiac troponins are markers of myocardial damage, normally in relation to myocardial infarction (Reichlin et al., 2009), which is not a notable clinical presentation in the great apes (Varki et al., 2009).

ELISA findings

The use of ELISA set out to validate the findings of the Olink discovery and evaluate the potential diagnostic capability of commercially available assay kits. A larger sample size was available for the ELISA portion of the study, which took place four years after the initial Olink discovery, meaning that more serum samples were available from chimpanzees whose hearts had been examined histologically. ICAM-2 was the only analyte to reach statistical significance between the groups when tested with ELISA.

Diagnostic value of ICAM-2

Further evaluation of ICAM-2, assessed via ELISA, showed a sensitivity of 66.67% and a specificity of 100% at the optimal cut-off point determined by ROC curve

analysis. The high specificity indicates that ICAM-2 is highly effective at correctly identifying healthy individuals, minimising the likelihood of false-positive results (Barrett and Fardy, 2021; Fabricant, 2024). The positive predictive value (PPV) of 100% confirms that all individuals with ICAM-2 levels exceeding the cut-off were accurately identified as diseased. However, the negative predictive value (NPV) of 60% reflects a limitation, as 40% of individuals with ICAM-2 levels below the threshold may still have the disease. This underlines a potential shortcoming in using ICAM-2 levels alone to exclude disease (Barrett and Fardy, 2021; Fabricant, 2024).

Comparison between methods: PEA and ELISA

The lack of absolute agreement between the findings of the Olink panel and the ELISAs in this case is not particularly unusual, as previous studies have found similar discordance (Schmidt et al., 2022; Vasbinder et al., 2023). This could be for a number of reasons, such as potential post-translational modifications being detected in one assay and not the other, the PEA having a higher degree of specificity than the ELISA kits, or differences in assay conditions such as sample volume (1 µL for Olink vs. 100 µL for ELISA) and dilution factors used (neat sample for Olink vs. diluted for ELISA) (Olink, 2021b). It is also possible that pre-analytical factors may have affected the results. The ELISA testing took place several years after the Olink screening, thus sample storage conditions may have affected the quality of the samples. Separate aliquots of the serum samples were used for the Olink and ELISA testing, which may have affected protein concentrations in each assay if the samples were not fully homogenised prior to aliquot separation (Olink, 2021b). There are several examples in the literature of strong positive correlations between PEA and ELISA, though often this does not apply to all proteins tested (Skau et al., 2023; Zhao et al., 2022).

Limitations and future directions

Although ICAM-2, AXL, and PECAM-1 showed altered serum expression in association with IMF in these cases, it is important to acknowledge that each is also modulated by a variety of non-cardiac disease states and inflammatory conditions. PECAM-1, for instance, is broadly involved in leukocyte transmigration and has been implicated in diverse inflammatory disorders including multiple sclerosis, rheumatoid arthritis, sepsis and even anaphylaxis (Woodfin et al. 2007). Similarly, AXL shows dysregulated expression in diseases such as systemic lupus erythematosus and gastrointestinal cancers (Hafizi and Dahlbäck, 2006; Pidkovka and Belkhiri, 2023;

Shao and Cohen, 2014). ICAM-2 can be upregulated by chronic inflammatory stimuli (e.g., in neutrophil-dominated lung inflammation) (Lyck and Enzmann, 2015). Because these proteins respond to general inflammatory or immune activation in several conditions, changes in their levels may not be unique to myocardial fibrosis, which limits their specificity as potential IMF biomarkers.

The performance of the ICAM-2 ELISA kit with chimpanzee serum was less optimal than the others, with an inter-assay variation of 17%, which is higher than the commonly accepted threshold of 15% (Jaedicke et al., 2012; Minic and Zivkovic, 2020). Additionally, the analytical sensitivity (limit of detection) overlapped with the standard curve range as reported by the manufacturer, indicating that the assay may not be sufficiently sensitive for some samples, particularly those with low analyte concentrations. This led to the exclusion of several samples from statistical analysis, reducing the effective sample size and limiting the statistical power of the study. Furthermore, excluding low-concentration samples may bias the results by disproportionately affecting the representation of certain groups or disease stages (Crowther, 2009; Armbruster and Pry, 2008). However, the intra-assay variation was acceptable at 7%, and the 91% analyte recovery was well within the acceptable boundaries of 80–120% (Andreasson et al., 2015). Overall, the mixed results of the ICAM-2 ELISA assay performance do not negate the importance of the findings here, and further exploration, perhaps using other commercially available kits, is warranted.

The small sample size in this study can be considered a limitation. A post-hoc sample size calculation based on the ICAM-2 ELISA data (observed effect size, Hedges' g = 1.16) revealed that the study groups (currently n=6 Controls; n=12 Affected for ICAM-2) would need an additional 20 samples (n=13 Controls; n=25 Affected) in order to achieve full statistical power (Faul et al., 2009). Additionally, while Olink technology is a technically robust method, it has been suggested elsewhere that moderate effect size proteins would require 400 samples per group (disease vs. control) in order to obtain full confidence in any statistical difference for an assay panel containing 100 test proteins (Mattingly et al., 2021). Given their potential relevance to IMF based on the literature, future work exploring all three candidate markers (ICAM-2, AXL and PECAM-1) in a larger number of chimpanzees could be beneficial.

There was limited control over how participating zoos collected, stored and transported samples, which may have affected pre-analytical conditions. While the median time between serum sampling and death in this study was 0 months, the range extended up to 215 months (17 years) in one case, reducing the relevance of some samples to the post-mortem phenotype. Conversely, many samples were collected at 0 months prior to death, either during post-mortem examination or at the time of euthanasia by the zoos of origin. While these may provide an accurate reflection of the end-stage disease phenotype, there is uncertainty regarding whether observed biomarkers represent terminal changes or were detectable during earlier disease stages. Interpreting biomarker expression across such a wide temporal range is not ideal, and reinforces the need for longitudinal sampling in future studies to better understand disease progression. Future studies should prioritise using samples collected within a narrower time window prior to death (e.g., 12 months or less) to ensure closer alignment with the post-mortem phenotype. Additionally, analyses should be conducted as soon as possible after sampling, with improved standardisation of storage and transport conditions to maintain sample quality (Revuelta-López et al., 2021). It is, however, important to consider the inherent challenges in obtaining samples from endangered wildlife species, including those housed in zoos and sanctuaries. In our case, all samples need to be collected opportunistically during routine veterinary procedures and the international network we have used to obtain paired samples (whole heart for post-mortem phenotyping in addition to an ante-mortem serum sample) has required extensive efforts over the course of a decade.

Another limitation of this study is that the Olink panel and ELISA kits used were designed and validated for human samples and antibodies only. Though chimpanzees have long been used as animal models in biomedical research due to their strong genetic similarity to humans, the two species can vary considerably in their natural genetic and proteomic expressions in serum and tissue (Pizzollo et al., 2018; Pavlovic et al., 2018; Howell et al., 2003; Schweigert et al., 2007). However, other studies have documented that assays developed for use with human serum also work as intended for non-human primate serum (Höglind et al., 2017; Stubenrauch et al., 2009; Cama et al., 2018; Niemuth et al., 2020), therefore it can be assumed that the same assay homology applies to the current study. Despite this, future work on the application and

performance of human-based protein assays for use with chimpanzee serum in a larger study population would be useful, particularly in the case of ICAM-2.

Additionally, the pathological classifications of chimpanzees in our study presents its own challenges. Individuals affected by IMF may have co-morbidities such as concurrent infections that may lead to systemic inflammation, potentially confounding the specificity of circulating biomarkers of IMF. Detailed post-mortem examinations revealed no macroscopic or microscopic signs of systemic infections, but the possibility of subclinical infections cannot be fully excluded. For instance, chronic renal disease leading to systemic hypertension and chronic cardiac remodelling has been documented in zoo-housed great apes (Ely et al., 2010; Chilton et al., 2016; Lowenstine et al., 2016), thus the potential overlap between IMF and other chronic cardiovascular diseases remains a diagnostic challenge (Strong et al., 2018b).

Wider implications of this study

Despite the inherent challenges described, this study is an important initial investigation into potential circulating biomarkers that are specific and sensitive to IMF in chimpanzees. Olink PEA is widely considered to be a robust and reliable method for modern biomarker discovery in humans (Mattingly et al., 2021) and its use in this study exemplifies the potential for its application in veterinary medicine. To date, Olink is yet to be widely employed for use with veterinary species, with the only dedicated non-human assay panel currently being for mouse models, and only very few published examples of the standard human panels being used in horses, pigs, and macaques (Verma et al., 2021; Bue et al., 2020; Donnelly et al., 2023). A key advantage of the Olink PEA is its requirement for a small sample volume (and higher output per sample volume), which is crucial for preserving valuable samples, especially in endangered or hard-to-sample populations such as chimpanzees. With further scope and development, Olink and other existing multiplex immunoassays could be an ideal choice for non-human studies where sample availability is a significant constraint, as it allows for comprehensive proteomic analyses without depleting the sample supply (Assarsson et al., 2014a). It is hoped that, in time, these currently expensive techniques may become more accessible and affordable.

In contrast to the advanced capabilities of Olink, traditional methods such as ELISA and point-of-care testing have been more commonly employed in veterinary patients

due to their accessibility, transportability and ease of use, providing rapid diagnostic information (Bora et al., 2022). However, their success in a veterinary context has been somewhat varied, often due to the challenges of validating these assays against commercial diagnostic laboratories and across different species (Anderson et al., 2022; Stratton et al., 2022; Feltrer et al., 2016). Point-of-care testing is something to strive for with the detection of biomarkers of IMF in chimpanzees, but more work is needed in this area to achieve reliable real-time monitoring, including species-specific validation of these assays. For now, diagnostics using ELISA has shown promise.

The uniqueness of this study lies not only in its use of advanced proteomic technologies for zoo-housed great apes, but also in its confirmation of the cardiovascular and systemic health status of the study animals, as assessed histologically. This is the most reliable way to determine if circulating biomarkers can accurately predict cardiovascular morbidity (Institute of Medicine, 2010) and is a significant strength of this research, further strengthening the evaluation of ICAM-2's diagnostic value.

With further validation, ICAM-2 could be integrated into a diagnostic panel alongside other blood-based biomarkers and non-invasive methods, such as cardiac ultrasound, to improve diagnostic accuracy for IMF in zoo-housed chimpanzees (Kosmala et al., 2019; Liu et al., 2024). Such an approach could eventually enable earlier detection and targeted interventions, which, for an idiopathic disease that often results in sudden death, would be highly valuable. For instance, in a zoo setting, a simple blood test for ICAM-2, combined with other inflammatory or fibrotic markers, could be used to triage individuals for more detailed cardiac assessments. Moreover, the high specificity of ICAM-2 suggests it could play a role in confirmatory testing, particularly when clinical resources are limited, reducing the risk of unnecessary interventions in healthy animals. Future studies could also explore longitudinal changes in ICAM-2 levels to assess its potential as a marker of disease progression or treatment efficacy (Kolamunnage-Dona and Williamson, 2018).

The coupling of highly sensitive, targeted approaches like Olink PEA and ELISA with untargeted methods such as mass spectrometry could enhance the identification of novel biomarkers by leveraging the strengths of both methods: the sensitivity and specificity of targeted assays with the broader scope of untargeted analyses (Petrera

et al., 2021). In the context of this thesis, a methodological pairing could be particularly advantageous in learning more about the pathophysiology of IMF, and will be explored in more detail in the coming chapters.

In conclusion, this work represents a promising first step towards the development of novel diagnostic tools for IMF in chimpanzees. The targeted approaches used here offer distinct advantages in terms of specificity and the potential for future application in point-of-care assays. The insights gained from this study pave the way for future research aimed at detecting early-stage IMF, eventually facilitating real-time monitoring of great ape health in zoos, and ultimately contributing to the health and welfare of great ape populations in human care.

2. THE CARDIAC TISSUE PROTEOME ASSOCIATED WITH IMF IN CHIMPANZEES

2.1 Introduction

Uncovering the molecular mechanisms underlying IMF is essential for developing effective interventions aimed at improving the health of zoo-housed great apes. In Chapter 1, circulating biomarkers of IMF were explored in serum samples from chimpanzees, providing valuable information about the systemic changes associated with the disease. However, cardiac tissue is where the pathology is localised, and studying the proteome specifically in the affected tissue offers a more detailed view of the molecular alterations that drive the disease (De La Cuesta et al., 2009).

Proteomics is the large-scale study of proteins, which are biomolecules responsible for most biological functions in a cell. It involves the identification, quantification, and analysis of the entire set of proteins (the proteome) present in a biological system, such as a cell, tissue or organism, at a given time under specific conditions (Domon and Aebersold, 2006). Proteomics aims to understand protein structure, function, interactions and changes in response to stimuli, diseases, or environmental conditions (Pandey and Mann, 2000). Since proteins are the functional molecules that mediate both normal physiological processes and disease pathology, their abundance and modifications in the heart tissue may offer insights into the progression and mechanisms of IMF (De La Cuesta et al., 2009).

Mass spectrometry (MS) is an analytical technique used to identify and quantify molecules, including proteins, based on their mass-to-charge ratio (m/z). MS is one of the most powerful and versatile tools for identifying and quantifying proteins in complex biological samples such as cardiac tissue (Cox and Mann, 2011). With optimisation of the sample preparation stage, MS is able to effectively identify and quantify proteins in fixed tissues (Ostasiewicz et al., 2010; Buczak et al., 2020; Azimzadeh et al., 2021), which is of particular importance here, as formalin fixed tissues are by far the most abundant sample type available from great ape hearts.

In exploratory proteomics, the goal is to discover as many proteins as possible from a sample, without preconceived hypotheses or specific targets in mind (Dunn et al., 2013). This untargeted approach allows for the unbiased identification of a large number of detectable proteins in a tissue sample, providing a comprehensive overview of the molecular environment associated with both the healthy and diseased states (Dunn et al., 2013; Fujii et al., 2017). This is relevant here, as the pathways and proteins involved specifically in IMF in great apes remain largely uncharacterised.

While the tissue proteome of the macaque heart (Rojsajjakul et al., 2023; Song et al., 2014) and chimpanzee brain (Bauernfeind et al., 2015) have been explored, there are no published studies about cardiac tissue proteomics in great apes. By investigating the cardiac tissue proteome in chimpanzees, this study aimed to:

1. Reveal molecular signatures that can potentially guide future diagnostic or therapeutic management, and improve our overall understanding, of IMF in zoo-housed great apes.

2.2 Materials and methods

Study subjects

Chimpanzees (*Pan troglodytes*) with a known cardiac phenotype were included in this study, which were the same 10 individuals from whom serum samples were used for biomarker discovery with Olink (Study A, as described in Chapter 1). Their formalin-fixed whole hearts were sent to Twycross Zoo (Burton Road, Atherstone, Warwickshire, CV9 3PX) at ambient temperature via the 'Ape Heart Project' framework, and examined at the University of Nottingham (Veterinary pathology service, Sutton Bonington Campus, College Road, Sutton Bonington, Leicestershire, LE12 5RA). Tissue sections were collected during standardised cardiac post-mortem examinations carried out by a board-certified veterinary pathologist (Strong et al., 2018c) and subsequently embedded in paraffin wax blocks. A summary of information regarding all study subjects and their disease classifications can be found in Table 2.1.

Table 2.1: Study subjects: chimpanzees with a known cardiac phenotype (n=10), as confirmed histologically, categorised as Affected (diseased) or Control (healthy). Their unique sample ID for mass spectrometry (MS), age at death (years), and sex (male or female) is also included.

Study ID	MS Sample ID	Age at death (years)	Sex	Disease phenotype
C2	127N	37	Male	Affected
C3	127C	33	Male	Affected
C4	128N	33	Male	Affected
C15	129N	46	Female	Affected
C18	129C	18	Male	Affected
C30	131N	21	Male	Affected
C9	128C	32	Female	Control
C31	131C	62	Female	Control
C20	130N	21	Male	Control
C26	130C	28	Male	Control

Mass spectrometry

Prior to the commencement of this PhD, formalin fixed myocardial tissue samples from chimpanzees affected by IMF (n=6) and healthy controls (n=4) were used for protein extraction. Formalin-fixed myocardial tissues were processed for proteomic analysis using LC-MS/MS (Shrader, 2013; El-Aneed et al., 2009) at the Advanced Mass Spectrometry Facility (AMSF), University of Birmingham (School of Biosciences, Edgbaston, B15 2TT). This method was based on a study by (Pasha et al., 2018), and modified for the purpose of this study. Proteins were extracted and prepared following a protocol adapted from (Wiśniewski et al., 2011). Approximately 500 mg of tissue per sample was minced and subjected to lysis using a buffer containing 0.1 M Tris (pH 8), 4% SDS, and 0.1 M DTT, with boiling at 99°C for 3.5 hours. The samples were further homogenised using a bead beater, and additional lysis buffer was used to maximise protein solubilisation. After centrifugation, the clarified supernatants yielded approximately 4–5 mL of protein solution per sample, with a concentration of ~4 mg/mL.

Protein digestion was performed using the Filter-Aided Sample Preparation (FASP) method (Wiśniewski et al., 2009). Pilot mass spectrometry (MS) runs were conducted to assess post-translational modifications (PTMs) introduced by formalin fixation, identifying methylation and formylation as relevant variable modifications for database searches. A broad chimpanzee protein database was selected to maximise protein identification. Digested peptides (100 µg per sample) were labelled with Tandem Mass Tags (TMT) 10plex (Thermo Fisher Scientific) following the manufacturer's instructions. Labelled peptides were combined and fractionated using basic reverse-phase chromatography on a XBridge Shield RPV18 column (Waters) into 10 fractions, desalted with SEPak, and analysed on an Orbitrap Eclipse mass spectrometer (Thermo Fisher Scientific). A data-dependent acquisition strategy was employed, with MS3 quantitation for enhanced accuracy and MS2 for peptide identification (Montero-Calle et al., 2023). Protein identification and quantification were performed using Proteome Discoverer 2.0 software (Thermo Fisher). This approach enabled the simultaneous quantification of proteins across all 10 chimpanzee tissue samples with high accuracy and reliability (Burton and Backus, 2024).

Data analysis

This chapter of the PhD was influenced by the COVID-19 pandemic, and the bioinformatics methods used here were learned and carried out by the author of this thesis whilst isolating at home between 2020–2021.

Data received from AMSF were received in a Microsoft Excel format having been exported from Proteome Discoverer computer software v2.1 (Thermo Fisher), and contained protein-level and peptide-level data with 24 other columns containing information about the proteins identified (Table 2.2). The analysis focused on the protein-level data. To ensure that there was at least one unique peptide used in the identification of proteins, data were filtered by the number of unique peptides and any with a value of 0 were excluded. Proteins for which there was no quantification were also removed from the dataset.

Protein abundance data were then transferred to GraphPad Prism (v10.3.0), and multiple unpaired t-tests were performed in order to produce a volcano plot of the data. When selecting proteins of interest from a volcano plot, the conventional approach typically involves identifying proteins that meet both statistical significance and a meaningful effect size threshold, i.e., a -log10(p value) >1.3 (equivalent to $p<0.05$) as well as a log2(fold change) >1 (Oveland et al., 2015). This dual-criteria method helps minimise false positives by focusing on proteins that are both statistically robust and biologically relevant. In this study, however, a more lenient approach was adopted due to the small sample size (n=10) and the exploratory nature of applying proteomics to chimpanzee myocardial tissue for the first time. Therefore, proteins meeting either a -log10(p value) >1.3 (equivalent to $p<0.05$) or a calculated log2(fold change) >1 (rather than meeting both criteria) were considered to be of interest.

The STRING (v12.0) website and database were then used to visualise the network of any associations between the proteins of interest using a high-confidence minimum interaction score. STRING integrates various types of interaction evidence, including experimental data, predicted interactions, and information from databases like the Kyoto Encyclopedia of Genes and Genomes (KEGG) and Reactome (Szklarczyk et al., 2023). Isoforms of the same protein, or proteins that were identified using reference genomes of different chimpanzee subspecies, were grouped together for the protein network analysis. STRING's built-in analysis tools were used to explore

biological processes, pathways, and molecular functions that were overrepresented in the interaction network compared with the reference genome. The UniProt database was used to gather any further relevant information about each protein of interest (The UniProt Consortium, 2021).

Table 2.2: Data column headings and descriptions as found in the original Excel spreadsheet of protein abundance data from mass spectrometry readout.

Column headings	Description
Protein FDR Confidence: Combined	Indicates the probability (high, medium, or low) that the protein was correctly identified.
Master	Identifies if this is the master protein (the one with the best score) that is being reported.
Accession	A unique identifier from the UniProt database
Description	A user-friendly protein name, including details such as OS=Organism Name, OX=Organism Identifier, GN=Gene Name, PE=Protein Existence, SV=Sequence Version.
Exp. q-value: Combined	The minimum false discovery rate (FDR) at which the identification of the protein is considered valid.
Contaminant	True/false – evaluated against a list of typical contaminants.
Sum PEP Score	The posterior error probability (PEP) reflects the likelihood that the observed peptide spectrum match (PSM) is incorrect.
Coverage [%]	The percentage of the protein sequence that was matched by identified peptides.
# Peptides	The total number of distinct peptide sequences identified within the protein group.
# PSMs	The total number of PSMs for the protein. The PSM count can exceed the number of identified peptides, especially for high-scoring proteins where peptides may be identified multiple times.
# Unique Peptides	The number of peptide sequences unique to a specific protein group. These peptides are shared within a protein group and are not found in proteins from other groups.

# Protein Groups	A group of proteins that share the same identified peptides. All proteins within a group will have the same or a lower number of identified peptides.
# AAs	The total length of the protein, measured in amino acids (AA).
MW [kDa]	The molecular weight of the protein, in kilodaltons (kDa).
calc. pI	The calculated isoelectric point (pI) of the protein.
Score Sequest HT	The protein's score as determined by the search engine used.
# Peptides (by Search Engine):	Displays the number of peptides identified by each search engine used, when multiple search engines are applied.
# Razor Peptides	A peptide assigned to the protein group with the largest number of total identified peptides. A unique razor peptide matches only one protein group, while a non-unique one is associated with the group having the most peptide IDs.
Abundance Ratio	The ratio of the intensity of the tag of interest to the control tag (e.g., 127/126).
Abundance Ratio Adj. P-Value	The p-value associated with the protein’s abundance ratio for the protein.
Abundances (Grouped)	The total calculated abundance for the protein.
Abundances (Grouped) CV [%]	The coefficient of variation (CV) for protein abundances.
Found in Sample	Indicates whether the protein was not found, or the quantity that was detected.
Modifications	Lists any post-translational modifications (PTMs), which can also be identified through peptide-level data exploration.

2.3 Results

A total of 584 proteins were identified, of which 514 proteins were quantified with at least one unique peptide across all 10 chimpanzee samples. Figure 2.1 shows the differential expression of these 514 proteins in the diseased versus the control group, with those of statistical significance (-log10[p value] > 1.3, n=10 proteins) or biological relevance (log2[fold change] > 1, n=3 proteins) highlighted. The direction of change on the graph represents either a protein upregulation (red, positive fold change) or downregulation (blue, negative fold change) in the diseased group.

On closer inspection of the proteins of interest, multiple unpaired t-tests revealed that 10 proteins were significantly different in chimpanzees affected by IMF (n=6) compared with healthy controls (n=4): Fibrillin-1 (FBN1) p=0.018; Collagen alpha-3(VI) chain isoform 6 (COL6A3[6]) p=0.022; Collagen alpha-2(VI) chain (COL6A2) p=0.026; Tubulin beta-4B chain (TUBB4B) p=0.029; Myosin regulatory light chain 12A (MYL12A) p=0.035; Cytochrome c oxidase subunit 6C (COX6C) p=0.041; Cytochrome c oxidase subunit 2 (subspecies A: *Pan troglodytes verus*) (COX2[A]) p=0.041; Alpha-parvin (PARVA) p=0.042; Collagen alpha-3(VI) chain isoform 1 (COL6A3[1]) p=0.044; Calcium-transporting ATPase 2 (ATP2A2) p=0.044. Three additional proteins were selected due to their high fold change, despite not being statistically significant: Periostin (POSTN) p=0.104; Collagen alpha-1(III) chain (COL3A1) p=0.314; Cytochrome c oxidase subunit 2 (subspecies B: *Pan troglodytes ellioti*) (COX2[B]) p=0.350. A summary of the proteins of interest can be found in Table 2.3.

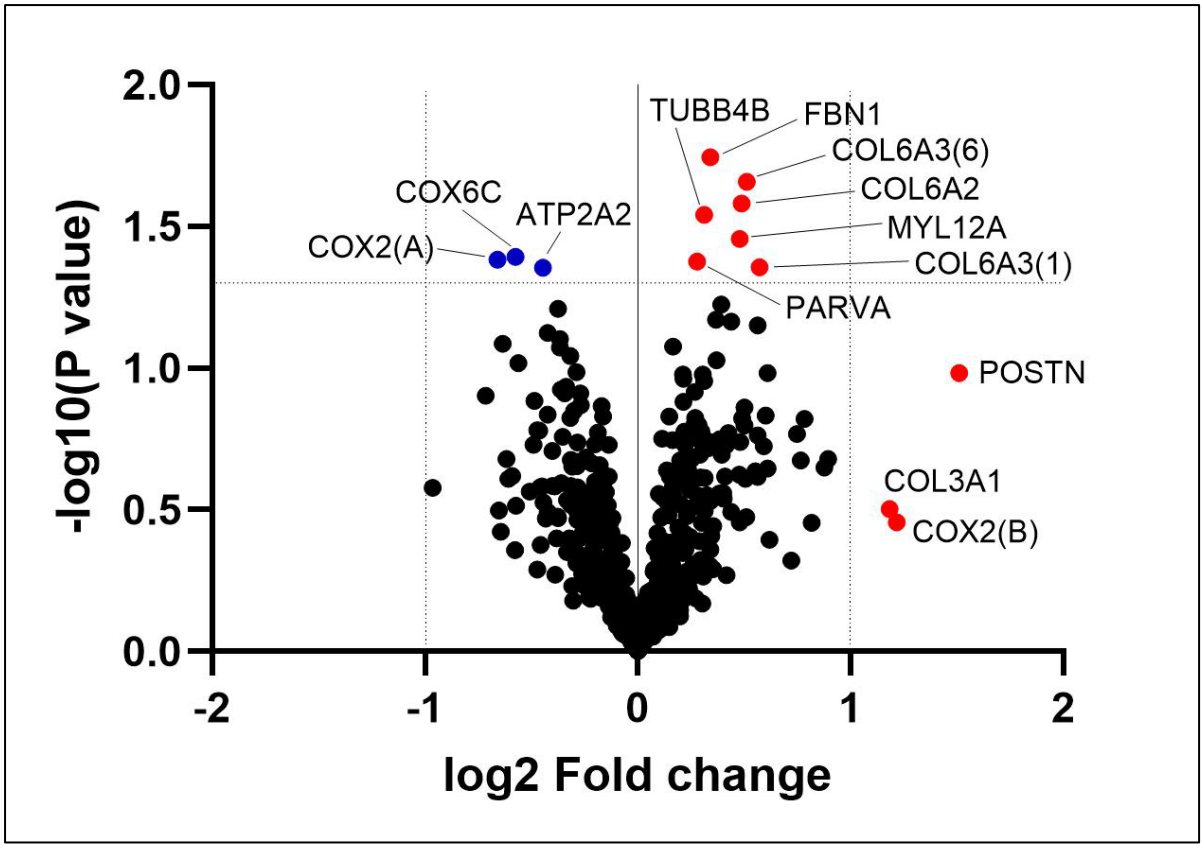

Figure 2.1: Volcano plot showing the -log10(p value) and log2(fold change) of relative abundance of 514 proteins discovered by mass spectrometry in chimpanzees affected by IMF (n=6) versus healthy controls (n=4).
Statistical significance (n=10 proteins) is reached above the horizontal dotted line (-log10[p value] > 1.3) and biological relevance (n=3 proteins) is reached at log2(fold change) > 1 or < -1. The direction of change is signified by the colour of the data points, where red = an upregulated protein in the diseased group, and blue = a downregulated protein in the diseased group.

Table 2.3: Proteins of interest (n=13) from proteomic exploration by mass spectrometry in chimpanzees (*Pan troglodytes*) affected by IMF (n=6) and healthy controls (n=4).
Statistically significant differences in relative abundance are represented by [*], indicating a -log10(p value) of >1.3. A log2(fold change) of >1 or <-1 is indicated by [#] and represents a biologically meaningful change in the affected group versus the control group. Corresponding gene names and reference genome species according to the UniProt database (The UniProt Consortium, 2021) are included.

Protein name	**Gene name**	**Reference species**	**-log10 p value**	**log2 Fold change**
Fibrillin-1	FBN1	*Pan troglodytes*	1.745 *	0.340
Collagen alpha-3(VI) chain isoform 6	COL6A3(6)	*Pan troglodytes*	1.657 *	0.512
Collagen alpha-2(VI) chain	COL6A2	*Pan troglodytes*	1.582 *	0.489
Tubulin beta-4B chain	TUBB4B	*Pan troglodytes*	1.542 *	0.312
Myosin regulatory light chain 12A	MYL12A	*Pan troglodytes*	1.455 *	0.479
Cytochrome c oxidase subunit 6C	COX6C	*Pan troglodytes*	1.392 *	-0.573
Cytochrome c oxidase subunit 2 (subspecies A)	COX2(A)	*Pan troglodytes verus*	1.383 *	-0.659
Alpha-parvin	PARVA	*Pan troglodytes*	1.375 *	0.278
Collagen alpha-3(VI) chain isoform 1	COL6A3(1)	*Pan troglodytes*	1.355 *	0.572
Calcium-transporting ATPase 2	ATP2A2	*Pan troglodytes*	1.355 *	-0.445
Periostin	POSTN	*Pan troglodytes*	0.982	1.509 #
Collagen alpha-1(III) chain	COL3A1	*Pan troglodytes*	0.502	1.183 #
Cytochrome c oxidase subunit 2 (subspecies B)	COX2(B)	*Pan troglodytes ellioti*	0.456	1.216 #

For the purpose of the STRING protein-protein interaction network, COL6A3(6) and COL6A3(1), and COX2(A) and COX2(B), were combined so that all proteins produced by a single protein-coding gene locus were represented by one node. The interaction network identified a central cluster comprising of five interconnected extracellular matrix (ECM) proteins: FBN1, COL3A1, COL6A2, COL6A3 and POSTN, as well as a peripheral cluster containing two proteins related to mitochondrial function: COX2 and COX6C. The remaining four proteins (PARVA, MYL12A, TUBB4B and ATP2A2) did not show any associations, though the physical proximity of the nodes on the network, such as that between PARVA and FBN1, may indicate a more closely related biological function (Figure 2.2). Functional enrichment analysis on STRING revealed more in-depth information regarding the biological functions associated with the proteins of interest, a summary of which can be found in Table 2.4.

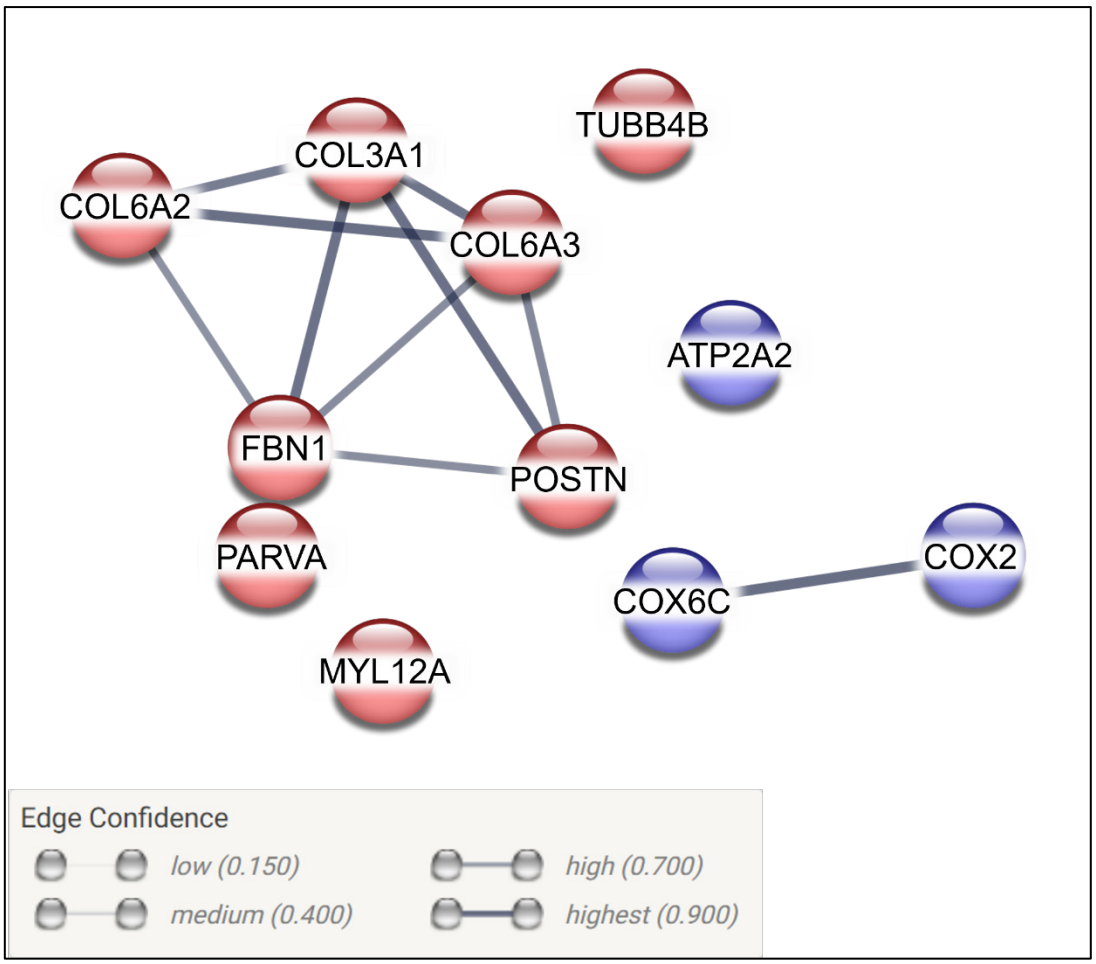

Figure 2.2: Interaction network for proteins differentially expressed in chimpanzees affected by IMF (n=6) compared with healthy controls (n=4), as discovered by mass spectrometry.

Isoforms are combined so that each node represents all proteins produced by a single protein-coding gene locus. Lines between nodes represent protein-protein associations. Only high-confidence associations (an Edge Confidence score of >0.7) are included. The node colour red = an upregulated protein in the diseased group, and blue = a downregulated protein in the diseased group. Network created via the STRING database v12.0 (Szklarczyk et al., 2023).

Table 2.4: Overrepresented biological functions implicated by networks involving proteins of interest (n=11) as discovered by mass spectrometry of myocardial tissue samples from chimpanzees affected by IMF (n=6) and healthy controls (n=4).
Effect strength is calculated by log10(observed/expected) and a false discovery rate (FDR) corrected p value was obtained via the Benjamini–Hochberg procedure. Both parameters were obtained using built-in analysis tools on STRING v12.0 (Szklarczyk et al., 2023). Database references: GO=Gene Ontology; CL=Cluster (STRING); KEGG=Kyoto Encyclopaedia of Genes and Genomes; R=Reactome.

Biological function	Involved proteins	Effect strength	Corrected p value	Database reference
Cell adhesion	FBN1, COL3A1, COL6A2, COL6A3, POSTN, MYL12A, PARVA, ATP2A2	1.17	0.000	GO:0007155
Extracellular matrix organisation	FBN1, COL3A1, COL6A2, COL6A3, POSTN	1.70	0.000	CL:19457
Focal adhesion	COL6A2, COL6A3, PARVA, MYL12A	1.57	0.001	KEGG:hsa04510
Axon guidance	TUBB4B, MYL12A, COL3A1, COL6A2, COL6A3	1.21	0.002	R:HSA-422475
Extracellular matrix structural constituent	FBN1, COL3A1, COL6A2, COL6A3	1.74	0.003	GO:0005201
Cardiac muscle contraction	COX2, COX6C, ATP2A2	1.79	0.003	KEGG:hsa04260
Mitochondrial electron transport	COX2, COX6C	2.47	0.015	CL:11193

2.4 Discussion

Identification of proteins

The proteomic analysis identified 514 proteins from the formalin fixed cardiac tissue of 10 chimpanzees, with 13 proteins emerging with statistically or biologically important differences in the diseased group. In comparison to other similar studies, the identification of 514 proteins from the samples suggests a sufficient depth of proteomic coverage, indicating that the samples were of reasonable quality and analysis by MS was effective despite the fixation process (Azimzadeh et al., 2012; Obi et al., 2023).

Among the 13 proteins of interest, five ECM proteins that are strongly associated with fibrotic disease were closely related in the protein-protein interaction network created by STRING: Fibrillin-1 (FBN1), Collagen alpha-1(III) chain (COL3A1), Collagen alpha-2(VI) chain (COL6A2), Collagen alpha-3(VI) chain (COL6A3), and Periostin (POSTN). FBN1 is a glycoprotein that plays an important role in the formation of microfibrils in the ECM, providing structural support to connective tissues such as the skin, lungs, and cardiovascular system (Li et al., 2023; Davis and Summers, 2012). FBN1 is essential for maintaining tissue elasticity and regulating growth factor signalling, especially transforming growth factor-beta (TGF-β), a key modulator of fibrosis (Olivieri et al., 2010). It has been shown that an increased FBN1 expression can drive fibrotic conditions by altering TGF-β availability, thereby promoting abnormal tissue remodelling and fibrosis (Velázquez-Enríquez et al., 2021; Li et al., 2021). Additionally, a mutation in the FBN1 gene causes Marfan syndrome, a connective tissue disorder responsible for aortic aneurism and dissection, and mitral valve prolapse in the heart (Lasne et al., 2020; Hibender et al., 2019). Collagens type III (COL3A1) and type VI (COL6A2 and COL6A3) are essential components of the ECM, providing structural support to help maintain the integrity and function of connective tissues. More specifically, type III collagen forms a supportive network alongside type I collagen, contributing to the elasticity and structural integrity of tissues (Karsdal, 2023; Liu et al., 1997). COL3A1 upregulation has been associated with liver fibrosis, pulmonary fibrosis, cardiac fibrosis and vascular remodelling (Nikolov and Popovski, 2022; Plavelil et al., 2020; Hoyer et al., 2021). Collagen type VI (COL6A2 and COL6A3) provides mechanical support to tissues and plays a role in cell adhesion, migration, and tissue repair (Karsdal, 2023). Overexpression of type VI collagen contributes to

increased tissue stiffness and abnormal ECM remodelling, and has been associated with pulmonary, adipose and cardiac fibrosis (Hoyer et al., 2021; Karsdal et al., 2020; Khan et al., 2009), as well as muscular dystrophy and certain cancers (Tonelotto et al., 2021; Li et al., 2022). POSTN is a non-structural ECM protein that plays a crucial role in the development and remodelling of connective tissues (Conway et al., 2014). POSTN activates TGF-β pathways and regulates tissue repair during ongoing remodelling, and is upregulated during tissue injury, inflammation, and fibrotic disease of the lungs, kidney and heart (Jang et al., 2022; Trundle et al., 2024; El-Adili et al., 2022; Ali et al., 2022; Bian et al., 2019). Overall, this network of five ECM proteins indicates a coordinated upregulation of fibrotic pathways in chimpanzees affected by IMF, and is consistent with known fibrotic mechanisms observed in other species. For instance, COL6A2, FBN1, POSTN, and COL3A1 have been implicated in cardiac fibrosis in zebrafish models (Simões et al., 2020), while COL3A1, POSTN, and other ECM components have been observed in obesity-related fibrosis models in mice (Chen et al., 2021b). Similar upregulation of these proteins has also been noted in a mouse model of dilated cardiomyopathy (Koshman et al., 2015). Future research could benefit from a more targeted proteomic approach, such as ECM-specific proteomic analysis by MS, to further clarify the molecular drivers of this apparent ECM-dominant disease (Barallobre-Barreiro et al., 2012, 2016a).

The decreased expression of Calcium-transporting ATPase 2 (ATP2A2), Cytochrome c oxidase subunit 2 (COX2) and Cytochrome c oxidase subunit 6C (COX6C) indicates alterations in myocyte contractility and mitochondrial function during IMF. ATP2A2 (also known as SERCA2) is an enzyme found in the sarcoplasmic reticulum of cardiomyocytes, which is responsible for the regulation of calcium ion (Ca^{2+}) transport during cardiac muscle contraction and relaxation (Kondrat'eva et al., 2014). Downregulation of ATPA2 is associated with impaired cardiac muscle relaxation during heart failure and cardiomyopathy (Frustaci et al., 2024; Rebrova et al., 2018; Lehnart et al., 2009; Kho et al., 2011). ATP2A2 has also been shown to interact specifically with cTnI in cardiomyocytes during Ca^{2+} regulation (Lu et al., 2022). COX2 is a core catalytic subunit of the Cytochrome c Oxidase (COX) complex and contributes directly to ATP production via oxidative phosphorylation (Srinivasan and Avadhani, 2012). COX6C is a regulatory subunit of the COX complex that modulates its stability and efficiency (Wright et al., 1984). Downregulations in both COX2 and

COX6C are known to increase ATP deficiency (and therefore decrease energy production), oxidative stress and apoptosis, particularly in high-energy-demand tissues such as the heart and brain (Srinivasan and Avadhani, 2012; Ramzan et al., 2020). This has been associated with cardiomyopathies, atherosclerosis, kidney disease and neurodegenerative disorders (Wang et al., 2022; Yin et al., 2018).

The presence of two distinct COX2 entries in the dataset likely reflects the broad protein database used for *Pan troglodytes*, which includes multiple subspecies and their respective peptide variations. One variant (COX2[A], *Pan troglodytes verus*) was significantly downregulated in the diseased group, while the other (COX2[B], *Pan troglodytes ellioti*) showed upregulation, albeit not statistically significant. This suggests that the peptide-level analysis grouped proteins from different subspecies based on their sequence similarities, but subtle differences in peptide matching strength or expression patterns may have led to these contrasting results. Further studies could explore the functional or technical implications of these variants (Modaber et al., 2019; Wibowo et al., 2021).

Three more proteins were upregulated in the diseased group but were independently positioned in the STRING network: Tubulin Beta-4B Chain (TUBB4B), Alpha-Parvin (PARVA) and Myosin Regulatory Light Chain 12A (MYL12A). TUBB4B is a component of cytoskeleton microtubules, which are important for maintaining cell shape, contractility, intracellular transport and mitosis (Murali et al., 2022). Excessive stabilisation or rigidity of microtubules in cardiomyocytes may lead to impaired contractility, worsening cardiac function and output during CVD (Chen et al., 2021a; Phyo et al., 2022). PARVA is involved in signalling pathways between the ECM and cytoskeleton, acting as a messenger between the two during the regulation of cell adhesion, migration and mechanical stability (Sepulveda and Wu, 2006). An increase in PARVA leads to more focal adhesions, and although this could reinforce cardiac tissue structure during stress, an excessive upregulation might contribute to fibrotic disease, since the balance between cell adhesion and migration is disrupted (Chen et al., 2005; Ain and Firdaus, 2022). MYL12A regulates phosphorylation of the myosin light chain, which affects cell motility, cytokinesis and muscle contraction (Toepfer et al., 2013; Markandran et al., 2022). An increase in MYL12A suggests enhanced contractile activity in the heart, and a compensatory upregulation is associated with

cardiac hypertrophy and heart failure (Dong et al., 2024; Szczesna-Cordary et al., 2004).

As expected from the study's inclusion criteria ('Affected' animals with histologically confirmed IMF), the proteomic profile revealed increased abundance of fibrosis-related proteins and reduced levels of cellular or metabolic proteins. This pattern reflects advanced myocardial remodelling, where ECM progressively replaces functional cardiac tissue (Strong et al., 2020; Lammey et al., 2008a). Similar remodelling is well documented in human myocardial fibrosis, where fibrillar collagens (e.g., COL1A1, COL3A1) and matricellular proteins such as POSTN are consistently upregulated (Sarohi et al. 2022; Zhao et al. 2014; Conway et al. 2014; Olivieri et al. 2010). These same components were prominent in IMF-affected chimpanzees, along with microfibrillar and basement membrane proteins like FBN1 and collagen VI (COL6A2, COL6A3), which are less frequently reported in human cardiac studies, but are recognised mediators of ECM stability and stiffness (Olivieri et al., 2010; Bouzeghrane et al., 2005). Mitochondrial dysfunction and impaired calcium handling were also apparent, with significant downregulation of COX2, COX6C, and ATP2A2, mirroring established changes in human heart failure and cardiomyopathy (Srinivasan and Avadhani, 2012; Rebrova et al., 2018; Frustaci et al., 2024). In contrast, this study identified cytoskeletal and contractile proteins such as tubulin-β4B (TUBB4B), α-parvin (PARVA), and myosin light chain 12A (MYL12A), which are not commonly reported in human cardiac fibrosis. These proteins are implicated in cytoskeletal integrity, contractile regulation, and focal adhesion signalling, and may reflect species-specific remodelling responses or underexplored contributors to fibrosis (Murali et al., 2022; Sepulveda and Wu, 2006; Toepfer et al., 2013).

Altogether, these findings suggest that IMF in chimpanzees involves a complex interplay of mitochondrial dysfunction, altered cellular architecture, and ECM remodelling. It may be that the heart attempts to compensate for impaired calcium regulation and energy production through structural adaptations and increased contractility (Cha et al., 2003; Tuomainen and Tavi, 2017; Chaanine, 2021; Johnson et al., 2024). These compensatory mechanisms likely then become maladaptive, driving a positive feedback loop of progressive fibrosis, electrical instability and cardiac dysfunction (Cha et al., 2003; Bround et al., 2013; Swynghedauw, 1999). This study adds to the growing body of evidence that Ca^{2+} regulation and mitochondrial health

are critical factors in the progression of myocardial fibrosis and heart failure, and could represent valuable therapeutic targets (Johnson et al., 2024; Van Mulders et al., 2024).

Limitations

The use of formalin-fixed cardiac tissue for this study was based on practicality, as this is the most abundant sample type available from chimpanzees with confirmed cardiac health status post-mortem. Fixed samples are widely used in veterinary and medical research because they are easily stored and highly stable over the long term, making them a valuable resource for retrospective studies (Balgley et al., 2009). However, formalin fixation causes protein cross-linking, which can hinder protein extraction and identification in mass spectrometry (Metz et al., 2004; Scicchitano et al., 2009; Klockenbusch et al., 2012). While advancements in proteomic methods have enabled the use of fixed tissue, it is likely that some low-abundance proteins were not detected (Maes et al., 2013; Sprung et al., 2009).

As in the previous chapter (Chapter 1), the small sample size of 10 chimpanzees reflects the exploratory nature of this study, which was conducted as a pilot study to evaluate whether formalin-fixed myocardial tissue could yield meaningful proteomic data in the context of understanding myocardial fibrosis in chimpanzees. Given that chimpanzees are endangered non-domestic animals, obtaining cardiac tissue from individuals with a confirmed cardiac health status is inherently challenging. The sample size also reflects practical and logistical constraints, as the mass spectrometry-based proteomic analysis used in this study is resource-intensive and costly. While the findings are limited in their generalisability due to the small sample size and potential pre-analytical variation such as differences in time between death and tissue fixation, as well as storage and transport conditions across zoos (Bass et al., 2014), this study represents an important first step. Future studies with larger cohorts and optimised sample handling protocols would be invaluable for improving statistical power and further validating the proteins identified here.

A challenge with untargeted proteomics is that it generates large, complex datasets, which can be difficult to analyse and interpret (Maes et al., 2013; Baldwin, 2004). Filtering through this data to identify the most relevant molecular changes requires careful interpretation, especially in a disease such as IMF that is not yet well-understood. This study used a more lenient statistical analysis approach than the

conventional criteria for volcano plots. While this approach increases the likelihood of identifying potentially relevant proteins in a small dataset, it also carries a higher risk of false positives. Nonetheless, this broader inclusion criterion provided a valuable starting point for exploratory studies and for guiding future, more targeted investigations, and does not detract from the biological relevance of the findings.

Conclusions

Overall, this study provides valuable insights into the pathogenesis of IMF in chimpanzees, revealing specific protein changes that have not been previously reported in this species. Key findings include alterations in pathways related to ATP production, calcium regulation, contractile function, and ECM organisation, which collectively highlight the multifaceted nature of IMF pathology. Aside from enhancing our understanding of IMF, these findings may inform the future development of therapeutic targets, utilising existing knowledge from human studies (Ali et al., 2022; Frangogiannis, 2019; Jang et al., 2022; Ravassa et al., 2023a; Li et al., 2022; Johnson et al., 2024).

This tissue-level proteomic analysis complements the circulating biomarkers identified in the previous chapter. While serum biomarkers provide a systemic view of disease processes, tissue proteomics offers direct insights into localised myocardial pathology. Together, these approaches provide a more comprehensive understanding of the molecular mechanisms underlying IMF, highlighting the potential of integrating systemic and localised markers to monitor disease progression and guide therapeutic strategies.

Looking ahead, the next chapter will build on these findings by employing a targeted approach using qPCR to quantify the expression of pre-selected genes that are potentially relevant to IMF. This progression from untargeted proteomics to targeted transcriptomics aims to refine our understanding of the molecular drivers of IMF and their potential as diagnostic or therapeutic targets.

3. TARGETED INVESTIGATION OF MYOCARDIAL GENE EXPRESSION IN CHIMPANZEES

3.1 Introduction

Following the untargeted proteomic analysis in Chapter 2, this chapter involves a more targeted investigation into the myocardial tissue expression of genes of interest, through the use of Reverse Transcription Quantitative Polymerase Chain Reaction (RT-qPCR). While the proteome reflects the functional and temporally stable protein landscape within the tissue, the transcriptome (gene expression) provides a dynamic snapshot of which genes were actively being transcribed into RNA at the time of sampling (Monk, 2003; Bathke et al., 2019). There is minimal overlap between the markers selected for this study and the findings presented in the previous chapter, due to the distinct focus of the two methodologies. The pre-selection of target genes here was also to account for any markers potentially underrepresented in the mass spectrometry due to their low relative abundance. The complementary use of such approaches allows for a more comprehensive understanding of pathways involved in IMF (Edfors et al., 2016; Zhang et al., 2011).

RT-qPCR is a widely used technique, during which purified total RNA is converted into complementary DNA (cDNA) through reverse transcription, before being amplified and quantified in real-time, using fluorescence to reflect the level of gene expression in the sample (Nolan et al., 2006). Due to the amplification step, RT-qPCR is particularly useful for studies involving limited-volume tissue samples, and performs with high sensitivity and specificity (Kubista et al., 2006). However, due to its analytical sensitivity, the pre-analytical quality of samples is of utmost importance, and any prior RNA degradation can have major downstream effects on results (Fleige and Pfaffl, 2006).

Purified RNA for use with RT-qPCR can originate from a range of sample types. FFPE tissue is commonly used in molecular studies, as it allows for retrospective studies on long-term archived samples, but it presents several challenges for RNA extraction (Lewis et al., 2001; Hedegaard et al., 2014). The formalin fixation process crosslinks nucleic acids with proteins, causing degradation, with subsequent RNA fragmentation

and reduced yields of intact RNA (von Ahlfen et al., 2007; Farragher et al., 2008). This can be a problem with fibrous tissues such as myocardium in particular, where the collagen and ECM content is proportionately high, making efficient extraction more difficult (Srinivasan et al., 2002). RNA Stabilisation Solution (such as RNAlater®) is an alternative tissue preservation method that generally yields higher quality RNA, as the solution stabilises the RNA immediately, preventing degradation (Florell et al., 2001). RNAlater has been successfully used for preserving myocardial tissue for molecular studies, offering superior RNA quality compared to FFPE, especially in fibrous tissues where RNA degradation can significantly affect gene expression results (Mutter et al., 2004).

Several studies have investigated tissue-level gene expression in great apes, particularly in relation to fibrosis and cardiovascular health. Comparative studies of gene expression in great ape fibroblasts and chimpanzee iPSC-derived cardiomyocytes have highlighted interspecies differences, particularly in regulatory pathways and extracellular matrix organisation, which are relevant to understanding species-specific cardiac phenotypes and potential pathologies (Pavlovic et al., 2018; Karaman et al., 2003). For example, Pavlovic et al. (2018) demonstrated the utility of chimpanzee iPSC-derived cardiomyocytes as models for studying gene regulatory differences that could predict human responses to cardiac disease. Karaman et al. (2003) identified interspecies differences in the expression of genes involved in extracellular matrix organisation, including collagen and structural protein regulation, as well as metabolic pathways related to cellular energy and stress responses, providing insights into molecular mechanisms that could influence myocardial fibrosis susceptibility. Additionally, genome-wide methylation studies (Pai et al., 2011) have shown epigenetic differences between humans and chimpanzees that could explain variability in tissue-specific gene expression and susceptibility to diseases. PCR has also been used to assess liver fibrosis in schistosomiasis-infected chimpanzees (Standley et al., 2013). Together, these studies underscore the importance of examining tissue gene expression in great apes to reveal molecular pathways relevant to myocardial fibrosis. However, there are no existing publications specifically highlighting the use of RT-qPCR to quantify CVD-related gene expression in chimpanzee myocardium post-mortem.

The primary objective of this study was to quantify the gene expression of markers of interest in myocardial tissue from chimpanzees affected by IMF versus healthy controls. The potential impact of tissue storage conditions on RNA quality was also explored. This transcriptome-level analysis complements the previously described proteomic findings, with the potential of refining our understanding of the molecular mechanisms and potential therapeutic targets of IMF in chimpanzees.

3.2 Materials and methods

Study subjects and samples

This study used myocardial tissue samples from zoo-housed chimpanzees (*Pan troglodytes*). In Stage I of the study, FFPE tissue was trialled. For this, 10 µm sections (wax scrolls) of FFPE left ventricular tissue blocks were obtained from the same 10 chimpanzees as described in the previous chapters (Chapters 1 and 2). This was done by the pathology technician at the University of Nottingham (Veterinary Pathology Service, Sutton Bonington Campus, College Road, Sutton Bonington, Leicestershire, LE12 5RA) before being transported at ambient temperature to the University of Birmingham School of Dentistry (5 Mill Pool Way, Edgbaston, B5 7EG).

After initial testing with the FFPE samples, it was decided that another sample type would be more suitable. Therefore, in Stage II of the study, tissue stored in RNA stabilisation solution (RNAlater) was used. Another group of chimpanzees, whose cardiac phenotype had been confirmed histologically, were included due to the availability of this sample type (see Table 3.1). While FFPE myocardial tissue was available from a total of 56 chimpanzees, there were only 13 chimpanzees with corresponding tissue samples in RNAlater, and this group of 13 did not contain all 10 of the individuals involved in the previous chapters. One individual also had a spleen tissue sample (preserved in RNAlater) available, which was included in the study as a positive Inter-Plate Control (IPC). The tissue sections were placed into RNAlater at the time of whole-body post-mortem examinations carried out by the respective zoos of origin (n=5 zoos) and stored frozen at -20°C to -80°C. They were then sent to Twycross Zoo (at varied temperatures, often pre-dating the commencement of this PhD) where they were stored at -80°C until analysis. The Affected group (n=9) included five females and four males, with a median age of 40 years (range: 21 to 46 years) and a median pre-analytical sample storage time of 74 months (range: 2 to 105 months). The Control group (n=4) included three females and one male, with a median age of 26.5 years (range: 10 to 62 years) and a median pre-analytical sample storage time of 82 months (range: 58 to 100 months). A summary of information regarding all study subjects and their disease classifications can be found in Table 3.1.

Table 3.1: Study subjects: chimpanzees with a known cardiac phenotype (n=13), as confirmed histologically, categorised as Affected (diseased) or Control (healthy). Their sex (male or female), age at death (years) length of pre-analytical sample storage time (months) is also included.

Disease phenotype	Study ID	Sex	Age at death (years)	Sample storage (months)
Affected	C4	Male	33	105
	C8	Male	39	100
	C15	Female	46	93
	C29	Female	44	96
	C30	Male	21	74
	C34	Female	42	71
	C54	Male	41	6
	C55	Female	28	5
	C56	Female	40	2
Control	C9	Female	32	100
	C20	Male	21	90
	C31	Female	62	74
	C36	Female	10	58

Stage I: Using FFPE tissue samples

RNA extraction

The RNeasy FFPE Kit (catalog no. 73504) and Deparaffinisation Solution (catalog no. 19093) from QIAGEN GmbH were used for the extraction and purification of total RNA from 10 µm FFPE tissue sections at room temperature. The kit contained RNeasy MinElute® Spin Columns, 1.5 mL and 2 mL Collection Tubes, Proteinase K, RNase-Free DNase I, DNase Booster Buffer, RNase-Free Buffers (RBC, PKD and RPE) and RNase-Free Water. Upon arrival, the RNase-Free DNase I and the Spin Columns were stored at +4°C, with the remaining kit contents stored at room temperature, as per the manufacturer instructions. Before first use, the Buffer RPE was reconstituted with 44 mL ethanol (100%), and the RNase-free DNase I was reconstituted with 550 µL of RNase-free water.

To begin with, two 10 µm tissue sections from two chimpanzees only (C2 and C3) were used for the initial evaluation of RNA yield from FFPE tissues, using the following method (adapted from the QIAGEN RNeasy FFPE Handbook):

1. 160 µL Deparaffinisation Solution was added to a 2 mL microcentrifuge tube containing two 10 µm tissue sections. This was then vortexed for 10 seconds, and centrifuged briefly (5-10 seconds) in a microcentrifuge.
2. The solution was then incubated at 56°C for three minutes using a thermocycler, then left to cool to room temperature.
3. 150 µL Buffer PKD was added to the solution, and mixed by vortexing.
4. The solution was then centrifuged for one minute at 10,000 revolutions per minute (rpm).
5. 10 µL Proteinase K was added to the lower, uncoloured phase of the solution (as separated during centrifugation) and mixed gently by pipetting.
6. The solution was then incubated at 56°C for 15 minutes, then at 80°C for 15 minutes.
7. The lower, uncoloured phase of the solution was carefully transferred into a new 2 mL microcentrifuge tube.

8. The solution was incubated on ice for three minutes, before centrifuging at 13,500 rpm for 15 minutes.
9. The supernatant was carefully transferred to a new 1.5 mL microcentrifuge tube, without disturbing the pellet containing insoluble tissue debris.
10. 16 µL DNase Booster Buffer and 10 µL DNase I were added to the solution, then mixed by tube inversion and incubated at room temperature for 15 minutes.
11. 320 µL Buffer RBC was added, before mixing by pipette.
12. 720 µL ethanol (100%) was added, before mixing by pipette.
13. 700 µL of the sample was transferred to a Spin Column placed in a 2 mL collection tube. The sample was centrifuged at ≥10,000 rpm for 15 seconds. The eluate (flow-through) was discarded.
14. Step 13 was repeated until the entire sample volume had passed through the Spin Column.
15. 500 µL Buffer RPE was added to the Spin Column and centrifuged at ≥10,000 rpm for 15 seconds. The eluate was discarded.
16. Another 500 µL Buffer RPE was added to the Spin Column and centrifuged at ≥10,000 rpm for 2 minutes. The collection tube and eluate were discarded, taking care not to allow the column to come into contact with the eluate.
17. The Spin Column was carefully placed into a new 2 mL collection tube, then centrifuged with the lid open at full speed for five minutes. The collection tube and eluate were discarded.
18. The Spin Column was carefully placed into a new 1.5 mL collection tube. 20 µL RNase-free water was added to the Spin Column before centrifuging for one minute at full speed. The resulting eluate was the purified RNA.

After this, an optimisation of the protocol to improve RNA yield and quality was attempted, by altering the following procedures:

1. Excess paraffin wax was trimmed from the tissue sections before use.
2. The reagent volumes added were increased, as advised by the manufacturer for the use of >2 tissue sections.
3. Step 1 (deparaffinisation) of the original protocol was repeated, twice.
4. The volume of deparaffinisation solution added was increased.
5. Step 2 (56°C incubation) of the original protocol was repeated, twice.
6. The original FFPE tissue blocks were obtained, and fresh tissue sections were cut immediately before use, to avoid prolonged exposure to air.

Stage II: Using tissue samples in RNAlater

RNA extraction

The RNeasy® Mini Kit from QIAGEN GmbH (catalog no. 74104), TRIzol™ Reagent from Invitrogen (catalog no. 15596026) and Chloroform from Sigma-Aldrich (catalog no. C2432) were used for the extraction and purification of total RNA from tissue sections that had been stored in RNAlater. The RNeasy Mini Kit contained RNeasy Mini Spin Columns, 1.5 mL and 2 mL Collection Tubes, RNase-Free Buffers (RLT, RW1 and RPE) and RNase-Free Water. Upon arrival, the kit contents were stored at room temperature, as per the manufacturer instructions. Before first use, the Buffer RPE was reconstituted with 44 mL ethanol (100%). Appropriate health and safety precautions were taken before and during the use of TRIzol Reagent.

Approximately 50 mg of tissue per sample (see Table 3.2) was sectioned using a scalpel prior to extracting total RNA using the following method (adapted from the QIAGEN RNeasy Mini Handbook):

1. Inside a flow hood, 1 mL TRIzol Reagent was added to a 1.5 mL tube containing the 50 mg tissue section.
2. The tissue was disrupted and homogenised using a rotor-stator tissue homogeniser, continuing until all tissue is visibly disrupted.
3. The sample was left to sit at room temperature for 5 minutes.
4. 200 µL chloroform was added, before replacing the lid and shaking vigorously for 15 seconds.
5. The sample was left to sit at room temperature for 3 minutes.
6. The sample was centrifuged for 15 minutes at ≥10,000 rpm.
7. The aqueous phase of the supernatant was carefully removed and transferred into a new microcentrifuge tube.
8. An equal volume (500-700 µL) of 70% ethanol was slowly added to the supernatant, then mixed by pipetting.
9. 700 µL of the sample, including any precipitate that may have formed, was transferred to a Spin Column placed inside a 2 mL collection tube.

10. The sample was centrifuged for 30 seconds at ≥10,000 rpm. The eluate was discarded.
11. If the sample volume exceeded 700 µL, successive aliquots were centrifuged in the same Spin Column. The eluate was discarded after each centrifugation.
12. 700 µL Buffer RW1 was added to the Spin Column. The lid was closed gently, then the sample was centrifuged for 30 seconds at ≥10,000 rpm.
13. The Spin Column was transferred to a new collection tube. 500 µL Buffer RPE was added to the Spin Column. The lid was closed gently, then the sample was centrifuged for 30 seconds at ≥10,000 rpm. The eluate was discarded.
14. 500 µL Buffer RPE was added to the Spin Column. The lid was closed gently, then the sample was centrifuged for 2 minutes at ≥10,000 rpm.
15. The Spin Column was transferred to a new collection tube and centrifuged (empty) for 2 minutes at ≥10,000 rpm.
16. The Spin Column was transferred to a new collection tube and 30 µL RNase-free water was added directly to the Spin Column membrane. The sample was left to sit at room temperature for 2 minutes. The lid was closed gently, then the sample was centrifuged for 1 minute at ≥10,000 rpm. The resulting eluate was the purified RNA.

Finally, the concentration (µg/mL) and purity (ratio of optical density absorbance at 260nm and 280nm) of the resultant RNA were assessed using a NanoDrop® instrument.

Table 3.2: Mass (g) of tissue samples used for the extraction and purification of total RNA from myocardial tissue stored in RNAlater (n=14).
Asterisk (*) denotes an insufficient sample quantity available to meet the 50 mg (0.050 g) minimum mass.

Disease phenotype	Study ID	Mass of tissue used (g)
Affected	C4	0.057
	C8	0.056
	C15	0.054
	C29	0.053
	C30	0.058
	C34	0.012 *
	C54	0.058
	C55	0.059
	C56	0.052
Control	C20.SP	0.056
	C9	0.053
	C20	0.052
	C31	0.055
	C36	0.053

Reverse transcription

The extracted and purified RNA was converted into cDNA via reverse transcription. This was carried out using the Tetro™ cDNA Synthesis Kit from Bioline (catalog no. BIO-65043), which contained 5x RT Buffer, Reverse Transcriptase (200 u/µL), RNase Inhibitor (10 u/µL), dNTP Mix (10 mM Total), Oligo (dT)18 Primer Mix, Random Hexamer Primer Mix, and DEPC-treated Water. Upon arrival, the kit contents were stored at -20°C, as per the manufacturer instructions.

The following method, adapted from the Tetro cDNA Synthesis Kit Protocol, was used:

1. On ice, a priming mastermix was prepared in an RNase-free reaction tube, according to the total number of samples it was needed for. The baseline ratio of components was as follows, which accounted for volume loss inside tubes and pipette tips:
    a. 1.5 µL Oligo(dT)18
    b. 1.5 µL dNTP mix (10 mM)
    c. 6 µL 5x RT Buffer
    d. 1.5 µL RNase Inhibitor
    e. 1.5 µL Reverse Transcriptase (200 u/µL)
2. 8 µL of the mastermix was aliquoted into separate PCR reaction tubes (one tube per sample).
3. The volumetric equivalent of 0.5 µg RNA (to a maximum of 12 µL) was added, using the concentration of each RNA sample as assessed by a NanoDrop® instrument, according to the equation:

$$Volume\ of\ RNA\ eluate\ needed\ (ml) = \frac{0.5\ (\mu g)}{RNA\ concentration}$$

4. DEPC-treated water was added to give a final reaction volume of 20 µL. RNA plus water should equal 12 µL. If the volume of RNA added was the maximum (12 µL), no water was added:

$$Volume\ of\ water\ needed\ (\mu L) = (12\ \mu L) - \big(volume\ of\ RNA\ added\ (\mu L)\big)$$

5. The solution was mixed gently by pipetting.

6. Using a thermocycler, the following incubation programme was run:
    a. 45°C for 60 minutes
    b. 85°C for 5 minutes
    c. 4°C indefinitely (until removed from thermocycler)
7. 30 µL RNase-free water was added.
8. The solution was stored at -20°C, if not proceeding immediately with RT-qPCR.

Reference and target gene selection

Accurate analysis of target gene expression via RT-qPCR requires normalisation to account for variations in RNA quality, sample quantity, and the efficiency of reverse transcription and amplification (Bustin et al., 2009). Reference genes (often called housekeeping genes) are used as internal controls for this purpose. The stability of reference genes is critical, as their expression must remain constant across all experimental conditions (Huggett et al., 2005). In this study, reference gene selection was conducted according to the Minimum Information for Publication of Quantitative Real-Time PCR Experiments (MIQE) guidelines (Bustin et al., 2009), which state that multiple reference genes should be evaluated and refined based on their stability within the samples in use. Eight candidate reference genes were therefore chosen based on their common use in RT-qPCR experiments and previous reports of stable expression in similar tissue types (De Jonge et al., 2007): Actin Beta (ACTB); Beta-2-Microglobulin (B2M); Glyceraldehyde-3-Phosphate Dehydrogenase (GAPDH); Lactate Dehydrogenase A (LDHA); Ribosomal Protein S12 (RPS12); Ribosomal Protein S20 (RPS20); Ribosomal Protein L27 (RPL27); and Tyrosine 3-Monooxygenase/Tryptophan 5-Monooxygenase Activation Protein Zeta (YWHAZ).

A review of the literature was carried out to identify appropriate target genes for this study, to ensure the inclusion of potentially important genes, even if they were not identified in the proteomic analysis. Fifteen markers were selected based on their biological relevance to inflammation, tissue remodelling, and fibrosis, as well as their logistical feasibility for analysis in myocardial tissue. These included cytokines (Interleukin-6 (IL-6) and Interleukin-11 (IL-11)), growth factors (Connective Tissue

Growth Factor (CCN2/CTGF), Transforming Growth Factor Beta 1 (TGF-β1), and Vascular Endothelial Growth Factor (VEGF)), receptors and binding proteins (Galectin-3 (GAL-3), Tissue Inhibitor of Metalloproteinases 1 (TIMP-1), and Vitamin D Receptor (VDR-01 and VDR-02)), matrix proteins (Collagen Type I Alpha 1 Chain (COL1A1), Collagen Type III Alpha 1 Chain (COL3A1), Fibronectin 1 (FN1), and Secreted Phosphoprotein 1/Osteopontin (SPP1/OPN)), and enzymes (Matrix Metallopeptidase 2 (MMP-2) and Matrix Metallopeptidase 9 (MMP-9)). These markers were chosen because they represent critical pathways implicated in extracellular matrix remodelling and inflammatory responses associated with myocardial fibrosis, as highlighted in prior research (Lok et al., 2015; Ogawa et al., 2001; Wang et al., 2017; Schafer et al., 2017; Chen et al., 2014; Teng et al., 2021; McDonald et al., 2020; Vanhoutte et al., 2013; Nemir et al., 2014; Shu et al., 2021; Martínez-Martínez et al., 2019; Suzuki et al., 2000).

The primer sequences for the reference and target genes were designed with the help of Dr Ben Hewitt (a collaborator on the wider study) using the online tools *ensembl.org* and *Primer3Web* (Thornton and Basu, 2011). Primers are short, single-stranded DNA sequences that are designed to bind to specific regions of the reference or target genes in the amplification process during RT-qPCR. Two primers per gene are required (‘forward’ and ‘reverse’), with each binding to opposite strands of the target DNA, enabling replication in both directions (Bustin and Huggett, 2017). Primers are typically 18–25 nucleotides long, with balanced G-C pairs, and are designed to avoid secondary structures for efficient amplification (Bustin et al., 2009; Taylor et al., 2010). Upon arrival, all primers were reconstituted with RNase-free water according to the manufacturer instructions and stored at -20°C to prevent degradation. The primer sequences for the selected reference and target genes can be found in Table 3.3.

Table 3.3: Primer sequences of selected reference genes (n=8): ACTB, B2M, GAPDH, LDHA, RPS12, RPS20, RPL27, YWHAZ; and target genes (n=15): CCN2, COL1A1, COL3A1, FN1, GAL-3, IL-6, IL-11, MMP-2, MMP-9, SPP1, TGF-β1, TIMP-1, VDR-01, VDR-02, VEGF.
Primers were designed for use with chimpanzee (*Pan troglodytes*) material using the online tools ensembl.org and Primer3Web.

Category	Gene name	Oligo name	Sequence
Reference genes	ACTB	ACTB_CHIMP_F	CTACAATGAGCTGCGTGTGG
		ACTB_CHIMP_R	AGCCTGGATAGCAACGTACA
	B2M	B2M_CHIMP_F	AAGATGAGTATGCCTGCCGT
		B2M_CHIMP_R	TGATGCTGCTTACATGTCTCG
	GAPDH	GAPDH_CHIMP_F	TCATCCATGACAACTTCGGTATC
		GAPDH_CHIMP_R	ATGATGTTCTGGAGAGCCCC
	LDHA	LDHA_CHIMP_F	CTCTGAAGACTCTGCACCCA
		LDHA_CHIMP_R	ATAGCCCAGGATGTGTAGCC
	RPS12	RPS12_CHIMP_F	CAAGAGGTTCTGAAGACCGC
		RPS12_CHIMP_R	TCACAGTTGGATGCAAGCAC
	RPS20	RPS20_CHIMP_F	GCGACTCATTGACTTGCACA
		RPS20_CHIMP_R	CTCAAAGTGTACTGCTGGCC
	RPL27	RPL27_CHIMP_F	ATGGGCAAGAAGAAGATCGC
		RPL27_CHIMP_R	AGACATCCTTATTGACGACAGTT
	YWHAZ	YWHAZ_CHIMP_F	GAGAGAAAATTGAGACGGAGCT
		YWHAZ_CHIMP_R	CAACCTCAGCCAAGTAACGG
Target genes	CCN2 / CTGF	CCN2_CHIMP_F	TACCAATGACAACGCCTCCT
		CCN2_CHIMP_R	TGGGAGTACGGATGCACTTT
	COL1A1	COL1A1_CHIMP_F	CAAGAGGCATGTCTGGTTCG
		COL1A1_CHIMP_R	TAGGTGATGTTCTGGGAGGC
	COL3A1	COL3A1_CHIMP_F	ACACGTTTGGTTTGGAGAGTC
		COL3A1_CHIMP_R	GCTGGAGAGAAGTCGAAGGA
	FN1	FN1_CHIMP_F	TCCACAGTTCAAAAGACCCCT
		FN1_CHIMP_R	TCCGCCTAAAACCATGTTCC
	Gal-3	LGALS3_CHIMP_F	AGGGAAGAAAGACAGTCGGT
		LGALS3_CHIMP_R	AACCCGATGATTGTACTGCA

	IL-6	IL6_CHIMP_F	AGACAGCCACTCACCTCTTC
		IL6_CHIMP_R	AGTGCCTCTTTGCTGCTTTC
	IL-11	IL11_CHIMP_F	GAGTTTCCCCAGACCCTCG
		IL11_CHIMP_R	CCGTCAGCTGGGAATTTGTC
	MMP-2	MMP2_CHIMP_F	GATGCCGCCTTTAACTGGAG
		MMP2_CHIMP_R	AGGTTATCGGGGATGGCATT
	MMP-9	MMP9_CHIMP_F	ACGACGTCTTCCAGTACCG
		MMP9_CHIMP_R	TGGTTCAACTCATTCCGGGA
	SPP1 / OPN	SPP1_CHIMP_F	ACTGATTTTCCCACGGACCT
		SPP1_CHIMP_R	GGATGTCAGGTCTGCGAAAC
	TGF-β1	TGFB1_CHIMP_F	TCAACACATCAGAGCTCCGA
		TGFB1_CHIMP_R	GTATCGCCAGGAATTGTTGCT
	TIMP-1	TIMP1_CHIMP_F	CTGTTGGCTGTGAGGAATGC
		TIMP1_CHIMP_R	CTGGAAGCCCTTTTCAGAGC
	VDR-01	VDRO1_CHIMP_F	CTGGTCAGTTACAGCATCCA
		VDRO1_CHIMP_R	TTGGAGCGCAACATGATGAC
	VDR-02	VDRO2_CHIMP_F	TGTCCCAGCTCTCCATGC
		VDRO2_CHIMP_R	ATGGCACTTGACTTCAGCAG
	VEGF	VEGFA_CHIMP_F	CCGGTATAAGTCCTGGAGCG
		VEGFA_CHIMP_R	TTTAACTCAAGCTGCCTCGC

RT-qPCR

After reverse transcription, the cDNA was amplified and quantified via qPCR. For this, PowerTrack™ SYBR Green Master Mix (catalog no. 16535231) from Applied Biosystems™, Axygen® 96-well Polypropylene PCR Microplates (catalog no. PCR-96-LC480-W), and a LightCycler® 480 II Instrument (catalog no. 05015278001) from Roche Diagnostics were used. Two genes were included per plate, with three technical replicates of all 13 biological samples per gene. This is in line with the sample maximisation strategy, which reduces inter-assay variation and allows for reliable gene expression comparison between samples (Hellemans et al., 2007). A No Template Control (NTC), which is a negative control containing the PCR Reaction Mix but no cDNA, was included in duplicate per gene. The spleen sample (C20.SP) was used as an IPC, which is a positive control used for the detection of PCR reaction failures, and to normalise for variability between plates. Two concentrations (100% and 10%) of the IPC cDNA were used, to ensure amplification efficiency and consistency (Bustin et al., 2009; Taylor et al., 2010). The reaction conditions set on the LightCycler instrument began with a preincubation step at 95°C for 5 minutes at a ramp rate of 4.4°C/s, followed by 45 amplification cycles. Each cycle consisted of three steps: denaturation at 90°C for 10 seconds (ramp rate 4.4°C/s), annealing at 60°C for 10 seconds (ramp rate 2.2°C/s), and elongation at 72°C for 10 seconds (ramp rate 4.4°C/s). A melting curve analysis followed, starting with heating at 95°C for 5 seconds, holding at 65°C for 1 minute, and then gradually heating from 65°C to 97°C at a rate of 0.11°C/s with continuous fluorescence acquisition (five acquisitions per °C). The protocol concluded with a cooling step at 4°C for 30 minutes at a ramp rate of 2.2°C/s.

The RT-qPCR plates were prepared according to a planned layout (see Appendix B) using the following protocol:

1. On ice, PCR Reaction Mixes were made up per gene:
    a. 250 µL SYBR Green
    b. 195 µL molecular-grade water
    c. 2.5 µL forward primer
    d. 2.5 µL reverse primer
2. The solution was vortexed and centrifuged briefly.

3. Microplates were prepared and labelled before placing on ice.
4. 9 µL Reaction Mix was added to wells corresponding to the correct genes (according to the planned layout).
5. 1 µL cDNA was added to wells corresponding to the correct biological samples (according to the planned layout).
6. The plate was carefully covered with a Sealing Film, then covered with aluminium foil to protect from light, before being brought to a microplate centrifuge.
7. Foil was removed, and the plate was centrifuged for 3 minutes using the following cycle settings:
    a. 130 mm Rotor Radius
    b. 9/\4 Ramp (acceleration/deceleration)
    c. 1500 Relative Centrifugal Force
    d. 3220 Revolutions Per Minute
    e. 25°C Temperature
8. The plate was inserted into the LightCycler 480 Instrument and the qPCR programme was run. If not proceeding immediately with RT-qPCR, the plate was covered with aluminium foil and stored at -20°C until use.

Data analysis

The LightCycler 480 Instrument's built-in computer software (Rasmussen, 2001) was used for initial data processing and quantification of the number of amplification cycles taken for fluorescence in the sample to become detectable above a defined threshold – otherwise known as Quantification Cycle (Cq) or Cycle Threshold (Ct). The Cq value corresponds to the quantity of target nucleic acid in a sample, with lower Cq values indicating higher initial amounts of target material (Bustin et al., 2009).

The exported Absolute Quantification data were then analysed with qbase+, a software programme used for the normalisation, calibration and relative quantification of target gene expression data against multiple candidate reference genes (Hellemans

et al., 2007). Quality control of all technical replicates for the reference and target genes for each RT-qPCR plate was carried out, whereby any replicates not within one Quantification Cycle (Cq) were excluded from further analysis. Geometric mean normalisation (GeNorm) was used to assess and rank the stability of the candidate reference genes in this study (Vandesompele et al., 2002). A minimum of 10 samples and eight candidate reference genes are recommended for an optimal GeNorm analysis (Vandesompele et al., 2002). By identifying the most stable genes (GeNorm M<1), GeNorm ensures accurate normalisation of target gene expression data, helping to improve the reliability of the results.

GraphPad Prism (v10.3.1) was used for statistical analysis of the resulting Calibrated Normalised Relative Quantity (CNRQ) target gene expression data. Data normality was tested using the Shapiro-Wilk test. Pearson (parametric) and Spearman (non-parametric) correlations were used to assess the relationship between sample storage time and RNA purity, RNA concentration and target gene expression data. Welch's t-tests (parametric) and Mann-Whitney tests (non-parametric) were used to assess for any differences in RNA concentration and purity between sample preservation methods, as well as in target gene expression between chimpanzees affected by IMF versus healthy controls. No outliers were excluded from the statistical analysis. Given the small sample size and the natural variability in the dataset, retaining all data points ensured transparency and captured the full range of biological variability in this population.

3.3 Results

Stage I: Using FFPE tissue samples

RNA purity and concentration

Two FFPE tissue samples (from chimpanzees C2 and C3) produced suboptimal RNA despite three attempts to modify the RNA extraction protocol (see Table 3.4). In the first attempt, using the original protocol, the concentration of 15.81 µg/mL and the purity ratio (260nm/280nm) of 1.55 was below the acceptable range for high-quality RNA, which is typically between 1.8 and 2.0 (Imbeaud et al., 2005; Sambrook and Russell, 2001). In the second attempt, the protocol was modified by trimming excess paraffin wax from tissue scrolls before use, increasing reagent volumes added, and repeating key deparaffinisation steps. However, these changes resulted in a lower RNA concentration of 6.05 µg/mL, with only a marginal improvement in purity (1.57). Further modifications in the third attempt, such as cutting tissue scrolls from the original wax tissue blocks immediately before use, and increasing the volume of deparaffinisation solution, resulted in a reduced RNA concentration from C2 (4.99 µg/mL) but a slight improvement in concentration (12.01 µg/mL) and purity (1.81) from C3.

Overall, despite alterations to the extraction protocol, RNA concentrations from the two FFPE samples tested remained low, and RNA purity was not consistently within the desired range for the downstream application of RT-qPCR. While one of the samples approached acceptable purity thresholds, the variability in results suggested that FFPE tissue posed significant challenges for reliable RNA extraction and subsequent analysis in this study. Consequently, it was decided to prioritise tissue stored in RNAlater for further work, as it typically allows for better preservation of RNA integrity and higher yields suitable for RT-qPCR (Florell et al., 2001; Mutter et al., 2004). However, FFPE tissue may still be considered a viable future option for specific analyses or under conditions where alternative storage methods, such as RNAlater, are unavailable.

Table 3.4: Concentration (µg/mL) and purity (260nm/280nm) of RNA extracted from FFPE myocardial tissue from two chimpanzees (*Pan troglodytes*) as assessed by a NanoDrop® instrument.

Attempt no.	Protocol alterations (cumulative)	Sample ID	RNA conc. (µg/mL)	RNA purity (260nm/280nm)
1	• None (original protocol)	C2.L1	15.81	1.55
2	• Trim excess paraffin wax • Increase reagent volumes • Repeat Step 1 (deparaffinisation) twice • Repeat Step 2 (56°C incubation) twice	C3.L2	6.05	1.57
3	• Cut tissue scrolls immediately before use • Increase volume of deparaffination solution	C2.L1	4.99	1.54
		C3.L2	12.01	1.81

Stage II: Using tissue samples in RNAlater

RNA purity and concentration

The median concentration of RNA extracted from myocardial tissue samples stored in RNAlater from chimpanzees was 78.11 µg/mL (range: 18.77 µg/mL to 167.32 µg/mL). The purity ratios (260nm/280nm) ranged from 1.65 to 2.02, with a median of 1.92. The spleen sample (C20.SP) had an RNA concentration of 200.76 µg/mL and a purity ratio of 1.98 (see Table 3.5). There was no correlation between sample storage time and RNA concentration (p=0.981, Pearson correlation) or RNA purity (p=0.102, Spearman correlation).

When comparing these results with RNA extracted from FFPE samples, both RNA concentration and purity were significantly different between the two preservation methods (see Figure 3.1). Concentration was higher in the RNAlater samples compared to FFPE samples ($p<0.0001$, Welch's t-test). Purity was also higher in RNAlater samples compared to FFPE samples (p=0.002, Mann-Whitney). Though RNA quality from RNAlater samples was variable, this sample type was considered acceptable for proceeding with RT-qPCR.

Table 3.5: RNA concentration (µg/mL), purity (260nm/280nm), and sample storage time (months) of myocardial tissue samples from chimpanzees affected by IMF (n=9) and healthy controls (n=4).
One spleen sample was included as a positive Inter-Plate Control (C20.SP). Asterisk (*) denotes that the quantity of tissue available was below the suggested minimum (<50 mg) required for the extraction of total RNA.

Disease phenotype	Sample	Sample storage (months)	RNA conc. (µg/mL)	RNA purity (260nm/280nm)
Affected	C4	105	100.44	2.02
	C8	100	43.51	1.91
	C15	93	57.76	1.90
	C29	96	49.58	1.92
	C30	74	92.59	1.92
	C34	71	40.05 *	1.82 *
	C54	6	159.74	1.98
	C55	5	18.77	1.65
	C56	2	39.31	1.75
Control	C20.SP	90	200.76	1.98
	C9	100	78.31	1.98
	C20	90	81.11	1.95
	C31	74	167.32	2.00
	C36	58	85.69	1.93

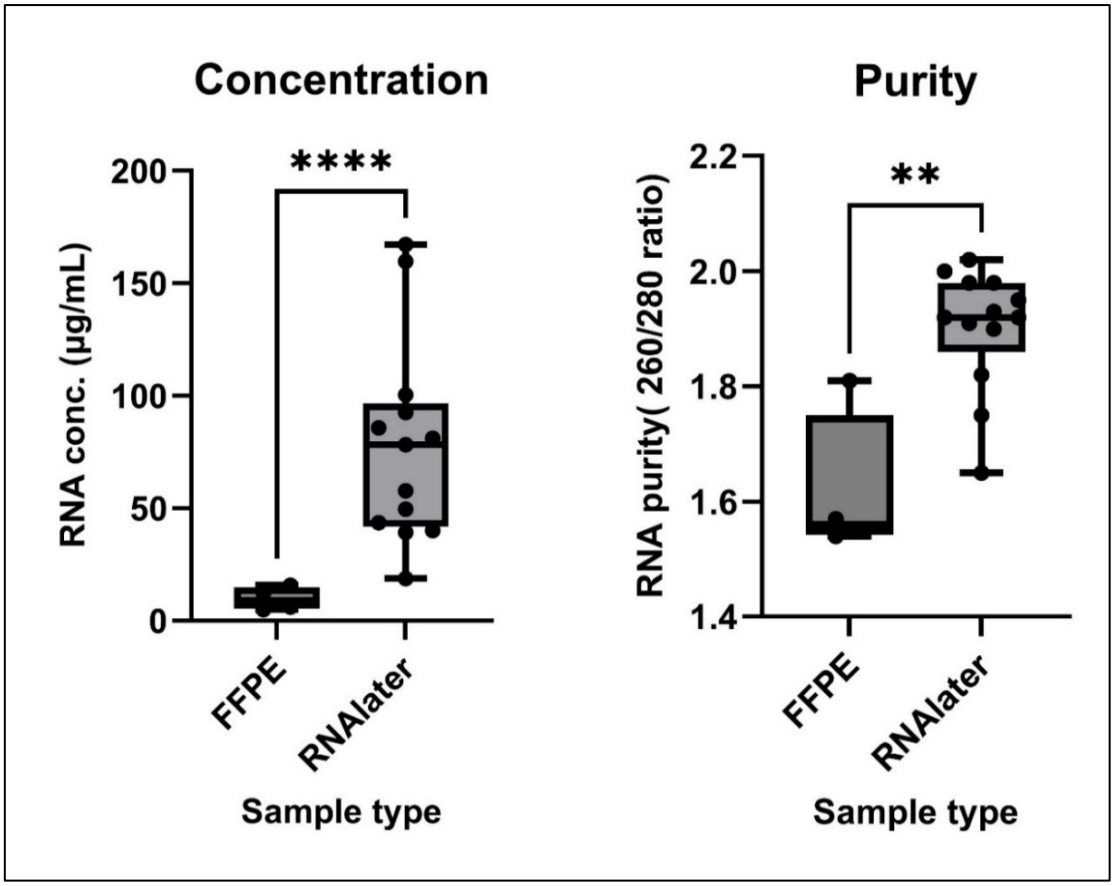

Figure 3.1: Difference in RNA concentration (µg/mL) and purity (260nm/280nm) between two sample preservation methods: FFPE and RNAlater.

The box and whisker plots display the median (horizontal line within the box), the interquartile range (IQR, the box itself), and the whiskers representing the minimum and maximum values within 1.5 times the IQR. Individual data points are shown as dots. Statistically significant differences between sample preservation methods are indicated by asterisks: **** = $p<0.0001$ for RNA concentration, and ** = $p<0.01$ for RNA purity, as determined by Welch's t-test and Mann-Whitney test, respectively.

Gene expression

One reference gene, RPS20, and two target genes, VDR-01 and VDR-02, showed no detectable expression at the gene transcript level and were subsequently excluded from further analysis. GeNorm analysis revealed that only one of the remaining seven candidate reference genes was optimally stable (RPL27, GeNorm M<1). In this instance, it was recommended by the software that the six most stable reference genes be retained for further analysis, since the use of multiple sub-optimal reference genes provides more accurate normalisation than one optimal reference gene (Taylor et al., 2010; Hellemans et al., 2007). LDHA was the least stable (M=1.42) and was removed, therefore the expression of the target genes was normalised according to RPL27, B2M, RPS12, ACTB, GAPDH and YWHAZ, in order of decreasing stability, respectively.

All biological samples (n=13) showed expression of the remaining target genes (n=13). However, no significant differences in CNRQ were observed between the Affected and Control group for any of the tested genes (see Figure 3.2): CCN2/CTGF (p=0.414, Mann-Whitney); COL1A1 (p=0.301, Welch's t-test); COL3A1 (p=0.826, Welch's t-test); FN1 (p=0.330, Mann-Whitney); GAL-3 (p=0.990, Welch's t-test); IL-6 (p=0.889, Mann-Whitney); IL-11 (p=0.436, Mann-Whitney); MMP-2 (p=0.199, Mann-Whitney); MMP-9 (p>0.999, Mann-Whitney); SPP1/OPN (p=0.504, Mann-Whitney); TGF-β1 (p=0.184, Welch's t-test); TIMP-1 (p=0.604, Mann-Whitney); VEGF (p=0.604, Mann-Whitney).

There was no correlation between sample storage time and gene expression for any of the target genes (p>0.05, Pearson and Spearman correlation).

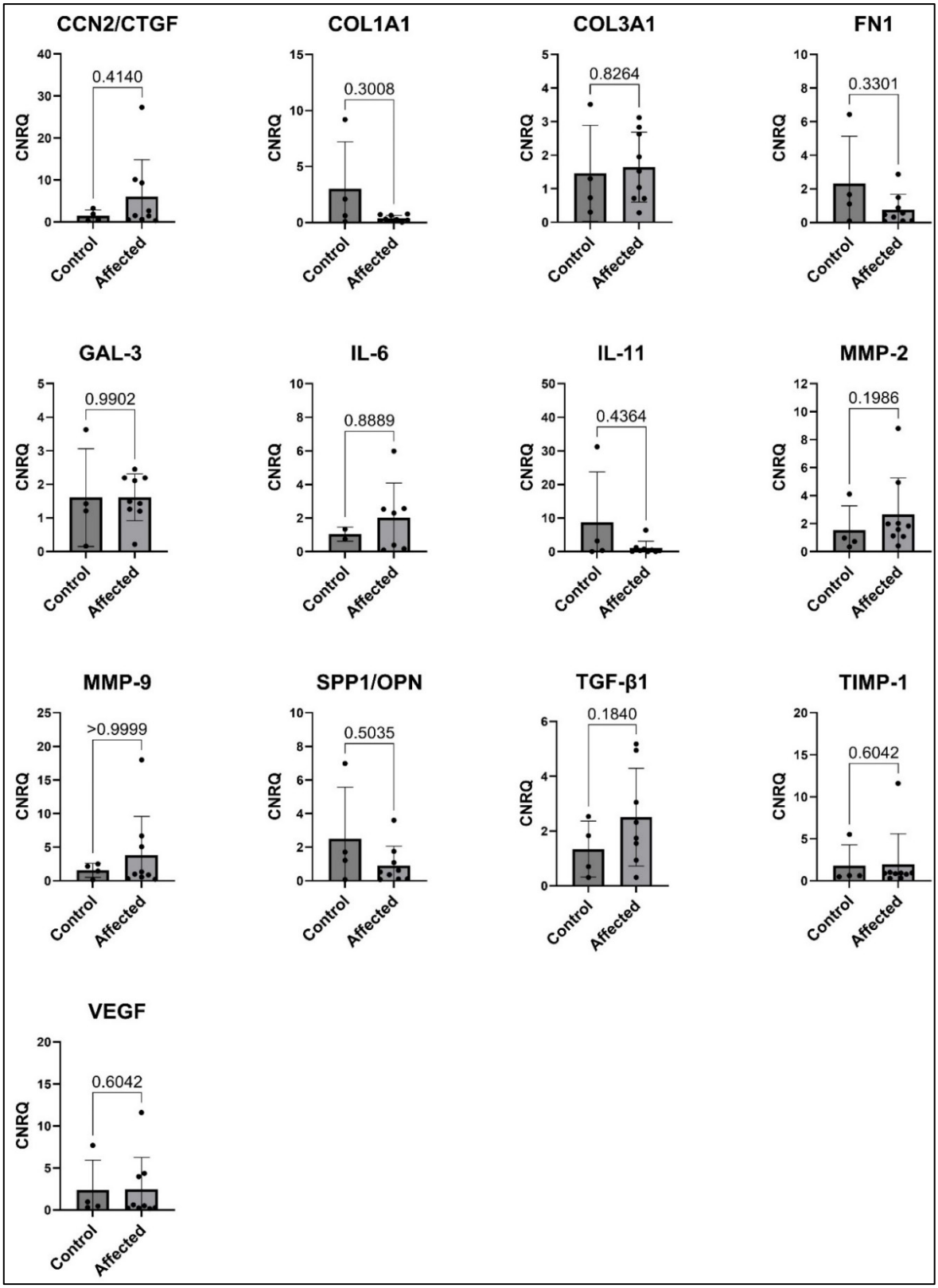

Figure 3.2: Expression of target genes (n=13) in myocardial tissue from chimpanzees affected by IMF (n=9) versus healthy controls (n=4).

The bars represent the mean Calibrated Normalised Relative Quantity (CNRQ) values, with error bars indicating the standard deviation (SD). Individual data points are represented by dots. Statistical significance was assessed using either Welch's t-test or the Mann-Whitney test.

3.4 Discussion

This study aimed to investigate the molecular signature of IMF in chimpanzees by quantifying the expression of 13 target genes associated with fibrosis, inflammation, and ECM remodelling using RT-qPCR. RNA was extracted from both FFPE and RNAlater-preserved myocardial tissues to assess gene expression. Despite rigorous methodology, no significant differences in gene expression were observed between affected and control groups, and VDR expression was undetectable at the transcript level. These findings highlight the potential technical challenges of using post-mortem tissue for transcriptomic analysis.

RNA quality

One of the most crucial aspects of any RT-qPCR study is the quality of the RNA extracted from tissue samples, which can significantly affect the downstream results. In this study, attempts to extract RNA from FFPE tissue produced poor yields and RNA purity, consistent with previous reports highlighting the challenges associated with RNA extraction from FFPE samples (Srinivasan et al., 2002; von Ahlfen et al., 2007). FFPE-induced crosslinking of nucleic acids and proteins often leads to RNA degradation, particularly in fibrous tissues such as myocardium, where collagen content is high (Lewis et al., 2001). Nevertheless, FFPE tissue remains a potential option for gene expression analysis in certain scenarios. While FFPE samples are inherently more processed than alternatives such as RNAlater-stored tissue, their suitability for retrospective studies make them an important resource. Optimising protocols for fixed fibrous tissues, as suggested in the literature (Ortega-Pinazo et al., 2023), or exploring alternative, high-throughput methods such as RNA-seq (Mortazavi et al., 2008; Chen et al., 2021c), may enable FFPE tissue to be used more effectively, particularly where no alternative tissue preservation method is available.

Tissue stored in RNAlater yielded significantly higher RNA concentrations and purities. RNAlater preserves RNA immediately by inhibiting RNase activity, offering superior RNA quality compared to FFPE (Florell et al., 2001; Mutter et al., 2004). The lack of correlation between sample storage time and RNA quality suggests that RNAlater preserves RNA adequately even over extended periods, a finding that aligns with the literature (Farragher et al., 2008). Although the purity and concentration yield of RNA

from RNAlater-stored tissue exhibited variability, these parameters were within acceptable ranges for RT-qPCR (Bustin et al., 2009).

Gene expression

The absence of significant differences in the expression of target genes between the affected and control groups raises important questions about technical and biological variability in this study. Although the selected reference genes were normalised using GeNorm to evaluate stability, only one of the eight candidates, RPL27, exhibited optimal stability (Vandesompele et al., 2002). The overall instability of the reference genes may have influenced the results of the target genes, the possible reasons for which will be discussed in more detail at a later point.

The absence of detectable VDR expression in chimpanzee myocardium raises questions about species-specific differences or potential technical limitations. In humans and other mammals, VDR is expressed in myocardial tissue, playing roles in mitigating fibrosis, inflammation, and hypertrophy (Chen et al., 2011; Rahman et al., 2007). One hypothesis is that the myocardium may not require high levels of VDR gene expression due to the long half-life and stability of the VDR protein, reducing the need for continuous transcription (Javan et al., 2024). Alternatively, VDR expression may be condition-dependent, increasing under specific pathological stimuli, such as cardiac hypertrophy or inflammation (Chen et al., 2008). While the presence of IMF in the Affected group represents a pathological trigger, the variability introduced by post-mortem interval and tissue handling may have obscured detectable transcription. Evidence from post-mortem transcriptomics suggests that degradation and transcriptional silencing during death may disproportionately affect certain genes, especially those with transient or low baseline expression, such as VDR (Ferreira et al., 2018; Javan et al., 2024). Furthermore, species-specific genetic factors, such as VDR polymorphisms, could influence VDR expression patterns and functional roles in chimpanzee myocardium (Gisbert-Ferrándiz et al., 2020; Jia et al., 2014), and this would be an important avenue for future research in light of the suspected importance of vitamin D in IMF (Strong et al., 2020; Moittié et al., 2022).

Despite the lack of statistically significant findings, trends in the expression of fibrosis-related markers, such as MMP-2, TGF-β1 and CCN2 (CTGF), merit further investigation. TGF-β1 is a well-known pro-fibrotic cytokine that promotes fibroblast

activation and ECM deposition in fibrotic tissues (Leask and Abraham, 2004). Similarly, CCN2 acts downstream of TGF-β1 to amplify fibrotic responses (Shi-Wen et al., 2008). Although these trends were not statistically significant in this study, their biological relevance is well-supported in the literature, suggesting that larger sample sizes and more homogenous pre-analytical conditions may provide clearer results.

Limitations and technical considerations

RNA extracted from samples preserved in RNAlater generally exhibited better quality, though variability in purity and concentration was still evident. This inconsistency likely arose from factors such as post-mortem interval (PMI), sample handling, and storage conditions. Extended PMIs are particularly problematic because RNA degrades rapidly, reflecting the transient and dynamic nature of the transcriptome at the time of sampling (Ferreira et al., 2018; Javan et al., 2024). For genes like VDR, whose expression may depend on specific physiological or pathological stimuli, this degradation likely contributed to the inability to detect transcription. Post-mortem transcriptomic analyses are further complicated by the molecular processes triggered by death. While DNA remains relatively stable, RNA is highly vulnerable to degradation by ribonucleases and environmental factors (Javan et al., 2024). In addition, some genes undergo active transcriptional changes post-mortem, while others are silenced, creating further complexity in interpreting gene expression (Ferreira et al., 2018; Javan et al., 2024). These pre-analytical challenges likely also affected the low stability of reference genes in this study.

Other pre-analytical factors, such as tissue sampling, storage, and transport conditions, likely contributed to the observed variations in RNA quality. For instance, while it is recommended that no more than 0.5 cm^3 of tissue is preserved in 2.5–5 mL of RNAlater (Ambion, 2010), some samples had substantially more tissue per solution volume, likely hindering the stabilisation of RNA within the core of the tissue. Storage conditions at the zoos also varied, with some samples stored at -80°C, others at -20°C, and some even at room temperature, according to communications with zoo veterinarians. Although RNAlater is generally effective in preserving RNA, inconsistent storage temperatures may have contributed to inter-sample variability (Ambion, 2010; Micke et al., 2006). Prolonged storage times, reaching up to 105 months in this study, may have further compounded these effects, as RNA degradation can occur even in stabilised samples over time (Imbeaud et al., 2005). While no direct correlation was

observed between storage time and RNA quality, future studies would benefit from assessing RNA integrity more comprehensively, rather than relying solely on purity and concentration measures (Fleige and Pfaffl, 2006).

As discussed in earlier chapters, distinguishing between the affected and control groups was further complicated by potential overlap in clinical and subclinical phenotypes. For example, some individuals in the control group exhibited mild fibrotic changes or were affected by co-morbidities or external factors not accounted for. Notably, two chimpanzees in this study (one from each group) died of hyperthermia, a condition known to induce acute molecular responses (Leon and Helwig, 2010). Although these individuals did not significantly alter the analysis outcomes, their cases highlight the potential influence of environmental stressors on gene expression.

Conclusions

This study provides further preliminary insights into the molecular landscape of IMF in chimpanzees, highlighting the challenges of measuring gene expression in post-mortem tissue. Pre-analytical variability, including PMI and storage conditions, likely influenced RNA quality, reference gene stability, and expression of the target genes. While the lack of detectable VDR expression may reflect species-specific or disease-specific regulation and merits further investigation, it is likely that the pre-analytical environment affected this too. While it is known that RNA expression does not always correlate with protein levels (Schwanhüusser et al., 2011; Vogel and Marcotte, 2012), further work involving the expression of genes corresponding to the proteins of interest from the previous chapter (Chapter 2) could also be beneficial.

With refinement of pre-analytical and technical considerations, the integration of gene expression analysis with complementary approaches such as tissue proteomics and serum biomarkers has the potential to offer valuable contributions to the broader understanding of IMF. In the meantime, the final chapter will explore circulating vitamin D levels in zoo-housed great apes as a potential risk factor for IMF, integrating these findings into a broader understanding of cardiovascular health in great apes.

4. EXPLORATION OF VITAMIN D STATUS IN EUROPEAN ZOO-HOUSED GREAT APES

4.1 Introduction

The aetiology of IMF in great apes is currently unknown, but previous work from the wider research group has suggested a possible link with vitamin D, while also ruling out other important hypotheses (Strong et al., 2020). Since vitamin D is known to be important for cardiovascular and overall health, a thorough investigation into the vitamin D status of the zoo-housed great ape populations is an important first step in learning more about this potential risk factor for IMF.

Vitamin D comprises a group of fat-soluble secosteroids, and its main source in humans and animals is dependent on direct, unfiltered sunlight. Cholecalciferol (vitamin D_3) is synthesised when ultraviolet B (UVB) radiation from the sun interacts with 7-dehydrocholesterol in the skin (Holick et al., 1980). Ergocalciferol (vitamin D_2) is synthesised by plants and fungi, and obtained by humans and animals from dietary sources (Holick et al., 1980). Both vitamin D_2 and D_3 are inactive forms that are converted by the liver into the major circulating metabolite: calcifediol. Otherwise known as 25-hydroxyvitamin D (25-OHD), calcifediol is the biomarker used to measure vitamin D status and is relatively stable with a half-life of 2-3 weeks (Jones et al., 1998; Lund et al., 1980). The active form, 1,25-dihydroxyvitamin D, interacts with cells via the VDR and is essential for calcium and phosphorus homeostasis, and a range of other physiological processes including immune function and cardiovascular health (Schwalfenberg, 2011; Calton et al., 2015; Wang et al., 2020; Holick, 2004a; Szodoray et al., 2008; Deluca et al., 2013).

Vitamin D is known to have a cardioprotective role, and may regulate fibrosis (such as IMF) by modulating anti-inflammatory and oxidative stress pathways (Meredith et al., 2015). Additionally, Chapter 2 of this thesis identified mitochondrial dysfunction and impaired calcium regulation as key molecular pathways associated with IMF in chimpanzees. These processes are intrinsically tied to oxidative stress and reactive oxygen species (ROS), which vitamin D is known to modulate via its anti-inflammatory and antioxidant effects (Srinivasan and Avadhani, 2012; Wimalawansa, 2019).

Additionally, gene expression analysis of cardiac tissue (Chapter 3) did not detect VDR expression at the transcript level, which requires more investigation.

Furthermore, reduced UVB exposure and subsequent vitamin D deficiency are implicated in the pathogenesis of hypertension (hypothesised to be a risk factor for IMF in great apes), as vitamin D plays a critical role in regulating the renin-angiotensin system, improving endothelial function, and reducing vascular inflammation (Rostand, 1997; Pilz et al., 2009). Widespread vitamin D deficiency is a public health concern for humans worldwide (Cashman et al., 2016; Prentice, 2008), and since non-human great apes share a high genetic and physiological similarity with humans, it is likely that their vitamin D requirements and metabolism are comparable.

In zoo-housed animals, maintaining adequate vitamin D status can be challenging. In the wild, great apes and other species obtain sufficient UVB exposure from sunlight, alongside a balanced, natural diet (Van Mulders et al., 2024). However, in managed populations, factors such as geographical latitude and enclosure design can restrict UVB exposure, and a human-managed diet can differ greatly from the naturally occurring foods in species' range countries (Van Mulders et al., 2024).

Great apes living in European zoos possess known human risk factors for vitamin D deficiency. For example, those with darker skin pigmentation require more UVB exposure to synthesise adequate vitamin D_3 because melanin, which protects against UVA damage and regulates UVB absorption, reduces the efficiency of vitamin D synthesis (Webb et al., 2018; Hall et al., 2010; Akeson et al., 2016; Jablonski and Chaplin, 2010). Being housed indoors and at northerly latitudes is also a risk factor – at latitudes above 37°N (level with southern Europe), UVB is not present in sufficient quantities in winter months for adequate vitamin D synthesis (Webb et al., 1988). The colder weather at more northerly latitudes also may make it less desirable to spend time outdoors (The Scientific Advisory Committee on Nutrition, 2016). Alongside this, the prevalence of cardiovascular disease, particularly IMF, in great apes is higher in zoos than in the wild (Strong et al., 2020; Van Mulders et al., 2024). Therefore, it is reasonable to investigate possible environmental differences that differ between the two settings, such as solar UV levels, thus impacting vitamin D status. Understanding how vitamin D status may influence health outcomes in great apes, and identifying

vulnerable groups and practical interventions within these populations, is therefore a highly important area of research.

Although research on vitamin D in zoo-housed great apes is very limited, with no published reports on bonobos or orangutans, it is becoming an increasingly prominent topic, and previous studies have provided important insights. Cases of rickets in juvenile chimpanzees raised without outdoor access highlight the risks of insufficient UVB exposure, while in another study, chimpanzees with greater sunlight access showed significantly higher serum vitamin D levels (Junge et al., 2000; Videan et al., 2007b). In gorillas, individuals housed indoors without direct sunlight exposure had lower serum 25-OHD concentrations compared to those with regular outdoor access, despite similar dietary provisions (Bartlett et al., 2017). These findings suggest that dietary intake alone is insufficient in maintaining adequate vitamin D levels and emphasise the need for species-specific research into the effects of diet, UVB exposure, and other husbandry practices (Crissey et al., 1999). In the first published research measuring 25-OHD in sanctuary-living chimpanzees in their range countries, median vitamin D status was insufficient by human standards, and varied by sex, age and sunlight exposure (Feltrer-Rambaud et al., 2023).

This thesis chapter builds on existing research on vitamin D status in a large portion of the European zoo-housed chimpanzee population (Moittié et al., 2022), which was the first large-scale, multi-zoo study of its kind, and identified widespread vitamin D insufficiency while highlighting significant predictors such as season, health status, and outdoor access. Despite the growing body of literature on this topic, several key knowledge gaps remain, and this chapter expands the scope to include all four great ape species for the first time. By incorporating a larger dataset and additional variables, this study aims to:

1. Evaluate 25-OHD concentrations in bonobos, chimpanzees, gorillas, and orangutans and determine the prevalence of deficient, insufficient, adequate, and optimal vitamin D statuses in line with human reference ranges.
2. Investigate the influence of individual (e.g., age, sex, health status, coat coverage), environmental (e.g., UVB irradiance, seasonality), and husbandry (e.g., outdoor access, diet) factors on vitamin D status.

3. Assess whether certain species or subpopulations are at greater risk of vitamin D insufficiency and explore potential underlying causes.
4. Inform evidence-based management for zoo-housed great apes by further highlighting considerations for health and husbandry practices.

4.2 Materials and methods

Study subjects

This study used serum and plasma samples from zoo-housed bonobos (*Pan paniscus*), chimpanzees (*Pan troglodytes*), gorillas (*Gorilla gorilla*) and orangutans (*Pongo abelii* and *Pongo pygmaeus*). A total of 473 samples (n=468 serum, n=5 plasma) from 322 animals were measured for vitamin D. Of these, 228 samples are yet to be published, while 245 chimpanzee samples were already published in the form of a peer-reviewed journal article in Scientific Reports (Moittié et al., 2022), which can be found in Appendix C. This thesis chapter is a follow-on from the published chimpanzee study, with additional novel results for the remaining great ape species.

From bonobos, there were 50 samples from 43 individuals. 20 samples were from males, and 30 from females, with an overall age range of 3 to 54 years (median = 18.5 years). From chimpanzees, there were 255 samples from 149 individuals. 100 samples were from males, and 154 from females, one with an unknown sex. The overall age range at the time of sampling was 1 to 65 years (median = 28 years), with age unknown for 4 samples. From gorillas, there were 107 samples from 86 individuals. 49 samples from males, and 58 from females, with an overall age range of 0 to 50 years (median = 14.5 years). From orangutans, there were 61 samples from 44 individuals. 34 samples were from males, and 27 from females, with an overall age range of 4 to 48 years (median = 22 years). A more detailed breakdown of the post-data-processing study animal demographics can be found in Table 4.3.

All samples were collected opportunistically during veterinary procedures at the zoos of origin (n=56 zoos), before being shipped frozen to the UK for subsequent vitamin D measurement. Where necessary, CITES permits and other import paperwork were obtained prior to sample transport. Repeated samples from the same animal were accepted if the sampling dates were at least 60 days (two months) apart.

25-OHD measurement

Once in the UK, serum and plasma samples were sent to a laboratory participating in the UK Accreditation Service (UKAS) Vitamin D External Quality Assessment Scheme (Clinical Biochemistry, Manchester University NHS Foundation Trust, M13 9WL). All samples were analysed at the same laboratory, in as few batches as possible, in order

to minimise analytical variability (Holmes et al., 2013; Viljoen et al., 2011; Ferrari et al., 2017). Measurements of 25-OHD_2, 25-OHD_3, and total 25-OHD were carried out using Liquid Chromatography and tandem Mass Spectrometry (LC-MS/MS). The analysis involved Transcend II liquid chromatography with TurboFlow online sample preparation technology, and a TSQ Endura tandem quadrupole mass spectrometer (Thermo Fisher Scientific), as previously described (Moittié et al., 2020b, 2022). Clinical interpretation of vitamin D status was based on total 25-OHD (the sum of 25-OHD_2 and 25-OHD_3) and was adapted from known human reference ranges (Holick et al., 2011; The Scientific Advisory Committee on Nutrition, 2016; British Association of Dermatologists et al., 2010), since no formal reference ranges currently exist for non-human great apes. The reference ranges used for this study can be found in Table 4.1.

Table 4.1: Reference ranges used for the interpretation of vitamin D status (total 25-OHD, nmol/L) of zoo-housed great apes, as adapted from known human ranges.

Total 25-OHD (nmol/L)	Category
<25	Deficient
25–50	Insufficient
51–75	Adequate
>75	Optimal

Zoo questionnaire and environmental data

In an effort to understand more about the factors affecting vitamin D status in non-human great apes, a survey including questions pertaining to the characteristics, health and husbandry of the study animals was developed and sent to all zoos of sample origin. The questions were filled out per sample, and details about the questions can be found in Table 4.2.

Mean UVB (Daily All Sky Surface UVB Irradiance, W/m^2) at each sampling location in the 60 days prior to sampling was obtained from the National Aeronautics and Space Administration (NASA) Langley Research Center (LaRC) Prediction of Worldwide

Energy Resource (POWER) Project (Data Access Viewer v2.4.2). For this, the latitude and longitude of each zoo of origin was obtained from the Species360 Zoological Information Management System (ZIMS), and an online date calculator (Time and Date AS 1995-2024, n.d.) was used to obtain the starting date for the UVB data time period (60 days prior to the sampling date). The mean UVB (W/m^2) was calculated for each 60-day pre-sampling period and used for further analysis.

To make a map visualising the geographic origins of samples in the context of global UVB irradiance, a different UVB dataset (in J/m^2) was downloaded (Beckmann et al., 2014). This was in the form of geospatial data and encompassed the global annual mean UVB levels from 2004–2013. This was used to build maps using QGIS Desktop v2.18.28 in conjunction with a world map shapefile and CSV files containing the latitude, longitude, and number of samples at each sampling location.

The season of the year was determined in the following way for each sampling date: Spring (21st March–20th June), Summer (21st June–21st September), Autumn (22nd September–20th December), and Winter (21st December–20th March).

The age group category (years) at the time of sampling was determined in the following way: Juvenile (<15 years), Adult (15–34 years), and Elderly (>34 years). While the categories were directly taken from the published chimpanzee study (Moittié et al., 2022), their application across bonobos, gorillas, and orangutans is supported by comparative data on life expectancy and maturational timelines. Juvenile cut-offs are supported by studies that defined “young” chimpanzees with a mean age well below 15 years (Videan et al., 2007b) and placed the end of adolescence at 15 years in both chimpanzees and orangutans (Weiss and King, 2015). Adulthood typically begins in the early teens and extends into the early 30s, with adulthood commonly defined as 15–35 years (Weiss and King, 2015). The elderly category is well supported, as individuals over 34 years are considered aged in studies of physiological and behavioural ageing (Strong et al., 2020; Baker, 2000), and 35+ is described as the onset of old age across great ape species (Lowenstine et al., 2016). Additionally, chimpanzees typically experience reproductive senescence by age 35, supporting this threshold as biologically meaningful (Alberts et al., 2013).

Data analysis

All data were gathered and processed using Microsoft Excel. Any repeated samples from the same individuals that overlapped the same sampling period were removed, keeping only one sample per 60-day period. For samples with 25-OHD concentrations reported as <5 nmol/L, the limit of detection (5 nmol/L) was assigned as the measured value. This conservative approach avoids underestimating values while enabling their inclusion in statistical analyses.

Statistical analysis was carried out using GraphPad Prism (v10.4.0). Shapiro-Wilk normality tests were performed prior to analysis. All variables were tested for significance against total 25-OHD: Continuous variables (UVB [W/m^2] and sample storage time [months]) were tested using parametric Pearson r or non-parametric Spearman r correlation; Binary categorical variables (Sex, sample type, health status, contraception [females only], pregnancy/lactation [females only], Pellets in diet, Supplement in diet, UV lighting/UV permeable materials in enclosure, Outdoor access) were tested using parametric t-tests or non-parametric Mann-Whitney tests; Ordinal categorical variables (Season of the year, Coat quality, Age group, Body condition score) were tested using ANOVA or non-parametric Kruskal-Wallis tests with Dunn's post-hoc test for multiple comparisons. For statistical analysis, the body condition score variable was condensed from nine ordinal levels, to three, where levels 1-3 became "Low (1-3)", levels 4-6 became "Medium (4-6)", and levels 7-9 became "High (7-9)". All variables were first tested using all great apes together, with those producing statistically significant results being further explored at the species level.

Table 4.2: Questionnaire sent to zoos of origin in order to gather additional data regarding vitamin D status of great apes.

Category	Question
Individual characteristics	Animal name
	Species
	GAN (ID #)
	Date of sampling
	What was the animal's coat quality in the 2 months before sampling? 1 = Intact coat cover 2 = Partial hair loss (e.g. due to overgrooming) 3 = Total hair loss (e.g. alopecia)
Health	What was the animal's overall health status in the 2 months before sampling? 1 = Healthy 2 = Abnormal
	Was the animal on contraception in the 2 months before sampling? If yes, what method? 1 = No 2 = Yes
	If female, was the animal pregnant or lactating in the 2 months before sampling? 1 = No 2 = Yes
	What was the animal's body condition score in the 2 months before sampling? On a scale of 1–9, where: 1 = Emaciated 5 = Ideal 9 = Obese
Husbandry	Was there commercial pellet feed in the animal's diet in the 2 months before sampling? If yes, please provide the exact brand and type of pellet. 1 = No 2 = Yes
	Was the animal receiving additional vitamin D supplementation (additional to the core diet/pellets) in the 2 months before sampling? If yes, in what form and dose? 1 = No 2 = Yes
	Did the animal's housing contain any artificial UV lighting or UV-permeable materials in the 2 months before sampling? If yes, please give details. 1 = No 2 = Yes
	Did the animal have unlimited daytime access to outdoors in the 2 months before sampling? If not, please give details. 1 = No 2 = Yes

4.3 Results

A total of 473 vitamin D concentrations were measured, 228 of which are yet to be published, while 245 were already-published chimpanzee data (Moittié et al., 2022). Nine samples were then excluded from further analysis due to overlapping sampling periods (more than one sample within a 60-day period from the same individual), or unknown core information such as animal identification or sampling dates. Thus, 464 samples from 321 individual animals were remaining for further analysis, the majority of which were serum (n=459). A total of 77.8% of the samples were accompanied by corresponding questionnaire data, though not every completed questionnaire had all questions answered.

Of the remaining 464 samples, the majority were from chimpanzees (54.1%, n=251), followed by gorillas (22.8%, n=106), orangutans (12.5%, n=58), and bonobos (10.6%, n=49). The mean age across all species was 23.3 years, with gorillas having the youngest mean age (18.3 years) and chimpanzees the oldest (26.6 years). Age group distribution revealed that gorillas had the highest proportion of juveniles (50.0%, n=53), whereas chimpanzees had the largest proportion of elderly individuals (28.2%, n=70). Females accounted for 57.4% (n=266) of all samples, with the proportion of females highest in chimpanzees (61.2%, n=153) and lowest in orangutans (46.6%, n=27). Samples originated from 55 unique locations, with the number of origin zoos varying by species, ranging from 5 zoos for bonobos to 34 zoos for chimpanzees.

Currently in European zoos, there are 1518 great apes (ZIMS data, 2024), of which 158 (10.4%) are bonobos, 301 (19.8%) are orangutans, 405 (26.7%) are gorillas, and 654 (43%) are chimpanzees. Therefore, as proportions of the total European zoo populations, this study includes 27.2% of all bonobos (from 45.5% of possible locations), 22.6% of all chimpanzees (from 37.4% of possible locations), 21.2% of all gorillas (from 12.4% of possible locations), and 14.6% of all orangutans (from 14% of possible locations).

Full species-specific details about study demographics are provided Table 4.3. Figure 4.1 shows the geographic origins of the samples from each species, in the context of mean global annual UVB (J/m^2) radiation for visualisation purposes.

Table 4.3: Demographics of study animals from which 25-OHD was measured.
For 'Samples/animals', species-specific percentages (%) represent the proportions of all species combined. For the age group and sex distributions, the percentages represent the proportions per species/row.

Species	Samples/ animals	Mean age (years)	Age group distribution	Sex distribution	Origin zoos
All (combined)	n=464 samples n=321 animals	23.3	*Juvenile (<15)*: 31.5% *Adult (15-34)*: 45.9% *Elderly (>34)*: 22.6%	*Female*: 57.4% *Male*: 42.6%	n=55
Bonobos	n=49 samples (10.6%) n=43 animals (13.4%)	19.2	*Juvenile (<15)*: 42.9% *Adult (15-34)*: 44.9% *Elderly (>34)*: 12.2%	*Female*: 59.2% *Male*: 40.8%	n=5
Chimpanzees	n=251 (54.1%) n=148 animals (46.1%)	26.6	*Juvenile (<15)*: 20.2% *Adult (15-34)*: 51.6% *Elderly (>34)*: 28.2%	*Female*: 61.2% *Male*: 38.8%	n=34
Gorillas	n=106 (22.8%) n=86 animals (26.8%)	18.3	*Juvenile (<15)*: 50.0% *Adult (15-34)*: 34.9% *Elderly (>34)*: 15.1%	*Female*: 53.8% *Male*: 46.2%	n=23
Orangutans	n=58 (12.5%) n=44 animals (13.7%)	22.0	*Juvenile (<15)*: 36.2% *Adult (15-34)*: 43.1% *Elderly (>34)*: 20.7%	*Female*: 46.6% *Male*: 53.4%	n=17

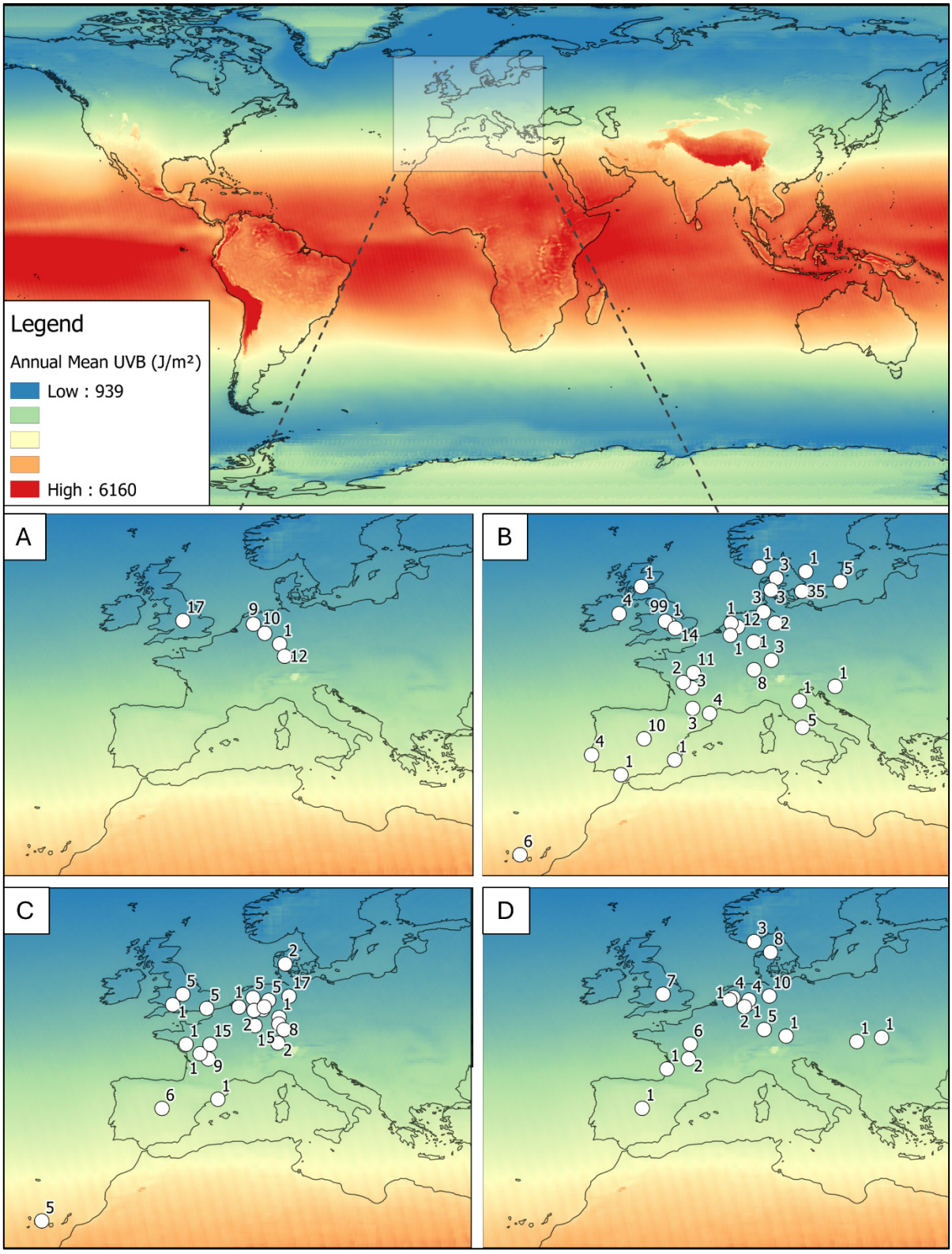

Figure 4.1: Map depicting global annual mean UVB (J/m^2) with corresponding colours ranging from 939 J/m^2 (blue) to 6160 J/m^2 (red), with four sub-maps showing geographic origins of samples from [A]: Bonobos (n=49 samples from 5 zoos); [B]: Chimpanzees (n=251 samples from 34 zoos); [C]: Gorillas (n=106 samples from 23 zoos); [D]: Orangutans (n=58 samples from 17 zoos).
Map created with QGIS Desktop (v2.18.28) using publicly available global UVB data (Beckmann et al., 2014).

Overall 25-OHD status and thresholds

The majority (99.4%) of samples had a total 25-OHD (25-OHD_2 + 25-OHD_3) that was equivalent to their 25-OHD_3 concentration, because the concentration of 25-OHD_2 was below the limit of detection (5 nmol/L) for all except three samples: two gorillas (25-OHD_2 = 9.60 and 5.51 nmol/L) and one bonobo (25-OHD_2 = 23.97 nmol/L). From this point forwards, the vitamin D status and key outcome variable is considered to be total 25-OHD (nmol/L). The proportion of total 25-OHD results that fell below the limit of detection, and were subsequently assigned as such (5 nmol/L), was 1.7% (8/464).

The overall mean 25-OHD concentration across all 464 samples was 54.96 nmol/L. Across all samples, 45.7% were below the human cut-off of ≤50 nmol/L ('Deficient' and 'Insufficient' combined, see Table 4.1), while 54.3% were >50 nmol/L ('Adequate' and 'Optimal' combined). At the species level, bonobos (n=49) had a mean 25-OHD concentration of 37.5 nmol/L, with 71.4% classified as deficient or insufficient (≤50 nmol/L). Chimpanzees (n=251) had the highest mean 25-OHD concentration of 62.16 nmol/L, with 35.9% classified as deficient or insufficient (≤50 nmol/L). Gorillas (n=106) had a mean 25-OHD concentration of 50.95 nmol/L, with 50.0% classified as deficient or insufficient (≤50 nmol/L). Orangutans (n=58) had a mean concentration of 45.88 nmol/L, with 58.6% classified as deficient or insufficient (≤50 nmol/L). This information is detailed in Table 4.4. Figure 4.2 show the overall distributions (median and inter-quartile ranges) of total 25-OHD for each species, while Figure 4.3 details the proportions of samples from each species that fell into each reference range category.

Table 4.4: Mean 25-OHD concentrations (nmol/L) and the proportion (%) of samples from each species that fell within the defined human reference range categories: Deficient (<25 nmol/L), Insufficient (25–50 nmol/L), Adequate (51–75 nmol/L), and Optimal (>75 nmol/L).

Species	Mean 25-OHD (nmol/L)	Deficient (<25 nmol/L)	Insufficient (25–50 nmol/L)	Adequate (51–75 nmol/L)	Optimal (>75 nmol/)
All (combined)	54.96	17.9%	27.8%	31.7%	22.6%
Bonobos	37.50	34.7%	36.7%	22.5%	6.1%
Chimpanzees	62.16	6.4%	29.5%	37.0%	27.1%
Gorillas	50.95	30.2%	19.8%	26.4%	23.6%
Orangutans	45.88	31.0%	27.6%	25.9%	15.5%

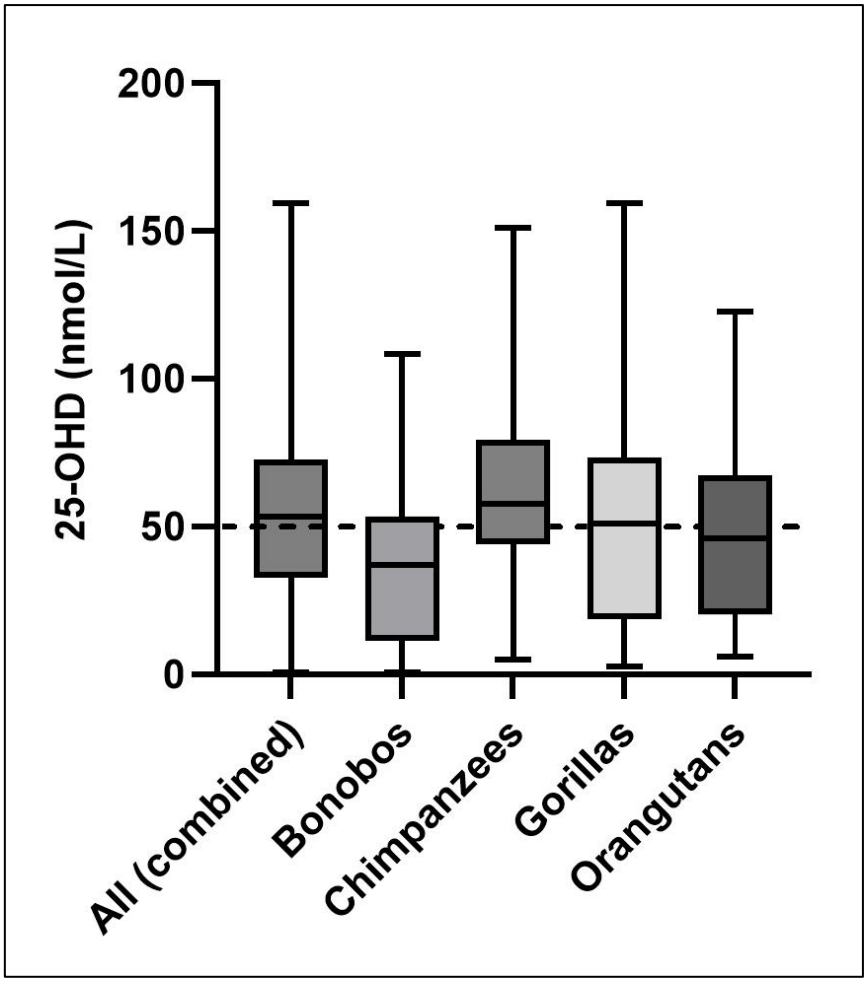

Figure 4.2: Total 25-OHD concentrations (nmol/L) across all species.
Box-and-whisker plots showing the distribution of total 25-OHD concentrations (nmol/L) for all samples combined (n=464) and for each species: bonobos (n=49), chimpanzees (n=251), gorillas (n=106), and orangutans (n=58). The horizontal dashed line at 50 nmol/L indicates the threshold separating insufficient/deficient (≤50 nmol/L) from adequate/optimal (>50 nmol/L) vitamin D status. The box represents the interquartile range (IQR), the horizontal line within each box indicates the median, and the whiskers extend to the minimum and maximum values within 1.5× the IQR.

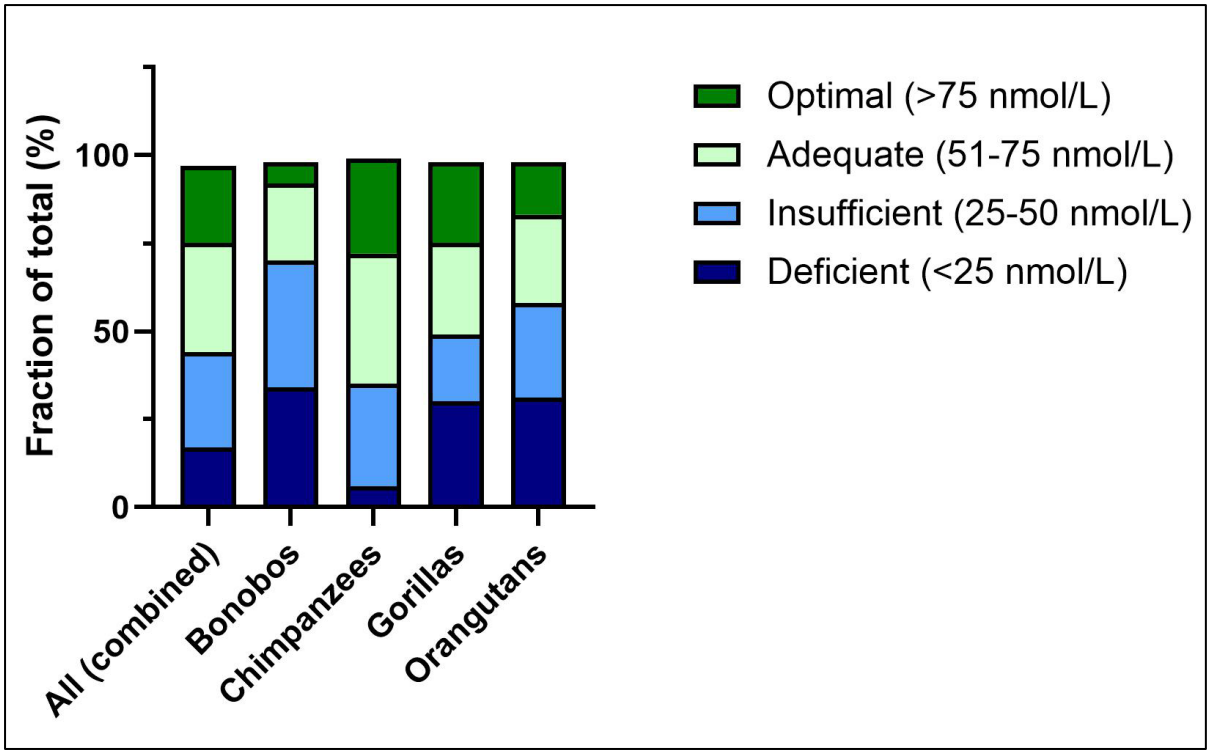

Figure 4.3: Distribution of total 25-OHD concentration categories across species. Stacked bar chart showing the proportion of samples (%) classified as Deficient (<25 nmol/L), Insufficient (25–50 nmol/L), Adequate (51–75 nmol/L), and Optimal (>75 nmol/L) for all samples combined (n=464) and for each species: bonobos (n=49), chimpanzees (n=251), gorillas (n=106), and orangutans (n=58).

Sample storage time and sample type

When all samples were considered together (n=464), there was a very weak but statistically significant negative correlation between sample storage time in months and total 25-OHD (Spearman r = −0.176, p < 0.001). Species-specific analysis revealed a moderate negative correlation in bonobos (Spearman r = −0.496, p < 0.001) and orangutans (Spearman r = −0.550, p < 0.001). No significant correlation was found for chimpanzees (Spearman r = -0.077, p = 0.225) or gorillas (Spearman r = -0.190, p = 0.052). Scatter plots illustrating these relationship are included below in Figure 4.4.

No significant difference in 25-OHD concentrations was observed between serum and plasma samples (n=459 serum, n=5 plasma, Mann-Whitney p = 0.971), as seen in Figure 4.5.

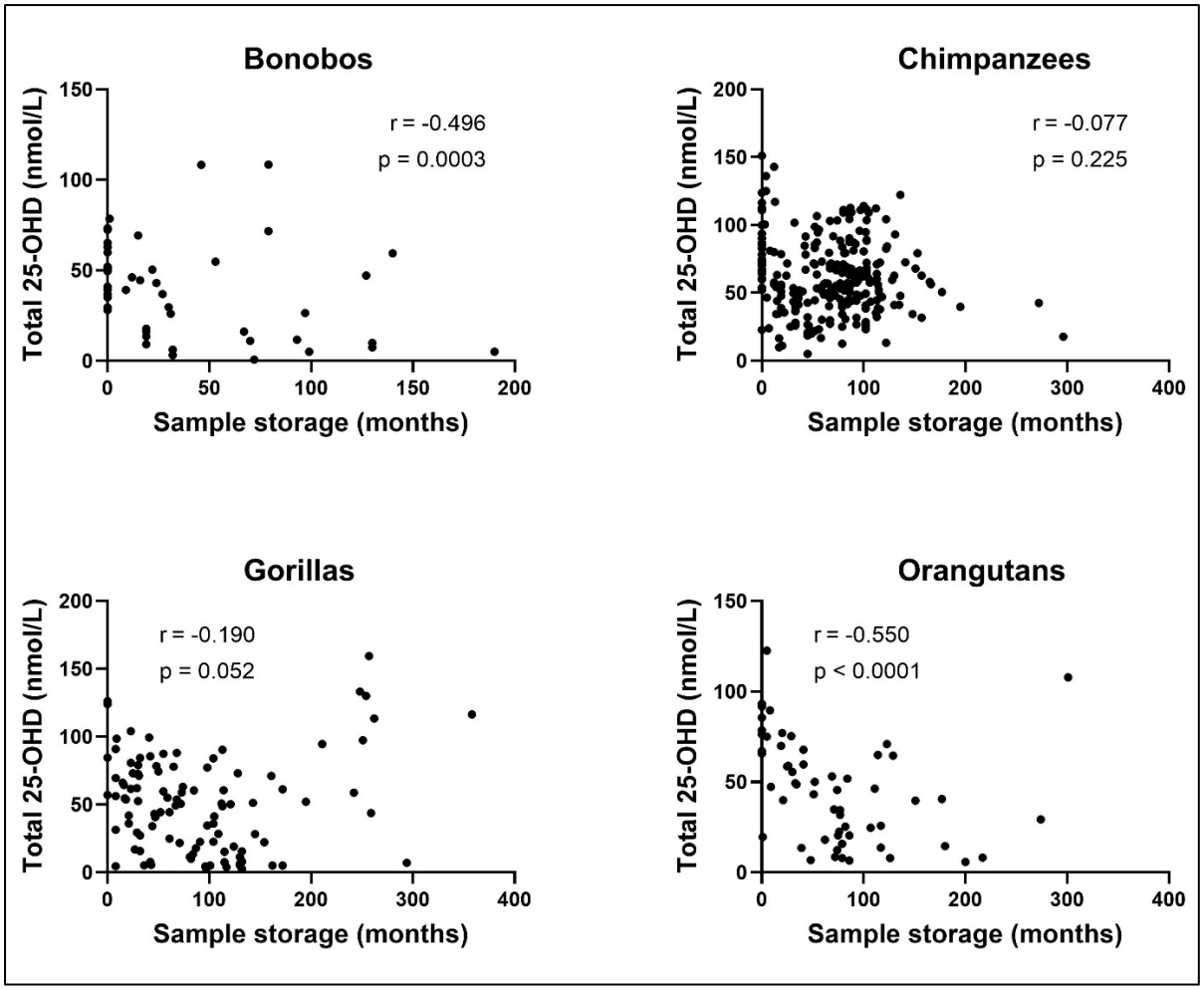

Figure 4.4: Scatterplots showing the relationship between sample storage time (months) and total 25-OHD (nmol/L) for bonobos (n=49), chimpanzees (n=251), gorillas (n=106), and orangutans (n=58).
Each data point represents an individual sample. Spearman r and p values are displayed on each plot.

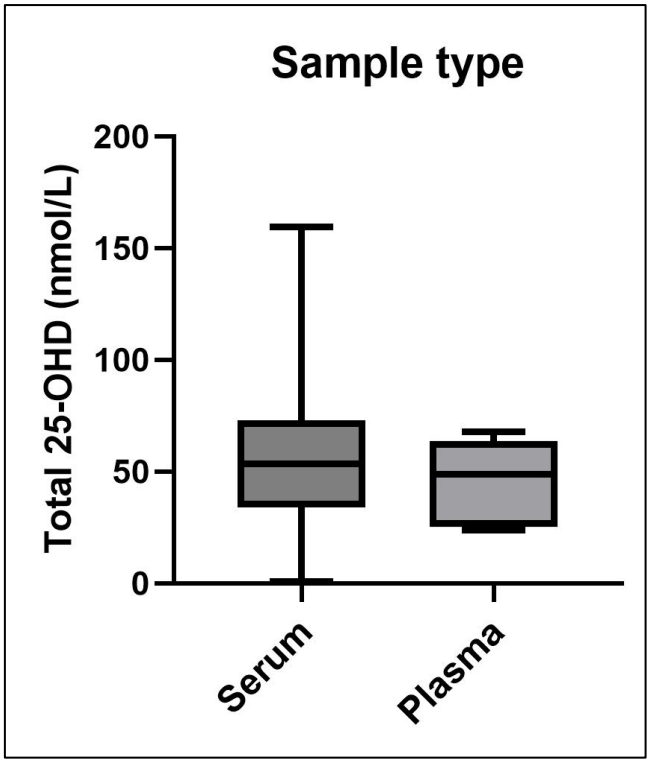

Figure 4.5: Total 25-OHD concentrations (nmol/L) for two sample types, serum and plasma.

Box-and-whisker plots showing the distribution of total 25-OHD (nmol/L) for serum (n=459) and plasma (n=5) samples. Boxes represent the interquartile range (IQR), with the median line shown inside each box, and whiskers extending to the minimum and maximum values. No significant difference in total 25-OHD was observed between the sample types (Mann-Whitney, p = 0.971).

Individual characteristics and health factors

Health status was significantly associated with 25-OHD concentrations when all species were analysed together, whereby animals classed as healthy had significantly higher total 25-OHD than individuals with abnormal health (Mann-Whitney, $p < 0.001$). However, when broken down by species, this association remained significant only in chimpanzees (Mann-Whitney, $p < 0.001$), while no significant differences were observed in bonobos ($p = 0.975$), gorillas ($p = 0.923$), or orangutans ($p = 0.269$). Figure 4.6 highlights the significant association in chimpanzees, and though the other species did not reach significance, there was still a trend towards a higher 25-OHD status in healthy individuals.

When all species were analysed together, coat quality showed a significant association with 25-OHD concentrations (Kruskal-Wallis, $p = 0.027$), with individuals classified as ‘Total hair loss’ showing significantly higher 25-OHD than those with an ‘Intact’ coat. However, cases of total hair loss were reported exclusively in chimpanzees, and in a very small number of samples (n=12 samples from three individuals with alopecia). Further analysis performed on only chimpanzees revealed no observed differences between coat quality categories (n=113 intact coat, n=49 partial hair loss, n=12 total hair loss, Kruskal-Wallis $p > 0.05$), as seen in Figure 4.7.

No significant associations were found between 25-OHD and sex (n=197 Male, n=266 Female, Mann Whitney $p = 0.971$), age group (n=145 Juvenile, n=212 Adult, n=104 Elderly, Kruskal-Wallis $p > 0.05$), body condition score (n=22 Low [1-3], n=236 Medium [4-6], n=38 High [7-9], Kruskal-Wallis $p > 0.05$), or contraception (n=128 None, n=28 Contraception, Mann-Whitney $p = 0.996$), pregnancy status (n=172 Not pregnant, n=6 Pregnant, Mann-Whitney $p = 0.996$), and lactation status in females (n=68 Not lactating, n=14 Lactating, Mann-Whitney $p = 0.996$), as seen in Figure 4.8.

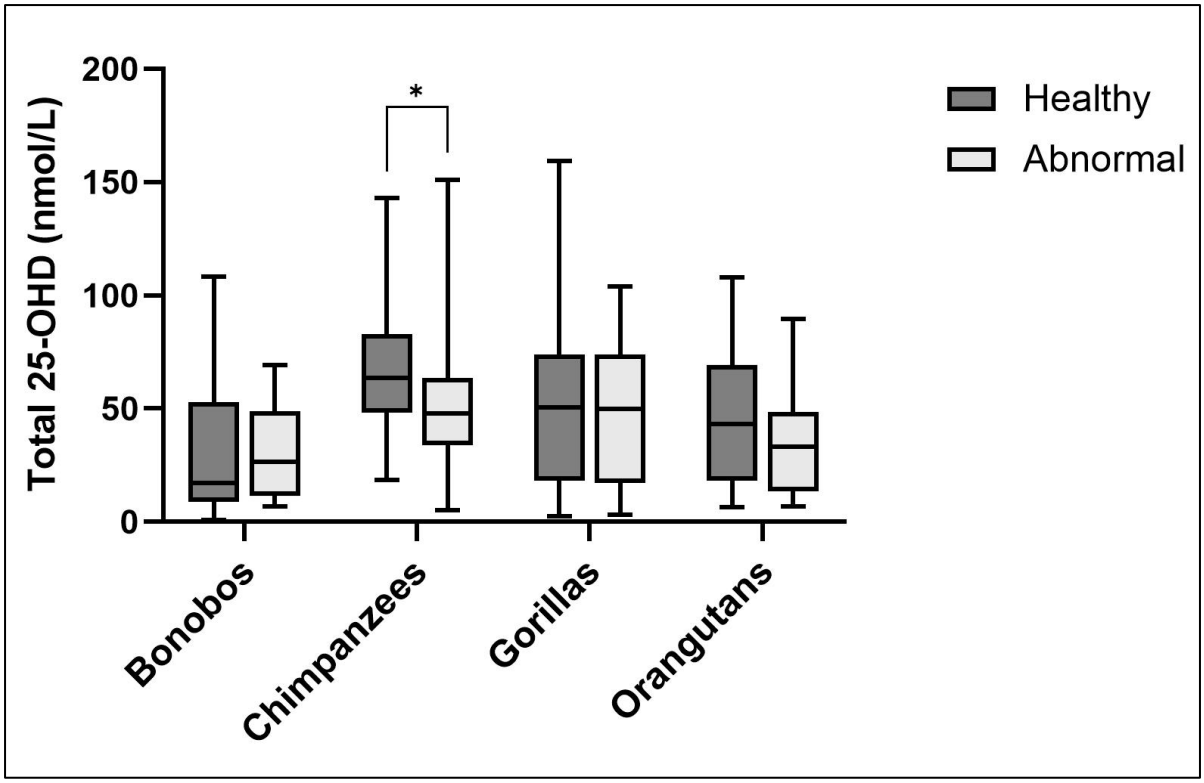

Figure 4.6: Total 25-OHD concentrations (nmol/L) by health status.
Box-and-whisker plots showing the distribution of total 25-OHD concentrations for individuals with healthy and abnormal health statuses across four great ape species: bonobos (n=23), chimpanzees (n=209), gorillas (n=90), and orangutans (n=39). Boxes represent the interquartile range (IQR), with the median line shown inside each box, and whiskers extending to the minimum and maximum values. A significant difference between health statuses was observed in chimpanzees (Mann-Whitney, $p<0.001$), as indicated by the asterisk (*). No significant differences were found for bonobos, gorillas, or orangutans.

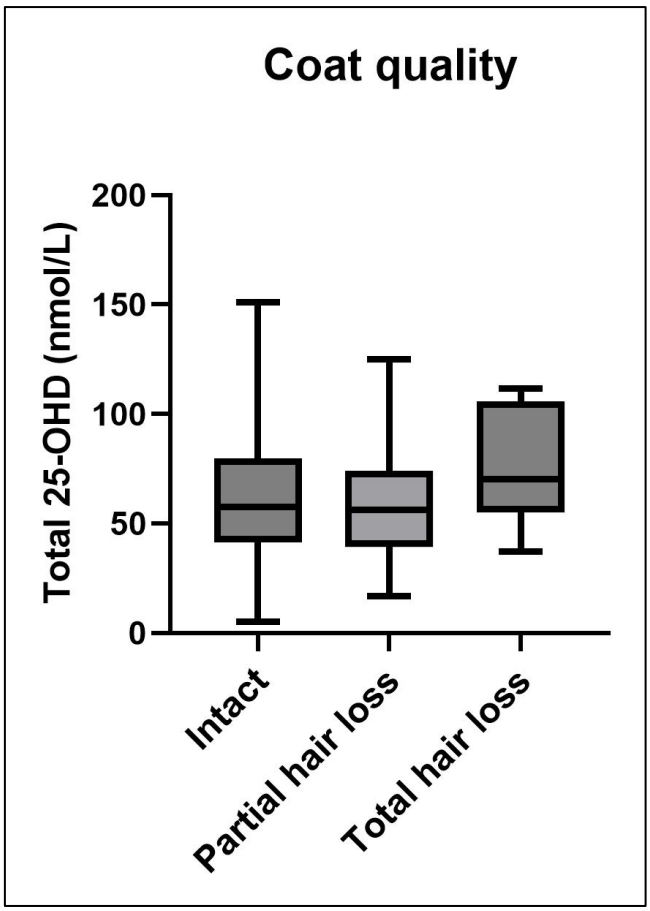

Figure 4.7: Total 25-OHD concentrations (nmol/L) by coat quality.
Box-and-whisker plots showing the distribution of total 25-OHD concentrations of samples from chimpanzees with an intact coat (n=113), partial hair loss (n=49), and total hair loss (n=12). Boxes represent the interquartile range (IQR), with the median line shown inside each box, and whiskers extending to the minimum and maximum values. No significant differences were observed between any of the categories (Kruskal-Wallis, $p > 0.05$).

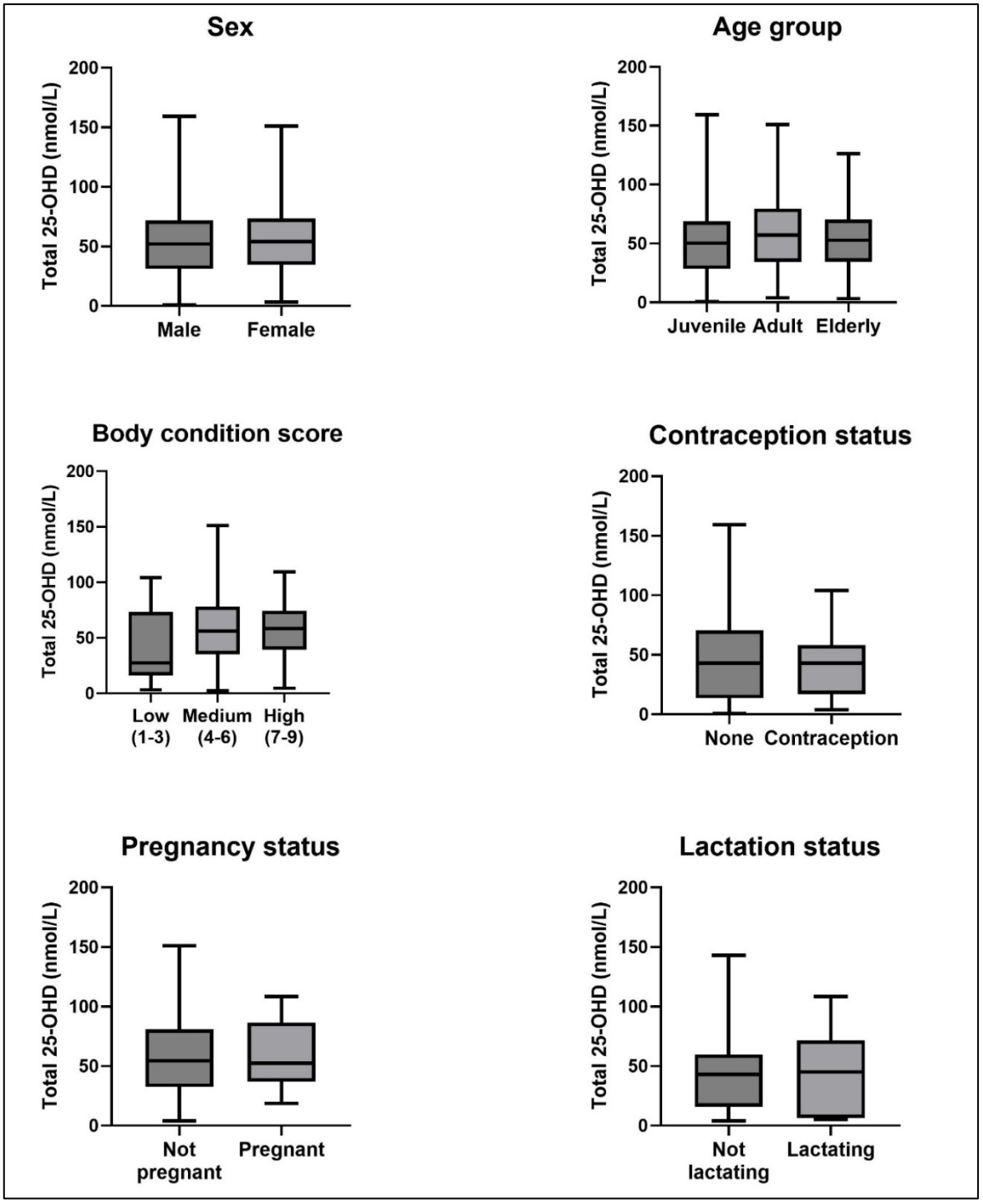

Figure 4.8: Total 25-OHD concentrations (nmol/L) by sex, age group, body condition score, contraception status, pregnancy status, and lactation status.

Boxes represent the interquartile range (IQR), with the median line shown inside each box, and whiskers extending to the minimum and maximum values. No significant differences were found for any of the variables: sex (n=197 Male, n=266 Female, Mann Whitney p = 0.971); age group (n=145 Juvenile, n=212 Adult, n=104 Elderly, Kruskal-Wallis p > 0.05); body condition score (n=22 Low [1-3], n=236 Medium [4-6], n=38 High [7-9], Kruskal-Wallis p > 0.05); contraception status (n=128 None, n=28 Contraception, Mann-Whitney p = 0.996); pregnancy status (n=172 Not pregnant, n=6 Pregnant, Mann-Whitney p = 0.996); or lactation status in females (n=68 Not lactating, n=14 Lactating, Mann-Whitney p = 0.996).

Environmental factors

Total 25-OHD concentrations varied significantly according to the season when all species were combined (Kruskal-Wallis, $p < 0.001$). Species-specific analyses revealed significant seasonal effects in bonobos (Kruskal-Wallis, $p = 0.002$), chimpanzees ($p < 0.001$), and gorillas ($p < 0.001$), but no significant differences were observed in orangutans. Figure 4.9 shows the seasonal variations in 25-OHD for each of the species.

UVB data were unavailable for samples collected prior to 2001 (n = 6), and these samples were excluded from this part of the analysis. The distribution of UVB irradiance levels at each sampling location in the 60 days prior to sampling can be seen in the form of a histogram in Figure 4.10.

A weak positive correlation was observed between UVB irradiance (W/m^2) and total 25-OHD concentrations across all species (Spearman $r = 0.341$, $p < 0.001$). Species-specific analyses demonstrated significant positive correlations between UVB and 25-OHD concentrations in bonobos (Pearson $r = 0.487$, $p < 0.001$), chimpanzees (Spearman $r = 0.312$, $p < 0.001$), and gorillas (Pearson $r = 0.512$, $p < 0.001$), but not in orangutans (Pearson $r = 0.200$, $p = 0.139$). Figure 4.11 displays the relationship between UVB and total 25-OHD concentrations for all species.

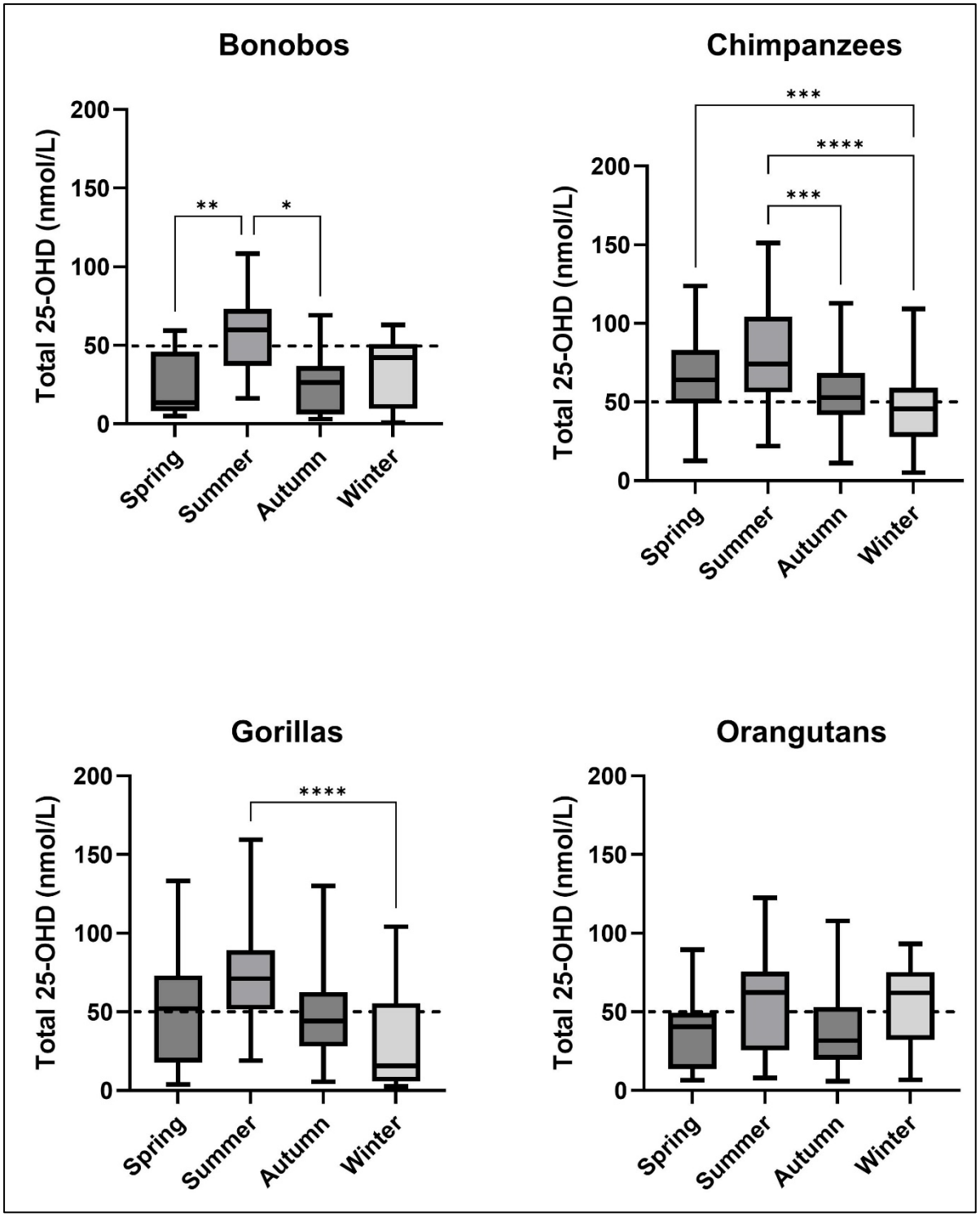

Figure 4.9: Seasonal variation in total 25-OHD concentrations (nmol/L) for each species.

Box-and-whisker plots showing the distribution of total 25-OHD concentrations (nmol/L) across four seasons (Spring, Summer, Autumn, and Winter) for bonobos (n=49), chimpanzees (n=251), gorillas (n=106), and orangutans (n=58). Pairwise comparisons between seasons are indicated with asterisks: *p < 0.05, **p < 0.01, ***p < 0.001, ****p < 0.0001 (Kruskal-Wallis tests with Dunn's multiple comparisons). The dashed horizontal line represents the threshold for insufficient/deficient vitamin D (≤50 nmol/L).

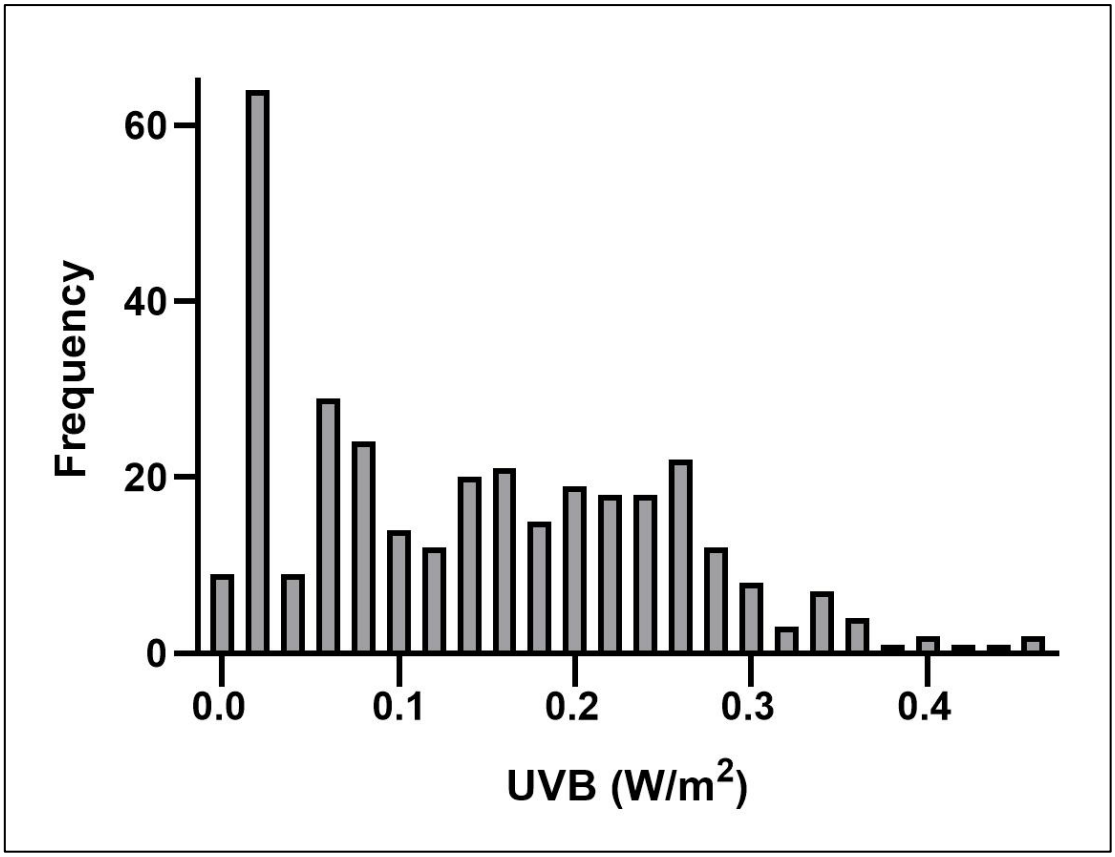

Figure 4.10: Frequency distribution of UVB irradiance (W/m²) across all samples. The histogram shows the range and frequency of UVB irradiance as calculated for each sample in the 60 days prior to sampling.

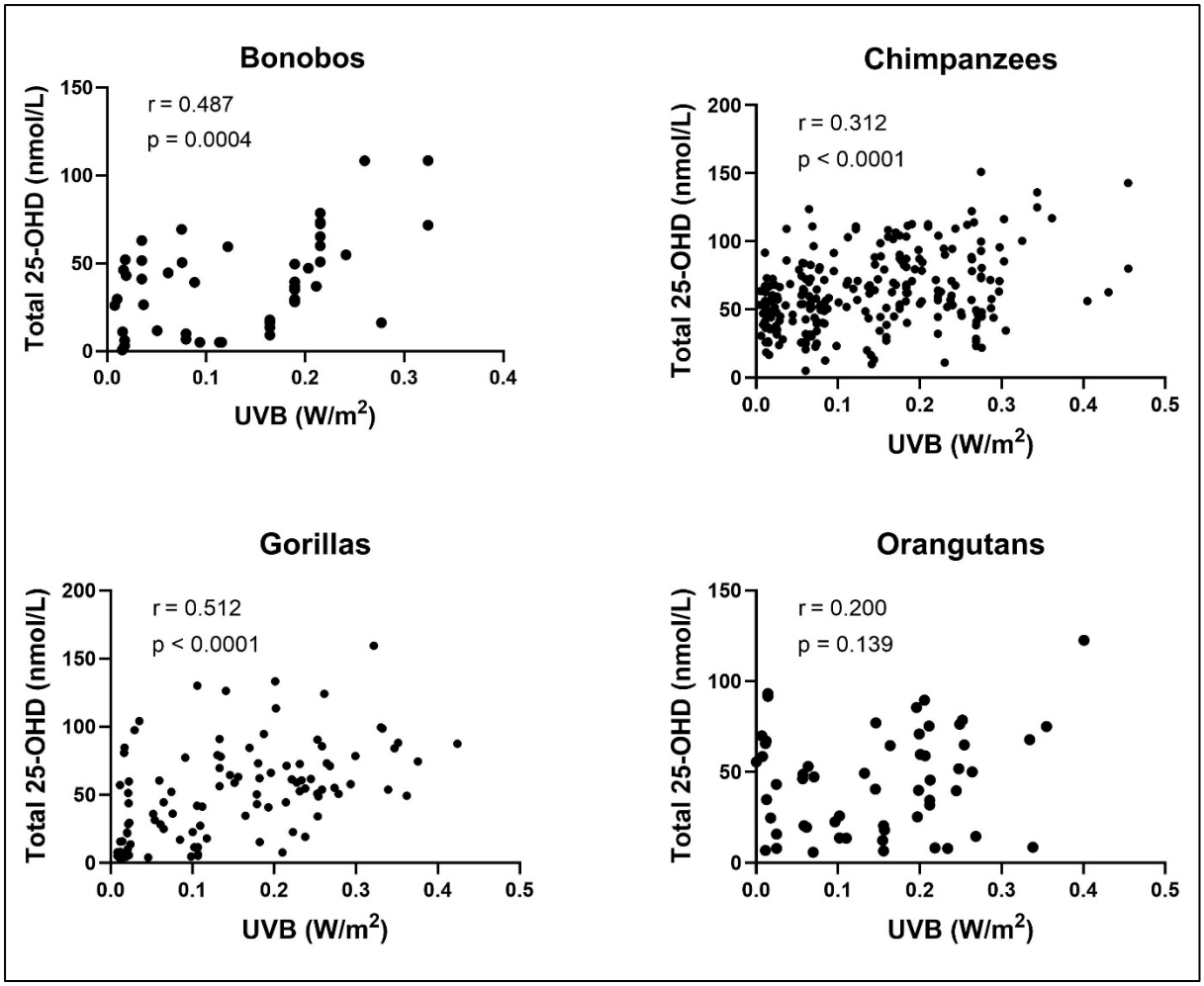

Figure 4.11: Relationship between UVB irradiance and total 25-OHD concentrations for each species.

Scatterplots showing the relationship between UVB irradiance (W/m²) and total 25-OHD concentrations (nmol/L) for bonobos (n=49), chimpanzees (n=251), gorillas (n=106), and orangutans (n=58). Each data point represents an individual sample. Spearman or Pearson r and p values are displayed on each plot.

Husbandry factors

Among the husbandry factors examined, outdoor access was significantly associated with 25-OHD concentrations when all species were analysed together (Mann-Whitney, $p < 0.001$). Species-specific analyses revealed a significant association only in chimpanzees (Mann-Whitney, $p < 0.001$), while no significant differences were observed in bonobos ($p = 0.238$), gorillas ($p = 0.160$), or orangutans ($p = 0.745$). In bonobos, chimpanzees and gorillas, outdoor access was associated with higher 25-OHD, although statistical significance was reached only in the chimpanzee dataset (see Figure 4.12).

Similarly, the presence of pellets in the diet was significantly associated with 25-OHD concentrations across all species (Mann-Whitney, $p < 0.001$). Species-specific results showed significantly higher 25-OHD in chimpanzees ($p = 0.050$) and orangutans ($p = 0.003$) that had pellets included in their diet, while the statistical tests could not be performed for bonobos or gorillas due to there being no reports of individuals with no pellets in their diet (see Figure 4.13).

Neither vitamin D supplement use (n=242 No, n=65 Yes, Mann-Whitney $p = 0.234$), nor the presence of UV lighting or UV-permeable materials in enclosures (n=155 No, n=6 Yes, Mann-Whitney $p = 0.742$, were significantly associated with 25-OHD concentrations, as seen in Figure 4.14.

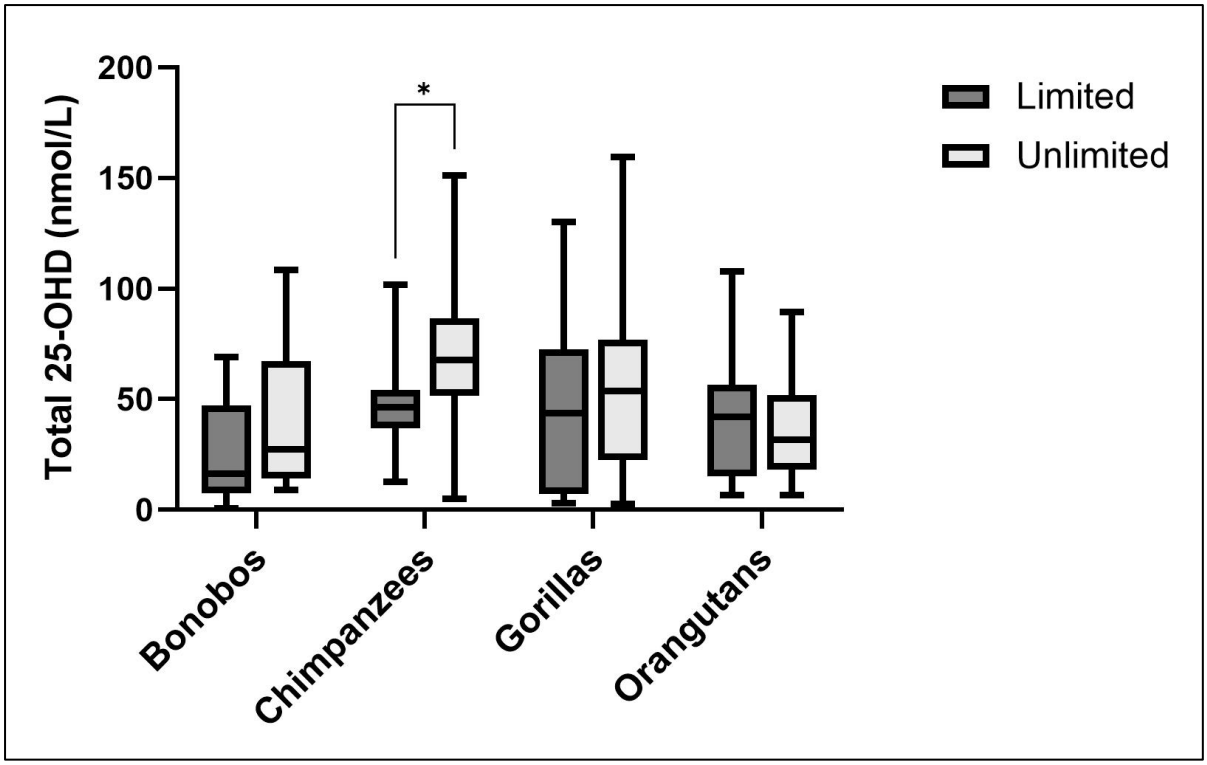

Figure 4.12: Total 25-OHD concentrations (nmol/L) by outdoor access.
Box-and-whisker plots showing the distribution of total 25-OHD concentrations for individuals with limited and unlimited outdoor access across four great ape species: bonobos (n=23) chimpanzees (n=189), gorillas (n=91), and orangutans (n=41). Boxes represent the interquartile range (IQR), with the median line shown inside each box, and whiskers extending to the minimum and maximum values. A significant difference between outdoor access groups was observed in chimpanzees (Mann-Whitney, $p<0.001$), as indicated by the asterisk (*). No significant differences were found for bonobos, gorillas, or orangutans.

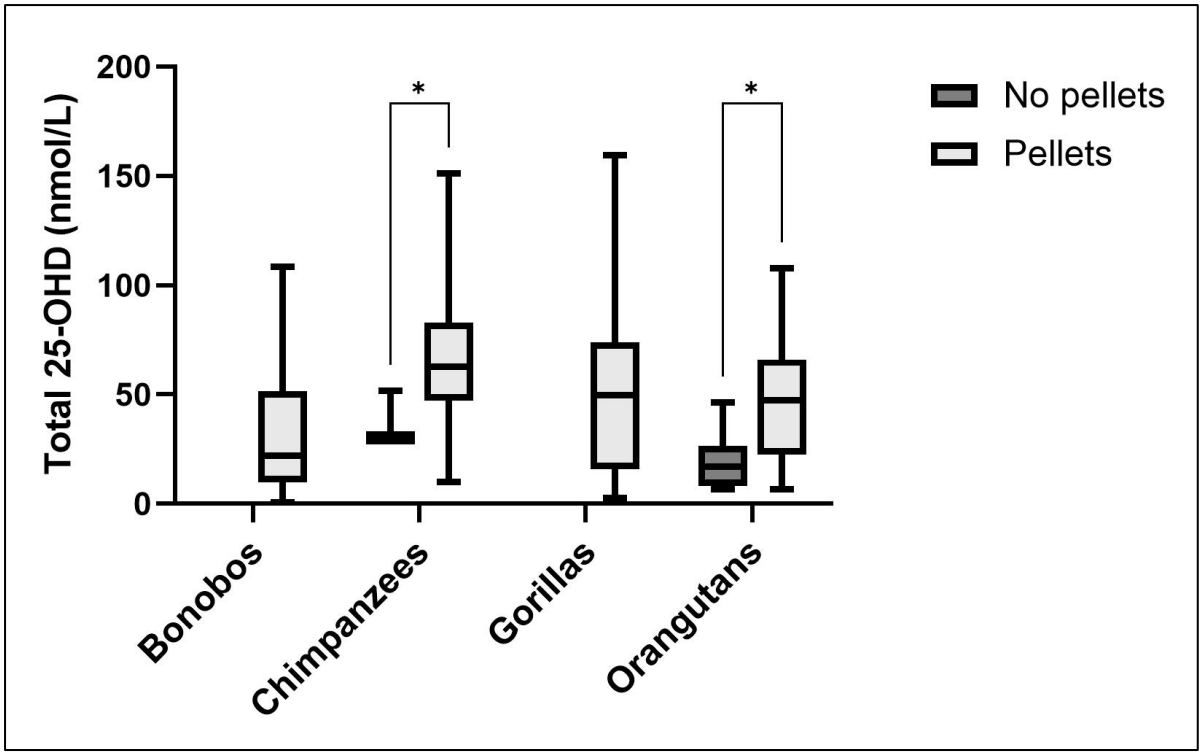

Figure 4.13: Total 25-OHD concentrations (nmol/L) by presence of pellets in the diet. Box-and-whisker plots showing the distribution of total 25-OHD concentrations for individuals with no pellets and pellets in their diet across four great ape species: bonobos (n=22), chimpanzees (n=181), gorillas (n=88), and orangutans (n=39). Boxes represent the interquartile range (IQR), with the median line shown inside each box, and whiskers extending to the minimum and maximum values. Significant differences were observed in chimpanzees and orangutans, with higher 25-OHD concentrations in individuals consuming pellets (Mann-Whitney, $p<0.001$), as indicated by the asterisks (*). Data for bonobos and gorillas are presented for comparison only, as all individuals in these species consumed pellets, precluding statistical comparisons.

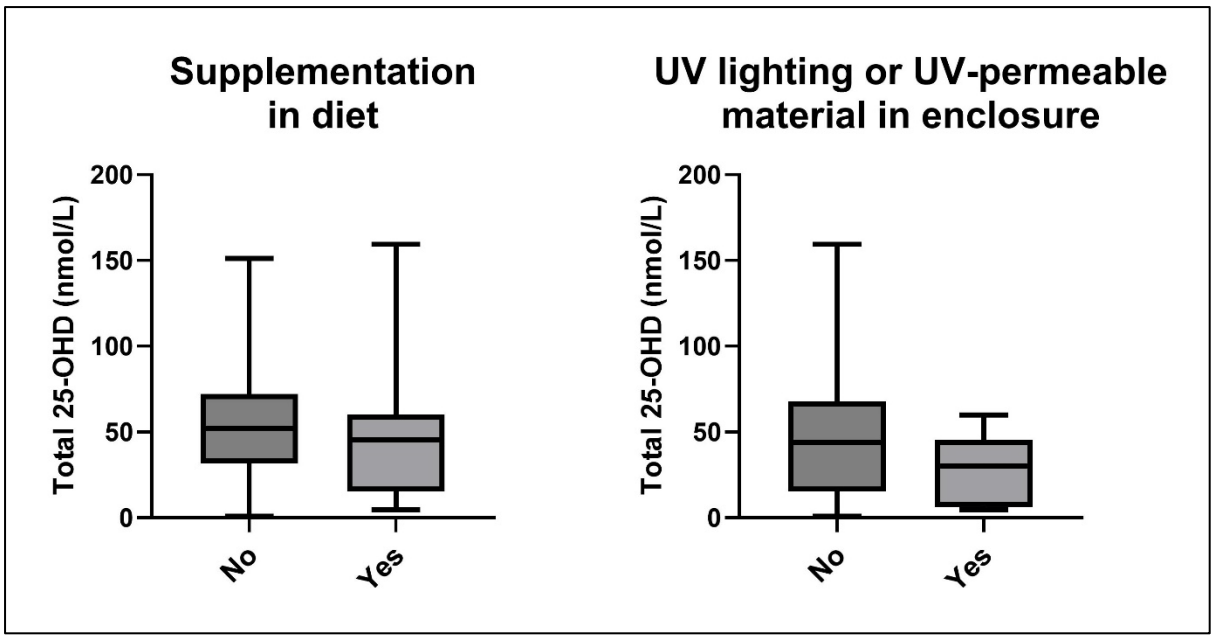

Figure 4.14: Total 25-OHD concentrations (nmol/L) by presence of supplementation in diet (left), and presence of artificial UV lighting or UV-permeable materials in enclosures (right).

Boxes represent the interquartile range (IQR), with the median line shown inside each box, and whiskers extending to the minimum and maximum values. No significant difference in total 25-OHD (nmol/L) was observed for supplementation in diet (n=242 No, n=65 Yes, Mann-Whitney p = 0.234), nor UV lighting or UV-permeable materials in enclosures (n=155 No, n=6 Yes, Mann-Whitney p = 0.742).

4.4 Discussion

This study investigated vitamin D (25-OHD) status in zoo-housed great apes across Europe, building on previous research (Moittié et al., 2022) to explore species-specific variability and the influence of individual, environmental and husbandry factors on vitamin D status in a larger cohort.

Overall 25-OHD status and thresholds

Across all samples, 45.7% were classified as vitamin D deficient or insufficient (≤50 nmol/L), indicating a risk of widespread vitamin D inadequacy in the zoo-housed great ape population in Europe. This raises major concerns about potential implications for great ape populations in human care, particularly given vitamin D's important role in immune function, musculoskeletal and cardiovascular health, among other physiological processes (Pilz et al., 2011; Wang et al., 2020; Ware et al., 2020; Szodoray et al., 2008; Schwalfenberg, 2011; Deluca et al., 2013). Bonobos exhibited the highest proportion of vitamin D deficient and insufficient samples (71.4%), followed by orangutans (58.6%), gorillas (50.0%), and chimpanzees (35.9%). Given that bonobos are the lowest in number in European zoos, this finding is of significant concern. The relatively higher vitamin D levels in chimpanzees may reflect better alignment of husbandry practices with their physiological requirements or enhanced UVB exposure. However, this observation could also be influenced by the larger sample size and broader geographic representation for chimpanzees, which reduces the risk of sampling bias compared to the other species.

An important overall consideration is to look at the sample sizes from each species as proportions of the total European zoo populations. While the absolute number of samples for bonobos may appear low (n=49), this actually represents 27.2% of the entire European bonobo population, sampled from nearly half (45.5%) of all bonobo-holding zoos. This is the highest proportion of all the species, and is a major strength in the study, especially given that bonobos are relatively less studied among the great apes – a simple literature database search returned 1304 results for bonobos, 10065 for chimpanzees, 5557 for gorillas, and 2542 for orangutans. In comparison, the study included 22.6% of all chimpanzees (from 37.4% of chimpanzee-holding zoos), 21.2%

of gorillas (from 12.4% of gorilla-holding zoos), and 14.6% of orangutans (from 14% of orangutan-holding zoos).

Sample storage time and sample type

Sample storage time showed a weak but statistically significant negative correlation with 25-OHD concentrations, suggesting minor degradation of vitamin D metabolites over time. While previous research has shown mixed results regarding this (Colak et al., 2013; Agborsangaya et al., 2010; Drammeh et al., 2008), vitamin D is generally considered highly stable in serum and plasma, even during long-term storage (Wielders and Wijnberg, 2009). In this study, the effect size of the correlation was small, indicating minimal impact of storage time on the statistical outcomes for this variable. Importantly, further analyses revealed that excluding older samples did not alter the statistical results, and the inclusion of all samples was deemed biologically relevant. Additionally, it is possible that older samples reflect genuinely lower 25-OHD concentrations due to historical differences in husbandry practices, such as less emphasis on outdoor access or dietary supplementation. In future, it would be interesting to explore whether there should be a maximum acceptable length of sample storage time before 25-OHD measurement, particularly in zoological settings where storage conditions may be less standardised than in human clinical contexts.

No significant differences were observed between serum and plasma samples, supporting the validity of using both sample types in vitamin D assessments as reported elsewhere (Colak et al., 2013; Zhang et al., 2014).

Individual characteristics and health factors

Health status was significantly associated with 25-OHD concentrations when all species were combined, with healthy individuals exhibiting higher 25-OHD than those with reported abnormal health. While this study cannot infer causality or determine the direction of this relationship, the association aligns with previous research suggesting that low vitamin D levels are linked to increased susceptibility to various health conditions, including cardiovascular disease (Pilz et al., 2010; Wang et al., 2020; Carbone et al., 2023; Mozos and Marginean, 2015; Nizami et al., 2019; Perge et al., 2019; Wang et al., 2012). While vitamin D deficiency may not directly cause conditions like IMF, it could exacerbate underlying cardiovascular pathology by contributing to hypertension, endothelial dysfunction, and vascular inflammation (Rostand, 1997; Pilz

et al., 2009). At the species level, this association was significant only in chimpanzees, possibly reflecting the larger sample size or species-specific health vulnerabilities, such as the reported high prevalence of IMF in chimpanzees compared to other great apes (Strong et al., 2018b, 2020). However, based on the wider research group's (unpublished) findings, a similar high prevalence of IMF in bonobos cannot be ruled out, despite a relative underrepresentation in the dataset (due to their lower population size). Although the trends in bonobos and gorillas suggest lower 25-OHD concentrations in individuals with abnormal health status, these relationships did not reach statistical significance, possibly due to smaller sample sizes or fewer zoos represented. Future research using controlled, longitudinal studies following the same individuals through different health states (e.g., chronic disease versus acute illness) would provide greater insight into the relationship between vitamin D status and health outcomes, and explore whether vitamin D deficiency influences disease progression.

Coat quality was significantly associated with 25-OHD concentrations when all species were analysed together, with individuals classified as having 'Total hair loss' exhibiting higher 25-OHD concentrations compared to those with an 'Intact' coat. This finding is likely explained by increased UVB penetration through exposed skin, enhancing cutaneous vitamin D synthesis in hairless individuals (Holick et al., 1980, 1981; Engelsen et al., 2005; Webb et al., 1988). However, it is important to note that cases of total hair loss were rare, and occurring only in chimpanzees. Furthermore, species-specific analysis in chimpanzees did not reveal significant differences between coat quality categories, limiting the generalisability of this finding.

Other individual characteristics, including sex, age group, body condition score, and contraception, pregnancy, and lactation in females, were not significantly associated with vitamin D levels in this study. This contrasts with findings from (Feltrer-Rambaud et al., 2023), which reported that female chimpanzees in range-country sanctuaries had higher 25-OHD concentrations than males, and adults had higher levels than infants. As one of the most comprehensive datasets from range countries, this study offers valuable insights into what might be expected under more natural conditions. In humans, elderly individuals typically have lower serum 25-OHD (MacLaughlin and Holick, 1985; Parfitt et al., 1982), and higher body fat composition is associated with lower vitamin D status (Wortsman et al., 2000). Pregnancy and lactation are known to influence vitamin D status in humans, with links to deficiency (Hollis and Wagner,

2004; Specker, 1994). Similarly, the use of hormonal contraception has been associated with increased 25-OHD concentrations (Harmon et al., 2016). In this study, the lack of significant findings may partly reflect the small number of reported cases for some variables, which likely reduced statistical power.

Environmental factors

Environmental variables, UVB irradiance and seasonality, emerged as key determinants of vitamin D status. A moderate positive correlation between UVB exposure and 25-OHD concentrations was observed across all species, with the strongest relationships in bonobos and gorillas. Seasonal effects were also significant, with higher concentrations observed in summer and autumn compared to winter and spring. This finding aligns with well-established knowledge about the role of UVB exposure in cutaneous vitamin D synthesis and the seasonal variability of UVB availability (O'Neill et al., 2016; Webb et al., 1988).

Interestingly, orangutans did not exhibit significant associations with UVB irradiance or seasonality. This divergence may partly reflect the relatively small sample size and limited geographic representation, which could have reduced statistical power and obscured potential relationships with environmental variables. Additionally, winter results being higher in orangutans cannot be easily explained by physiological adaptations, and it is more likely influenced by husbandry practices, such as dietary supplementation or differences in outdoor access across seasons. While orangutans are genetically divergent from the other great ape species, and may indeed possess physiological differences (e.g., skin pigmentation, hair density) that affect UVB-driven vitamin D synthesis, further research would be needed to explore this unusual result.

It is clear from the histogram of UVB irradiance that the majority of samples were collected under relatively low natural UVB exposure. Average annual UVB irradiance in the natural ranges of great apes is typically ≥0.3 W/m² (NASA LaRC POWER Project, Data Access Viewer v2.0.0). Only 5.6% (26/464) of samples in this study were from individuals exposed to comparable UVB levels in the 60 days prior to sampling, with five of these samples originating from a zoo in Tenerife. This highlights the potential inadequacy of solar UVB irradiance in Europe compared to the natural ranges of great ape species. The samples from Tenerife provided a valuable addition to this dataset, as they were collected under UVB irradiance levels closer to those

found in great ape natural ranges (≥0.3 W/m^2). Although only 11 samples originated from there (n=6 chimpanzees; n=5 gorillas), the mean UVB irradiance was 0.28 W/m², compared to an average of 0.14 W/m² across all other samples. This difference highlights the importance of obtaining more samples from locations that more closely match the species' natural ranges. It also supports the idea that UVB irradiance could be a more important variable than season alone for evaluating vitamin D status, as UVB exposure can vary substantially within the same season depending on geographic location. As research expands to include a wider geographic range, including the Southern Hemisphere where seasonality patterns are reversed, UVB irradiance will provide a consistent and biologically relevant measure of solar exposure.

Husbandry factors

Outdoor access was significantly associated with 25-OHD concentrations across all species, with individuals provided with unlimited daytime access to outdoor areas exhibiting higher vitamin D levels compared to those with limited access. However, when analysed by species, this association reached statistical significance only in chimpanzees, a result that persisted even when considering summer samples alone. The smaller sample sizes for bonobos and gorillas may have reduced statistical power to detect significant associations, though observed trends suggest outdoor access is likely an important husbandry factor for these species as well. It is also worth noting that all bonobos and gorillas in this study received nutritional supplementation via pellets, which may have partially masked the impact of outdoor access on vitamin D levels. Similarly to the environmental factors (UVB and seasonality), orangutans' vitamin D status did not seem to respond in the same way to the provision of unlimited outdoor access. Further research is needed to explore these species-specific patterns and their implications for husbandry practices.

The provision of commercial pellets in the diet was another important factor for vitamin D status, with chimpanzees and orangutans that were receiving pellets exhibiting higher 25-OHD concentrations. This is the first study to demonstrate a clear positive impact of pellet consumption on vitamin D levels in zoo-housed great apes, underscoring the importance of dietary fortification, particularly in regions with limited UVB availability. While it was not possible to assess this relationship in bonobos and gorillas, because all individuals for whom dietary information was available were

consuming pellets, this finding has important implications for zoo management. There is ongoing discussion in the literature regarding both the benefits and drawbacks of pellet feeding. While fortified pellets provide essential nutrients, including vitamin D, their use has also been associated with behavioural issues such as increased regurgitation and reingestion in great apes (Mulder et al., 2016; Cabana et al., 2018; Less et al., 2014). Consequently, some zoos have moved towards pellet-free diets, which may inadvertently compromise vitamin D status. It is highly challenging to quantify dietary vitamin D intake at the individual level, as zoo-housed great apes are typically scatter-fed as a group, making it difficult to determine exact consumption. However, this study demonstrates an overall potential benefit of pellet supplementation, and a retrospective study using matched comparisons could provide further insights into its specific impact on vitamin D status. Additionally, controlled dietary studies focusing solely on changes in vitamin D intake, while minimising other husbandry changes, would be valuable for confirming these findings and guiding evidence-based management practices.

The limited number of reports regarding the use of supplements (14% of all samples) and UV-related interventions, including UV lighting and UV-permeable materials (1.3% of all samples), likely contributed to the lack of statistical significance observed in this study. However, this does not rule out their potential importance in influencing vitamin D status in zoo-housed great apes. In this study, UV lighting and UV-permeable materials were analysed together as a single variable due to the small number of cases for each. However, it would be important for future research to examine these factors independently to better assess their individual efficacy. While no published studies have explored UVB lighting or UV-permeable materials in great apes, studies in other zoo-housed taxa have demonstrated their efficacy in improving vitamin D status (Woodhouse and Rick, 2016; Baines et al., 2016). As the awareness and implementation of these strategies become more widespread, they are likely to emerge as more prominent determinants of vitamin D concentrations in future research. It is important to note that the implementation of artificial UVB lighting poses logistical challenges, including maintenance, space constraints, and cost (Baines and Cusack, 2019; Bernard et al., 1997), which may make it prohibitive for many great ape facilities. Oral supplementation, on the other hand, is a more logistically feasible approach, and it has the potential to be more cost-effective (Hiligsmann et al., 2015).

While results from human studies remain mixed regarding the efficacy of vitamin D supplementation (Ford et al., 2014; Moslemi et al., 2022; Scragg et al., 2017; Ala-Houhala et al., 2012; Bogh et al., 2012), and the results of this study do not support its use, it may still hold potential especially in regions with limited UVB availability, though more work is needed to clarify this.

Future directions

Future research should prioritise the development of species-specific 25-OHD reference ranges and explore longitudinal changes in vitamin D status to better understand its clinical relevance to health outcomes in these species. Additionally, controlled trials investigating the efficacy of a pellet-based diet, additional dietary supplementation, UVB lighting, and outdoor access would offer valuable insights into evidence-based husbandry practices.

Here, the data variables were explored individually. However, more complex statistical analysis such as mixed models would be highly beneficial so that the many variables and their interactions with each other, as well as with 25-OHD, and the repeated measures, can be evaluated in a more robust manner. This would be especially important for the variables that are likely to have a similar impact on vitamin D status, such as UVB, season, and outdoor access.

To improve the statistical power of the conclusions drawn for bonobos and orangutans, a higher number of samples from these species would be necessary. For instance, the bonobo samples originated from only five different zoos, all of which were situated in northern Europe (latitudes >46°N) and likely lead to skew in bonobo results (i.e. samples from locations with lower UVB levels). However, there are major practical challenges in obtaining more samples from these species, as they represent much smaller population sizes in zoos.

Expanding the geographic scope of this research to include zoos outside of Europe and incorporating more range-country populations will provide a more comprehensive perspective on naturalistic vitamin D concentrations and their determinants, but only if the same methodology is used between studies in order to facilitate accurate comparisons (Ferrari et al., 2017; Holmes et al., 2013). In fact, work is currently underway by the author of this thesis and the wider research group to obtain samples from Singapore, Australia, and Cameroon, in an effort to achieve this.

Due to the potential impact of such low vitamin D status on health outcomes in these species, the relationship between cardiovascular health and vitamin D status should be more closely examined. This is challenging, due to the requirement of obtaining paired serum or plasma samples with post-mortem cardiovascular histopathology. Due to time constraints, it was not possible to include in this thesis, though such a dataset is currently being gathered and is expected to be explored in more detail at a later point, when a larger sample size is obtained.

Conclusions

This study reveals an extremely prominent risk of vitamin D deficiency, a potential risk factor for CVD, in all zoo-housed great apes. The multifactorial nature of vitamin D status, and the importance of UVB exposure, diet, and outdoor access, has been highlighted. However, the study also raises important questions about interspecies differences in vitamin D requirements and metabolism, which require further investigation. Bonobos and orangutans appear particularly vulnerable to low 25-OHD levels under managed care, which may necessitate targeted interventions to improve their wellbeing. Overall, this study provides a novel and valuable contribution to our understanding of vitamin D status in zoo-housed great apes, identifying key areas for husbandry improvements and further investigation.

THESIS CONCLUSIONS

This thesis has investigated the health of zoo-housed great apes, with a specific focus on CVD. In particular, IMF, a poorly understood but prevalent phenotype that can lead to sudden death, was investigated. Across four research chapters, novel insights were gained through a comprehensive approach involving biomarker discovery, proteomic and gene expression analyses, and a large-scale assessment of vitamin D status in great apes.

The first chapter identified potential serum biomarkers of IMF in chimpanzees. Through an advanced multiplex immunoassay, significant differences in the expression of three biomarkers between healthy individuals and those affected by IMF were detected, including AXL, ICAM-2 and PECAM-1. In further validation testing with ELISA, one marker, ICAM-2, showed continued promise as a non-invasive diagnostic tool with the potential to aid ante-mortem detection and intervention, reducing the reliance on retrospective post-mortem analyses. ICAM-2 showed a high specificity and strong diagnostic utility in confirming disease, though its ability to rule out disease was weaker (i.e. no false positives, but some false negatives). Future studies should aim to investigate these biomarkers in a larger cohort and across different species, incorporating longitudinal data to track their response to environmental or clinical changes, in order to pave the way for real-time monitoring of great ape cardiovascular health in zoos.

The second chapter used mass spectrometry and data exploration techniques to investigate the cardiac tissue proteome of chimpanzees affected by IMF, revealing for the first time important changes in proteins associated with myocardial calcium homeostasis, mitochondrial function, contractility, and ECM remodelling. These findings highlight key biological pathways involved in IMF pathophysiology, and could also provide a foundation for targeted therapeutic strategies in future. Further research should confirm these findings in a larger cohort, ideally with more controlled pre-analytical conditions, though this is not always feasible in the context of zoo and wildlife research. The exploration of alternative sample types, storage conditions, and methods such as ECM-specific proteomics, would also be beneficial.

The third chapter examined the myocardial tissue expression of 15 genes using RT-qPCR, and highlighted the challenges of measuring gene expression in post-mortem tissue. Pre-analytical variability, including post-mortem interval and storage conditions, likely influenced the RNA quality, reference gene stability, and expression of the target genes. Despite the lack of statistically significant findings, trends in the expression of fibrosis-related markers, such as MMP-2, TGF-β1 and CCN2 (CTGF), could warrant further investigation, especially given their high biological relevance. While the lack of detectable VDR expression may reflect species-specific or disease-specific regulation and could benefit from additional investigation, it is likely that the pre-analytical environment affected this too. Although RNA expression does not always correlate with protein levels, further work involving the expression of genes corresponding to the proteins of interest from the second chapter would also be valuable. With refinement of pre-analytical and technical considerations, the approach used in this chapter could still add substantial value to our growing understanding of IMF.

The fourth chapter provided a detailed analysis of vitamin D status in a large sample of zoo-housed great apes, building on previous work in chimpanzees, but including bonobos, gorillas and orangutans for the first time. All species exhibited widespread low vitamin D status, which likely exacerbates the risk of IMF, though species-specific differences and trends require additional exploration. These findings highlight the importance of optimising husbandry practices, including the quality of diet and access to UVB, to mitigate potential health impacts. The expansion of geographical scope to include great apes exposed to naturally higher levels of solar UVB would be a useful comparison to the populations in Europe, but only where there is consistency in sampling and analytical methods. Establishing reference ranges would enhance the accuracy of clinical interpretation, though this would require a large number of samples from animals living in fully natural conditions, measured with a consistent and reliable analytical method. A closer examination of the relationship between vitamin D status and cardiovascular health is needed, through the analysis of paired data in the form of serum vitamin D measured by LC-MS/MS, as well as post-mortem cardiac histopathology.

Overall, the findings of this thesis significantly advance our understanding of IMF, an enigmatic but prevalent cardiovascular phenotype in zoo-housed great apes. By

addressing critical knowledge gaps about the aetiopathogeneses of IMF for the first time, as well as vitamin D status in the broader context of cardiovascular health, this research builds a stronger foundation for evidence-based strategies to improve outcomes and quality of life for great apes. The use of modern and high-throughput techniques demonstrates the potential for such approaches to address complex health issues in zoo-housed populations, and lay the groundwork for future studies, with the overall aim of reducing the burden of this disease and supporting the wellbeing, and wider conservation, of these endangered species.

LITERATURE CITED

Agborsangaya, C., Toriola, A.T., Grankvist, K., et al. (2010) The effects of storage time and sampling season on the stability of serum 25-hydroxy vitamin D and androstenedione. *Nutrition and Cancer*, 62 (1): 51–57. doi:10.1080/01635580903191460.

von Ahlfen, S., Missel, A., Bendrat, K., et al. (2007) Determinants of RNA quality from FFPE samples. *PLoS ONE*, 2 (12). doi:10.1371/journal.pone.0001261.

Ain, U. and Firdaus, H. (2022) Parvin: A hub of intracellular signalling pathways regulating cellular behaviour and disease progression. *Acta Histochemica*. 124 (7). doi:10.1016/j.acthis.2022.151935.

Akeson, P.K., Lind, T., Hernell, O., et al. (2016) Serum Vitamin D Depends Less on Latitude Than on Skin Color and Dietary Intake During Early Winter in Northern Europe. *Journal of Pediatric Gastroenterology and Nutrition*, 62 (4): 643–649. doi:10.1097/MPG.0000000000001028.

Ala-Houhala, M.J., Vähävihu, K., Hasan, T., et al. (2012) Comparison of narrowband ultraviolet B exposure and oral vitamin D substitution on serum 25-hydroxyvitamin D concentration. *British Journal of Dermatology*, 167 (1): 160–164. doi:10.1111/j.1365-2133.2012.10990.x.

Alberts, S.C., Altmann, J., Brockman, D.K., et al. (2013) Reproductive aging patterns in primates reveal that humans are distinct. *Proceedings of the National Academy of Sciences of the United States of America*, 110 (33): 13440–13445. doi:10.1073/PNAS.1311857110/SUPPL_FILE/PNAS.201311857SI.PDF.

Ali, N.H., Rehman, S., Naqvi, M., et al. (2022) Periostin: A Potential Biomarker and Therapeutic Target in Pulmonary Diseases. *Journal of Pharmacy and Pharmaceutical Sciences*, 25. doi:10.18433/jpps32306.

Ambion (2010) RNAlater® Tissue Collection: RNA Stabilization Solution. *Ambion Protocols and Manuals*. Available at: https://www.thermofisher.com/content/dam/LifeTech/migration/en/filelibrary/nucleic-

acid-purification-analysis/pdfs.par.18819.file.dat/bp-7020.pdf (Accessed: 13 December 2024).

Amsellem, V., Dryden, N.H., Martinelli, R., et al. (2014) ICAM-2 regulates vascular permeability and N-cadherin localization through ezrin-radixin-moesin (ERM) proteins and Rac-1 signalling. *Cell Communication and Signaling*, 12 (1). doi:10.1186/1478-811X-12-12.

Ancrenaz, M., Gumal, M., Marshall, A.J., et al. (2016) *Pongo pygmaeus (errata version published in 2018)*.

Anderson, J.L., May, H.T., Horne, B.D., et al. (2010) Relation of vitamin D deficiency to cardiovascular risk factors, disease status, and incident events in a general healthcare population. *American Journal of Cardiology*, 106 (7): 963–968. doi:10.1016/j.amjcard.2010.05.027.

Anderson, N.L., De La Cruz, S.E.W., Brenn-White, M., et al. (2022) Reference Values and Comparison of Blood Chemistry and Plasma Protein Values Between Gold Standard Analyzers and Four Point-of-care Devices in Free-ranging Canvasbacks (Aythya Valisineria). *Journal of Zoo and Wildlife Medicine*, 53 (2): 302–318. doi:10.1638/2021-0035.

Andreasson, U., Perret-Liaudet, A., van Waalwijk van Doorn, L.J.C., et al. (2015) A Practical Guide to Immunoassay Method Validation. *Frontiers in Neurology*, 6 (Aug): 179. doi:10.3389/FNEUR.2015.00179.

Antman, E., Bassand, J.P., Klein, W., et al. (2000) Myocardial infarction redefined - A consensus document of The Joint European Society of Cardiology/American College of Cardiology Committee f or the redefinition of myocardial infarction. *Journal of the American College of Cardiology*, 36 (3): 959–969. doi:10.1016/S0735-1097(00)00804-4.

Armbruster, D.A. and Pry, T. (2008) Limit of blank, limit of detection and limit of quantitation. *The Clinical biochemist. Reviews*, 29 Suppl 1.

Assarsson, E., Lundberg, M., Holmquist, G., et al. (2014a) Homogenous 96-Plex PEA Immunoassay Exhibiting High Sensitivity, Specificity, and Excellent Scalability. *PLOS ONE*, 9 (4): e95192. doi:10.1371/JOURNAL.PONE.0095192.

Assarsson, E., Lundberg, M., Holmquist, G., et al. (2014b) Homogenous 96-Plex PEA Immunoassay Exhibiting High Sensitivity, Specificity, and Excellent Scalability. *PLOS ONE*, 9 (4): e95192. doi:10.1371/JOURNAL.PONE.0095192.

Azimzadeh, O., Atkinson, M.J. and Tapio, S. (2021) "Quantitative Proteomic Analysis Using Formalin-Fixed, Paraffin-Embedded (FFPE) Human Cardiac Tissue." In *Methods in Molecular Biology*. doi:10.1007/978-1-0716-1186-9_33.

Azimzadeh, O., Scherthan, H., Yentrapalli, R., et al. (2012) Label-free protein profiling of formalin-fixed paraffin-embedded (FFPE) heart tissue reveals immediate mitochondrial impairment after ionising radiation. *Journal of Proteomics*, 75 (8). doi:10.1016/j.jprot.2012.02.019.

Baiker, K., Moittie, S., Liptovszky, M., et al. (2020) "Targeted Proteomics for Insight into Cardiovascular Disease in Great Apes." In *Journal of Comparative Pathology*. 2020. Elsevier Ltd. p. 154. doi:10.1016/j.jcpa.2019.10.041.

Baiker, K., Strong, V., Moittie, S., et al. (2018) New Insights into the Pathogenesis of Idiopathic Cardiac Fibrosis in European Captive Chimps. *Journal of Comparative Pathology*, 158: 112. doi:10.1016/j.jcpa.2017.10.051.

Baines, F.M., Chattell, J., Dale, J., et al. (2016) How much UVB does my reptile need? The UV-Tool, a guide to the selection of UV lighting for reptiles and amphibians in captivity. *Journal of Zoo and Aquarium Research*, 4 (1): 42–63. doi:10.19227/JZAR.V4I1.150.

Baines, F.M. and Cusack, L.M. (2019) "Environmental Lighting." In Divers, S. and Stahl, S. (eds.) *Mader's Reptile and Amphibian Medicine and Surgery*. 3rd ed. W.B. Saunders. pp. 131-138.e1. doi:10.1016/B978-0-323-48253-0.00017-9.

Baker, K.C. (2000) Advanced age influences chimpanzee behavior in small social groups. *Zoo Biology*, 19 (2). doi:10.1002/1098-2361(2000)19:2<111::AID-ZOO2>3.0.CO;2-5.

Baldessari, A., Snyder, J., Ahrens, J., et al. (2013) Fatal myocardial fibrosis in an aged chimpanzee (Pan troglodytes). *Pathobiology of aging & age related diseases*, 3 (1): 21073–5. doi:10.3402/pba.v3i0.21073.

Baldwin, M.A. (2004) Protein Identification by Mass Spectrometry. *Molecular & Cellular Proteomics*, 3 (1). doi:10.1074/mcp.r300012-mcp200.

Balgley, B.M., Guo, T., Zhao, K., et al. (2009) Evaluation of archival time on shotgun proteomics of formalin-fixed and paraffin-embedded tissues. *Journal of Proteome Research*, 8 (2). doi:10.1021/pr800503u.

Ballou, J.D., Lees, C., Faust, L.J., et al. (2010) Demographic and Genetic Management of Captive Populations. *Wild mammals in captivity, principles and techniques*, pp. 263–283.

Barallobre-Barreiro, J., Didangelos, A., Schoendube, F.A., et al. (2012) Proteomics analysis of cardiac extracellular matrix remodeling in a porcine model of ischemia/reperfusion injury. *Circulation*, 125 (6): 789–802. doi:10.1161/CIRCULATIONAHA.111.056952.

Barallobre-Barreiro, J., Lynch, M., Yin, X., et al. (2016a) Systems biology—opportunities and challenges: the application of proteomics to study the cardiovascular extracellular matrix. *Cardiovascular Research*, 112 (3): 626–636. doi:10.1093/CVR/CVW206.

Barallobre-Barreiro, J., Oklu, R., Lynch, M., et al. (2016b) Extracellular matrix remodelling in response to venous hypertension: proteomics of human varicose veins. *Cardiovascular Research*, 110 (3): 419–430. doi:10.1093/CVR/CVW075.

Barrett, B.J. and Fardy, J.M. (2021) “Evaluation of Diagnostic Tests.” In *Methods in Molecular Biology*. doi:10.1007/978-1-0716-1138-8_18.

Bartlett, S.L., Chen, T.C., Murphy, H., et al. (2017) Assessment of Serum 25-Hydroxyvitamin D Concentrations in Two Collections of Captive Gorillas (Gorilla gorilla gorilla). *Journal of Zoo and Wildlife Medicine*, 48 (1): 144–151. doi:10.1638/2015-0299.1.

Bass, B.P., Engel, K.B., Greytak, S.R., et al. (2014) A review of preanalytical factors affecting molecular, protein, and morphological analysis of Formalin-Fixed, Paraffin-Embedded (FFPE) tissue: How well do you know your FFPE specimen? *Archives of Pathology and Laboratory Medicine*. 138 (11). doi:10.5858/arpa.2013-0691-RA.

Bathke, J., Konzer, A., Remes, B., et al. (2019) Comparative analyses of the variation of the transcriptome and proteome of Rhodobacter sphaeroides throughout growth. *BMC Genomics*, 20 (1). doi:10.1186/s12864-019-5749-3.

Batlle, M., Castillo, N., Alcarraz, A., et al. (2019) Axl expression is increased in early stages of left ventricular remodeling in an animal model with pressure-overload. *PLoS ONE*, 14 (6). doi:10.1371/JOURNAL.PONE.0217926.

Batlle, M., Recarte-Pelz, P., Roig, E., et al. (2014) AXL receptor tyrosine kinase is increased in patients with heart failure. *International Journal of Cardiology*, 173 (3): 402–409. doi:10.1016/J.IJCARD.2014.03.016.

Bauernfeind, A.L., Reyzer, M.L., Caprioli, R.M., et al. (2015) High spatial resolution proteomic comparison of the brain in humans and chimpanzees. *Journal of Comparative Neurology*, 523 (14). doi:10.1002/cne.23777.

Beckmann, M., Václavík, T., Manceur, A.M., et al. (2014) glUV: a global UV-B radiation data set for macroecological studies. *Methods in Ecology and Evolution*, 5 (4): 372–383. doi:10.1111/2041-210X.12168.

Bernard, J.B., Ofterdal, O.T. and Ullrey, D.E. (1997) Vitamin D and ultraviolet radiation: Meeting lighting needs for captive animals. *Saf. Health*, (July).

Bian, X., Su, X., Wang, Y., et al. (2019) Periostin contributes to renal and cardiac dysfunction in rats with chronic kidney disease: Reduction of PPARα. *Biochimie*, 160. doi:10.1016/j.biochi.2019.03.003.

Boesch, C. and Boesch-Achermann, H. (2000) “Demography of the Taï chimpanzee community.” In *The Chimpanzees of the Taï Forest: Behavioural Ecology and Evolution*. Oxford University Press. p. 27.

Bogh, M.K.B., Gullstrand, J., Svensson, A., et al. (2012) Narrowband ultraviolet B three times per week is more effective in treating vitamin D deficiency than 1600 IU oral vitamin D3 per day: A randomized clinical trial. *British Journal of Dermatology*, 167 (3): 625–630. doi:10.1111/j.1365-2133.2012.11069.x.

Bora, M., Manu, M., Mathew, D.D., et al. (2022) Point of care diagnostics and non-invasive sampling strategy: a review on major advances in veterinary diagnostics. *Acta Veterinaria Brno*, 91 (1). doi:10.2754/avb202291010017.

Borenstein, M., Hedges, L. V., Higgins, J.P.T., et al. (2009) “Effect Sizes Based on Means.” In *Introduction to Meta-Analysis*. doi:10.1002/9780470743386.ch4.

Bouillon, R., Carmeliet, G., Verlinden, L., et al. (2008) Vitamin D and human health: Lessons from vitamin D receptor null mice. *Endocrine Reviews*, 29 (6): 726–776. doi:10.1210/er.2008-0004.

Bouwens, E., van den Berg, V.J., Akkerhuis, K.M., et al. (2020) Circulating biomarkers of cell adhesion predict clinical outcome in patients with chronic heart failure. *Journal of Clinical Medicine*, 9 (1). doi:10.3390/jcm9010195.

Bouzeghrane, F., Reinhardt, D.P., Reudelhuber, T.L., et al. (2005) Enhanced expression of fibrillin-1, a constituent of the myocardial extracellular matrix in fibrosis. *American Journal of Physiology - Heart and Circulatory Physiology*, 289 (3 58-3). doi:10.1152/ajpheart.00151.2005.

Boyd, R., Danforth, M.D., Rapoport, G., et al. (2019) Great ape heart project guidelines for the echocardiographic assessment of great apes. *Journal of Zoo and Wildlife Medicine*, 50 (4): 822–836. doi:10.1638/2018-0164.

Braadt, L., Naumann, M., Freuer, D., et al. (2023) Novel inflammatory biomarkers associated with stroke severity: results from a cross-sectional stroke cohort study. *Neurological Research and Practice*, 5 (1). doi:10.1186/s42466-023-00259-3.

British Association of Dermatologists, Cancer Research UK, Diabetes UK, et al. (2010) *Consensus Vitamin D position statement*. Available at: https://www.nhs.uk/livewell/summerhealth/documents/concensus_statement%20_vitd_dec_2010.pdf (Accessed: 23 April 2021).

Brookes, O., Gray, S., Bennett, P., et al. (2022) Evaluating Cognitive Enrichment for Zoo-Housed Gorillas Using Facial Recognition. *Frontiers in Veterinary Science*, 9. doi:10.3389/fvets.2022.886720.

Bround, M.J., Wambolt, R., Luciani, D.S., et al. (2013) Cardiomyocyte ATP production, metabolic flexibility, and survival require calcium flux through cardiac ryanodine receptors in vivo. *Journal of Biological Chemistry*, 288 (26). doi:10.1074/jbc.M112.427062.

Brown, J.L., Paris, S., Prado-Oviedo, N.A., et al. (2016) Reproductive health assessment of female elephants in north American zoos and association of husbandry practices with reproductive dysfunction in african elephants (loxodonta africana). *PLoS ONE*, 11 (7). doi:10.1371/journal.pone.0145673.

Bucknell, P., Dobbs, P., Martin, M., et al. (2023) Cardiorespiratory effects of isoflurane and medetomidine–tiletamine–zolazepam in 12 bonobos (Pan paniscus). *Veterinary Record*, 192 (4): e2589. doi:10.1002/VETR.2589.

Buczak, K., Kirkpatrick, J.M., Truckenmueller, F., et al. (2020) Spatially resolved analysis of FFPE tissue proteomes by quantitative mass spectrometry. *Nature Protocols*, 15 (9). doi:10.1038/s41596-020-0356-y.

Bue, M., Bergholt, N.L., Jensen, L.K., et al. (2020) Inflammatory proteins in infected bone tissue – An explorative porcine study. *Bone Reports*, 13: 100292. doi:10.1016/J.BONR.2020.100292.

Burton, N.R. and Backus, K.M. (2024) Functionalizing tandem mass tags for streamlining click-based quantitative chemoproteomics. *Communications Chemistry 2024 7:1*, 7 (1): 1–12. doi:10.1038/s42004-024-01162-x.

Bustin, S. and Huggett, J. (2017) qPCR primer design revisited. *Biomolecular Detection and Quantification*. 14. doi:10.1016/j.bdq.2017.11.001.

Bustin, S.A., Benes, V., Garson, J.A., et al. (2009) The MIQE guidelines: Minimum information for publication of quantitative real-time PCR experiments. *Clinical Chemistry*, 55 (4). doi:10.1373/clinchem.2008.112797.

Cabana, F., Jasmi, R. and Maguire, R. (2018) Great ape nutrition: low-sugar and high-fibre diets can lead to increased natural behaviours, decreased regurgitation and reingestion, and reversal of prediabetes. *International Zoo Yearbook*, 52 (1). doi:10.1111/izy.12172.

Caldentey, G., García De Frutos, P., Cristóbal, H., et al. (2019) Serum levels of Growth Arrest-Specific 6 protein and soluble AXL in patients with ST-segment elevation myocardial infarction. *European Heart Journal: Acute Cardiovascular Care*, 8 (8). doi:10.1177/2048872617740833.

Calton, E.K., Keane, K.N., Newsholme, P., et al. (2015) The impact of Vitamin D levels on inflammatory status: A systematic review of immune cell studies. *PLoS ONE*, 10 (11). doi:10.1371/JOURNAL.PONE.0141770.

Cama, V.A., McDonald, C., Arcury-Quandt, A., et al. (2018) Evaluation of an OV-16 IgG4 Enzyme-Linked Immunosorbent Assay in Humans and Its Application to Determine the Dynamics of Antibody Responses in a Non-Human Primate Model of Onchocerca volvulus Infection. *The American Journal of Tropical Medicine and Hygiene*, 99 (4): 1041. doi:10.4269/AJTMH.18-0132.

Carbone, F., Liberale, L., Libby, P., et al. (2023) Vitamin D in atherosclerosis and cardiovascular events. *European Heart Journal*. doi:10.1093/EURHEARTJ/EHAD165.

Cashman, K.D., Dowling, K.G., Škrabáková, Z., et al. (2016) Vitamin D deficiency in Europe: pandemic? *The American Journal of Clinical Nutrition*, 103 (4): 1033–1044. doi:10.3945/AJCN.115.120873.

Cha, Y.M., Dzeja, P.P., Shen, W.K., et al. (2003) Failing atrial myocardium: Energetic deficits accompany structural remodeling and electrical instability. *American Journal of Physiology - Heart and Circulatory Physiology*, 284 (4 53-4). doi:10.1152/ajpheart.00337.2002.

Chaanine, A.H. (2021) Metabolic remodeling and implicated calcium and signal transduction pathways in the pathogenesis of heart failure. *International Journal of Molecular Sciences*. 22 (19). doi:10.3390/ijms221910579.

Chapman, S., Chapman, J. and Chatterton, J. (2023) “Euthanasia of Geriatric Zoo Animals: Decision-Making and Procedure.” In *Optimal Wellbeing of Ageing Wild Animals in Human Care*. doi:10.1007/978-3-031-30659-4_11.

Chatfield, J., Stones, G. and Jalil, T. (2012) Severe Idiopathic Hypocalcemia in a Juvenile Western Lowland Gorilla (Gorilla gorilla gorilla). *Journal of Zoo and Wildlife Medicine*, 43 (1): 171–173.

Chen, H., Huang, X.N., Yan, W., et al. (2005) Role of the integrin-linked kinase/PINCH1/alpha-parvin complex in cardiac myocyte hypertrophy. *Laboratory Investigation*, 85 (11). doi:10.1038/labinvest.3700345.

Chen, N., Qin, M., Gong, Q., et al. (2021a) Construction of mRNA Regulatory Networks Reveals the Key Genes in Atrial Fibrillation. *Computational and Mathematical Methods in Medicine*, 2021. doi:10.1155/2021/5527240.

Chen, Q., Lai, S.M., Xu, S., et al. (2021b) Resident macrophages restrain pathological adipose tissue remodeling and protect vascular integrity in obese mice. *EMBO reports*, 22 (8). doi:10.15252/EMBR.202152835.

Chen, S., Glenn, D.J., Ni, W., et al. (2008) Expression of the vitamin D receptor is increased in the hypertrophic heart. *Hypertension*, 52 (6). doi:10.1161/HYPERTENSIONAHA.108.119602.

Chen, S., Law, C.S., Grigsby, C.L., et al. (2011) Cardiomyocyte-specific deletion of the vitamin D receptor gene results in cardiac hypertrophy. *Circulation*, 124 (17). doi:10.1161/CIRCULATIONAHA.111.032680.

Chen, S., Puthanveetil, P., Feng, B., et al. (2014) Cardiac miR-133a overexpression prevents early cardiac fibrosis in diabetes. *Journal of Cellular and Molecular Medicine*, 18 (3): 415–421. doi:10.1111/JCMM.12218.

Chen, S., Wu, Y., Qin, X., et al. (2021c) Global gene expression analysis using RNA-seq reveals the new roles of Panax notoginseng Saponins in ischemic cardiomyocytes. *Journal of Ethnopharmacology*, 268. doi:10.1016/j.jep.2020.113639.

Chevalier, C., Wendner, M., Suling, A., et al. (2022) Association of NT-proBNP and hs-cTnT with Imaging Markers of Diastolic Dysfunction and Focal Myocardial Fibrosis in Hypertrophic Cardiomyopathy. *Life*, 12 (8): 1241. doi:10.3390/LIFE12081241.

Chilton, J., Wilcox, A., Lammey, M., et al. (2016) Characterization of a Cardiorenal-like Syndrome in Aged Chimpanzees (Pan troglodytes). *Veterinary Pathology*, 53 (2): 417–424. doi:10.1177/0300985815618435.

Cho, H.C. and Abe, S. (2013) Is two-tailed testing for directional research hypotheses tests legitimate? *Journal of Business Research*, 66 (9). doi:10.1016/j.jbusres.2012.02.023.

Chong, D.L.W., Rebeyrol, C., José, R.J., et al. (2021) ICAM-1 and ICAM-2 Are Differentially Expressed and Up-Regulated on Inflamed Pulmonary Epithelium, but Neither ICAM-2 nor LFA-1: ICAM-1 Are Required for Neutrophil Migration Into the

Airways In Vivo. *Frontiers in Immunology*, 12: 691957. doi:10.3389/FIMMU.2021.691957/BIBTEX.

Clark, F.E. (2011) Great ape cognition and captive care: Can cognitive challenges enhance well-being? *Applied Animal Behaviour Science*. 135 (1–2). doi:10.1016/j.applanim.2011.10.010.

Clemens, T.L., Henderson, S.L., Adams, J.S., et al. (1982) Increased skin pigment reduces the capacity of skin to synthesise vitamin D3. *The Lancet*, 319 (8263): 74–76. doi:10.1016/S0140-6736(82)90214-8.

Cloutier Barbour, C., Danforth, M.D., Murphy, H., et al. (2020) Monitoring great ape heart health through innovative electrocardiogram technology: Training methodologies and welfare implications. *Zoo biology*, pp. 1–5. doi:10.1002/zoo.21567.

Cohen, J. (1988) *Statistical Power Analysis for the Behavioral Sciences Second Edition*.

Colak, A., Toprak, B., Dogan, N., et al. (2013) Effect of sample type, centrifugation and storage conditions on vitamin D concentration. *Biochemia Medica*, 23 (3): 321. doi:10.11613/BM.2013.039.

Conway, S.J., Izuhara, K., Kudo, Y., et al. (2014) The role of periostin in tissue remodeling across health and disease. *Cellular and Molecular Life Sciences*. 71 (7). doi:10.1007/s00018-013-1494-y.

Cox, J. and Mann, M. (2011) Quantitative, high-resolution proteomics for data-driven systems biology. *Annual Review of Biochemistry*, 80. doi:10.1146/annurev-biochem-061308-093216.

Crissey, S., Barr, J.E., Slifka, K.A., et al. (1999) Serum concentrations of lipids, vitamins A and E, vitamin D metabolites, and carotenoids in nine primate species at four zoos. *Zoo Biology*, 18 (6): 551–564. doi:10.1002/(SICI)1098-2361(1999)18:6<551::AID-ZOO9>3.0.CO;2-S.

Crissey, S., Pribyl, L., Pruett-Jones, M., et al. (1998) Nutritional management of Old World primates with special consideration for vitamin D. *International Zoo Yearbook*, 36 (1): 122–130. doi:10.1111/j.1748-1090.1998.tb02894.x.

Crowther, J.R. (2009) *Methods in Molecular Biology: The ELISA Guidebook*. Methods in Molecular Biology. 2nd ed. Totowa, NJ: Humana Press. doi:10.1007/978-1-60327-254-4.

Davis, M.R. and Summers, K.M. (2012) Structure and function of the mammalian fibrillin gene family: Implications for human connective tissue diseases. *Molecular Genetics and Metabolism*. 107 (4). doi:10.1016/j.ymgme.2012.07.023.

DeBerge, M., Glinton, K., Subramanian, M., et al. (2021) Macrophage AXL receptor tyrosine kinase inflames the heart after reperfused myocardial infarction. *Journal of Clinical Investigation*, 131 (6). doi:10.1172/JCI139576.

Deluca, G.C., Kimball, S.M., Kolasinski, J., et al. (2013) The role of vitamin D in nervous system health and disease. *Neuropathology and Applied Neurobiology*, 39 (5): 458–484. doi:10.1111/nan.12020.

DeLuca, H.F. (2004) Overview of general physiologic features and functions of vitamin D. *The American Journal of Clinical Nutrition*, 80 (6 Suppl): 1689S-1696S. doi:10.1093/ajcn/80.6.1689s.

Dennis, P.M., Raghanti, M.A., Meindl, R.S., et al. (2019) Cardiac disease is linked to adiposity in male gorillas (Gorilla gorilla gorilla). *PloS one*, 14 (6): e0218763–e0218763. doi:10.1371/journal.pone.0218763.

Diacovo, T.G., DeFougerolles, A.R., Bainton, D.F., et al. (1994) A functional integrin ligand on the surface of platelets: intercellular adhesion molecule-2. *The Journal of Clinical Investigation*, 94 (3): 1243–1251. doi:10.1172/JCI117442.

Dietl, A. and Maack, C. (2017) Targeting Mitochondrial Calcium Handling and Reactive Oxygen Species in Heart Failure. *Current Heart Failure Reports*. 14 (4). doi:10.1007/s11897-017-0347-7.

Domon, B. and Aebersold, R. (2006) Mass spectrometry and protein analysis. *Science*. 312 (5771). doi:10.1126/science.1124619.

Dong, Y., Lu, R., Cao, H., et al. (2024) Deficiency in Prader-Willi syndrome gene necdin leads to attenuated cardiac contractility. *iScience*, 27 (6). doi:10.1016/j.isci.2024.109974.

Donnelly, C.G., Johnson, A.L., Reed, S., et al. (2023) Cerebrospinal fluid and serum proteomic profiles accurately distinguish neuroaxonal dystrophy from cervical vertebral compressive myelopathy in horses. *Journal of Veterinary Internal Medicine*, 37 (2): 689–696. doi:10.1111/JVIM.16660.

Drammeh, B.S., Schleicher, R.L., Pfeiffer, C.M., et al. (2008) Effects of Delayed Sample Processing and Freezing on Serum Concentrations of Selected Nutritional Indicators. *Clinical Chemistry*, 54 (11): 1883–1891. doi:10.1373/CLINCHEM.2008.108761.

Drane, A.L., Atencia, R., Cooper, S.M., et al. (2019) Cardiac structure and function characterized across age groups and between sexes in healthy wild-born captive chimpanzees (Pan troglodytes) living in sanctuaries. *American Journal of Veterinary Research*, 80 (6): 547–557. doi:10.2460/ajvr.80.6.547.

Drane, A.L., Atencia, R., Cooper, S.M., et al. (2020) Evaluation of relationships between results of electrocardiography and echocardiography in 341 chimpanzees (Pan troglodytes). *American Journal of Veterinary Research*, 81 (6): 488–498. doi:10.2460/ajvr.81.6.488.

Dunn, W.B., Erban, A., Weber, R.J.M., et al. (2013) Mass appeal: Metabolite identification in mass spectrometry-focused untargeted metabolomics. *Metabolomics*. 9 (SUPPL.1). doi:10.1007/s11306-012-0434-4.

Edes, A.N. (2020) “Cumulative stressful events predict disease and mortality risk in gorillas.” In *The 89th Annual Meeting of the American Association of Physical Anthropologists*. 2020. p. 77. Available at: https://meeting.physanth.org/program/2020/session55/edes-2020-cumulative-stressful-events-predict-disease-and-mortality-risk-in-gorillas.html (Accessed: 5 November 2020).

Edes, A.N. and Brand, C.M. (2021) Age, sex, and inflammatory markers predict chronic conditions, cardiac disease, and mortality among captive western lowland gorillas (Gorilla gorilla gorilla). *Primates*. doi:10.1007/s10329-021-00942-6.

Edes, A.N., Brown, J.L. and Edwards, K.L. (2020a) Testing lipid markers as predictors of all-cause morbidity, cardiac disease, and mortality risk in captive western lowland gorillas (Gorilla gorilla gorilla). *Primate Biology*, 7: 41–59. doi:10.5194/pb-7-41-2020.

Edes, A.N., Brown, J.L. and Edwards, K.L. (2023) Evaluating individual biomarkers for predicting health risks in zoo-housed chimpanzees (Pan troglodytes) and bonobos (Pan paniscus). *American Journal of Primatology*, 85 (3). doi:10.1002/ajp.23457.

Edes, A.N. and Crews, D.E. (2019) Do inflammatory markers predict heart disease and mortality in gorillas as they do in humans? *American Journal of Human Biology: ABSTRACTS*, 31 (2): 14. doi:10.1002/ajhb.23214.

Edes, A.N., Edwards, K.L., Wolfe, B.A., et al. (2020b) Allostatic Load Indices With Cholesterol and Triglycerides Predict Disease and Mortality Risk in Zoo-Housed Western Lowland Gorillas (Gorilla gorilla gorilla). *Biomarker Insights*, 15: 1–13. doi:10.1177/1177271920914585.

Edes, A.N., Wolfe, B.A. and Crews, D.E. (2020c) Testing a method to improve predictions of disease and mortality risk in western lowland gorillas (gorilla gorilla gorilla) using allostatic load. *The International Journal on the Biology of Stress*, pp. 1–11. doi:10.1080/10253890.2020.1748003.

Edes, A.N., Zimmerman, D., Jourdan, B., et al. (2022) Value Ranges and Clinical Comparisons of Serum DHEA-S, IL-6, and TNF-α in Western Lowland Gorillas. *Animals*, 12 (19). doi:10.3390/ani12192705.

Edfors, F., Danielsson, F., Hallström, B.M., et al. (2016) Gene-specific correlation of RNA and protein levels in human cells and tissues . *Molecular Systems Biology*, 12 (10). doi:10.15252/msb.20167144.

El-Adili, F., Lui, J.K., Najem, M., et al. (2022) Periostin overexpression in scleroderma cardiac tissue and its utility as a marker for disease complications. *Arthritis Research and Therapy*, 24 (1). doi:10.1186/s13075-022-02943-2.

El-Aneed, A., Cohen, A. and Banoub, J. (2009) Mass spectrometry, review of the basics: Electrospray, MALDI, and commonly used mass analyzers. *Applied Spectroscopy Reviews*. 44 (3). doi:10.1080/05704920902717872.

Elliott, P., Walker, L.L., Little, M.P., et al. (2007) Change in Salt Intake Affects Blood Pressure of Chimpanzees: Implications for Human Populations. *Circulation*, 116: 1563–1568. doi:10.1161/CIRCULATIONAHA.106.675579.

Ely, J.J., Bishop, M.A., Lammey, M.L., et al. (2010) Use of biomarkers of collagen types I and III fibrosis metabolism to detect cardiovascular and renal disease in chimpanzees (Pan troglodytes). *Comparative Medicine*.

Ely, J.J., Zavaskis, T., Lammey, M.L., et al. (2011a) Association of Brain-Type Natriuretic Protein and Cardiac Troponin I with Incipient Cardiovascular Disease in Chimpanzees (Pan troglodytes). *Comparative Medicine*, 61 (2): 163–169.

Ely, J.J., Zavaskis, T., Lammey, M.L., et al. (2011b) Blood pressure reference intervals for healthy adult chimpanzees (Pan troglodytes). *Journal of Medical Primatology*, 40 (3): 171–180. doi:10.1111/j.1600-0684.2011.00467.x.

Ely, J.J., Zavaskis, T. and Lammey, M.L. (2013) Hypertension increases with Aging and Obesity in chimpanzees (Pan troglodytes). *Zoo Biology*, 32 (1): 79–87. doi:10.1002/zoo.21044.

Engelsen, O., Brustad, M., Aksnes, L., et al. (2005) Daily Duration of Vitamin D Synthesis in Human Skin with Relation to Latitude, Total Ozone, Altitude, Ground Cover, Aerosols and Cloud Thickness. *Photochemistry and Photobiology*, 81: 1287–1290. doi:10.1562/2004-11-19-RN-375.

Fabricant, P.D. (2024) Characteristics of a Diagnostic Test: Sensitivity, Specificity, Positive Predictive Value, and Negative Predictive Value. *Practical Clinical Research Design and Application*, pp. 31–36. doi:10.1007/978-3-031-58380-3_5.

Farhangi, M.A., Nameni, G., Hajiluian, G., et al. (2017) Cardiac tissue oxidative stress and inflammation after vitamin D administrations in high fat- diet induced obese rats. *BMC Cardiovascular Disorders*, 17 (1): 1–7. doi:10.1186/s12872-017-0597-z.

Farragher, S.M., Tanney, A., Kennedy, R.D., et al. (2008) RNA expression analysis from formalin fixed paraffin embedded tissues. *Histochemistry and Cell Biology*. 130 (3). doi:10.1007/s00418-008-0479-7.

Faul, F., Erdfelder, E., Buchner, A., et al. (2009) Statistical power analyses using G*Power 3.1: Tests for correlation and regression analyses. *Behavior Research Methods*, 41 (4): 1149–1160. doi:10.3758/BRM.41.4.1149/METRICS.

Feltrer, Y., Strike, T., Routh, A., et al. (2016) Point-of-care cardiac troponin I in non-domestic species: a feasibility study. *Journal of Zoo and Aquarium Research*, 4 (2): 99–103. Available at: http://woodleyequipment.com, (Accessed: 3 November 2020).

Feltrer-Rambaud, Y., Moresco, A., Ange-van Heugten, K., et al. (2023) Serum vitamin D in sanctuary chimpanzees (Pan troglodytes) in range countries: A pilot study. *Veterinary Medicine and Science*, 9 (6): 2937–2945. doi:10.1002/VMS3.1279.

Ferrari, D., Lombardi, G. and Banfi, G. (2017) Concerning the vitamin D reference range: pre-analytical and analytical variability of vitamin D measurement. *Biochemia Medica*, 27 (3): 453–466. doi:10.11613/BM.2017.030501.

Ferreira, P.G., Muñoz-Aguirre, M., Reverter, F., et al. (2018) The effects of death and post-mortem cold ischemia on human tissue transcriptomes. *Nature Communications*, 9 (1). doi:10.1038/s41467-017-02772-x.

Flach, E.J., Tong, L., Banerjee, A.A., et al. (2010) "Investigation of cardiac pathology in chimpanzees (Pan troglodytes)." In *British Veterinary Zoological Society Proceedings*. 2010.

Fleige, S. and Pfaffl, M.W. (2006) RNA integrity and the effect on the real-time qRT-PCR performance. *Molecular Aspects of Medicine*. 27 (2–3). doi:10.1016/j.mam.2005.12.003.

Florell, S.R., Coffin, C.M., Holden, J.A., et al. (2001) Preservation of RNA for functional genomic studies: A multidisciplinary tumor bank protocol. *Modern Pathology*, 14 (2). doi:10.1038/modpathol.3880267.

Ford, J.A., MacLennan, G.S., Avenell, A., et al. (2014) Cardiovascular disease and vitamin D supplementation: Trial analysis, systematic review, and meta-analysis. *American Journal of Clinical Nutrition*, 100 (3): 746–755. doi:10.3945/ajcn.113.082602.

Fourage, A., Shepherd, C.R., Campera, M., et al. (2023) It's a sign: Animal welfare and zoo type are predictors of animal identification signage usage and quality at zoo exhibits. *Zoo Biology*, 42 (2). doi:10.1002/zoo.21734.

Frangogiannis, N.G. (2019) Cardiac fibrosis: Cell biological mechanisms, molecular pathways and therapeutic opportunities. *Molecular Aspects of Medicine*, 65: 70–99. doi:10.1016/j.mam.2018.07.001.

Freire, R. and Nicol, C.J. (2019) A bibliometric analysis of past and emergent trends in animal welfare science. *Animal Welfare*, 28 (4). doi:10.7120/09627286.28.4.465.

Friedrichs, K.R., Harr, K.E., Freeman, K.P., et al. (2012) ASVCP reference interval guidelines: Determination of de novo reference intervals in veterinary species and other related topics. *Veterinary Clinical Pathology*, 41 (4): 441–453. doi:10.1111/vcp.12006.

Frustaci, A., De Luca, A., Verardo, R., et al. (2024) Novel ATP2A2 Gene Mutation c.118G>A Causing Keratinocyte and Cardiomyocyte Disconnection in Darier Disease. *Biomedicines*, 12 (5). doi:10.3390/BIOMEDICINES12051060/S1.

Fruth, B., Hickey, J.R., André, C., et al. (2016) *Pan paniscus (errata version published in 2016)*.

Fu, Q. and Van Eyk, J.E. (2006) Proteomics and heart disease: identifying biomarkers of clinical utility. *Expert Rev. Proteomics*, 3 (2): 237–249. doi:10.1586/14789450.3.2.237.

Fujii, K., Nakamura, H. and Nishimura, T. (2017) Recent mass spectrometry-based proteomics for biomarker discovery in lung cancer, COPD, and asthma. *Expert Review of Proteomics*. 14 (4). doi:10.1080/14789450.2017.1304215.

Furuichi, T., Idani, G., Ihobe, H., et al. (1998) Population dynamics of wild bonobos (Pan paniscus) at Wamba. *International Journal of Primatology*, 19 (6): 1029–1043. doi:10.1023/A:1020326304074/METRICS.

Galdikas, B.M.F. (1981) “Orangutan reproduction in the wild.” In Graham, C.E. (ed.) *Reproductive Biology of the Great Apes: Comparative and Biomedical Perspectives*. London: Academic Press, Inc. pp. 281–299.

Geyer, P.E., Holdt, L.M., Teupser, D., et al. (2017) Revisiting biomarker discovery by plasma proteomics. *Molecular Systems Biology*, 13 (9): 942. doi:10.15252/msb.20156297.

Ghosal, R., Edwards, K.L., Chiarelli, T.L., et al. (2023) Biomarkers of reproductive health in wildlife and techniques for their assessment. *Theriogenology Wild*, 3. doi:10.1016/j.therwi.2023.100052.

Gisbert-Ferrándiz, L., Cosin-Roger, J., Hernández, C., et al. (2020) The vitamin D receptor Taq I polymorphism is associated with reduced VDR and increased PDIA3 protein levels in human intestinal fibroblasts. *Journal of Steroid Biochemistry and Molecular Biology*, 202. doi:10.1016/j.jsbmb.2020.105720.

Głogowska-Ligus, J., Dąbek, J., Zych-Twardowska, E., et al. (2013) Expression analysis of intercellular adhesion molecule-2 (ICAM-2) in the context of classical cardiovascular risk factors in acute coronary syndrome patients. *Archives of Medical Science*, 9 (6): 1035–1039. doi:10.5114/AOMS.2012.28808.

Golbidi, S., Frisbee, J.C. and Laher, I.X. (2015) Chronic stress impacts the cardiovascular system: Animal models and clinical outcomes. *American Journal of Physiology - Heart and Circulatory Physiology*. 308 (12). doi:10.1152/ajpheart.00859.2014.

González, A., López, B. and Díezl, J. (2002) Myocardial fibrosis in arterial hypertension. *European Heart Journal Supplements*, 4 (suppl_D): D18–D22. doi:10.1016/S1520-765X(02)90156-2.

Goulet-Pelletier, J.-C. and Cousineau, D. (2018) A review of effect sizes and their confidence intervals, Part I: The Cohen's d family. *The Quantitative Methods for Psychology*, 14 (4). doi:10.20982/tqmp.14.4.p242.

Grimes, D.S., Hindle, E. and Dyer, T. (1996) Sunlight, cholesterol and coronary heart disease. *QJM: An International Journal of Medicine*, 89 (8): 579–589. doi:10.1093/qjmed/89.8.579.

Hafizi, S. and Dahlbäck, B. (2006) Signalling and functional diversity within the Axl subfamily of receptor tyrosine kinases. *Cytokine & Growth Factor Reviews*, 17 (4): 295–304. doi:10.1016/J.CYTOGFR.2006.04.004.

Hall, L.M., Kimlin, M.G., Aronov, P.A., et al. (2010) Vitamin D intake needed to maintain target serum 25-hydroxyvitamin D concentrations in participants with low sun

exposure and dark skin pigmentation is substantially higher than current recommendations. *Journal of Nutrition*, 140 (3): 542–550. doi:10.3945/jn.109.115253.

Hanamura, S., Kiyono, M., Lukasik-Braum, M., et al. (2008) Chimpanzee deaths at Mahale caused by a flu-like disease. *Primates*, 49 (1): 77–80. doi:10.1007/s10329-007-0054-1.

Hanley, J.A. and McNeil, B.J. (1982) The meaning and use of the area under a receiver operating characteristic (ROC) curve. *Radiology*, 143 (1): 29–36. doi:10.1148/radiology.143.1.7063747.

Harmon, Q.E., Umbach, D.M. and Baird, D.D. (2016) Use of Estrogen-Containing Contraception Is Associated With Increased Concentrations of 25-Hydroxy Vitamin D. *The Journal of Clinical Endocrinology & Metabolism*, 101 (9): 3370–3377. doi:10.1210/JC.2016-1658.

Hedegaard, J., Thorsen, K., Lund, M.K., et al. (2014) Next-generation sequencing of RNA and DNA isolated from paired fresh-frozen and formalin-fixed paraffin-embedded samples of human cancer and normal tissue. *PLoS ONE*, 9 (5). doi:10.1371/journal.pone.0098187.

Hedges, L. V. (1981) Distribution Theory for Glass's Estimator of Effect Size and Related Estimators. *Journal of Educational Statistics*, 6 (2). doi:10.2307/1164588.

Hellemans, J., Mortier, G., De Paepe, A., et al. (2007) qBase relative quantification framework and software for management and automated analysis of real-time quantitative PCR data. *Genome Biology*, 8 (2): 1–14. doi:10.1186/GB-2007-8-2-R19/FIGURES/5.

Henderson, N.C., Rieder, F. and Wynn, T.A. (2020) Fibrosis: from mechanisms to medicines. *Nature*. 587 (7835). doi:10.1038/s41586-020-2938-9.

Heymans, S., Lakdawala, N.K., Tschöpe, C., et al. (2023) Dilated cardiomyopathy: causes, mechanisms, and current and future treatment approaches. *The Lancet*. 402 (10406). doi:10.1016/S0140-6736(23)01241-2.

Hibender, S., Wanga, S., van der Made, I., et al. (2019) Renal cystic disease in the Fbn1C1039G/+ Marfan mouse is associated with enhanced aortic aneurysm formation. *Cardiovascular Pathology*, 38: 1–6. doi:10.1016/J.CARPATH.2018.10.002.

Hiligsmann, M., Sedrine, W. Ben, Bruyère, O., et al. (2015) Cost-effectiveness of vitamin D and calcium supplementation in the treatment of elderly women and men with osteoporosis. *European Journal of Public Health*. 25 (1). doi:10.1093/eurpub/cku119.

Hill, K., Boesch, C., Goodall, J., et al. (2001) Mortality rates among wild chimpanzees. *Journal of Human Evolution*, 40: 437–450. doi:10.1006/jhev.2001.0469.

Hoegh, H.J., Davis, B.D. and Manthe, A.F. (1999) Sun avoidance practices among non-Hispanic white Californians. *Health Education and Behavior*, 26 (3): 360–368. doi:10.1177/109019819902600306.

Höglind, A., Areström, I., Ehrnfelt, C., et al. (2017) Systematic evaluation of monoclonal antibodies and immunoassays for the detection of Interferon-γ and Interleukin-2 in old and new world non-human primates. *Journal of Immunological Methods*, 441: 39–48. doi:10.1016/J.JIM.2016.11.011.

Holick, M.F. (2004a) Sunlight and vitamin D for bone health and prevention of autoimmune diseases, cancers, and cardiovascular disease. *The American Journal of Clinical Nutrition*, 80 (6): 1678S-1688S. doi:10.1093/ajcn/80.6.1678S.

Holick, M.F. (2004b) Vitamin D: Importance in the prevention of cancers, type 1 diabetes, heart disease, and osteoporosis. *American Journal of Clinical Nutrition*, 79 (3): 362–371. doi:10.1093/ajcn/79.3.362.

Holick, M.F., Binkley, N.C., Bischoff-Ferrari, H.A., et al. (2011) Evaluation, Treatment, and Prevention of Vitamin D Deficiency: an Endocrine Society Clinical Practice Guideline. *The Journal of Clinical Endocrinology & Metabolism*, 96 (7): 1911–1930. doi:10.1210/JC.2011-0385.

Holick, M.F., Maclaughlin, J.A., Clark, M.B., et al. (1980) Photosynthesis of previtamin D3 in human skin and the physiologic consequences. *Science*, 210 (4466): 203–205. doi:10.1126/science.6251551.

Holick, M.F., MacLaughlin, J.A. and Doppelt, S.H. (1981) Regulation of cutaneous previtamin D3 photosynthesis in man: Skin pigment is not an essential regulator. *Science*, 211 (4482): 590–593. doi:10.1126/science.6256855.

Hollis, B.W. and Wagner, C.L. (2004) Assessment of dietary vitamin D requirements during pregnancy and lactation. *The American Journal of Clinical Nutrition*, 79 (5): 717–726. doi:10.1093/AJCN/79.5.717.

Holmes, E.W., Garbincius, J. and Mckenna, K.M. (2013) Analytical Variability Among Methods for the Measurement of 25-Hydroxyvitamin D. *Am J Clin Pathol*, 140: 550–560. doi:10.1309/AJCPU2SKW1TFKSWY.

Howell, S., Hoffman, K., Bartel, L., et al. (2003) Normal Hematologic and Serum Clinical Chemistry Values for Captive Chimpanzees (Pan troglodytes). *Comparative Medicine*, 53 (4): 413–423.

Hoyer, N., Jessen, H., Prior, T.S., et al. (2021) High turnover of types III and VI collagen in progressive idiopathic pulmonary fibrosis. *Respirology*, 26 (6). doi:10.1111/resp.14056.

Hubbard, G.B., Lee, R. and Eichberg, J.W. (1991) Diseases and Pathology of Chimpanzees at the Southwest Foundation for Biomedical Research. *American Journal of Primatology*, 24: 273–282.

Huggett, J., Dheda, K., Bustin, S., et al. (2005) Real-time RT-PCR normalisation; strategies and considerations. *Genes and Immunity*. 6 (4). doi:10.1038/sj.gene.6364190.

Humle, T., Maisels, F., Oates, J.F., et al. (2016) *Pan troglodytes (errata version published in 2018)*. Available at: https://dx.doi.org/10.2305/IUCN.UK.2016-2.RLTS.T15933A17964454.en.

Imbeaud, S., Graudens, E., Boulanger, V., et al. (2005) Towards standardization of RNA quality assessment using user-independent classifiers of microcapillary electrophoresis traces. *Nucleic Acids Research*, 33 (6). doi:10.1093/nar/gni054.

Institute of Medicine (2010) *Evaluation of biomarkers and surrogate endpoints in chronic disease*. Micheel, C. and Ball, J. (eds.). Washington, DC: The National Academies Press. doi:10.17226/12869.

Jablonski, N.G. and Chaplin, G. (2010) Human skin pigmentation as an adaptation to UV radiation. *Proceedings of the National Academy of Sciences of the United States of America*, 107 (SUPPL. 2): 8962–8968. doi:10.1073/pnas.0914628107.

Jaedicke, K.M., Taylor, J.J. and Preshaw, P.M. (2012) Validation and quality control of ELISAs for the use with human saliva samples. *Journal of Immunological Methods*, 377 (1–2): 62–65. doi:10.1016/J.JIM.2012.01.010.

Jang, S.Y., Kim, J., Park, J.T., et al. (2022) Therapeutic Potential of Targeting Periostin in the Treatment of Graves' Orbitopathy. *Frontiers in Endocrinology*, 13. doi:10.3389/fendo.2022.900791.

Javan, G.T., Singh, K., Finley, S.J., et al. (2024) Complexity of human death: its physiological, transcriptomic, and microbiological implications. *Frontiers in Microbiology*. 14. doi:10.3389/fmicb.2023.1345633.

Jia, J., Shen, C., Mao, L., et al. (2014) Vitamin D receptor genetic polymorphism is significantly associated with decreased risk of hypertension in a Chinese han population. *Journal of Clinical Hypertension*, 16 (9). doi:10.1111/jch.12386.

Joblon, M.J., Flower, J.E., Thompson, L.A., et al. (2022) Investigation of the use of serum biomarkers for the detection of cardiac disease in marine mammals. *Journal of Zoo and Wildlife Medicine*, 53 (2): 373–382. doi:10.1638/2021-0152.

Johnson, E., Nguyen, L., Albakri, J.S., et al. (2024) Mitochondrial Dysfunction and Calcium Homeostasis in Heart Failure: Exploring the Interplay Between Oxidative Stress and Cardiac Remodeling for Future Therapeutic Innovations. *Current Problems in Cardiology*, p. 102968. doi:10.1016/J.CPCARDIOL.2024.102968.

Jones, G., Strugnell, S.A. and DeLuca, H.F. (1998) Current understanding of the molecular actions of vitamin D. *Physiological Reviews*, 78 (4): 1193–1231. doi:10.1152/physrev.1998.78.4.1193.

Jones, P., Cordonnier, N., Mahamba, C., et al. (2011) Encephalomyocarditis virus mortality in semi-wild bonobos (Pan panicus). *Journal of Medical Primatology*, 40 (3): 157–163. doi:10.1111/j.1600-0684.2010.00464.x.

Jones, P., Mahamba, C., Rest, J., et al. (2005) Fatal inflammatory heart disease in a bonobo (Pan paniscus). *Journal of Medical Primatology*, 34 (1): 45–49. doi:10.1111/j.1600-0684.2004.00091.x.

De Jonge, H.J.M., Fehrmann, R.S.N., De Bont, E.S.J.M., et al. (2007) Evidence Based Selection of Housekeeping Genes. *PLoS ONE*, 2 (9): 898. doi:10.1371/journal.pone.0000898.

Jorde, R. and Grimnes, G. (2015) Vitamin D and health: The need for more randomized controlled trials. *Journal of Steroid Biochemistry and Molecular Biology*, 148: 269–274. doi:10.1016/j.jsbmb.2015.01.021.

Junge, R.E., Gannon, F.H., Porton, I., et al. (2000) Management and Prevention of Vitamin D Deficiency Rickets in Captive-Born Juvenile Chimpanzees (Pan troglodytes). *Journal of Zoo and Wildlife Medicine*, 31 (3): 361–369.

Kambale, E., Ramer, J., Gilardi, K., et al. (2014) “Cardiovascular and Hepatic Disease in Wild Eastern Lowland Gorillas (Gorilla beringei graueri).” In *American Association of Zoo Veterinarians Conference*. 2 July 2014.

Karaman, M.W., Houck, M.L., Chemnick, L.G., et al. (2003) Comparative analysis of gene-expression patterns in human and African great ape cultured fibroblasts. *Genome Research*. 13 (7). doi:10.1101/gr.1289803.

Karsdal, M., Nielsen, M.J., Sand, J.M., et al. (2020) Endotrophin, a hormone derived from type VI collagen, activates fibroblasts and drives fibrosis in the liver, lung, kidney, and heart. *Journal of Hepatology*, 73. doi:10.1016/s0168-8278(20)31523-3.

Karsdal, M.A. (2023) *Biochemistry of Collagens, Laminins and Elastin: Structure, Function and Biomarkers*. 3rd ed. doi:10.1016/C2022-0-01635-4.

Kaur, T., Singh, J., Tong, S., et al. (2008) Descriptive Epidemiology of Fatal Respiratory Outbreaks and Detection of a Human-Related Metapneumovirus in Wild Chimpanzees (Pan troglodytes) at Mahale Mountains National Park, Western Tanzania. *American Journal of Primatology*, 70: 1–11. doi:10.1002/ajp.20565.

Kenny, D.E., Cambre, R.C., Alvarado, T.P., et al. (1994) Aortic Dissection: An Important Cardiovascular Disease in Captive Gorillas (Gorilla gorilla gorilla). *Journal of Zoo and Wildlife Medicine*, 25 (4): 561–568.

Khan, T., Muise, E.S., Iyengar, P., et al. (2009) Metabolic Dysregulation and Adipose Tissue Fibrosis: Role of Collagen VI. *Molecular and Cellular Biology*, 29 (6). doi:10.1128/mcb.01300-08.

Kho, C., Lee, A., Jeong, D., et al. (2011) SUMO1-dependent modulation of SERCA2a in heart failure. *Nature*, 477 (7366). doi:10.1038/nature10407.

Kilbourn, A.M., Karesh, W.B., Wolfe, N.D., et al. (2003) Health evaluation of free-ranging and semi-captive orangutans (Pongo pygmaeus pygmaeus) in Sabah, Malaysia. *Journal of Wildlife Diseases*, 39 (1): 73–83. doi:10.7589/0090-3558-39.1.73.

Klockenbusch, C., O'Hara, J.E. and Kast, J. (2012) Advancing formaldehyde cross-linking towards quantitative proteomic applications. *Analytical and Bioanalytical Chemistry*. 404 (4). doi:10.1007/s00216-012-6065-9.

Koitabashi, N., Arai, M., Kogure, S., et al. (2007) Increased Connective Tissue Growth Factor Relative to Brain Natriuretic Peptide as a Determinant of Myocardial Fibrosis. *Hypertension*, 49 (5): 1120–1127. doi:10.1161/HYPERTENSIONAHA.106.077537.

Kolamunnage-Dona, R. and Williamson, P.R. (2018) Time-dependent efficacy of longitudinal biomarker for clinical endpoint. *Statistical Methods in Medical Research*, 27 (6). doi:10.1177/0962280216673084.

Kondrat'eva, D.S., Afanas'ev, S.A. and Popov, S. V. (2014) Expression of Ca2+-ATPase in sarcoplasmic reticulum in rat cardiomyocytes during experimental postinfarction cardiosclerosis and diabetes mellitus. *Bulletin of Experimental Biology and Medicine*, 156 (6). doi:10.1007/s10517-014-2440-1.

Kongsbak, M., Levring, T.B., Geisler, C., et al. (2013) The vitamin D receptor and T cell function. *Frontiers in Immunology*. 4 (JUN). doi:10.3389/fimmu.2013.00148.

Koshman, Y.E., Sternlicht, M.D., Kim, T., et al. (2015) Connective tissue growth factor regulates cardiac function and tissue remodeling in a mouse model of dilated cardiomyopathy. *Journal of molecular and cellular cardiology*, 89 (Pt B): 214–222. doi:10.1016/J.YJMCC.2015.11.003.

Kosmala, W., Przewlocka-Kosmala, M., Rojek, A., et al. (2019) Comparison of the Diastolic Stress Test With a Combined Resting Echocardiography and Biomarker Approach to Patients With Exertional Dyspnea: Diagnostic and Prognostic Implications. *JACC: Cardiovascular Imaging*, 12 (5): 771–780. doi:10.1016/J.JCMG.2017.10.008.

Krebs, B.L., Marrin, D., Phelps, A., et al. (2018) Managing Aged Animals in Zoos to Promote Positive Welfare: A Review and Future Directions. *Animals*, 8 (116). doi:10.3390/ani8070116.

Kruger, M. and Viljoen, A. (2023) Encouraging pro-conservation intentions in urban recreational spaces: a South African zoo perspective. *International Journal of Tourism Cities*, 9 (1). doi:10.1108/IJTC-06-2022-0156.

Kubista, M., Andrade, J.M., Bengtsson, M., et al. (2006) The real-time polymerase chain reaction. *Molecular Aspects of Medicine*, 27 (2–3): 95–125. doi:10.1016/J.MAM.2005.12.007.

De La Cuesta, F., Alvarez-Llamas, G., Gil-Dones, F., et al. (2009) Tissue proteomics in atherosclerosis: Elucidating the molecular mechanisms of cardiovascular diseases. *Expert Review of Proteomics*, 6 (4). doi:10.1586/epr.09.60.

Lakatta, E.G. (1993) Cardiovascular regulatory mechanisms in advanced age. *Physiological Reviews*, 73 (2). doi:10.1152/physrev.1993.73.2.413.

Lammey, M.L., Baskin, G.B., Gigliotti, A.P., et al. (2008a) Interstitial myocardial fibrosis in a captive chimpanzee (Pan troglodytes) population. *Comparative Medicine*.

Lammey, M.L., Lee, D.R., Ely, J.J., et al. (2008b) Sudden cardiac death in 13 captive chimpanzees (Pan troglodytes). *Journal of medical primatology*, 37 (s1): 39–43. doi:10.1111/j.1600-0684.2007.00260.x.

Lasne, A., Milleron, O., Delorme, G., et al. (2020) Clinical, electrical and morphological cardiac disorders in Marfan patients with FBN1 mutations. *Archives of Cardiovascular Diseases Supplements*, 12 (1). doi:10.1016/j.acvdsp.2019.09.217.

Leask, A. and Abraham, D.J. (2004) TGF-β signaling and the fibrotic response. *The FASEB Journal*, 18 (7). doi:10.1096/fj.03-1273rev.

Leendertz, F.H., Ellerbrok, H., Boesch, C., et al. (2004) Anthrax kills wild chimpanzees in a tropical rainforest. *Nature*, 430 (6998): 451–452. doi:10.1038/nature02722.

Leendertz, F.H., Pauli, G., Maetz-Rensing, K., et al. (2006) Pathogens as drivers of population declines: The importance of systematic monitoring in great apes and other threatened mammals. *Biological Conservation*, 131 (2): 325–337. doi:10.1016/j.biocon.2006.05.002.

Lehnart, S.E., Maier, L.S. and Hasenfuss, G. (2009) Abnormalities of calcium metabolism and myocardial contractility depression in the failing heart. *Heart Failure Reviews*. 14 (4). doi:10.1007/s10741-009-9146-x.

Leon, L.R. and Helwig, B.G. (2010) Heat stroke: Role of the systemic inflammatory response. *Journal of Applied Physiology*. 109 (6). doi:10.1152/japplphysiol.00301.2010.

Less, E.H., Bergl, R., Ball, R., et al. (2014) Implementing a low-starch biscuit-free diet in zoo gorillas: The impact on behavior. *Zoo Biology*, 33 (1). doi:10.1002/zoo.21116.

Lewis, F., Maughan, N.J., Smith, V., et al. (2001) Unlocking the archive - Gene expression in paraffin-embedded tissue. *Journal of Pathology*. 195 (1). doi:10.1002/1096-9896(200109)195:1<66::AID-PATH921>3.0.CO;2-F.

Li, L., Huang, J. and Liu, Y. (2023) The extracellular matrix glycoprotein fibrillin-1 in health and disease. *Frontiers in Cell and Developmental Biology*. 11. doi:10.3389/fcell.2023.1302285.

Li, L., Liao, J., Yuan, Q., et al. (2021) Fibrillin-1-enriched microenvironment drives endothelial injury and vascular rarefaction in chronic kidney disease. *Science Advances*, 7 (5). doi:10.1126/sciadv.abc7170.

Li, X., Li, Z., Gu, S., et al. (2022) A pan-cancer analysis of collagen VI family on prognosis, tumor microenvironment, and its potential therapeutic effect. *BMC Bioinformatics*, 23 (1). doi:10.1186/s12859-022-04951-0.

Lijnen, P.J., Petrov, V. V. and Fagard, R.H. (2000) Induction of cardiac fibrosis by transforming growth factor-β1. *Molecular Genetics and Metabolism*, 71 (1–2): 418–435. doi:10.1006/mgme.2000.3032.

Linger, R.M.A., Keating, A.K., Earp, H.S., et al. (2008) TAM Receptor Tyrosine Kinases: Biologic Functions, Signaling, and Potential Therapeutic Targeting in Human Cancer. *Advances in Cancer Research*, 100: 35–83. doi:10.1016/S0065-230X(08)00002-X.

Linos, E., Keiser, E., Kanzler, M., et al. (2012) Sun protective behaviors and vitamin D levels in the US population: NHANES 2003-2006. *Cancer Causes and Control*, 23 (1): 133–140. doi:10.1007/s10552-011-9862-0.

Van Linthout, S. and Tschöpe, C. (2017) Inflammation – Cause or Consequence of Heart Failure or Both? *Current Heart Failure Reports*. 14 (4). doi:10.1007/s11897-017-0337-9.

Lips, P. (2010) Worldwide status of vitamin D nutrition. *Journal of Steroid Biochemistry and Molecular Biology*, 121 (1–2): 297–300. doi:10.1016/j.jsbmb.2010.02.021.

Liptovszky, M. (2024) Advancing zoo animal welfare through data science: scaling up continuous improvement efforts. *Frontiers in Veterinary Science*, 11. doi:10.3389/fvets.2024.1313182.

Liu, X., Li, Y., Li, W., et al. (2024) Diagnostic value of multimodal cardiovascular imaging technology coupled with biomarker detection in elderly patients with coronary heart disease. *British Journal of Hospital Medicine*, 85 (6). doi:10.12968/HMED.2024.0123/ASSET/IMAGES/LARGE/HMED.2024.0123_F01.JPEG.

Liu, X., Wu, H., Byrne, M., et al. (1997) Type III collagen is crucial for collagen I fibrillogenesis and for normal cardiovascular development. *Proceedings of the National Academy of Sciences of the United States of America*, 94 (5). doi:10.1073/pnas.94.5.1852.

Lok, D.J.A., Van Der Meer, P., De La Porte, P.W.B.A., et al. (2010) Prognostic value of galectin-3, a novel marker of fibrosis,in patients with chronic heart failure: Data from the DEAL-HF study. *Clinical Research in Cardiology*, 99 (5). doi:10.1007/s00392-010-0125-y.

Lok, S.I., Nous, F.M.A., van Kuik, J., et al. (2015) Myocardial fibrosis and pro-fibrotic markers in end-stage heart failure patients during continuous-flow left ventricular assist device support. *European Journal of Cardio-Thoracic Surgery*, 48 (3): 407–415. doi:10.1093/EJCTS/EZU539.

Loushin, M.K. (2005) “The effects of anesthetic agents on cardiac function.” In *Handbook of Cardiac Anatomy, Physiology, and Devices*. Humana Press. pp. 171–180. doi:10.1007/978-1-59259-835-9_13/COVER.

Lowenstine, L.J., Mcmanamon, R. and Terio, K.A. (2016) Comparative Pathology of Aging Great Apes: Bonobos, Chimpanzees, Gorillas, and Orangutans. *Veterinary Pathology*, 53 (2): 250–276. doi:10.1177/0300985815612154.

Lu, Q., Pan, B., Bai, H., et al. (2022) Intranuclear cardiac troponin I plays a functional role in regulating Atp2a2 expression in cardiomyocytes. *Genes and Diseases*, 9 (6). doi:10.1016/j.gendis.2021.04.007.

Lund, B.J., Sørensen, O.H., Lund, B.I., et al. (1980) Vitamin D metabolism in hypoparathyroidism. *Journal of Clinical Endocrinology and Metabolism*, 51 (3): 606–610. doi:10.1210/jcem-51-3-606.

Lyck, R. and Enzmann, G. (2015) The physiological roles of ICAM-1 and ICAM-2 in neutrophil migration into tissues. *Current Opinion in Hematology*, 22 (1): 53–59. doi:10.1097/MOH.0000000000000103.

MacLaughlin, J. and Holick, M.F. (1985) Aging decreases the capacity of human skin to produce vitamin D3. *Journal of Clinical Investigation*, 76 (4): 1536–1538. doi:10.1172/JCI112134.

Maes, E., Broeckx, V., Mertens, I., et al. (2013) Analysis of the formalin-fixed paraffin-embedded tissue proteome: Pitfalls, challenges, and future prospectives. *Amino Acids*. 45 (2). doi:10.1007/s00726-013-1494-0.

Magden, E.R., Sleeper, M.M., Buchl, S.J., et al. (2016) *Use of an Implantable Loop Recorder in a Chimpanzee (Pan troglodytes) to Monitor Cardiac Arrhythmias and Assess the Effects of Acupuncture and Laser Therapy*., (September 2018).

Maisels, F., Bergl, R.A. and Williamson, E.A. (2018) *Gorilla gorilla (amended version of 2016 assessment)*.

Markandran, K., Yu, H., Song, W., et al. (2022) Functional and Molecular Characterisation of Heart Failure Progression in Mice and the Role of Myosin Regulatory Light Chains in the Recovery of Cardiac Muscle Function. *International Journal of Molecular Sciences*, 23 (1). doi:10.3390/ijms23010088.

Martínez-Martínez, E., Brugnolaro, C., Ibarrola, J., et al. (2019) CT-1 (Cardiotrophin-1)-Gal-3 (Galectin-3) Axis in Cardiac Fibrosis and Inflammation: Mechanistic Insights

and Clinical Implications. *Hypertension*, 73 (3): 602–611. doi:10.1161/HYPERTENSIONAHA.118.11874.

Mattingly, Z.A., Celia, A.M., Kuo, Y., et al. (2021) Technical performance and biotemporal stability evaluation of Olink proximity extension assay for blood-based biomarker discovery. *Alzheimer's & Dementia*, 17 (S5). doi:10.1002/ALZ.056318.

McCormick, M.E., Collins, C., Makarewich, C.A., et al. (2015) Platelet endothelial cell adhesion molecule-1 mediates endothelial-cardiomyocyte communication and regulates cardiac function. *Journal of the American Heart Association*, 4 (1): e001210. doi:10.1161/JAHA.114.001210.

McDonald, K., Glezeva, N., Collier, P., et al. (2020) Tetranectin, a potential novel diagnostic biomarker of heart failure, is expressed within the myocardium and associates with cardiac fibrosis. *Scientific Reports*, 10 (1). doi:10.1038/S41598-020-64558-4.

Mellor, E.L., McDonald Kinkaid, H.K., Mendl, M.T., et al. (2021) Nature calls: Intelligence and natural foraging style predict poor welfare in captive parrots. *Proceedings of the Royal Society B: Biological Sciences*, 288 (1960). doi:10.1098/rspb.2021.1952.

Meredith, A., Boroomand, S., Carthy, J., et al. (2015) 1,25 Dihydroxyvitamin D3 Inhibits TGFβ1-Mediated Primary Human Cardiac Myofibroblast Activation. *PLoS ONE*, 10 (6): e0128655. doi:10.1371/JOURNAL.PONE.0128655.

Metz, B., Kersten, G.F.A., Hoogerhout, P., et al. (2004) Identification of formaldehyde-induced modifications in proteins: Reactions with model peptides. *Journal of Biological Chemistry*, 279 (8). doi:10.1074/jbc.M310752200.

Micke, P., Ohshima, M., Tahmasebpoor, S., et al. (2006) Biobanking of fresh frozen tissue: RNA is stable in nonfixed surgical specimens. *Laboratory Investigation*, 86 (2). doi:10.1038/labinvest.3700372.

Miller, C.L., Schwartz, A.M., Barnhart, J.S., et al. (1999) Chronic Hypertension with Subsequent Congestive Heart Failure in a Western Lowland Gorilla (Gorilla gorilla gorilla). *Journal of Zoo and Wildlife Medicine*, 30 (2): 262–267.

Minic, R. and Zivkovic, I. (2020) “Optimization, Validation and Standardization of ELISA.” In Mózsik, G. (ed.) *Norovirus*. London: IntechOpen. doi:10.5772/INTECHOPEN.94338.

Mishra, P., Pandey, C.M., Singh, U., et al. (2019) Descriptive Statistics and Normality Tests for Statistical Data. *Annals of Cardiac Anaesthesia*, 22 (1): 67. doi:10.4103/ACA.ACA_157_18.

Modaber, M., Nazemi Rafie, J. and Rajabi-Maham, H. (2019) Population genetic structure of native Iranian population of Apis mellifera meda based on intergenic region and COX2 gene of mtDNA. *Insectes Sociaux*, 66 (3). doi:10.1007/s00040-019-00701-3.

Moittié, S. (2021) *Great ape cardiovascular disease: aetiopathogenesis, risk factors and diagnostic tools*.

Moittié, S., Baiker, K., Strong, V., et al. (2020a) Discovery of os cordis in the cardiac skeleton of chimpanzees (Pan troglodytes). *Scientific Reports*, 10 (1): 9417. doi:10.1038/s41598-020-66345-7.

Moittié, S., Graham, P.A., Barlow, N., et al. (2020b) Comparison of 25-hydroxyvitamin D concentration in chimpanzee dried blood spots and serum. *Veterinary Clinical Pathology*, 49 (2): 299–306. doi:10.1111/vcp.12863.

Moittié, S., Jarvis, R., Bandelow, S., et al. (2022) Vitamin D status in chimpanzees in human care: a Europe wide study. *Scientific Reports*, 12: 17625. doi:10.1038/s41598-022-21211-6.

Moittié, S., N Sheppard, M., Thiele, T., et al. (2020c) Non-Infectious, Necrotizing and Granulomatous Aortitis in a Female Gorilla. *Journal of Comparative Pathology*, 181: 7–12. doi:10.1016/J.JCPA.2020.09.009.

Mongirdienė, A., Skrodenis, L., Varoneckaitė, L., et al. (2022) Reactive Oxygen Species Induced Pathways in Heart Failure Pathogenesis and Potential Therapeutic Strategies. *Biomedicines*. 10 (3). doi:10.3390/biomedicines10030602.

Monk, N.A.M. (2003) Oscillatory expression of Hes1, p53, and NF-κB driven by transcriptional time delays. *Current Biology*, 13 (16). doi:10.1016/S0960-9822(03)00494-9.

Montero-Calle, A., Garranzo-Asensio, M., Rejas-González, R., et al. (2023) Benefits of FAIMS to Improve the Proteome Coverage of Deteriorated and/or Cross-Linked TMT 10-Plex FFPE Tissue and Plasma-Derived Exosomes Samples. *Proteomes*, 11 (4). doi:10.3390/proteomes11040035.

Moresco, A., Feltrer-Rambaud, Y., Wolfman, D., et al. (2022) Reproductive one health in primates. *American Journal of Primatology*. 84 (4–5). doi:10.1002/ajp.23325.

Morrow, D.A. and De Lemos, J.A. (2007) Benchmarks for the assessment of novel cardiovascular biomarkers. *Circulation*, 115 (8): 949–952. doi:10.1161/CIRCULATIONAHA.106.683110.

Mortazavi, A., Williams, B.A., McCue, K., et al. (2008) Mapping and quantifying mammalian transcriptomes by RNA-Seq. *Nature Methods*, 5 (7). doi:10.1038/nmeth.1226.

Moslemi, E., Musazadeh, V., Kavyani, Z., et al. (2022) Efficacy of vitamin D supplementation as an adjunct therapy for improving inflammatory and oxidative stress biomarkers: An umbrella meta-analysis. *Pharmacological Research*, p. 106484. doi:10.1016/J.PHRS.2022.106484.

Mozos, I. and Marginean, O. (2015) Links between Vitamin D Deficiency and Cardiovascular Diseases. *BioMed Research International*, pp. 1–12. doi:10.1155/2015/109275.

Mulder, I., Van Der Meer, R., De Vries, H., et al. (2016) The effect of a diet change on regurgitation and reingestion in captive chimpanzees. *Journal of Zoo and Aquarium Research*, 4 (4).

Van Mulders, L., Locquet, L., Kaandorp, C., et al. (2024) An overview of nutritional factors in the aetiopathogenesis of myocardial fibrosis in great apes. *Nutrition Research Reviews*, pp. 1–16. doi:10.1017/S0954422424000076.

Munson, L. and Montali, R.J. (1990) Pathology and diseases of great apes at the National Zoological Park. *Zoo Biology*, 9 (2). doi:10.1002/zoo.1430090204.

Murali, E., Nagle, A., Yoo, D., et al. (2022) Microtubules maintain passive tension and myofibril formation in developing cardiomyocytes. *Biophysical Journal*, 121 (3). doi:10.1016/j.bpj.2021.11.1456.

Murray, S., Kishbaugh, J.C., Hayek, L.A.C., et al. (2019) Diagnosing cardiovascular disease in western lowland gorillas (Gorilla gorilla gorilla) with brain natriuretic peptide. *PLoS ONE*, 14 (3). doi:10.1371/journal.pone.0214101.

Mutter, G.L., Zahrieh, D., Liu, C., et al. (2004) Comparison of frozen and RNALater solid tissue storage methods for use in RNA expression microarrays. *BMC Genomics*, 5. doi:10.1186/1471-2164-5-88.

Myers, M.J., Smith, E.R. and Turfle, P.G. (2017) Biomarkers in Veterinary Medicine. *Annual Review of Animal Biosciences*, 5: 65–87. doi:10.1146/annurev-animal-021815-111431.

Nemir, M., Metrich, M., Plaisance, I., et al. (2014) The Notch pathway controls fibrotic and regenerative repair in the adult heart. *European Heart Journal*, 35 (32): 2174–2185. doi:10.1093/EURHEARTJ/EHS269.

Newman, P.J., Berndt, M.C., Gorski, J., et al. (1990) PECAM-1 (CD31) Cloning and Relation to Adhesion Molecules of the Immunoglobulin Gene Superfamily. *Science*, 247 (4947): 1219–1222. doi:10.1126/SCIENCE.1690453.

Niemuth, N.A., Rudge, T.L., Sankovich, K.A., et al. (2020) Method feasibility for cross-species testing, qualification, and validation of the Filovirus Animal Nonclinical Group anti-Ebola virus glycoprotein immunoglobulin G enzyme-linked immunosorbent assay for non-human primate serum samples. *PLOS ONE*, 15 (10): e0241016. doi:10.1371/JOURNAL.PONE.0241016.

Nikolov, A. and Popovski, N. (2022) Extracellular Matrix in Heart Disease: Focus on Circulating Collagen Type I and III Derived Peptides as Biomarkers of Myocardial Fibrosis and Their Potential in the Prognosis of Heart Failure: A Concise Review. *Metabolites*. 12 (4). doi:10.3390/metabo12040297.

Nilsson, L.H., Grøndal, S.M., Blø, M., et al. (2021) Tilvestamab, a function-blocking monoclonal antibody inhibitor of AXL RTK signalling, limits the onset of renal fibrotic changes in human kidneys ex vivo. *Nephrology Dialysis Transplantation*, 36 (Supplement_1). doi:10.1093/ndt/gfab078.0010.

Nishida, T., Corp, N., Hamai, M., et al. (2003) Demography, female life history, and reproductive profiles among the chimpanzees of Mahale. *American Journal of Primatology*, 59 (3): 99–121. doi:10.1002/ajp.10068.

Nizami, H.L., Katare, P., Prabhakar, P., et al. (2019) Vitamin D Deficiency in Rats Causes Cardiac Dysfunction by Inducing Myocardial Insulin Resistance. *Molecular nutrition & food research*, 63 (17): 1900109-n/a. doi:10.1002/mnfr.201900109.

Nolan, T., Hands, R.E. and Bustin, S.A. (2006) Quantification of mRNA using real-time RT-PCR. *Nature Protocols*, 1 (3). doi:10.1038/nprot.2006.236.

Nowak, M.G., Rianti, P., Wich, S.A., et al. (2017) *Pongo tapanuliensis*.

Nunamaker, E.A., Lee, D.R. and Lammey, M.L. (2012) Chronic diseases in captive geriatric female Chimpanzees (Pan troglodytes). *Comparative medicine*, 62 (2): 131–136.

Obanda, V., Omondi, G.P. and Chiyo, P.I. (2014) The Influence of Body Mass Index, Age and Sex on Inflammatory Disease Risk in Semi-Captive Chimpanzees. *PloS one*, 9 (8): e104602–e104602. doi:10.1371/journal.pone.0104602.

Obi, E.N., Tellock, D.A., Thomas, G.J., et al. (2023) Biomarker Analysis of Formalin-Fixed Paraffin-Embedded Clinical Tissues Using Proteomics. *Biomolecules*. 13 (1). doi:10.3390/biom13010096.

Ogawa, Y., Tamura, N., Chusho, H., et al. (2001) Brain natriuretic peptide appears to act locally as an antifibrotic factor in the heart. *Canadian Journal of Physiology and Pharmacology*, 79 (8): 723–729. doi:10.1139/Y01-052.

Olds, J.E., Goldacker, A., Huneycutt, D., et al. (2023) The AliveCor KardiaMobile ECG device allows electrocardiogram assessment in awake bonobos (Pan paniscus). *American Journal of Veterinary Research*, 84 (6). doi:10.2460/ajvr.23.01.0013.

Olink (2021a) *Data normalization and standardization (White paper)*. Available at: https://7074596.fs1.hubspotusercontent-na1.net/hubfs/7074596/05-white%20paper%20for%20website/1096-olink-data-normalization-white-paper.pdf (Accessed: 24 May 2025).

Olink (2021b) *Measuring protein biomarkers with Olink — technical comparisons and orthogonal validation*. Available at: https://olink.com/application/measuring-protein-biomarkers-with-olink/ (Accessed: 14 May 2024).

Olivieri, J., Smaldone, S. and Ramirez, F. (2010) Fibrillin assemblies: Extracellular determinants of tissue formation and fibrosis. *Fibrogenesis and Tissue Repair*. 3 (1). doi:10.1186/1755-1536-3-24.

O'Neill, C.M., Kazantzidis, A., Ryan, M.J., et al. (2016) Seasonal Changes in Vitamin D-Effective UVB Availability in Europe and Associations with Population Serum 25-Hydroxyvitamin D. *Nutrients*, 8 (9): 533. doi:10.3390/NU8090533.

Ortega-Pinazo, J., Pacheco-Rodríguez, M.J., Serrano-Castro, P.J., et al. (2023) Comparing RNA extraction methods to face the variations in RNA quality using two human biological matrices. *Molecular Biology Reports*, 50 (11): 9263–9271. doi:10.1007/S11033-023-08761-2/TABLES/3.

Ostasiewicz, P., Zielinska, D.F., Mann, M., et al. (2010) Proteome, phosphoproteome, and N-glycoproteome are quantitatively preserved in formalin-fixed paraffin-embedded tissue and analyzable by high-resolution mass spectrometry. *Journal of Proteome Research*, 9 (7). doi:10.1021/pr100234w.

Oveland, E., Muth, T., Rapp, E., et al. (2015) Viewing the proteome: How to visualize proteomics data? *PROTEOMICS*, 15 (8): 1341–1355. doi:10.1002/PMIC.201400412.

Oyama, M.A. (2013) Using Cardiac Biomarkers in Veterinary Practice. *Veterinary Clinics of North America - Small Animal Practice*, 43 (6): 1261–1272. doi:10.1016/j.cvsm.2013.07.010.

Pai, A.A., Bell, J.T., Marioni, J.C., et al. (2011) A genome-wide study of DNA methylation patterns and gene expression levels in multiple human and chimpanzee tissues. *PLoS Genetics*, 7 (2). doi:10.1371/journal.pgen.1001316.

Pandey, A. and Mann, M. (2000) Proteomics to study genes and genomes. *Nature*. 405 (6788). doi:10.1038/35015709.

Paola Gómez-Mendoza, D., Lara-Ribeiro, A.C. and Verano-Braga, T. (2021) Pathological cardiac remodeling seen by the eyes of proteomics. *BBA-Proteins and Proteomics*, 1869: 140622. doi:10.1016/j.bbapap.2021.140622.

Parfitt, A.M., Gallagher, J.C., Heaney, R.P., et al. (1982) Vitamin D and bone health in the elderly. *American Journal of Clinical Nutrition*, 36 (5 Suppl.): 1014–1031. doi:10.1093/ajcn/36.5.1014.

Pasha, S., Inui, T., Chapple, I., et al. (2018) The Saliva Proteome of Dogs: Variations Within and Between Breeds and Between Species. *Proteomics*, 18 (3–4): 1700293. doi:10.1002/PMIC.201700293.

Pavlovic, B.J., Blake, L.E., Roux, J., et al. (2018) A Comparative Assessment of Human and Chimpanzee iPSC-derived Cardiomyocytes with Primary Heart Tissues. *Scientific Reports*, 8 (1): 1–14. doi:10.1038/s41598-018-33478-9.

Pearson, E.L., Lowry, R., Dorrian, J., et al. (2014) Evaluating the conservation impact of an innovative zoo-based educational campaign: “Don’t Palm Us Off” for orang-utan conservation. *Zoo Biology*, 33 (3). doi:10.1002/zoo.21120.

Pepe, M.S. (2003) *The Statistical Evaluation of Medical Tests for Classification and Prediction*. doi:10.1093/oso/9780198509844.001.0001.

Perge, P., Boros, A.M., Gellér, L., et al. (2019) Vitamin D Deficiency Predicts Poor Clinical Outcomes in Heart Failure Patients Undergoing Cardiac Resynchronization Therapy. *Disease markers*, 2019: 1–7. doi:10.1155/2019/4145821.

Petrera, A., Von Toerne, C., Behler, J., et al. (2021) Multiplatform Approach for Plasma Proteomics: Complementarity of Olink Proximity Extension Assay Technology to Mass Spectrometry-Based Protein Profiling. *Journal of Proteome Research*, 20 (1): 751–762. doi:10.1021/ACS.JPROTEOME.0C00641/ASSET/IMAGES/LARGE/PR0C00641_0006.JPEG.

Phyo, S.A., Uchida, K., Chen, C.Y., et al. (2022) Transcriptional, Post-Transcriptional, and Post-Translational Mechanisms Rewrite the Tubulin Code During Cardiac Hypertrophy and Failure. *Frontiers in Cell and Developmental Biology*, 10. doi:10.3389/fcell.2022.837486.

Pidkovka, N. and Belkhiri, A. (2023) Altered expression of AXL receptor tyrosine kinase in gastrointestinal cancers: a promising therapeutic target. *Frontiers in Oncology*, 13: 1079041. doi:10.3389/FONC.2023.1079041/BIBTEX.

Pilz, S., Tomaschitz, A., Drechsler, C., et al. (2010) Vitamin D deficiency and myocardial diseases. *Molecular Nutrition and Food Research*, 54 (8): 1103–1113. doi:10.1002/mnfr.200900474.

Pilz, S., Tomaschitz, A., März, W., et al. (2011) Vitamin D, cardiovascular disease and mortality. *Clinical Endocrinology*, 75 (5): 575–584. doi:10.1111/J.1365-2265.2011.04147.X.

Pilz, S., Tomaschitz, A., Ritz, E., et al. (2009) Vitamin D status and arterial hypertension: a systematic review. *Nature Reviews Cardiology 2009 6:10*, 6 (10): 621–630. doi:10.1038/nrcardio.2009.135.

Pizzollo, J., Nielsen, W.J., Shibata, Y., et al. (2018) Comparative Serum Challenges Show Divergent Patterns of Gene Expression and Open Chromatin in Human and Chimpanzee. *Genome Biology and Evolution*, 10 (3): 826–839. doi:10.1093/GBE/EVY041.

Plavelil, N., Goldstein, R., Klein, M., et al. (2020) Tachycardia-Induced Matrix Metalloproteinases Activation Associated with Collagen Type III Cardiac Fibrosis and Heart Failure in Swine. *The FASEB Journal*, 34 (S1). doi:10.1096/fasebj.2020.34.s1.08987.

Plumptre, A., Robbins, M.M. and Williamson, E.A. (2019) *Gorilla beringei*.

Prentice, A. (2008) Vitamin D deficiency: A global perspective. *Nutrition Reviews*, 66 (Suppl.2): S153–S164. doi:10.1111/j.1753-4887.2008.00100.x.

Rabb, G.B. (1994) The changing roles of zoological parks in conserving biological diversity. *Integrative and Comparative Biology*, 34 (1). doi:10.1093/icb/34.1.159.

Rahman, A., Hershey, S., Ahmed, S., et al. (2007) Heart extracellular matrix gene expression profile in the vitamin D receptor knockout mice. *Journal of Steroid Biochemistry and Molecular Biology*, 103 (3–5). doi:10.1016/j.jsbmb.2006.12.081.

Raindi, D., Rees, J., Hirschfeld, J., et al. (2022) Periodontal health, neutrophil activity and cardiovascular health in captive chimpanzees. *Archives of Oral Biology*, 134: 105342. doi:10.1016/J.ARCHORALBIO.2021.105342.

Ramzan, R., Vogt, S. and Kadenbach, B. (2020) Stress-mediated generation of deleterious ROS in healthy individuals - role of cytochrome c oxidase. *Journal of Molecular Medicine*. 98 (5). doi:10.1007/s00109-020-01905-y.

Raskopf, E., Gonzalez Carmona, M.A., Van Cayzeele, C.J., et al. (2014) Toxic damage increases angiogenesis and metastasis in fibrotic livers via PECAM-1. *BioMed Research International*, 2014. doi:10.1155/2014/712893.

Rasmussen, R. (2001) “Quantification on the LightCycler.” In *Rapid Cycle Real-Time PCR*. doi:10.1007/978-3-642-59524-0_3.

Ravassa, S., López, B., Treibel, T.A., et al. (2023a) Cardiac Fibrosis in heart failure: Focus on non-invasive diagnosis and emerging therapeutic strategies. *Molecular Aspects of Medicine*, 93: 101194. doi:10.1016/J.MAM.2023.101194.

Ravassa, S., López, B., Treibel, T.A., et al. (2023b) Cardiac Fibrosis in heart failure: Focus on non-invasive diagnosis and emerging therapeutic strategies. *Molecular Aspects of Medicine*, 93: 101194. doi:10.1016/J.MAM.2023.101194.

Reagan, W.J., Barnes, R., Harris, P., et al. (2017) Assessment of Cardiac Troponin I Responses in Nonhuman Primates during Restraint , Blood Collection , and Dosing in Preclinical Safety Studies. *Toxicologic Pathology*, 45 (2): 335–343. doi:10.1177/0192623316663865.

Rebrova, T.Y., Muslimova, E.F., Kondratieva, D.S., et al. (2018) The Role of Ca2+-ATPase 2a (ATP2A2), Ryanodine Receptors (RYR2), and Calsequestrin (CASQ2) Gene Polymorphisms in the Development of Heart Failure. *Russian Journal of Genetics*. 54 (6). doi:10.1134/S102279541806008X.

Reichlin, T., Hochholzer, W., Bassetti, S., et al. (2009) Early Diagnosis of Myocardial Infarction with Sensitive Cardiac Troponin Assays. *New England Journal of Medicine*, 361 (9): 858–867. doi:10.1056/NEJMOA0900428/SUPPL_FILE/NEJM_REICHLIN_858SA1.PDF.

Reschner, H., Milutinovic, A. and Petrovič, D. (2009) The PECAM-1 gene polymorphism - a genetic marker of myocardial infarction. *Central European Journal of Biology*, 4 (4): 515–520. doi:10.2478/S11535-009-0042-0/MACHINEREADABLECITATION/RIS.

Revuelta-López, E., Barallat, J., Cserkoóvá, A., et al. (2021) Pre-analytical considerations in biomarker research: Focus on cardiovascular disease. *Clinical Chemistry and Laboratory Medicine*, 59 (11): 1747–1760. doi:10.1515/CCLM-2021-0377/ASSET/GRAPHIC/J_CCLM-2021-0377_FIG_003.JPG.

Rivera, S. and Leach, K.S. (2023) “Voluntary Medical Procedures in Great Apes.” In Miller, E., Lamberski, N. and Calle, P. (eds.) *Fowler’s Zoo and Wild Animal Medicine Current Therapy*. 10th ed. pp. 673–678. doi:10.1016/B978-0-323-82852-9.00097-6.

Rojsajjakul, T., Hordeaux, J.J., Choudhury, G.R., et al. (2023) Quantification of human mature frataxin protein expression in nonhuman primate hearts after gene therapy. *Communications Biology*, 6 (1). doi:10.1038/s42003-023-05472-z.

Ronghai, Y., Weiping, Y., Yingfeng, L., et al. (2019) Salvia miltiorrhiza injection ameliorates myocardial ischemia-reperfusion injury via downregulation of PECAM-1. *Tropical Journal of Pharmaceutical Research*, 18 (7): 1467–1473. doi:10.4314/TJPR.V18I7.15.

Ross, S.R., Joshi, P.B., Terio, K.A., et al. (2022) A 25-Year Retrospective Review of Mortality in Chimpanzees (Pan troglodytes) in Accredited U.S. Zoos from a Management and Welfare Perspective. *Animals*, 12 (15): 1878. doi:10.3390/ANI12151878.

Rostand, S.G. (1997) Ultraviolet light may contribute to geographic and racial blood pressure differences. *Hypertension*, 30 (2): 150–156. doi:10.1161/01.HYP.30.2.150.

Ruopp, M.D., Perkins, N.J., Whitcomb, B.W., et al. (2008) Youden Index and Optimal Cut-Point Estimated from Observations Affected by a Lower Limit of Detection. *Biometrical journal. Biometrische Zeitschrift*, 50 (3): 419. doi:10.1002/BIMJ.200710415.

Sambrook, J. and Russell, D.W. (2001) *Molecular Cloning: A Laboratory Manual. Third Edition*.

Sarohi, V., Chakraborty, S. and Basak, T. (2022) Exploring the cardiac ECM during fibrosis: A new era with next-gen proteomics. *Frontiers in Molecular Biosciences*. 9. doi:10.3389/fmolb.2022.1030226.

Schafer, S., Viswanathan, S., Widjaja, A.A., et al. (2017) IL-11 is a crucial determinant of cardiovascular fibrosis. *Nature 2017 552:7683*, 552 (7683): 110–115. doi:10.1038/nature24676.

Schmidt, I.M., Colona, M.R., Srivastava, A., et al. (2022) Plasma Kidney Injury Molecule-1 in Systemic Lupus Erythematosus: Discordance Between ELISA and Proximity Extension Assay. *Kidney Medicine*, 4 (8): 100496. doi:10.1016/J.XKME.2022.100496.

Schmidt, R.E. (1978) Systemic Pathology of Chimpanzees. *Journal of Medical Primatology*, 7: 274–318. doi:10.1159/000459914.

Schwalfenberg, G.K. (2011) A review of the critical role of vitamin D in the functioning of the immune system and the clinical implications of vitamin D deficiency. *Molecular Nutrition and Food Research*, 55 (1): 96–108. doi:10.1002/mnfr.201000174.

Schwanhüusser, B., Busse, D., Li, N., et al. (2011) Global quantification of mammalian gene expression control. *Nature*, 473 (7347). doi:10.1038/nature10098.

Schweigert, F.J., Gerike, B., Raila, J., et al. (2007) Proteomic distinction between humans and great apes based on plasma transthyretin microheterogeneity. *Comparative Biochemistry and Physiology Part D: Genomics and Proteomics*, 2 (2): 144–149. doi:10.1016/J.CBD.2007.02.001.

Scicchitano, M.S., Dalmas, D.A., Boyce, R.W., et al. (2009) Protein extraction of formalin-fixed, paraffin-embedded tissue enables robust proteomic profiles by mass spectrometry. *Journal of Histochemistry and Cytochemistry*, 57 (9). doi:10.1369/jhc.2009.953497.

Scragg, R., Stewart, A.W., Waayer, D., et al. (2017) Effect of monthly high-dose vitamin D supplementation on cardiovascular disease in the vitamin D assessment study: A randomized clinical trial. *JAMA Cardiology*, 2 (6): 608–616. doi:10.1001/jamacardio.2017.0175.

Seiler, B.M., Dick, E.J., Guardado-Mendoza, R., et al. (2009) Spontaneous heart disease in the adult chimpanzee (Pan troglodytes). *Journal of Medical Primatology*, 38 (1): 51–58. doi:10.1111/j.1600-0684.2008.00307.x.

Sen-Chowdhry, S., Lowe, M.D., Sporton, S.C., et al. (2004) Arrhythmogenic right ventricular cardiomyopathy: Clinical presentation, diagnosis, and management. *The American Journal of Medicine*, 117 (9): 685–695. doi:10.1016/J.AMJMED.2004.04.028.

Sepulveda, J.L. and Wu, C. (2006) The parvins. *Cellular and Molecular Life Sciences*. 63 (1). doi:10.1007/s00018-005-5355-1.

Serebruany, V.L., Murugesan, S.R., Pothula, A., et al. (1999) Soluble PECAM-1, but Not P-Selectin, Nor Osteonectin Identify Acute Myocardial Infarction in Patients Presenting with Chest Pain. *Cardiology*, 91 (1): 50–55. doi:10.1159/000006876.

Shao, W.H. and Cohen, P.L. (2014) The role of tyrosine kinases in systemic lupus erythematosus and their potential as therapeutic targets. *Expert Review of Clinical Immunology*. 10 (5). doi:10.1586/1744666X.2014.893827.

Shave, R., Oxborough, D., Somauroo, J., et al. (2014) Echocardiographic assessment of cardiac structure and function in great apes: a practical guide. *International Zoo Yearbook*, 48 (1): 218–233. doi:10.1111/izy.12026.

Shaw, P.W., Yang, Y., Gonzalez, J.A., et al. (2016) Extracellular volume by CMR is associated with serum biomarkers of extracellular matrix turnover and inflammation in hypertensive heart disease. *Journal of Cardiovascular Magnetic Resonance*. 18. doi:10.1186/1532-429X-18-S1-O103.

Shing, C., Id, R.H., Mü Ller-Nurasyid Id, M., et al. (2023) Proteomics biomarker discovery for individualized prevention of familial pancreatic cancer using statistical learning. *PLOS ONE*, 18 (1): e0280399. doi:10.1371/JOURNAL.PONE.0280399.

Shi-Wen, X., Leask, A. and Abraham, D. (2008) Regulation and function of connective tissue growth factor/CCN2 in tissue repair, scarring and fibrosis. *Cytokine and Growth Factor Reviews*. 19 (2). doi:10.1016/j.cytogfr.2008.01.002.

Shrader, S. (2013) “Introductory mass spectrometry.” In *Introductory Mass Spectrometry*. pp. 1–11. doi:10.1201/b15584.

Shu, J., Gu, Y., Jin, L., et al. (2021) Matrix metalloproteinase 3 regulates angiotensin II-induced myocardial fibrosis cell viability, migration and apoptosis. *Molecular Medicine Reports*, 23 (2). doi:10.3892/MMR.2020.11790.

Simões, F.C., Cahill, T.J., Kenyon, A., et al. (2020) Macrophages directly contribute collagen to scar formation during zebrafish heart regeneration and mouse heart repair. *Nature Communications*, 11 (1). doi:10.1038/S41467-019-14263-2.

Singleton, I., Wich, S.A., Nowak, M., et al. (2017) *Pongo abelii (errata version published in 2018)*.

Skau, E., Wagner, P., Leppert, J., et al. (2023) Are the results from a multiplex proteomic assay and a conventional immunoassay for NT-proBNP and GDF-15 comparable? *Clinical Proteomics*, 20 (1). doi:10.1186/S12014-023-09393-1.

Slaffer, S.N. and Allchurch, A.F. (1995) Diagnosis and treatment of dilated (congestive) cardio-myopathy in a Sumatran orang-utan Pongo pygmaeus abelii. *Dodo*, 31: 147–152.

Sleeper, M.M. (2009) Is it acute heart failure or sudden cardiac death in the chimpanzee? *Journal of medical primatology*, 38 (2): 75–75. doi:10.1111/j.1600-0684.2009.00351.x.

Sleeper, M.M., Doane, C.J., Langner, P.H., et al. (2005) Successful treatment of idiopathic dilated cardiomyopathy in an adult chimpanzee (Pan troglodytes). *Comparative Medicine*, 55 (1): 80–84.

Song, B., Liu, Y., Parman, T., et al. (2014) Quantitative Proteomics for Cardiac Biomarker Discovery Using Isoproterenol-Treated Nonhuman Primates. *Journal of proteome research*, 13 (12): 5909–5917. doi:10.1021/pr500835w.

Sonnenschein, K., Fiedler, J., de Gonzalo-Calvo, D., et al. (2021) Blood-based protein profiling identifies serum protein c-KIT as a novel biomarker for hypertrophic cardiomyopathy. *Scientific Reports*, 11 (1). doi:10.1038/s41598-020-80868-z.

Specker, B.L. (1994) Do North American women need supplemental vitamin D during pregnancy or lactation? *The American Journal of Clinical Nutrition*, 59 (2): 484S-491S. doi:10.1093/AJCN/59.2.484S.

Sprung, R.W., Brock, J.W.C., Tanksley, J.P., et al. (2009) Equivalence of protein inventories obtained from formalin-fixed paraffin-embedded and frozen tissue in multidimensional liquid chromatography-tandem mass spectrometry shotgun

proteomic analysis. *Molecular and Cellular Proteomics*, 8 (8). doi:10.1074/mcp.M800518-MCP200.

Srinivasan, M., Sedmak, D. and Jewell, S. (2002) Effect of fixatives and tissue processing on the content and integrity of nucleic acids. *American Journal of Pathology*. 161 (6). doi:10.1016/S0002-9440(10)64472-0.

Srinivasan, S. and Avadhani, N.G. (2012) Cytochrome c oxidase dysfunction in oxidative stress. *Free Radical Biology and Medicine*. 53 (6). doi:10.1016/j.freeradbiomed.2012.07.021.

Standley, C.J., Mugisha, L., Adriko, M., et al. (2013) Intestinal schistosomiasis in chimpanzees on Ngamba Island, Uganda: Observations on liver fibrosis, schistosome genetic diversity and praziquantel treatment. *Parasitology*, 140 (3). doi:10.1017/S0031182012001576.

Staufer, K., Dengler, M., Huber, H., et al. (2017) The non-invasive serum biomarker soluble Axl accurately detects advanced liver fibrosis and cirrhosis. *Cell Death and Disease*, 8 (10). doi:10.1038/CDDIS.2017.554.

Steiner, C.A., Rodansky, E.S., Johnson, L.A., et al. (2021) AXL Is a Potential Target for the Treatment of Intestinal Fibrosis. *Inflammatory Bowel Diseases*, 27 (3). doi:10.1093/ibd/izaa169.

Stratton, H.S., Ange-van Heugten, K.D. and Minter, L.J. (2022) Comparison of Hematocrit and Biochemical Analytes among Two Point-of-Care Analyzers (EPOC and i-STAT Alinity v) and a Veterinary Diagnostic Laboratory in the African Savanna Elephant (Loxodonta africana) and the Southern White Rhinoceros (Ceratotherium simum simum). *Journal of Zoological and Botanical Gardens 2022, Vol. 3, Pages 653-664*, 3 (4): 653–664. doi:10.3390/JZBG3040048.

Strong, V., Baiker, K., Brennan, M.L., et al. (2017) A retrospective review of western lowland gorilla (gorilla, gorilla, gorilla) mortality in European zoological collections between 2004 and 2014. *Journal of Zoo and Wildlife Medicine*, 48 (2): 277–286. doi:10.1638/2016-0132R.1.

Strong, V., Moittié, S., Sheppard, M.N., et al. (2020) Idiopathic Myocardial Fibrosis in Captive Chimpanzees (Pan troglodytes). *Veterinary Pathology*, 57 (1): 183–191. doi:10.1177/0300985819879442.

Strong, V., Möller, T., Tillman, A.S., et al. (2018a) A clinical study to evaluate the cardiopulmonary characteristics of two different anaesthetic protocols for immobilization of healthy chimpanzees (Pan troglodytes). *Veterinary Anaesthesia and Analgesia*, 45 (6): 794–801. doi:10.1016/j.vaa.2018.06.015.

Strong, V.J. (2017) *Getting to the heart of the matter: an investigation into captive great ape mortality and cardiovascular disease*.

Strong, V.J., Grindlay, D., Redrobe, S., et al. (2016) A systematic review of the literature relating to captive great ape morbidity and mortality. *Journal of Zoo and Wildlife Medicine*, 47 (3): 697–710. doi:10.1638/2015-0240.1.

Strong, V.J., Martin, M., Redrobe, S., et al. (2018b) A retrospective review of great ape cardiovascular disease epidemiology and pathology. *International Zoo Yearbook*, 52 (1): 113–125. doi:10.1111/izy.12193.

Strong, V.J., Sheppard, M.N., Redrobe, S., et al. (2018c) Guidelines for consistent cardiovascular post-mortem examination, sampling and reporting of lesions in European zoo-housed great apes. *International Zoo Yearbook*. doi:10.1111/izy.12191.

Stubenrauch, K., Wessels, U. and Lenz, H. (2009) Evaluation of an immunoassay for human-specific quantitation of therapeutic antibodies in serum samples from non-human primates. *Journal of Pharmaceutical and Biomedical Analysis*, 49 (4): 1003–1008. doi:10.1016/J.JPBA.2009.01.030.

Suzuki, J.I., Isobe, M., Kawauchi, M., et al. (2000) Altered expression of matrix metalloproteinases and tissue inhibitors of metalloproteinases in acutely rejected myocardium and coronary arteriosclerosis in cardiac allografts of nonhuman primates. *Transplant International*, 13 (2). doi:10.1111/j.1432-2277.2000.tb01049.x.

Swynghedauw, B. (1999) Molecular mechanisms of myocardial remodeling. *Physiological Reviews*. 79 (1). doi:10.1152/physrev.1999.79.1.215.

Szczesna-Cordary, D., Guzman, G., Ng, S.S., et al. (2004) Familial Hypertrophic Cardiomyopathy-linked Alterations in Ca2+ Binding of Human Cardiac Myosin

Regulatory Light Chain Affect Cardiac Muscle Contraction. *Journal of Biological Chemistry*, 279 (5). doi:10.1074/jbc.M307092200.

Szklarczyk, D., Kirsch, R., Koutrouli, M., et al. (2023) The STRING database in 2023: protein-protein association networks and functional enrichment analyses for any sequenced genome of interest. *Nucleic acids research*, 51 (D1): D638–D646. doi:10.1093/NAR/GKAC1000.

Szodoray, P., Nakken, B., Gaal, J., et al. (2008) The complex role of vitamin D in autoimmune diseases. *Scandinavian Journal of Immunology*, 68 (3): 261–269. doi:10.1111/j.1365-3083.2008.02127.x.

Tallo-Parra, O., Salas, M. and Manteca, X. (2023) Zoo Animal Welfare Assessment: Where Do We Stand? *Animals*. 13 (12). doi:10.3390/ani13121966.

Tang, W.H.W., Francis, G.S., Morrow, D.A., et al. (2007) National Academy of Clinical Biochemistry Laboratory Medicine Practice Guidelines: Clinical utilization of cardiac biomarker testing in heart failure. *Circulation*, 116 (5): 99–109. doi:10.1161/CIRCULATIONAHA.107.185267.

Tangpricha, V., Pearce, E.N., Chen, T.C., et al. (2002) Vitamin D insufficiency among free-living healthy young adults. *American Journal of Medicine*, 112 (8): 659–662. doi:10.1016/S0002-9343(02)01091-4.

Taylor, S., Wakem, M., Dijkman, G., et al. (2010) A practical approach to RT-qPCR—Publishing data that conform to the MIQE guidelines. *Methods*, 50 (4): S1–S5. doi:10.1016/J.YMETH.2010.01.005.

Teng, L., Huang, Y., Guo, J., et al. (2021) Cardiac fibroblast miR-27a may function as an endogenous anti-fibrotic by negatively regulating Early Growth Response Protein 3 (EGR3). *Journal of Cellular and Molecular Medicine*, 25 (1): 73–83. doi:10.1111/JCMM.15814.

Terio, K.A., Acvp, D., Kinsel, M.J., et al. (2011) Pathologic Lesions in Chimpanzees (Pan troglodytes schweinfurthii) from Gombe National Park, Tanzania, 2004-2010. *Journal of Zoo and Wildlife Medicine*, 42 (4): 597–607.

The Scientific Advisory Committee on Nutrition (2016) *Vitamin D and Health*. Available at: https://www.gov.uk/government/publications/sacn-vitamin-d-and-health-report (Accessed: 1 June 2021).

The UniProt Consortium (2021) UniProt: the universal protein knowledgebase in 2021. *Nucleic Acids Research*, 49 (D1): D480–D489. doi:10.1093/NAR/GKAA1100.

Thermo Scientific (2007) *Spike-and-recovery and linearity-of-dilution assessment*. Available at: https://tools.thermofisher.com/content/sfs/brochures/TR0058-Spike-and-Recovery.pdf (Accessed: 9 July 2022).

Thornton, B. and Basu, C. (2011) Real-time PCR (qPCR) primer design using free online software. *Biochemistry and Molecular Biology Education*, 39 (2). doi:10.1002/bmb.20461.

Time and Date AS 1995-2024 (n.d.) *Date Calculator: Add to or subtract from a date*. Available at: https://www.timeanddate.com/date/dateadd.html (Accessed: 15 December 2024).

Toepfer, C., Caorsi, V., Kampourakis, T., et al. (2013) Myosin regulatory light chain (RLC) phosphorylation change as a modulator of cardiac muscle contraction in disease. *Journal of Biological Chemistry*, 288 (19). doi:10.1074/jbc.M113.455444.

Tonelotto, V., Castagnaro, S., Cescon, M., et al. (2021) “Collagens and Muscle Diseases: A Focus on Collagen VI.” In *Biology of Extracellular Matrix*. doi:10.1007/978-3-030-67592-9_6.

Tong, L.J., Flach, E.J., Sheppard, M.N., et al. (2014) Fatal Arrhythmogenic Right Ventricular Cardiomyopathy in 2 Related Subadult Chimpanzees (Pan troglodytes). *Veterinary Pathology*, 51 (4): 858–867. doi:10.1177/0300985813501333.

Towbin, J.A. and Jefferies, J.L. (2017) Cardiomyopathies due to left ventricular noncompaction, mitochondrial and storage diseases, and inborn errors of metabolism. *Circulation Research*, 121 (7). doi:10.1161/CIRCRESAHA.117.310987.

Trundle, J., Lu-Nguyen, N., Malerba, A., et al. (2024) Targeted Antisense Oligonucleotide-Mediated Skipping of Murine Postn Exon 17 Partially Addresses Fibrosis in D2.mdx Mice. *International Journal of Molecular Sciences*, 25 (11): 6113. doi:10.3390/IJMS25116113/S1.

Tsoutsou, P.G., Gourgoulianis, K.I., Petinaki, E., et al. (2004) ICAM-1, ICAM-2 and ICAM-3 in the sera of patients with idiopathic pulmonary fibrosis. *Inflammation*, 28 (6): 359–364. doi:10.1007/S10753-004-6647-6/METRICS.

Tuomainen, T. and Tavi, P. (2017) The role of cardiac energy metabolism in cardiac hypertrophy and failure. *Experimental Cell Research*. 360 (1). doi:10.1016/j.yexcr.2017.03.052.

Vandesompele, J., De Preter, K., Pattyn, F., et al. (2002) Accurate normalization of real-time quantitative RT-PCR data by geometric averaging of multiple internal control genes. *Genome Biology*, 3 (7). doi:10.1186/gb-2002-3-7-research0034.

Vanhoutte, D., Van Almen, G.C., Van Aelst, L.N.L., et al. (2013) Matricellular proteins and matrix metalloproteinases mark the inflammatory and fibrotic response in human cardiac allograft rejection. *European Heart Journal*, 34 (25): 1930–1941. doi:10.1093/EURHEARTJ/EHS375.

Varki, N., Anderson, D., Herndon, J.G., et al. (2009) Heart disease is common in humans and chimpanzees, but is caused by different pathological processes. *Evolutionary Applications*, 2 (1): 101–112. doi:10.1111/j.1752-4571.2008.00064.x.

Vasbinder, A., Raffield, L.M., Gao, Y., et al. (2023) Assay-related differences in SuPAR levels: implications for measurement and data interpretation. *Journal of Nephrology*, 36 (1): 157–159. doi:10.1007/S40620-022-01344-7/TABLES/1.

Velázquez-Enríquez, J.M., Santos-álvarez, J.C., Ramírez-Hernández, A.A., et al. (2021) Proteomic analysis reveals key proteins in extracellular vesicles cargo associated with idiopathic pulmonary fibrosis in vitro. *Biomedicines*, 9 (8). doi:10.3390/biomedicines9081058.

Verma, A., Hawes, C.E., Lakshmanappa, Y.S., et al. (2021) Monoclonal antibodies protect aged rhesus macaques from SARS-CoV-2-induced immune activation and neuroinflammation. *Cell Reports*, 37 (5): 109942. doi:10.1016/j.celrep.2021.109942.

Videan, E.N., Cutler, R., Heward, C.B., et al. (2007a) Identification of Cardiovascular Disease Risk Factors in Male Chimpanzees (Pan troglodytes): Implications for Captive Management. *American Journal of Primatology: Abstract 184*, 69: 121. doi:10.1002/ajp.20448.

Videan, E.N., Heward, C.B., Chowdhury, K., et al. (2009) Comparison of Biomarkers of Oxidative Stress and Cardiovascular Disease in Humans and Chimpanzees (Pan troglodytes). *Comparative Medicine*, 59 (3): 287–296.

Videan, E.N., Heward, C.B., Fritz, J., et al. (2007b) Relationship between sunlight exposure, housing condition, and serum vitamin D and related physiologic biomarker levels in captive chimpanzees (Pan troglodytes). *Comparative Medicine*.

Viljoen, A., Singh, D.K., Farrington, K., et al. (2011) Analytical quality goals for 25-vitamin D based on biological variation. *Journal of Clinical Laboratory Analysis*, 25 (2): 130–133. doi:10.1002/JCLA.20446.

Vogel, C. and Marcotte, E.M. (2012) Insights into the regulation of protein abundance from proteomic and transcriptomic analyses. *Nature Reviews Genetics*, 13 (4). doi:10.1038/nrg3185.

Wang, C., Lv, J., Xue, C., et al. (2022) Novel role of COX6c in the regulation of oxidative phosphorylation and diseases. *Cell Death Discovery*. 8 (1). doi:10.1038/s41420-022-01130-1.

Wang, J., Gong, X., Chen, H., et al. (2017) Effect of Cardiac Resynchronization Therapy on Myocardial Fibrosis and Relevant Cytokines in a Canine Model With Experimental Heart Failure. *Journal of Cardiovascular Electrophysiology*, 28 (4): 438–445. doi:10.1111/JCE.13171.

Wang, L., Song, Y., Manson, J.A.E., et al. (2012) Circulating 25-Hydroxy-Vitamin D and risk of cardiovascular disease: A meta-analysis of prospective studies. *Circulation: Cardiovascular Quality and Outcomes*, 5 (6): 819–829. doi:10.1161/CIRCOUTCOMES.112.967604.

Wang, Y., Zhou, S., Lei, S., et al. (2020) Vitamin D Deficiency and Cardiovascular Diseases. *Science of advanced materials*, 12 (1): 27–37. doi:10.1166/sam.2020.3715.

Ware, W.A., Freeman, L.M., Rush, J.E., et al. (2020) Vitamin D status in cats with cardiomyopathy. *Journal of Veterinary Internal Medicine*, 34 (4): 1389–1398. doi:10.1111/jvim.15833.

Webb, A.R., Kazantzidis, A., Kift, R.C., et al. (2018) Colour counts: Sunlight and skin type as drivers of vitamin D deficiency at UK latitudes. *Nutrients*, 10 (4). doi:10.3390/nu10040457.

Webb, A.R., Kline, L. and Holick, M.F. (1988) Influence of Season and Latitude on the Cutaneous Synthesis of Vitamin D3: Exposure to Winter Sunlight in Boston and Edmonton Will Not Promote Vitamin D3 Synthesis in Human Skin. *Journal of Clinical Endocrinology and Metabolism*, 67 (2): 373–378. doi:10.1210/jcem-67-2-373.

Weiss, A. and King, J.E. (2015) Great ape origins of personality maturation and sex differences: A study of orangutans and chimpanzees. *Journal of Personality and Social Psychology*, 108 (4). doi:10.1037/pspp0000022.

Wibowo, D.S., Widayanti, R., Asvan, M., et al. (2021) Short communication: Molecular study on mt-dna cox2 gene of sumatran elephant (elephas maximus sumatranus). *Biodiversitas*, 22 (2). doi:10.13057/BIODIV/D220263.

Wielders, J.P.M. and Wijnberg, F.A. (2009) Preanalytical stability of 25(OH)-vitamin D3 in human blood or serum at room temperature: Solid as a rock. *Clinical Chemistry*, 55 (8): 1584–1585. doi:10.1373/clinchem.2008.117366.

Williams, J.M., Lonsdorf, E. V, Wilson, M.L., et al. (2008) Causes of Death in the Kasekela Chimpanzees of Gombe National Park, Tanzania. *American Journal of Primatology*, 70: 766–777. doi:10.1002/ajp.20573.

Wimalawansa, S.J. (2019) Vitamin D deficiency: Effects on oxidative stress, epigenetics, gene regulation, and aging. *Biology*. 8 (2). doi:10.3390/biology8020030.

Wiśniewski, J.R., Ostasiewicz, P. and Mann, M. (2011) High recovery FASP applied to the proteomic analysis of microdissected formalin fixed paraffin embedded cancer tissues retrieves known colon cancer markers. *Journal of Proteome Research*, 10 (7): 3040–3049. doi:10.1021/PR200019M/SUPPL_FILE/PR200019M_SI_005.XLS.

Wiśniewski, J.R., Zougman, A., Nagaraj, N., et al. (2009) Universal sample preparation method for proteome analysis. *Nature Methods*, 6 (5). doi:10.1038/nmeth.1322.

Wittig, R.M., Crockford, C., Weltring, A., et al. (2015) Single aggressive interactions increase urinary glucocorticoid levels in wild male chimpanzees. *PLoS ONE*, 10 (2): e0118695. doi:10.1371/journal.pone.0118695.

Wobeser, G.A. (2006) “How Disease is Detected, Described, and Measured.” In *Essentials of Disease in Wild Animals*. Blackwell Publishing.

Woodfin, A., Voisin, M.B. and Nourshargh, S. (2007) PECAM-1: A multi-functional molecule in inflammation and vascular biology. *Arteriosclerosis, Thrombosis, and Vascular Biology*. 27 (12). doi:10.1161/ATVBAHA.107.151456.

Woodhouse, S.J. and Rick, M. (2016) The effect of UVB radiation on serum vitamin D and ionized calcium in the African spoonbill (Platalea alba). *Journal of Zoo and Wildlife Medicine*, 47 (2). doi:10.1638/2014-0239.1.

Wortsman, J., Matsuoka, L.Y., Chen, T.C., et al. (2000) Decreased bioavailability of vitamin D in obesity. *American Journal of Clinical Nutrition*, 72 (3): 690–693. doi:10.1093/ajcn/72.3.690.

Wright, R.M., Ko, C., Cumsky, M.G., et al. (1984) Isolation and sequence of the structural gene for cytochrome c oxidase subunit VI from Saccharomyces cerevisiae. *Journal of Biological Chemistry*, 259 (24). doi:10.1016/s0021-9258(17)42563-4.

Wynn, T.A. (2008) Cellular and molecular mechanisms of fibrosis. *Journal of Pathology*. 214 (2). doi:10.1002/path.2277.

Yang, D.C., Gu, S., Li, J.M., et al. (2021) Targeting the AXL receptor in combating smoking-related pulmonary fibrosis. *American Journal of Respiratory Cell and Molecular Biology*, 64 (6): 734–746. doi:10.1165/RCMB.2020-0303OC/SUPPL_FILE/DISCLOSURES.PDF.

Yin, W., Li, R., Feng, X., et al. (2018) The Involvement of Cytochrome c Oxidase in Mitochondrial Fusion in Primary Cultures of Neonatal Rat Cardiomyocytes. *Cardiovascular Toxicology*, 18 (4). doi:10.1007/s12012-018-9447-1.

Youden, W.J. (1950) Index for rating diagnostic tests. *Cancer*, 3 (1): 32–35. doi:10.1002/1097-0142(1950)3:1<32::AID-CNCR2820030106>3.0.CO;2-3.

Zabka, T.S., Goldstein, T., Cross, C., et al. (2009) Characterization of a degenerative cardiomyopathy associated with domoic acid toxicity in california sea lions (Zalophus californianus). *Veterinary Pathology*, 46 (1): 105–119. doi:10.1354/VP.46-1-105/ASSET/IMAGES/LARGE/10.1354_VP.46-1-105-FIG1.JPEG.

Zhang, C., Liu, R., Yuan, J., et al. (2016) Predictive Values of N-Terminal Pro-B-Type Natriuretic Peptide and Cardiac Troponin I for Myocardial Fibrosis in Hypertrophic Obstructive Cardiomyopathy. *PLOS ONE*, 11 (1): e0146572. doi:10.1371/JOURNAL.PONE.0146572.

Zhang, S., Jian, W., Sullivan, S., et al. (2014) Development and validation of an LC–MS/MS based method for quantification of 25 hydroxyvitamin D2 and 25 hydroxyvitamin D3 in human serum and plasma. *Journal of Chromatography B*, 961: 62–70. doi:10.1016/J.JCHROMB.2014.05.006.

Zhang, Z., Tan, M., Xie, Z., et al. (2011) Identification of lysine succinylation as a new post-translational modification. *Nature Chemical Biology*, 7 (1). doi:10.1038/nchembio.495.

Zhao, H., Wang, M., Muthelo, P., et al. (2022) Detection of SARS-CoV-2 antibodies in serum and dried blood spot samples of vaccinated individuals using a sensitive homogeneous proximity extension assay. *New Biotechnology*, 72: 139–148. doi:10.1016/J.NBT.2022.11.004.

Zhao, S., Wu, H., Xia, W., et al. (2014) Periostin expression is upregulated and associated with myocardial fibrosis in human failing hearts. *Journal of Cardiology*, 63 (5). doi:10.1016/j.jjcc.2013.09.013.

Zhu, L., Wang, Y., Zhao, S., et al. (2022) Detection of myocardial fibrosis: Where we stand. *Frontiers in Cardiovascular Medicine*, 9: 926378. doi:10.3389/FCVM.2022.926378/BIBTEX.

Van Zijll Langhout, M., Wolters, M., Horvath, K.M., et al. (2017) Clinical signs, diagnostics and successful treatment of a myocarditis in an adult chimpanzee (Pan troglodytes). *Journal of Medical Primatology*, 46: 263–266. doi:10.1111/jmp.12273.

Zile, M.R., Claggett, B.L., Prescott, M.F., et al. (2016) Prognostic Implications of Changes in N-Terminal Pro-B-Type Natriuretic Peptide in Patients With Heart Failure. *Journal of the American College of Cardiology*, 68 (22): 2425–2436. doi:10.1016/J.JACC.2016.09.931/SUPPL_FILE/MMC1.DOCX.

APPENDICES

Appendix A: An overview of post-mortem cardiac examinations carried out between October 2020 and August 2023.

Introduction

Cardiovascular disease (CVD) is a significant cause of morbidity and mortality in zoo-housed great apes, though it tends to be associated with different pathological changes than those commonly found in humans (Varki et al., 2009; Strong et al., 2016, 2018b)(Varki et al., 2009; Strong et al., 2016, 2018b). In order to improve understanding of the pathophysiology and aetiopathogeneses of great ape CVD, an interdisciplinary team of pathologists, clinicians and researchers began investigating collaboratively as the Ape Heart Project (based at Twycross Zoo, UK). To date, the project has received and examined the hearts of 59 chimpanzees, 29 gorillas, 20 orangutans and 11 bonobos (total n=119). Past doctoral theses and papers have described the morphology of many of these hearts in great detail (Moittié, 2021; Strong, 2017)(Moittié, 2021; Strong, 2017), and have characterised important phenotypes including IMF (Strong et al., 2020)(Strong et al., 2020).

While the detailed characterisation of cardiac phenotypes was not part of the novel research focus of this thesis, cardiac examinations continued throughout the duration of this PhD, and a brief description of the cases examined during this time are included here for interest, to complement and further contextualise the main research chapters. Emphasis is placed on the individuals whose samples were included in other chapters of this thesis (n=4 chimpanzees), or who were deemed to be cases of marked CVD.

European zoos were invited to submit samples (as defined below) in the event of a great ape death, regardless of whether or not the clinical history was indicative of CVD. Following a great ape death, participating zoos extracted the heart during initial postmortem investigation and were advised to section it at the apex in order to expose the ventricular chambers (Figure A.1) prior to fixing in 10% neutrally buffered formalin for a minimum of one week. Once fully fixed, the hearts were submitted to the Ape Heart Project (Twycross Zoo, Burton Road, Atherstone, UK, CV9 3PX) in accordance with relevant legislation pertaining to the import of research and diagnostic samples into the UK from Europe. The European EAZA Biobank at Copenhagen Zoo served as a central collection point for samples originating from within the EU. Subsequently, the hearts were sent from Copenhagen Zoo to Twycross Zoo using the CITES Registered Scientific Institution scheme for further pathological examination.

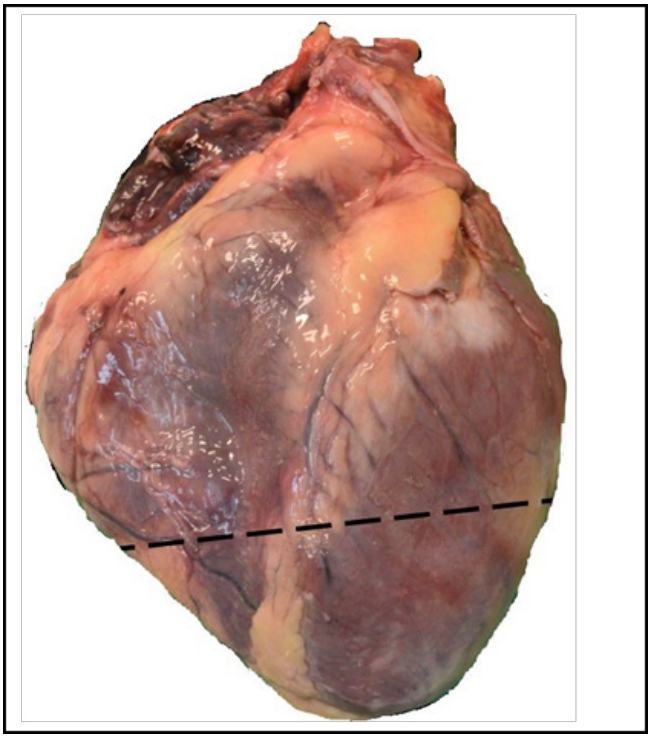

Figure A.1: The approximate location of the transverse cut to be made across the lower third of the apex during the postmortem sampling and fixation process (as depicted by the black dashed line). The cut should be perpendicular to the long axis of the heart, exposing the chambers of both ventricles.

Macroscopic examination

Once received in the UK, the hearts were examined at the University of Nottingham School of Veterinary Medicine and Science (Veterinary Pathology Service, LE12 5RA) by the author of this thesis (October 2020 – August 2023), under the guidance of one of the following veterinary pathologists: Kerstin Baiker (Dr med vet, MRCVS, CertForensicVP, SFHEA, DiplECVP), Antonia Morey Matamalas (DVM, MVM, MRCVS, AFHEA), or Marta Nobre de Castro Pereira (DVM, MSc WAH, MRCVS). The macroscopic examination and sampling methods were adapted from a standardised protocol that was previously developed (Strong et al., 2018c)(Strong et al., 2018c).

A summarised version of the adapted examination protocol is as follows:

I. Comment on the condition of the sample:
    a. Previous sectioning or trimming
    b. Quality of tissue preservation/fixing
    c. Overall shape of the heart – effects of fixing/transport
II. Describe the gross morphology:
    a. Amount of epicardial fat
    b. Any gross chamber enlargement or anatomical abnormalities
    c. Any colour changes or visible lesions on the epicardium
    d. Weight of the heart (g)
    e. The length (cm) from the coronary groove to the apex (posterior aspect)
    f. The circumference (cm) of the heart at the level of the coronary groove
III. Making a new transverse incision, above where the submitting institution had opened the chambers already and describe/measure:
    a. The transverse section of the myocardium (colour variation, wall thickness)
    b. The width (cm) of the left ventricular free wall (LVFW), inter-ventricular septum (IVS) and right ventricular free wall (RVFW), excluding papillary muscles and epicardial fat
IV. Open the right chambers and pulmonary artery as follows:
    a. Open the right atrium laterally from the inferior vena cava (IVC) to the right atrial appendage (RAA), assess and describe any lesions

b. Open the right ventricle laterally, assess and describe any lesions, paying particular attention to the right ventricular outflow tract (RVOT)
c. Measure the circumference (cm) of the tricuspid valve, assess and describe any lesions
d. Open the pulmonary artery by incising along the septum of the anterior right ventricle, assess and describe any lesions
e. Measure the circumference (cm) of the pulmonary valve, assess and describe any lesions

V. Open the left chambers and aorta as follows:

a. Open the left atrium along the top wall (pulmonic veins), assess and describe any lesions
b. Open the left ventricle laterally, assess and describe any
c. Measure the circumference (cm) of the mitral valve, assess and describe any lesions
d. Open the aorta by incising along the septum of the anterior left ventricle, assess and describe any lesions
e. Measure the circumference (cm) of the aortic valve, assess and describe any lesions

VI. Inspect the coronary vasculature as follows:

a. Within the opened aorta, identify the ostia of the coronary arteries and probe
b. Comment on the number, locations and sizes of the ostia and check whether they branch normally
c. Cut across the coronary arteries at 3mm intervals, assess and describe any lesions

VII. Take samples for histopathology from the following tissue sections, labelling each cassette with animal ID and sample ID. The sample IDs are as follows:

a. Left ventricle – L1 (anterior); L2 (posterior); L3 (lateral)
b. Inter-ventricular septum – S1 (anterior); S2 (posterior)
c. Right ventricle – R1 (anterior); R2 (posterior); R3 (lateral), R4 (RVOT)
d. Others – SA (Sinoatrial node); AV (Atrioventricular node); A (Aorta); Any lesions found during the examination

Histopathological examination

A minimum of 12 standardised tissue sections were taken from each heart, with additional samples taken from any identified lesions. Once the tissue sections were placed into cassettes, they were re-submerged in formalin and submitted for processing and staining with Haematoxylin and Eosin (H&E), and sliced by the histology technician at the University of Nottingham's Veterinary Pathology Service (LE12 5RA, UK). The processed slides were sent to a digital histology slide scanning and storage service at University College London (UCL IQPath, UCL Institute of Neurology, Queen Square, London, WC1N 3BG).

Once digitalised, the slides were systematically examined for histopathologic lesions that may indicate acute or chronic cardiac changes. Final diagnoses were established by the overseeing board-certified veterinary pathologist, Kerstin Baiker (Dr med vet, MRCVS, CertForensicVP, SFHEA, DiplECVP), in accordance with any clinical information received from the submitting zoo pertaining to the animal's ante-mortem health and circumstances of death.

Reporting and analysis

A written report was produced and sent to the submitting zoo from which the animal's heart came, detailing to what extent the animal had cardiovascular changes (mild, moderate or marked, and acute or chronic), if any, and whether any changes were likely to have been clinically important. The individual results were collated and stored in a database, along with other relevant information such as clinical history when available.

Results

Formalin-fixed whole hearts (n=25) were received from 19 European zoological collections (as depicted in Figure A.2) between October 2020 and August 2023. 44% of the hearts were from chimpanzees (*Pan troglodytes* n=11), 32% from Western lowland gorillas (*Gorilla gorilla* n=8), 20% from orangutans (*Pongo sp*. n=1, *Pongo abelii* n=2, *Pongo pygmaeus* n=2), and one heart (4%) was from a bonobo (*Pan paniscus*). The median age at death of all animals was 31.4 years (range: 0.0 – 49.8 years). The age of the single bonobo was 31.4 years. The median age of chimpanzees was 34.9 years (range: 12.9 – 49.8 years), for gorillas it was 28.7 years (range: 8.8 – 47.8 years), and for orangutans it was 31.4 years (range: 0.0 – 44.7 years). All median ages listed here are considered to be in the adult, but not elderly, age category, according to various sources (Alberts et al., 2013; Furuichi et al., 1998; Galdikas, 1981; Strong, 2017; Strong et al., 2018b)(Alberts et al., 2013; Furuichi et al., 1998; Galdikas, 1981; Strong, 2017; Strong et al., 2018b). 52% (n=13) of the hearts were from female animals, and 48% (n=12) from males. The demographics of each study animal can be found in Table A.1, alongside a summary of the pathological findings.

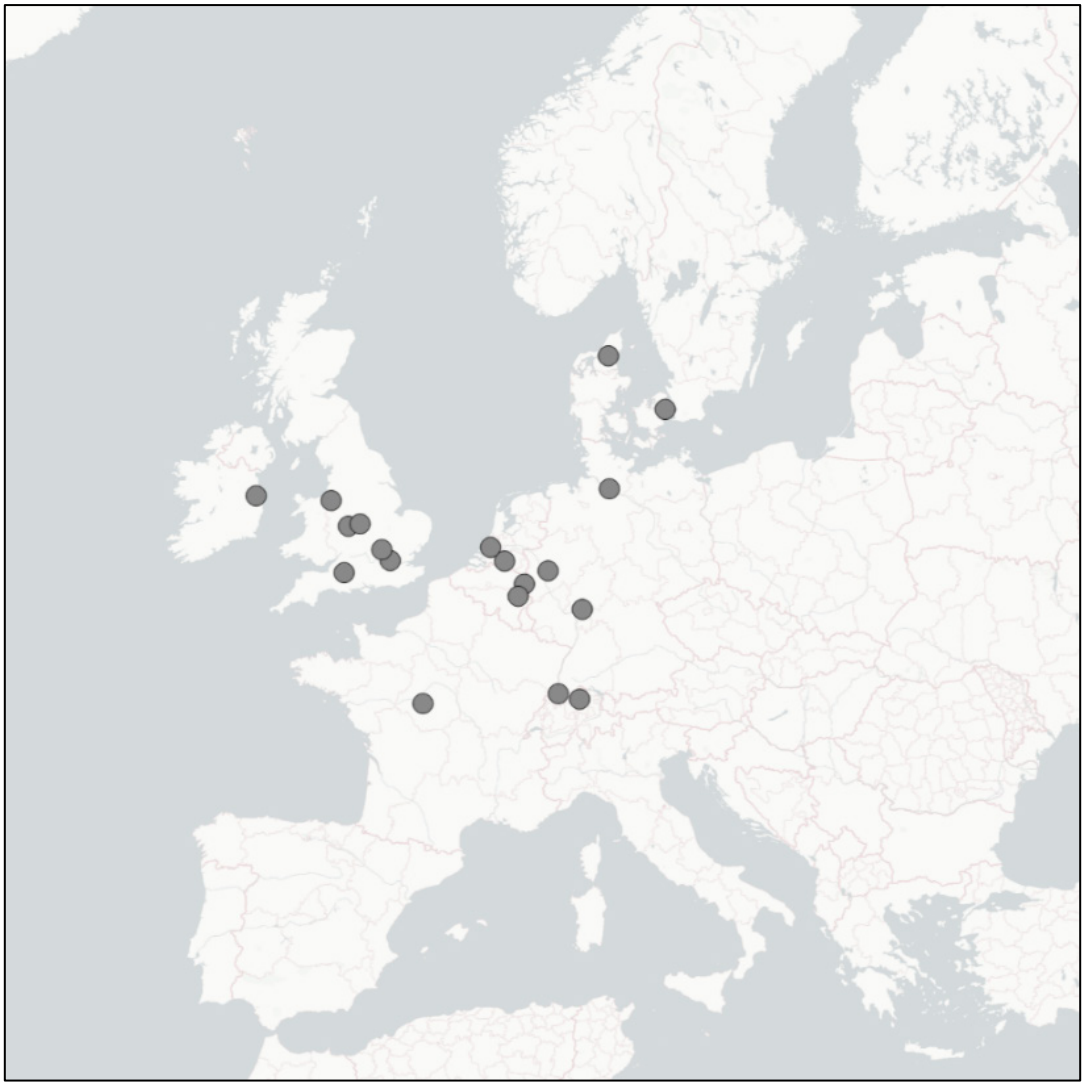

Figure A.2: Map showing the origin locations (n=19) of great ape hearts submitted by European zoos for postmortem examination between October 2020 and August 2023. Map generated with QGIS Desktop v2.18.28.

Table A.1: Summary of cardiovascular findings resulting from the histopathological phenotyping of the submitted great ape hearts (n=25). The study ID, sex, and age (years) of the animal at the time of death is included, as well as information relating to the nature of the death and the findings upon cardiovascular examination. The severity (mild, moderate, or marked) and chronicity (chronic or acute) of any pathological changes is included. Asterisk (*) in the study ID column denotes an individual whose samples were included in other chapters of this thesis (n=4 chimpanzees). Hash symbol (#) in the cardiovascular abnormalities column denotes advanced CVD cases. Abbreviations: IMF = Idiopathic Myocardial Fibrosis; CBN = Contraction Band Necrosis; ACM = Arrhythmogenic Cardiomyopathy; DCM = Dilated Cardiomyopathy.

Taxonomy	Study ID	Sex	Age (years)	Circumstances of death	Cardiovascular abnormalities	Severity and chronicity
Bonobo	B10	Male	31	Euthanasia	Yes	Mild, acute
Chimpanzee	C43	Female	40	Sudden death (cardiac)	Yes (IMF) #	Marked, chronic
	C44 *	Male	32	Euthanasia	Yes (IMF) #	Moderate, chronic Marked, acute
	C45	Female	34	Sudden death (cardiac)	Yes (IMF) #	Marked, chronic Moderate, acute
	C46 *	Female	49	Sudden death (non-cardiac)	Yes	Mild, chronic Mild, acute
	C47 *	Female	47	Euthanasia	Yes	Mild to moderate, chronic
	C48	Female	12	Peri-anaesthesia death (non-cardiac)	No	–
	C49	Male	30	Traumatic injuries	Yes	Mild to moderate, chronic
	C50	Male	15	Euthanasia	Yes	Mild to moderate, acute
	C51	Male	32	Peri-anaesthesia death (cardiac)	Yes (IMF) #	Marked, chronic Mild, acute
	C52	Male	38	Sudden death (cardiac)	Yes (ACM) #	Marked, chronic Moderate, acute
	C54 *	Male	41	Sudden death (cardiac)	Yes (thrombi / IMF / DCM) #	Marked, chronic Moderate, acute

Gorilla	G20	Female	25	Peri-anaesthesia death (cardiac)	Yes (chronic infarction) #	Marked, chronic
	G21	Female	45	Sudden death (non-cardiac)	No	–
	G22	Female	47	Euthanasia	Yes (CBN) #	Mild, chronic Marked, acute
	G23	Male	16	Euthanasia	Yes	Mild, chronic Mild, acute
	G24	Female	33	Euthanasia	Yes	Moderate, chronic Moderate, acute
	G25	Female	8	Euthanasia	Yes	Moderate, acute
	G26	Male	31	Sudden death (cardiac)	Yes (ACM) #	Marked, chronic
	G27	Female	21	Euthanasia	No	–
Orangutan	O13	Female	31	Sudden death (non-cardiac)	Yes	Mild, chronic Moderate, acute
	O14	Male	25	Peri-anaesthesia death (non-cardiac)	No	–
	O15	Female	44	Euthanasia	Yes	Mild, chronic
	O16	Male	0	Traumatic injuries	No	–
	O17	Male	31	Euthanasia	Yes (DCM) #	Marked, chronic

Of all 25 hearts received, 20 (80%) showed cardiovascular abnormalities of some kind. At the species level, the prevalence of abnormalities was 91% (10/11) in chimpanzees, 75% (6/8) in gorillas, and 60% (3/5) in orangutans. The bonobo individual also showed abnormalities (1/1). Of all individuals with abnormalities, half were female (10/20) and half were male (10/20). The median age of individuals with abnormalities was 32.5 years (range: 8.8 – 49.8 years). Euthanasia was the cause of death in 50% (10/20) of the cases with observed abnormalities, while 35% (7/20) were classed as a sudden or unexpected death, 10% (2/20) listed as peri-anaesthesia, and 5% (1/20) due to physical trauma.

Half (10/20) of the individuals with abnormalities were considered to have mild or moderate CVD (i.e. subclinical). The median age of mild or moderate CVD cases was 31.4 years (range: 8.8 – 49.8 years). Euthanasia was the cause of death in 70% (7/10) of these cases, with sudden or unexpected death and physical trauma making up 20% (2/10) and 10% (1/10) of the deaths, respectively. Observed chronic changes included myocardial fibrosis (interstitial, perivascular and replacement) and vascular changes (arterial media thickening, arteriolosclerosis, mineralisation, aortic media degeneration, intimal thickening and root dilation). Acute changes included myocarditis, fibrinous endocarditis, cardiomyofibre degeneration, myocardial necrosis, contraction band necrosis (CBN), and subendocardial and epicardial haemorrhages.

Two chimpanzees whose serum samples were included in Chapter 1 of this thesis had mild to moderate CVD. More specifically, a 49.8 year old female chimpanzee (C46) who died suddenly and was diagnosed with acute haemorrhagic colitis and chronic kidney disease post-mortem, showed chronic myocardial fibrosis (mild to moderate interstitial and replacement fibrosis), mild peracute CBN, and chronic focal aortic media degeneration with mineralisation. The second, a 47.6 year old female chimpanzee who was euthanised due to perceived age-related deterioration, showed chronic myocardial fibrosis (mild to moderate interstitial, perivascular, and replacement fibrosis) with mild chronic arterial media thickening, mineralisation and arteriosclerosis.

The remaining half (10/20) of those with observed cardiovascular abnormalities were considered to have marked CVD (i.e. likely to lead to incurable disease or death), according to the post-mortem findings. The median age of marked CVD cases was

33.8 years (range: 26.0 – 47.8 years). Among the cases of marked CVD, 50% (5/10) had a sudden or unexpected death, 30% (3/10) were euthanised, and 20% (2/10) were peri-anaesthesia deaths. The majority (7/10) of the marked CVD cases were attributed to cardiomyopathy, while the remaining three involved acute CBN, intracardial thrombi, and a prior focally extensive infarction.

Idiopathic myocardial fibrosis (IMF) was the most common cardiomyopathy, affecting 57% (4/7). Sudden death occurred in half (2/4) of the IMF cases, with euthanasia (1/4) and peri-anaesthetic death (1/4) also recorded. All IMF cases were chimpanzees (C43, C44, C45, C51), and were characterised by multifocal extensive areas of chronic interstitial and replacement fibrosis with no clear aetiology (Strong et al., 2020)(Strong et al., 2020). In all cases, IMF was accompanied by acute changes including cardiomyofibre degeneration, haemorrhages and CBN. Figure A.3 shows the extensive myocardial fibrosis in these cases. Serum from C44 was also included in Chapter 1 of this thesis. C44 was a 32.2 year old male chimpanzee who was euthanised due to physical trauma, and showed chronic moderate interstitial and replacement fibrosis, acute CBN, and multifocal acute haemorrhages.

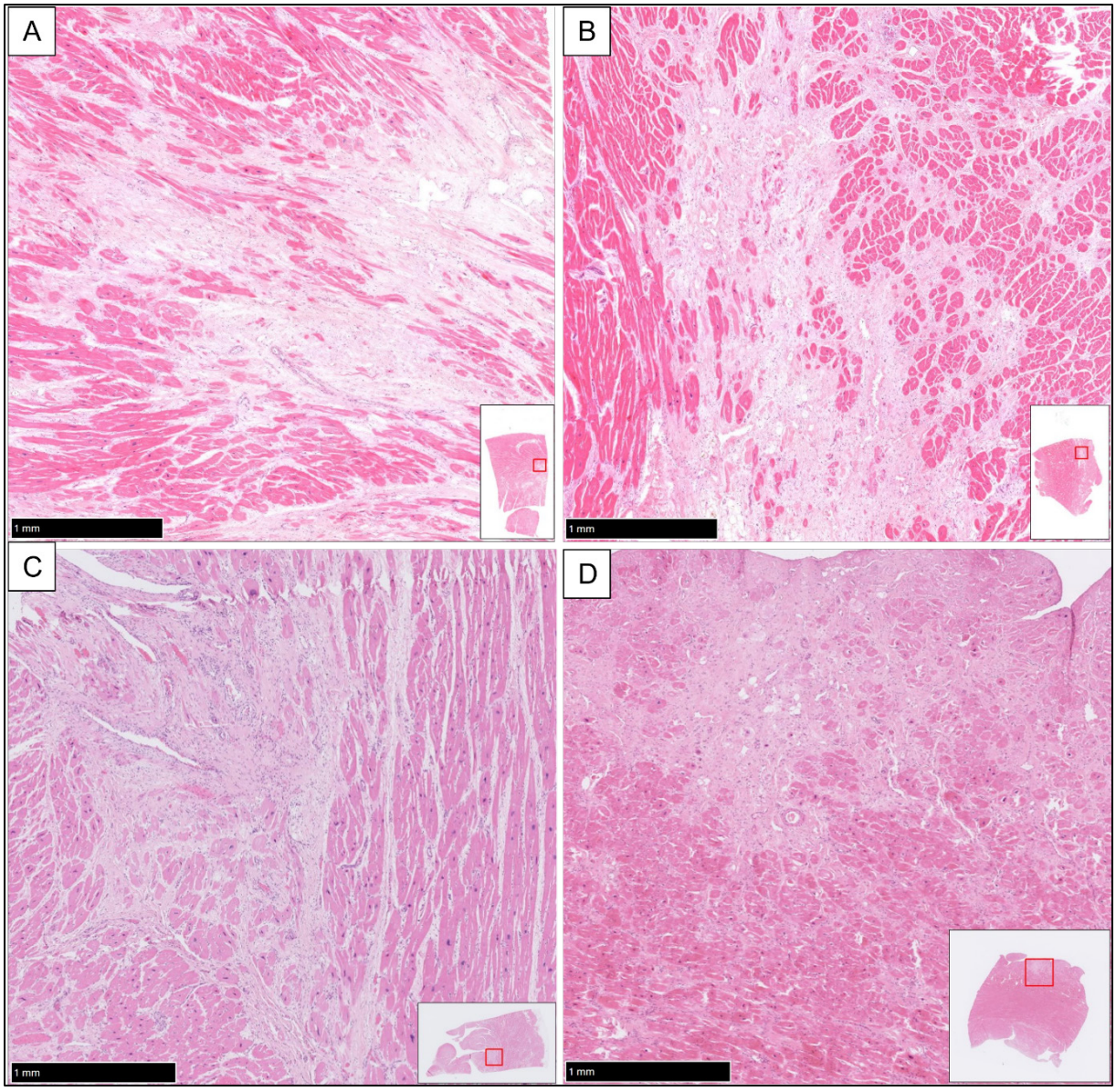

Figure A.3 (A-D): Histology slides showing idiopathic myocardial fibrosis (IMF) in the left ventricular myocardium of four chimpanzees (*Pan troglodytes*): C43, C44, C45 and C51 (Figs. A-D respectively). All histology slides stained with H&E and shown at a 2.5x magnification with a 1mm scalebar. Images produced from an online digital slide viewer (NZConnect 1.0.36).

Another cardiomyopathy phenotype, arrhythmogenic cardiomyopathy (ACM), affected two male individuals, C52 and G26, who both experienced a sudden cardiac death. While myocardial fibrosis is also a feature of ACM, it is more specifically characterised by extensive fibrofatty replacement of the cardiac muscle tissue. This fibrofatty replacement normally begins in the right chambers and is thought to impact the heart's electrical conductivity. Figure A.4 shows the marked fibrofatty replacement of cardiomyocytes in the right ventricular myocardium of C52 and G26, which ultimately led to arrhythmia and sudden death.

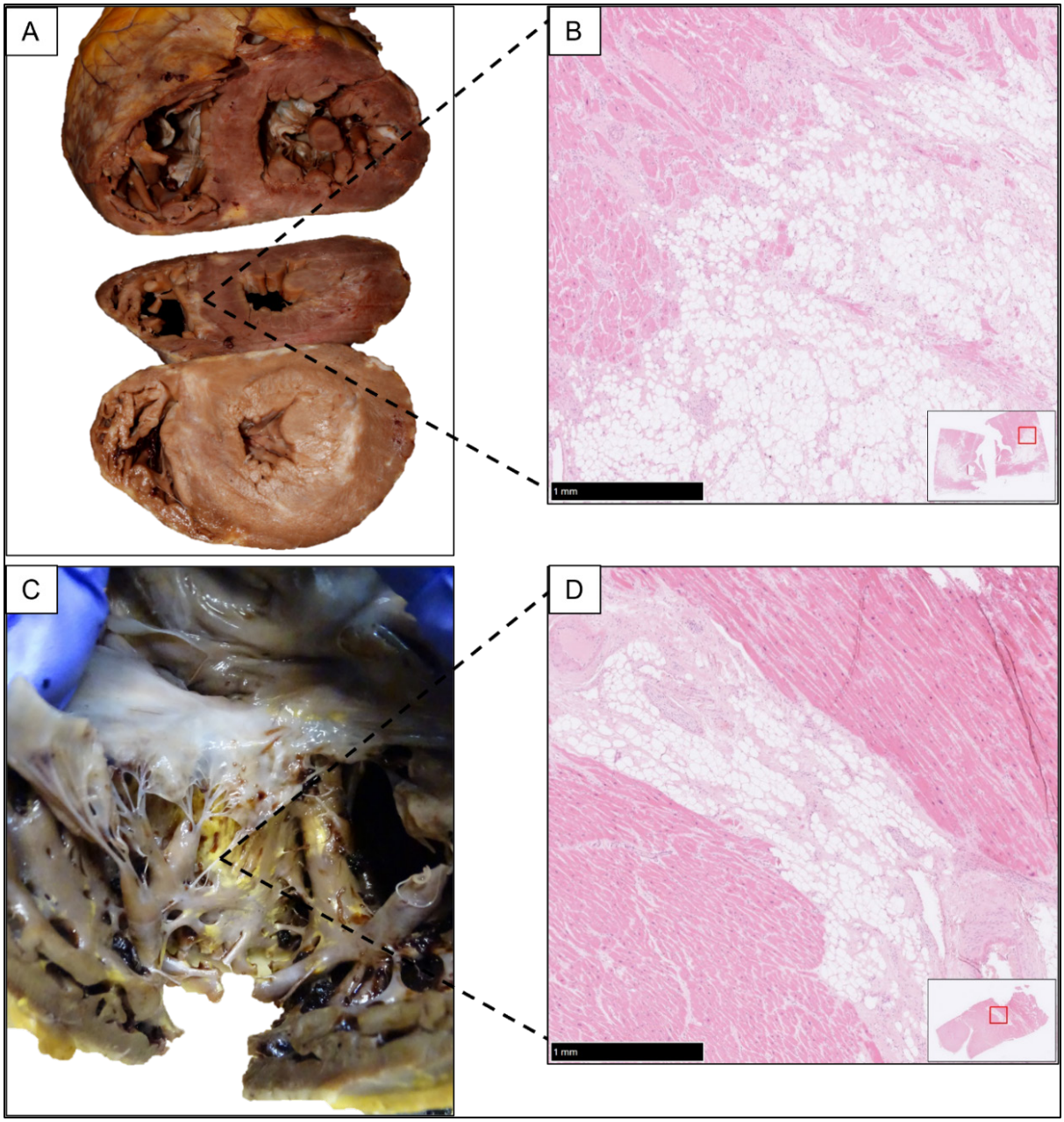

Figure A.4 (A-D): Right ventricular fibrofatty replacement of cardiomyocytes characteristic of Arrhythmogenic Cardiomyopathy (ACM) as seen macroscopically and histologically in two great apes: C52 (*Pan troglodytes,* Figs. A-B) and G26 (*Gorilla gorilla gorilla,* Figs. C-D). All histology slides stained with H&E and shown at a 2.5x magnification with a 1mm scalebar. Images produced from an online digital slide viewer (NZConnect 1.0.36).

The final cardiomyopathy identified was dilated cardiomyopathy (DCM), which was diagnosed in one male orangutan (O17), who showed a marked dilation of the left chambers (Figure A.5 A-B), with cardiomyocyte hypertrophy (Figure A.5 C), which culminated in systolic dysfunction and congestive heart failure. Additionally, the heart-weight-to-bodyweight ratio of O17 was 0.66%, which is considered indicative of cardiomegaly in chimpanzees (Baldessari et al., 2013; Lammey et al., 2008b, 2008a; González et al., 2002)(Baldessari et al., 2013; Lammey et al., 2008b, 2008a; González et al., 2002), but there is currently no published data about this in orangutans. This individual had been euthanised due to a poor clinical outlook.

There were two marked CVD cases where cardiomyopathy was not the accompanying phenotype. Evidence of a previous myocardial infarction, signified by a focally extensive area of fibrofatty replacement within the right side of the septal wall, was identified in a female gorilla (G20) who died upon general anaesthesia induction. In an elderly female gorilla (G22), more acute changes in the form of marked CBN were found, which suggests that if she hadn’t been euthanised due to poor clinical prognosis, the extent of the irreversible ischaemic myocardial damage in this case may have led to her death anyway.

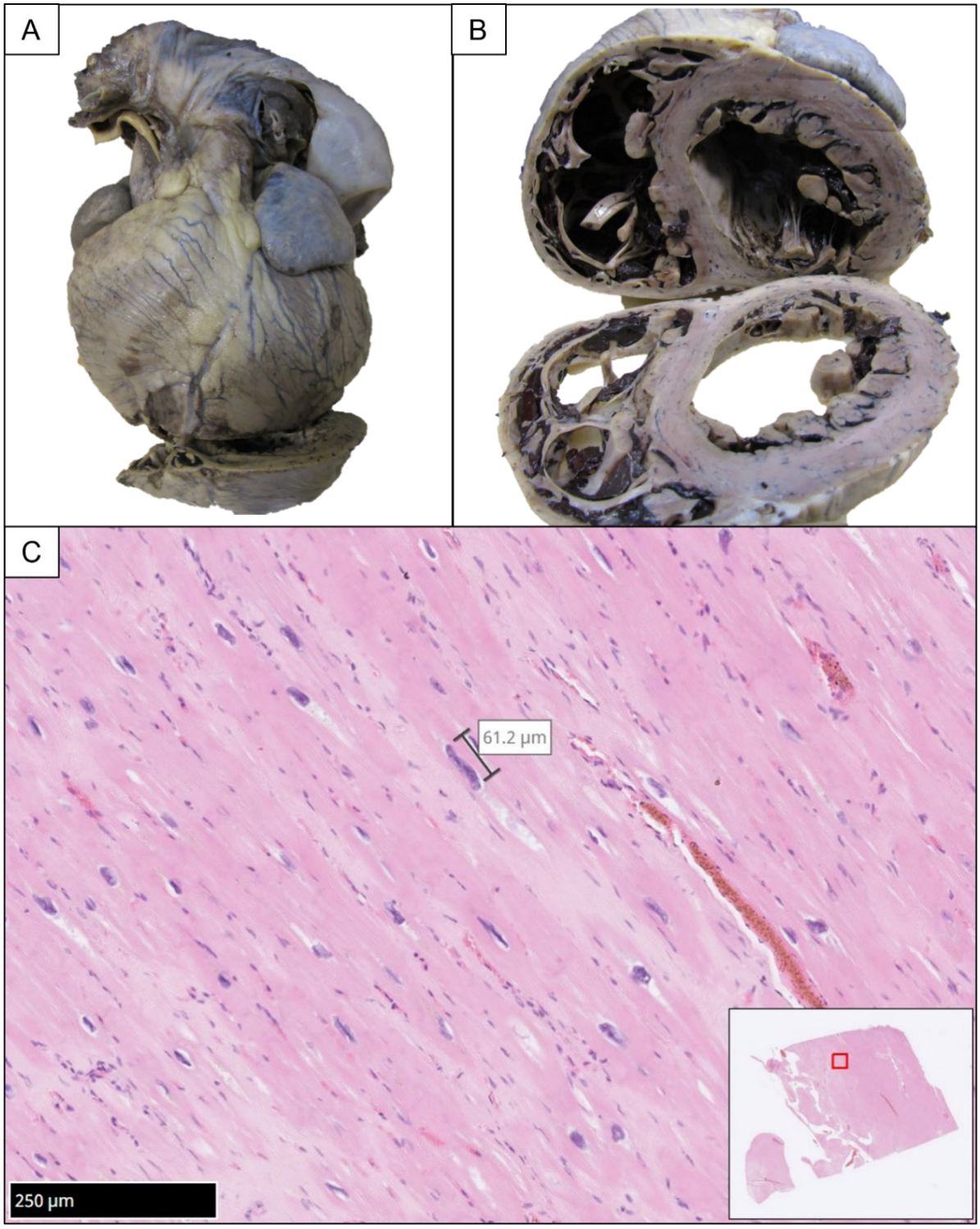

Figure A.5 (A-C): Dilated Cardiomyopathy (DCM) as observed in O17 (*Pongo abelii*). Figs A-B show macroscopic cardiomegaly and left ventricular and atrial dilation as seen externally (Fig. A) and internally (Fig. B). Fig. C shows cardiomyocyte hypertrophy as seen during histological examination. An enlarged (61.2µm), hyperchromatic nucleus has been identified and labelled. Histology slide stained with H&E and shown at a 7x magnification with a 250µm scalebar. Images produced from an online digital slide viewer (NZConnect 1.0.36).

The final case of marked CVD was a male chimpanzee (C54), who died suddenly and was affected by multiple cardiovascular changes. Though there were characteristics of both IMF and DCM – namely, marked chronic interstitial and replacement fibrosis with a left ventricular dilation – there were also multiple fibrinous thrombi within the left ventricle (Figure A.6). The large thrombi were adhered multifocally to the papillary muscles and leaflets of the mitral valve and were most likely the cause of the sudden death in this individual, though the aetiopathogenesis of these remains unclear. Within the aorta, there were chronic mild intimal thickenings and an acute focal adventitial haemorrhage. Acute CBN and moderate cardiomyofibre degeneration were also present, reflecting the terminal dysrhythmic event observed in this case. Myocardial tissue from C54 was included in Chapter 3 of this thesis.

A summary of the prevalence of the observed CVD phenotypes among the marked CVD cases in each species can be found in Figure A.7.

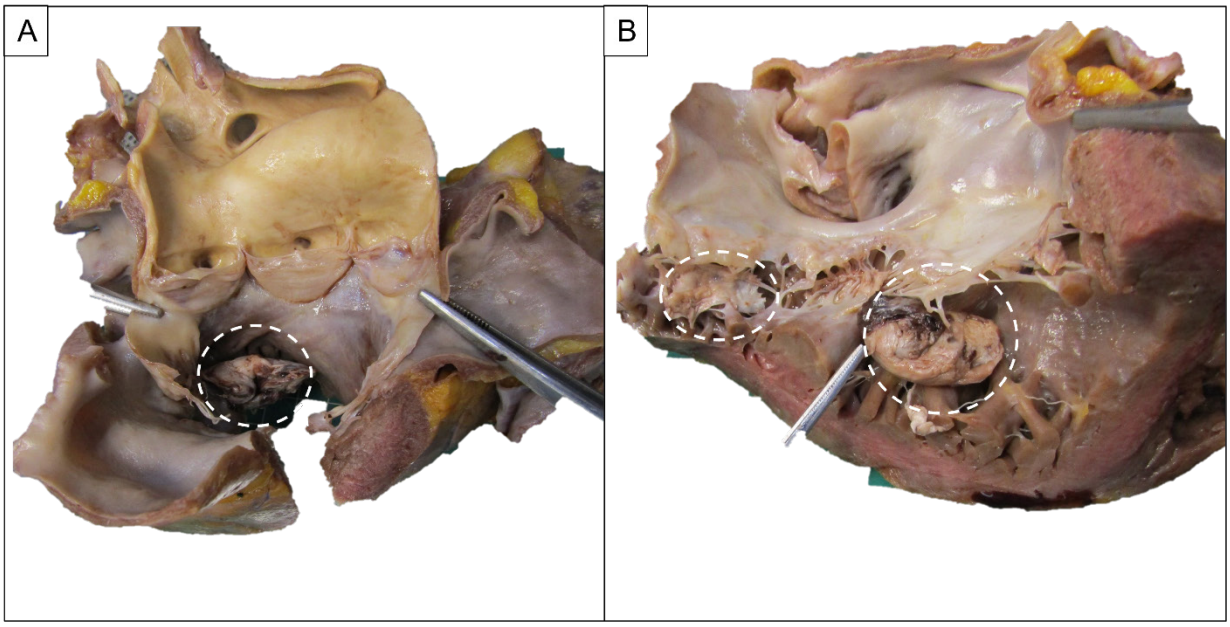

Figure A.6 (A-B): Intracardial left ventricular thrombi of C54 (*Pan troglodytes*) as seen macroscopically from within the left atrium (Fig. A) and left ventricle (Fig. B). White dashed circles have been used to outline the thrombi, which are adhered multifocally to the papillary muscles and leaflets of the mitral valve.

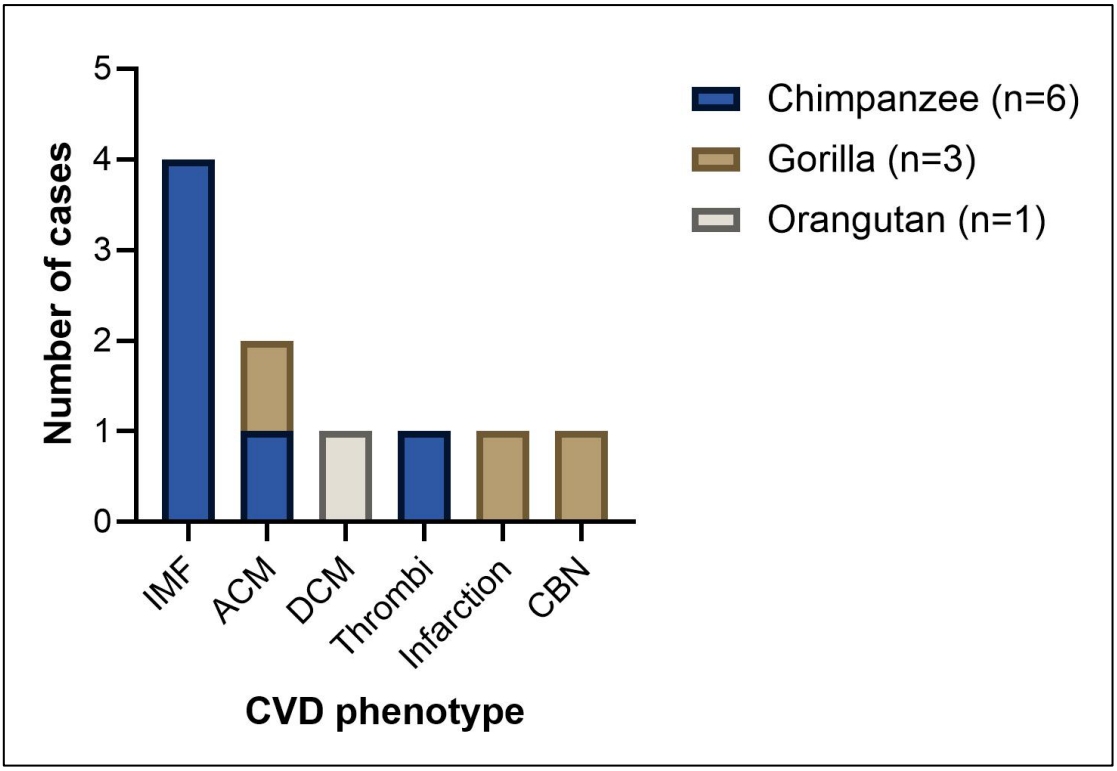

Figure A.7: Prevalence of observed phenotypes among great apes (n=10) presenting with marked cardiovascular disease (CVD). IMF = Idiopathic Myocardial Fibrosis; ACM = Arrhythmogenic Cardiomyopathy; DCM = Dilated Cardiomyopathy; CBN = Contraction Band Necrosis.

Conclusions

This Appendix has provided a brief description of cases examined during the timeframe of the PhD, by the author of this thesis, in conjunction with a board-certified veterinary pathologist. Four of the individuals described here were also included elsewhere in other chapters of this thesis: serum from C44, C46 and C47 in Chapter 1 (serum biomarkers), and C54 in Chapter 3 (myocardial gene expression).

The overall prevalence of cardiovascular abnormalities in all great apes examined, regardless of the cause of death, was 80% (20 out of 25 animals), with species-specific prevalence of abnormalities as follows: chimpanzees 91% (10 out of 11), gorillas 75% (six out of eight), orangutans 60% (three out of five) and bonobos 100% (one out of one). This is consistent with a previous morbidity and mortality review on great apes, with reported prevalence of CVD higher in chimpanzees and bonobos than gorillas and orangutans, with orangutans consistently showing the lowest rate of cardiovascular disease across the studies reviewed (Strong et al., 2016)(Strong et al., 2016).

The high observed rate of sudden or unexpected deaths in the study animals (43% of animals with any cardiovascular abnormality, and 70% of animals with marked CVD) reinforces the findings of previous reports, though the species-specific rates of sudden death tend to differ according to the particular disease phenotypes seen. For example, vascular disease, including aortic dissection, appear to be more notable in gorillas (Kenny et al., 1994)(Kenny et al., 1994) and may be responsible for the particularly high rate of sudden death reported in gorillas elsewhere (Strong et al., 2018b)(Strong et al., 2018b), even though it did not feature in this dataset.

Cardiomyopathies (ACM, DCM and IMF) were responsible for 70% of the observed marked CVD cases. Arrhythmogenic Cardiomyopathy (ACM), otherwise termed Arrhythmogenic Right Ventricular Cardiomyopathy (ARVC), was observed in two males (C52 and G26). In humans, ACM is a genetic disorder characterised by the replacement of myocardial tissue with fibrofatty tissue, primarily in the right ventricle of affected individuals, resulting in arrhythmia and sudden death (Sen-Chowdhry et al., 2004)(Sen-Chowdhry et al., 2004). Though reported cases of ACM in great apes are rare, previously reported cases were from male chimpanzees and gorillas (Tong

et al., 2014; Strong et al., 2018b)(Tong et al., 2014; Strong et al., 2018b), as confirmed in the present dataset. Dilated Cardiomyopathy (DCM), which is characterised primarily by left ventricular dilation, cardiomegaly and systolic dysfunction (Heymans et al., 2023)(Heymans et al., 2023), was identified in one adult male orangutan (O17) here. DCM has previously been reported in three male chimpanzees and one male orangutan (Sleeper et al., 2005; Slaffer and Allchurch, 1995; Strong et al., 2018b)(Sleeper et al., 2005; Slaffer and Allchurch, 1995; Strong et al., 2018b). Neither ACM nor DCM are considered to be major contributors to cardiovascular morbidity and mortality in great apes (Strong et al., 2016)(Strong et al., 2016) and may be due to genetic mutations that may not currently be widespread in the zoo populations. Despite this, it could be important to investigate these cases further in order to inform population and breeding management within zoo settings, so as not to proliferate the conditions further.

IMF was the most prevalent of all observed phenotypes, affecting 40% of the great apes with marked CVD. All individuals diagnosed with IMF here were chimpanzees. IMF has received great attention in the literature in recent years due to its high prevalence in all great apes, and in particular, chimpanzees. IMF is repeatedly reported as the most prominent form of CVD in chimpanzees, and while males and older individuals are at higher risk, the sex and age of affected individuals varies (Varki et al., 2009; Strong et al., 2018b; Baldessari et al., 2013; Lammey et al., 2008a; Strong et al., 2020, 2016)(Varki et al., 2009; Strong et al., 2018b; Baldessari et al., 2013; Lammey et al., 2008a; Strong et al., 2020, 2016). Despite ever-increasing knowledge about the prevalence and characteristics of IMF (as assessed post-mortem), there is still a great deal to learn about this idiopathic condition before any effective preventative measures or treatments can be adopted. Therefore, the research chapters of this thesis present novel insights into the ante-mortem diagnosis, pathogeneses and risk factors for IMF.

Appendix B: Example layout used for 96-well microplates for RT-qPCR.

Letters (e.g. A and B) represent genes, and numbers (e.g. 1–13) represent biological samples, in this case chimpanzees (Pan troglodytes). Two genes were included per plate, with three technical replicates of all biological samples per gene. A No Template Control (NTC), which is a negative control containing the PCR Reaction Mix but no cDNA, was included in duplicate per gene. Two concentrations (100% and 10%) of an Inter Plate Control (IPC) were included, in duplicate, to ensure amplification efficiency and consistency.

	1	2	3	4	5	6	7	8	9	10	11	12
A	A 1	A 2	A 3	A 4	A 5	A 6	A 7	A 8	A 9	A 10	A 11	A 12
B	A 1	A 2	A 3	A 4	A 5	A 6	A 7	A 8	A 9	A 10	A 11	A 12
C	A 1	A 2	A 3	A 4	A 5	A 6	A 7	A 8	A 9	A 10	A 11	A 12
D	B 1	B 2	B 3	B 4	B 5	B 6	B 7	B 8	B 9	B 10	B 11	B 12
E	B 1	B 2	B 3	B 4	B 5	B 6	B 7	B 8	B 9	B 10	B 11	B 12
F	B 1	B 2	B 3	B 4	B 5	B 6	B 7	B 8	B 9	B 10	B 11	B 12
G	A NTC	B NTC	A IPC. 10	A IPC. 100	B IPC. 10	B IPC. 100	A 13	A 13	A 13	B 13	B 13	B 13
H	A NTC	B NTC	A IPC. 10	A IPC. 100	B IPC. 10	B IPC. 100						

Appendix C: Moittié, S., Jarvis, R., Bandelow, S., et al. (2022) Vitamin D status in chimpanzees in human care: a Europe wide study. Scientific Reports, 12: 17625. doi:10.1038/s41598-022-21211-6.

www.nature.com/scientificreports

scientific reports

Check for updates

OPEN

Vitamin D status in chimpanzees in human care: a Europe wide study

Sophie Moittié[1,2], Rachel Jarvis[2], Stephan Bandelow[3], Sarah Byrne[4,8], Phillipa Dobbs[4], Melissa Grant[5], Christopher Reeves[6], Kate White[2], Mátyás Liptovszky[4,9] & Kerstin Baiker[7]

While vitamin D deficiency is a public health concern in humans, comparatively little is known about vitamin D levels in non-human primates. Vitamin D plays a crucial role in overall health and its deficiency is associated with a range of disorders, including cardiovascular disease, which is a leading cause of death in great apes. Serum samples (n = 245) from chimpanzees (*Pan troglodytes*) housed at 32 European zoos were measured for 25-hydroxyvitamin D_2, 25-hydroxyvitamin D_3 and total 25-hydroxyvitamin D (25-OHD) using liquid chromatography and tandem mass spectrometry. Of these samples, 33.1% indicated inadequate vitamin D status, using the human reference interval (25-OHD < 50 nmol/L). The season of the year, health status of the animal, and the provision of daily outdoor access had a significant effect on vitamin D status. This is the first large-scale study on vitamin D status of non-human great apes in human care. Inadequate 25-OHD serum concentrations are widespread in the chimpanzee population in Europe and could be a risk factor for the development of idiopathic myocardial fibrosis, a major cause of mortality in this species, as well as other diseases. A review of husbandry and nutrition practices is recommended to ensure optimal vitamin D supply for these endangered animals.

Vitamin D deficiency in humans is being described as a pandemic, and is associated with healthcare costs of billions of Euros in Europe[1,2]. Apart from the well-known role of vitamin D in calcium homeostasis and the musculoskeletal system, vitamin D has a wide range of other biological functions and prolonged vitamin D deficiency has been associated with a variety of disorders in humans such as cardiovascular diseases, neurological disorders, cancers, autoimmune diseases, and respiratory infections[3–6].

Vitamin D comprises a range of fat-soluble secosteroids that are synthesised in the skin from ultraviolet B (UVB) radiation (vitamin D_3) or obtained from dietary sources (vitamin D_2 and D_3)[4]. Both vitamin D_2 and D_3 are inactive forms that are converted in the liver into 25-hydroxyvitamin D_2 (25-OHD_2) and 25-hydroxyvitamin D_3 (25-OHD_3), the sum of which is referred to as total 25-hydroxyvitamin D (25-OHD). 25-OHD is the major circulating metabolite and the recommended biomarker used to measure vitamin D status due to its stability and long half-life[7,8]. 25-OHD is converted by the kidneys into the active form 1,25-hydroxyvitamin D, which interacts via the vitamin D receptor, a nuclear hormone receptor expressed in many cells including cardiomyocytes and is thought to directly regulate over 2000 genes[4,9].

The effects of vitamin D are likely to be similar in great apes and humans due to their genetic and phenotypic similarities, thus vitamin D deficiency could have a severe negative impact on the health of great apes. The authors have previously hypothesised the role of vitamin D deficiency in ape cardiovascular disease (CVD), which is a major cause of morbidity and mortality in captive great apes[10,11]. One such CVD, idiopathic myocardial fibrosis (IMF), where cardiac muscle is progressively replaced by connective tissue, affects up to 91% of zoo-housed chimpanzees (*Pan troglodytes*) in Europe and 77% in the United States[11,12]. However, little has been published regarding the actiopathogenesis and risk factors associated with myocardial fibrosis in chimpanzees[13,14]. Husbandry and nutrition need to be investigated as possible risk factors in great ape CVD, as research indicates that zoo-housed great apes are more affected by CVD than their wild counterparts[11]. An inhibitory role for vitamin D in cardiac fibrosis has been demonstrated in humans and animals[15–17], principally through inhibition of the main pro-fibrotic factor transforming growth factor beta 1 (TGF-β1). There is also an inverse relationship between

[1]School of Veterinary Medicine, St. George's University, West Indies, Grenada. [2]School of Veterinary Medicine and Science, University of Nottingham, Sutton Bonington LE12 5RD, UK. [3]School of Medicine, St. George's University, West Indies, Grenada. [4]Twycross Zoo, Atherstone CV9 3PX, UK. [5]School of Dentistry, Institute of Clinical Science, University of Birmingham and Birmingham Community Healthcare Foundation Trust, Birmingham B5 7ET, UK. [6]Department of Clinical Biochemistry, Manchester University NHS Foundation Trust, Manchester, UK. [7]Department of Veterinary Clinical Sciences, City University of Hong Kong, Kowloon, Hong Kong SAR, Hong Kong. [8]Present address: Dublin Zoo, Saint James', Dublin 8, Ireland. [9]Present address: Department of Life Sciences, Perth Zoo, South Perth, WA 6151, Australia. ✉email: smoittie@sgu.edu; rachel.jarvis@nottingham.ac.uk

serum 25-OHD and parathyroid hormone (PTH) concentrations in humans, with progressively increasing PTH when 25-OHD falls under 75 nmol/L. It was previously demonstrated that increasing PTH levels increase blood pressure, cause cardiomyocyte hypertrophy, and interstitial fibrosis of the heart[18]. Inadequate vitamin D status could thus be a risk factor for the development of IMF in chimpanzees[11].

Solar UV radiation exposure is significantly more effective at increasing serum 25-OHD than dietary vitamin D_2 or D_3 supplementation[19–21]. Vitamin D synthesis in the skin is affected by environmental and individual variables such as available UVB, exposure time, skin pigmentation, and age[21,22]. All wild non-human great apes, including chimpanzees, live in tropical areas that receive high amounts of direct sunlight. They are thus likely poorly adapted to restricted UVB exposure and may not synthesise enough cutaneous vitamin D when housed in zoos at more northern or southern latitudes than their natural range[23]. Melanin, the main skin pigment, has an important adaptive role in protecting against UVA damage and in regulating UVB absorption, thus decreasing cutaneous vitamin D_3 synthesis[8,22,24]. Therefore, dark skin is a well-known risk factor in humans for vitamin D deficiency, especially at northern latitudes, due to the lower average solar UV radiation[24,25]. Skin pigmentation also had an effect on vitamin D status in wild baboons, in that darker-skinned species were shown to have lower levels of vitamin D_3 metabolites than lighter species[26]. Though some natural variation occurs with age and sun exposure, chimpanzees commonly have dark skin pigmentation, which may affect their ability to synthesise vitamin D when living outside their natural distribution range[27]. Although reference intervals for serum 25-OHD have not yet been established in non-human great apes, some small-scale studies suggest that both juvenile and adult captive chimpanzees may suffer from vitamin D deficiencies despite vitamin D supplementation[28–31]. At one US institution, chimpanzees housed in indoor-only enclosures had significantly lower vitamin D levels than chimpanzees with daily outdoor access[28].

While vitamin D may have significant health impacts in chimpanzees, there are no standardised methods for measuring vitamin D status in this species. Analytical variability is one of the main challenges in measuring vitamin D metabolites, as it has been demonstrated that inter-assay and inter- and intra-laboratory variability commonly exceeds recommended allowable error[32,33]. Studies on vitamin D status in the European human population show very different estimates of prevalence of vitamin D deficiency, partly due to differences in analytical methods, and although it has been suggested to use centralised laboratories and standardised methods to make these studies more reliable, this has not yet been achieved[1,34]. A recent method validation study measuring 25-OHD in chimpanzees also highlighted the significant analytical variability between assays and laboratories when measuring 25-OHD in great apes[35]. Using liquid chromatography and tandem mass spectrometry (LC–MS/MS), which is considered the gold-standard method in human laboratory practice, at a single laboratory is thus key to precisely assess the vitamin D status of the chimpanzee population in Europe[36]. The aims of the present study were the following:

1. Evaluate the vitamin D status of European zoo chimpanzees using LC–MS/MS on serum samples at a single accredited laboratory.
2. Assess the effect of environmental variables (latitude, UVB irradiance, season) on chimpanzee 25-OHD concentrations.
3. Assess the impact of individual variables (health status, skin tone, body condition score, age, sex) on chimpanzee 25-OHD concentrations.
4. Evaluate the influence of husbandry practices in European zoos (provision of daily outside access, diet and vitamin D supplementation) on chimpanzee 25-OHD concentrations.

Methods

Serum samples were received from European zoos and sanctuaries, that agreed to participate in this study and had available banked serum samples. Samples were in all cases taken opportunistically while chimpanzees were under anaesthesia for procedures such as scheduled health-checks, disease investigation, surgery, or transport within or between facilities. Samples were kept frozen at − 20 °C to − 80 °C and protected from the light after sampling at their facility of origin or at the European Association of Zoos and Aquaria (EAZA) Biobank. All available samples were sent on ice to an accredited laboratory participating in the United Kingdom Accreditation Service (UKAS) Vitamin D External Quality Assessment Scheme (Clinical Biochemistry—Manchester University NHS Foundation Trust) for measurements of 25-OHD_2, 25-OHD_3 and total 25-OHD using Transcend II liquid chromatography. The analysis required a sample preparation system with TurboFlow online sample preparation technology and a TSQ Endura tandem quadrupole mass spectrometer (Thermo Fisher Scientific), as detailed elsewhere[35]. Known human reference intervals were used to interpret chimpanzee vitamin D status, where 25-OHD > 50 nmol/L is currently considered sufficient[21,37].

The following epidemiological information about each animal was obtained from participating zoos: age, sex, health status, body condition score, skin tone, body hair coverage, diet including any commercial dry feed (referred to as pellets) and vitamin D supplementation given, and details on provision of outdoor access in the 2 months prior to sampling. The geographic location (latitude and longitude) of each zoo was determined using Google Maps. Northern Europe was defined as latitudes above 46°N, where levels of UVB are too low to allow cutaneous vitamin D_3 synthesis for most of the year[23]. For each sample, the mean UVB irradiance in W/m^2 for the corresponding zoo location during the 2 months before sampling was calculated using daily local irradiance data available from the National Aeronautics and Space Administration (NASA) Langley Research Center (LaRC) Prediction of Worldwide Energy Resource (POWER) Project (Data Access Viewer v2.0.0). The time of sample storage before analysis was calculated in months. Animals were classified as healthy when reported as such or when reported to suffer from acute traumatic injuries only. Details on the categorical variables and the ordinal level grouping used for statistical analysis are shown in Table 1.

Variable	Type	Levels
Age group[38]	Ordinal	Juvenile: < 15 years
		Adult: 15–34 years
		Elderly: > 34 years
Sex	Binary	Male
		Female
Zoo latitude[23]	Binary	Northern Europe: > 46°N
		Southern Europe: ≤ 46°N
Season of sampling	Categorical	Summer: 21st of June–21st of September
		Autumn: 22nd of September–20th of December
		Winter: 21st of December–20th of March
		Spring: 21st of March–20th of June
Skin tone	Binary	Dark coloured face
		Light coloured face
Hair coverage	Ordinal	Good coat condition
		Partial hair loss
		Total hair loss
Provision of vitamin D in the form of oral supplementation (not including fortified pellets) at the time of sampling	Binary	No provision of extra vitamin D
		Provision of extra vitamin D
Provision of outside access in the 2 months before sampling	Binary	Limited outside access
		Unlimited outside access
Body condition score (BCS) reported on a scale of 1–9	Ordinal	Underweight (BCS 1–3)
		Optimal (BCS 4–6)
		Overweight (BCS 7–9)
Health status at the time of sampling	Binary	Healthy (including acute trauma)
		Abnormal health (any disease reported except acute trauma)

Table 1. Categorical variables used for statistical analysis.

To account for the repeated measures of vitamin D levels within the same individuals, mixed effects models with a random effect for each individual were used. The analyses were performed with R version 4.1.1 and the lme4 package for mixed effects models, which were built with a restricted maximum likelihood (REML) criterion. There is no requirement for normality of the outcome variable for these models, normality of the model residuals was assessed to establish model fit. Package lmerTest was used for significance testing and degrees of freedom estimation in these models, using the conservative Satterthwaite method[39]. The significance cut-off was set at alpha = 0.05.

The project was under ethical review and was granted full ethical permission by The University of Nottingham, School of Veterinary Medicine and Science Ethics committee in adherence to institutional, national and international guidelines (ethics number 3064200106). Permission from each facility was given for investigation of every animal and no chimpanzees were euthanised or harmed for the purposes of research. Blood samples were taken in each zoo under the Veterinary Surgeons Act (VSA) or equivalent guidelines and regulations in their country. All samples were shipped with full CITES (Convention on International Trade in Endangered Species of Wild Fauna and Flora) export and import permits. Study methods were carried out in accordance with the ARRIVE guidelines.

Results

A total of n = 245 serum samples were analysed, from 140 individual chimpanzees from 32 European zoos and sanctuaries. The number of samples per individual chimpanzee ranged from 1 to 10.

The numbers of samples per facility ranged from 1 to 100. The largest number of samples was obtained from a British zoo (n = 100, latitude 52.65°). Figure 1 shows the number of samples submitted by European zoos and sanctuaries.

Chimpanzees' median age at the time of sampling was 27 years (range 1–65 years), with 46 samples corresponding to juvenile individuals, 130 to adults and 65 to elderly.

A total of 97 samples were from male chimpanzees, and 147 from females. Reported health conditions of the chimpanzees were varied and included metabolic diseases like diabetes mellitus, neoplastic processes, chronic renal disease, cardiac, dental, and infectious diseases. A total of seven chimpanzees (corresponding to 11 samples) were known or suspected to suffer from cardiac disease at the time of sampling.

General vitamin D status. The concentration of 25-OHD_2 was less than 5 nmol/L thus negligible for all samples except for three: one chimpanzee from a British zoo with 25-OHD_3 = 26.2 nmol/L and 25-OHD_2 = 14.8 nmol/L, and two chimpanzees from a Danish zoo with concentrations of 25-OHD_3/25-

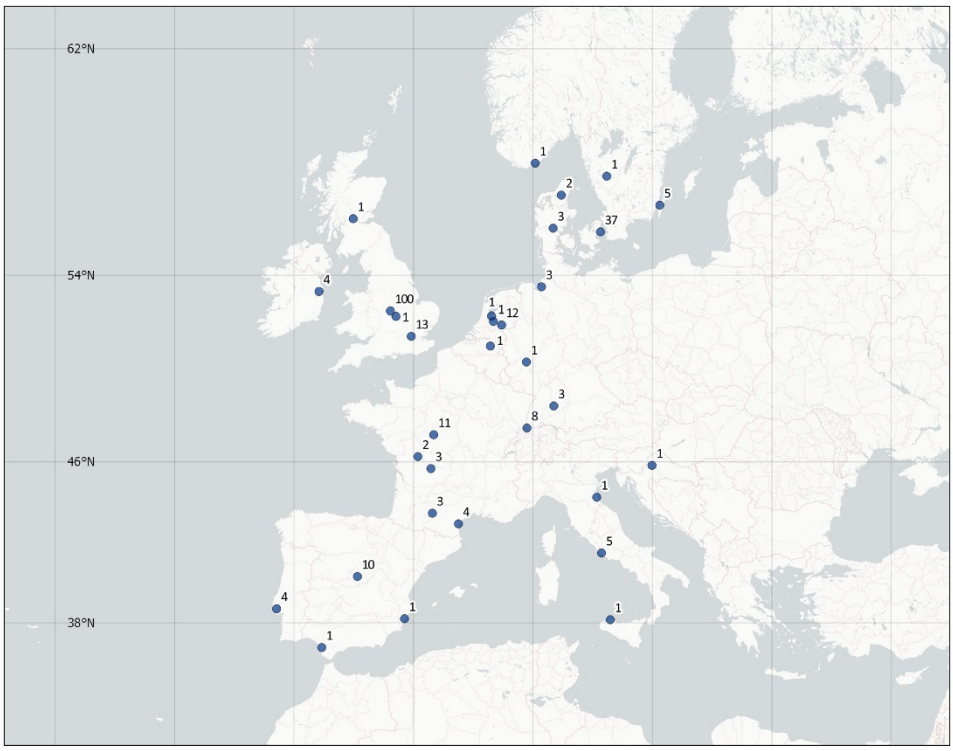

Figure 1. Geographic distribution and number of samples obtained from European zoos and sanctuaries for serum 25-OHD measurement. This map was created using QGIS Desktop v2.18.28.

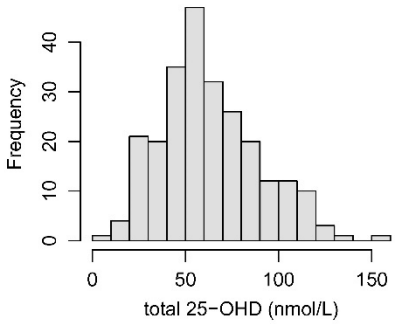

Figure 2. Frequency distribution of total 25-OHD in European zoo chimpanzees.

OHD_2 = 23/15.7 nmol/L and 25.9/27.7 nmol/L respectively. Thus, apart from these 3 chimpanzees, the total 25-OHD results in this study were equivalent to the concentrations of 25-OHD_3, thus total 25-OHD was used as the key outcome variable. One sample that had a total 25-OHD concentration below the detection limit of 5 nmol/L, this result was considered equal to 5 nmol/L for statistical analysis.

A histogram of 25-OHD concentrations showed some indication of skew (Fig. 2), but a log-transformation did not result in a more normal distribution of values. Accordingly, the uncorrected total 25-OHD levels were

Predictor	Effect size (nmol/L)	df	t	p
Unlimited outdoor access	19.9	113	5.32	5.35e−07
Season: autumn	−14.4	152	−3.06	0.0026
Season: winter	−25.5	146	5.53	1.43e−07
Season: spring	−11.8	148	−2.96	0.036
Health status	−9.8	165	−2.61	0.0098

Table 2. Effect sizes and significance estimates for all significant predictors of total 25-OHD levels.

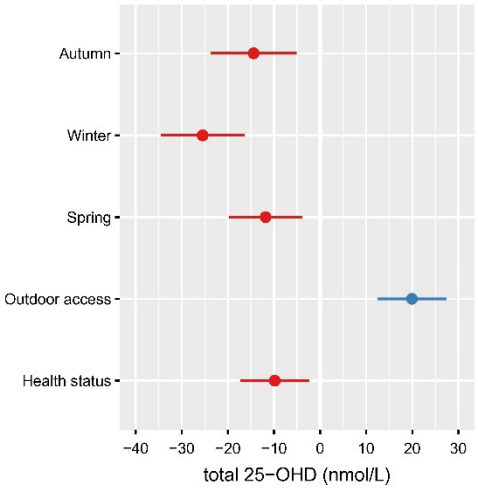

Figure 3. Effect size estimates and 95% confidence intervals for the main effects of all significant predictors of total 25-OHD levels. Summer 25-OHD levels are used as the baseline reference.

used as the outcome scores reflecting overall vitamin D status. 25-OHD concentrations ranged from < 5 to 151 nmol/L with a median of 57.7 nmol/L. A total of 81 samples (33.1%) had concentrations of 25-OHD below the human deficiency threshold of 50 nmol/L.

Significant predictors of vitamin D levels. To build a robust model of vitamin D status, all individually significant predictor variables for total 25-OHD levels were entered into a mixed effects model with main effects only at the first step. UVB irradiance analysed continuously dropped out of significance ($p = 0.07$) when sampling season was added into the same model, indicating that the latter explains the variance in 25-OHD levels better than the 2-month UVB irradiance. To build the most robust model, UVB irradiance scores were removed from the global model and analysed separately instead (see section on UVB irradiance below).

The model then contained only significant main effects. Interactions were also included where theoretically plausible but did not improve model fit in any case. The final model was thus restricted to only include significant main effects, which yielded a good fit with a conditional coefficient of determination (adjusted R^2) of 53%. The distribution of residuals resembled a normal distribution very closely, and Q-Q plots also indicated good model fit. The model results are listed in Table 2 and illustrated in Fig. 3. Summer 25-OHD levels were used as the baseline reference for seasonal effects. Compared to the summer season, 25-OHD concentrations were 14.4 nmol/L lower in autumn, 25.5 nmol/L lower in winter, and 11.8 nmol/L lower in spring. Unlimited outdoor access increased 25-OHD levels by 19.9 nmol/L whereas poor health status was associated with a 9.8 nmol/L decrease in 25-OHD levels.

Seasonal effects. Because the global model showed a significant effect of sampling season on vitamin D levels, uncorrected seasonal levels are presented in more detail in this section. Sampling date was known for 244 samples. 49 samples were taken in winter, 100 in spring, 47 in summer, and 48 in autumn. Median 25-OHD concentrations were 47 nmol/L in winter (IQR = 31.2–59.5 nmol/L), 64.20 nmol/L in spring (IQR = 49–83.1), 71.8 in summer (IQR = 51.1–100.4) and 54.5 in autumn (IQR = 46.2–69.5) (Fig. 4). The percentage of samples that were

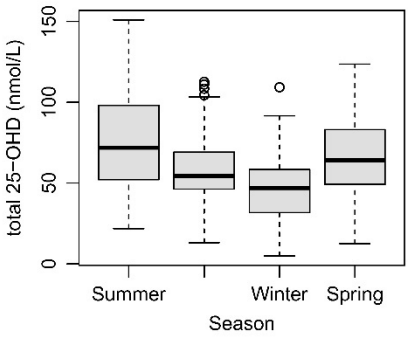

Figure 4. Total 25-OHD by season in European zoo chimpanzees. Central black bar: median. Inner box: interquartile range. Whiskers: range without outliers. Circles: outliers.

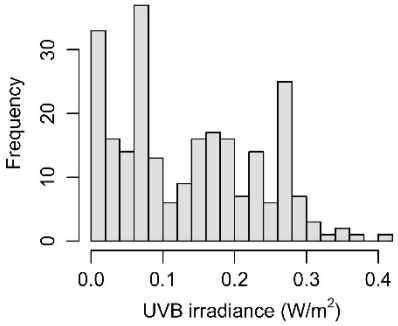

Figure 5. Distribution of UVB irradiance means in the 2 months before taking the sample. Bin size = 0.02.

below the human deficiency threshold of 50 nmol/L per season were: 55.1% in winter, 28% in spring, 23.4% in summer, and 31.3% in autumn.

UVB irradiance. Mean UVB irradiance in the 2 months before sampling was analysed separately as a continuous variable. As expected, the distribution also exhibited some right-hand skew (Fig. 5), but again a log transformation did not lead to a more symmetrical distribution. The uncorrected UVB irradiance scores were thus used for further analysis. Although sampling season appears to be a more robust predictor of 25-OHD levels than UVB irradiance in the 2 months prior to taking the sample, the continuous UVB irradiance scores are a significant predictor of 25-OHD levels when analysed in isolation (effect size = 49.6 nmol/L per 1 W/m^2, $t(1, 232) = 3.24$, $p = 0.0014$, see Fig. 6). The continuous UVB irradiance was then used to determine if there is a significant non-linear relationship in the effect on 25-OHD levels, which might indicate saturation at higher levels of UVB radiation. However, the non-linear effect was not significant ($p = 0.42$), which implies that there was no saturation effect for UVB radiation.

Variables that did not predict vitamin D levels. All other variables were also tested for a significant main effect on 25-OHD levels in separate mixed effects models containing no other co-variates. They did not exhibit significant effects, also when included in the more complex main model. Their main effect p-values and total number of valid data points are listed in Table 3 for reference.

Diet and supplementation. Information on the chimpanzees' diet at the time of sampling was available for 196 (80%) samples. For 187 (95.4%) of these samples, the animals were reported to eat primate pellets as part of their diet at the time of sampling. Diets were largely based on green and root vegetables, pellet, fruits, nuts and occasional other food items, such as eggs, vegetable oil, or meat. The total and relative amount eaten by each individual animal was not possible to ascertain, as diets were reported for whole chimpanzee groups.

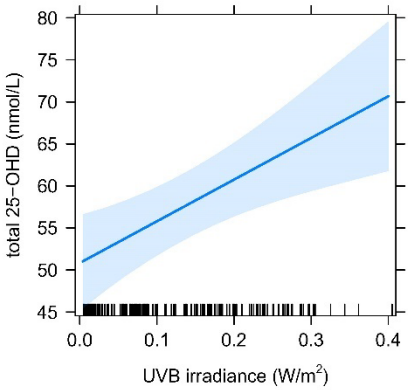

Figure 6. Estimates for the effect of UVB irradiance on 25-OHD levels, showing regression line and 95% confidence interval (shaded band).

Variable	Valid n	p
Sample storage (months)	244	0.147
Sex	244	0.732
Latitude (continuous)	245	0.647
Latitude (binary North/South)	245	0.245
Skin tone	181	0.463
Hair coverage	168	0.491
Vitamin D supplementation	162	0.964
BCS	187	0.288
Age category	241	0.384

Table 3. Non-significant predictors of 25-OHD levels.

Although at least seven different types of primate pellets were identified as offered to animals included in this study, but many facilities were unable to ascertain exactly which type of pellets the animals were receiving at the time of sampling. The amount of vitamin D present in commercial pellets varied greatly depending on the type, ranging from 1600 to 10,170 IU/kg. One food distributor reported to have markedly increased the vitamin D amount in their pellets in 2018 from 3500 to 8500 IU/kg. It was not possible to statistically assess the effect of pellet type on serum 25-OHD concentrations, due to the limited number of samples for each type of pellet and the uncertainty on which and how much pellet was consumed by the animal at the time of sampling.

Only 21 animals (from seven different zoos) were reported to receive extra oral vitamin D supplementation in addition of the vitamin D present in the rest of their diet at the time of sampling (n = 23 samples). It was, however, difficult to ascertain the exact amount of vitamin D received by each animal due to the zoos mixing the supplementation with the group diet, or due to lack of detail on the exact vitamin D amount present in the supplementation. The provision of extra vitamin D supplementation did not appear to have an effect on serum 25-OHD concentrations (see Table 2).

Discussion

This study represents the largest survey on vitamin D status of non-human great apes under human care. A significant strength in the methods used was the reduction in analytical variability by analysing all samples at the same laboratory with the same gold-standard assay, thus allowing a more accurate comparison between results[7]. Although pre-analytical factors such as storage and shipment conditions were expected to be different for all samples, the high stability of 25-OHD in serum samples, even if transiently kept at room temperature, justifies our choice of study methods[40,41].

Though a number of studies have measured vitamin D status in non-human primates, reference intervals for 25-OHD in apes have not yet been established. Juvenile chimpanzees with serum 25-OHD of 4 to 32 nmol/L were diagnosed with dietary rickets, while in the same group apparently healthy adult chimpanzees had average 25-OHD levels of 31 nmol/L. Interestingly, when some of these chimpanzees were later moved to a facility with year-round sun exposure in Hawaii, their average 25-OHD levels raised to 97.3 nmol/L. Another study suggests

that adult chimpanzees housed in indoor-only enclosures experience vitamin D deficiency, with 25-OHD levels averaging 38.2 nmol/L despite dietary supplementation[28,29]. When vitamin D status was assessed in nine species of zoo-housed primates, chimpanzees were found to have the lowest average 25-OHD serum levels (32.7 nmol/L) despite dietary levels above recommendations[30]. In zoo-housed Western lowland gorillas (*Gorilla gorilla gorilla*), serum 25-OHD levels were found to be low despite oral supplementation, with 25-OHD concentrations averaging 35.5 nmol/L in animals managed indoors and 66.6 nmol/L in animals with unrestricted outdoor access[42]. A study on the vitamin D status of baboons showed that sun exposed and supplemented olive baboons (*Papio anubis*) housed outdoor in Texas (USA) had average 25-OHD_3 levels of 220 nmol/L, and that average 25-OHD_3 levels for wild baboons were between 149.5 and 315.5 nmol/L depending on the species[26]. Reported levels of serum vitamin D metabolites in non-human primates differ widely depending on species, with New-World monkeys such as marmosets having significantly higher levels than other species (serum 25-OHD_3 of supplemented zoo marmosets are often above 500 nmol/L)[43]. Although these studies give an insight about vitamin D status of captive and wild primates, cautious interpretation is warranted and comparison between studies is problematic, due to the relatively small number of samples analysed, different species studied and the use of heterogeneous methods.

For humans, the suggested definition of vitamin D deficiency varies depending on sources, but serum 25-OHD concentrations between 50 and 125 nmol/L are generally recommended, while levels below 30 nmol/L are considered severely deficient and can increase the risk of developing diseases such as rickets or osteomalacia[44–46]. Applying a conservative 50 nmol/L cut-off for chimpanzees, more than 33% of all samples collected in the present study could be considered deficient, with the proportion rising to 55.1% in winter. Zoo latitude was not a significant predictor of 25-OHD levels in chimpanzees, and 13 out of 81 samples (16%) with 25-OHD below 50 nmol/L were from chimpanzees living in Southern European facilities. This means that the whole European chimpanzee population could be at risk of increased morbidity and mortality due to a suboptimal vitamin D status.

There was a clear difference in 25-OHD concentration between seasons, with higher levels observed in summer while lower levels were observed in winter. It seems, however, that for a large proportion of chimpanzees, even at the end of summer serum 25-OHD concentrations may not be high enough to ensure that they will not become deficient by winter. In humans in the United Kingdom (UK), 25-OHD serum levels in September needs to be at least 80.5 nmol/L in order to exceed a concentration of 25 nmol/L in February[47]. Unsurprisingly, mean UVB irradiance the two months before sampling was also significantly associated with 25-OHD levels.

Of interest is the lack of significant plateau in the relationship between UVB radiation and 25-OHD levels, which suggests that maximal cutaneous vitamin D synthesis is not reached within the sampled range of UVB levels. Accordingly, more exposure to UVB radiation should result in higher 25-OHD levels in the entire chimpanzee population, which may yield additional health benefits even for individuals above the deficiency cut-off for humans. Average annual UVB irradiance in chimpanzee natural range areas is between 0.3–0.4 W/m^2 (NASA LaRC POWER Project, Data Access Viewer v2.0.0), however in this study only eight samples were available where individuals were exposed to these levels. This highlights that solar UVB irradiance in Europe may be inadequate compared with levels encountered in the natural range of the species, further emphasising the need to review husbandry and nutrition practices for non-human great apes in human care.

The provision of unlimited daily outdoor access was associated with higher 25-OHD concentrations year-round. This is in accordance with the results of other studies on zoo gorillas and chimpanzees[28,42]. Although the provision of outdoor access during the majority of the year is recommended by the North American Association of Zoos and Aquariums' Chimpanzee Species Survival Plan[48], no recommendations have been published by the EAZA, and outdoor access is often restricted for chimpanzees in some zoos and sanctuaries for climatic, husbandry, or other animal management reasons. It is thus necessary to raise awareness about the importance of encouraging animals to spend time outdoors, especially during the high-UV season when cutaneous vitamin D synthesis is possible. In Caucasian humans in the UK, only nine minutes of daily sunshine exposure (with about one third of the total skin area exposed) during the high-UV season have been proposed to maintain 25-OHD levels above 25 nmol/L throughout winter[47]. Longer exposure times are likely to be necessary in chimpanzees to maintain healthy 25-OHD concentrations year-round, due to their darker skin and more extensive hair coverage. It may be safer to recommend daily sun or UVB exposure for zoo-housed chimpanzees, rather than advocate for vitamin D supplementation in the diet, as hypervitaminosis D can occur with supplementation, but not with UVB exposure[34,49]. Moreover, conflictive evidence exists from human studies regarding the impact of oral vitamin D supplementation on health outcomes[46,50]. And although sun-exposed captive baboons receiving oral supplementation had circulating 25-OHD levels comparable to wild baboons, cholecalciferol (vitamin D_3) conversion to 25-OHD_3 was higher in wild baboons compared to captive baboons receiving oral supplementation, supporting the assumption that UV exposure is more efficient than supplementation at raising circulating 25-OHD levels in non-human primate species[26]. Artificial UVB lighting is widely used in certain nondomestic taxa in human care, especially in reptiles and some small non-human primates (Callitrichids), but currently is not commonly utilised for non-human great apes due to cost, safety and efficacy considerations. This study provides some further evidence that investigating artificial UVB lighting as part of standard husbandry practices for non-human great apes at locations where available UVB levels are under the natural range (0.3–0.4 W/m^2) might be of benefit, justifying the above-mentioned costs and difficulties.

There appeared to be a relationship between 25-OHD levels and health status in chimpanzees. Reported health conditions were diverse and clinical information was transmitted with different levels of details depending on the institution. The effect of vitamin D status on cardiac disease as such could not been statistically explored due to the relatively small number of chimpanzees known to suffer from cardiac disease at the time of sampling. This is not overly surprising as the ante-mortem diagnosis of CVD in chimpanzees is challenging, with the only definitive diagnostic method for chronic degenerative heart diseases like the commonly diagnosed IMF being post-mortem by cardiac histopathology. Chimpanzees with an abnormal health status in our study showed a significantly lower serum 25-OHD level than their healthy counterparts, but future studies will need to investigate

this correlation further. In humans, vitamin D deficiency can not only lead to ill-health, but the inverse relationship is also observed, as chronic and acute inflammation can lead to a decrease in 25-OHD levels[44,51].

Interestingly, age was not found to have significant effect on chimpanzee vitamin D status. In humans, prevalence of vitamin D deficiency has been shown to vary depending on age group in some, but not all, large-scale studies, with teenagers and the elderly often considered most at risk[1,52,53]. In wild baboons, juveniles were found to have higher vitamin D_3 (cholecalciferol) levels, but not 25-OHD_3 levels, than adults[26]. Other primate studies have shown an absent or weak effect of age on levels of vitamin D metabolites[28,42,43,54].

The lack of a significant effect for variables with a smaller valid sample size, for which the analysis has reduced statistical power, is less likely to imply the confirmed absence of an effect. For example, analysing more samples from chimpanzees receiving extra vitamin D supplementation may have resulted in a significant effect of oral vitamin D supplementation on chimpanzee 25-OHD levels. However, the main limitations of this study were the relatively low number of samples from Southern Europe and the overrepresentation of samples from a single British zoo which likely led to bias when analysing the data. To have a clearer picture of vitamin D status in chimpanzees in Europe, ideally a wider and more balanced representation of latitudes would be needed, with a similar number of samples from Northern and Southern European zoos. This may however be difficult to achieve, as only one fifth of the European zoo chimpanzee population live in Southern Europe (according to Species360 Zoological Information Management System). That said, this study included samples from approximately 20% of the chimpanzee population kept in European zoos, which is an exceptional achievement considering that, due to the dangerous nature of these animals, samples are usually only taken opportunistically when chimpanzees are under general anaesthesia for health-checks, surgical procedures or enclosure moves.

Another limitation of our study is the inconsistency in information received from participating institutions about chimpanzee husbandry and nutrition at the time of sampling. Some institutions were not able to provide some or all of this information, which affected data analysis. This is common in large scale studies with numerous participating institutions, especially with archived data where some records may be incomplete or lost.

Hypovitaminosis D is a public health concern in humans and it has been linked to numerous chronic conditions including cancer, autoimmune, metabolic, and cardiovascular diseases, and a higher risk of overall mortality[55]. Growing evidence suggests that low vitamin D levels are associated with cardiovascular diseases such as hypertension, coronary heart disease, stroke, myocardial infarction, and cardiac fibrosis[15,16,56,57]. It is possible that vitamin D deficiency is a significant risk factor for cardiac disease in zoo-housed chimpanzees as macrophage-mediated fibrosis has been shown to induce differentiation of cardiac stromal cells into myofibroblasts[58–60]. A fibrosis-associated increase of macrophages and myofibroblasts was also shown in a previous study in chimpanzees[11]. Considering the results of this study, together with the high prevalence of idiopathic myocardial fibrosis (IMF) in chimpanzees[11], a relationship between vitamin D status and cardiovascular disease seems plausible. Transforming growth factor beta1 (TGFβ1) is the principal pro-fibrotic factor and its selective inhibition or of one of its downstream effectors like Interleukin 11 could be a promising therapeutic target in cardiac fibrosis in humans and apes and needs to be further investigated[61,62]. Furthermore, models in rats and mice have shown that activation of the vitamin D receptor (VDR) can prevent adverse cardiac remodelling by fibrosis[63,64]. Clinical trials using a TGFβ inhibitor, increased UVB exposure and/or vitamin D supplementation could potentially represent an important treatment strategy not only for great apes in our care but also be a very valuable and suitable treatment option for humans with increased cardiac, renal, pulmonary, or hepatic fibrosis. Beyond cardiovascular diseases, vitamin D insufficiency could result in non-human great apes being more susceptible to bacterial or viral upper respiratory tract infections or pneumonia which are a common cause of morbidity in these species[65–67].

Our study shows that a considerable proportion of European zoo-housed chimpanzees can be considered vitamin D deficient according to human reference levels. Health status and provision of outside access had significant impact on vitamin D status. Whether zoos should provide vitamin D supplementation cannot be decided based on this study, but similarly to humans, it may be advisable when sufficient cutaneous vitamin D synthesis is not possible. The provision of unlimited outdoor access, as well as regular health screenings including the measurement of serum 25-OHD concentrations are recommended to safeguard the health and welfare of the non-human great ape populations in human care.

Data availability

The datasets generated during and/or analysed during the current study are available from the corresponding author on reasonable request.

Received: 2 July 2022; Accepted: 23 September 2022
Published online: 21 October 2022

References

1. Cashman, K. D. *et al.* Vitamin D deficiency in Europe: Pandemic?. *Am. J. Clin. Nutr.* **103**, 1033–1044 (2016).
2. Holick, M. F. The vitamin D deficiency pandemic: Approaches for diagnosis, treatment and prevention. *Rev. Endocr. Metab. Disord.* **18**, 153–165 (2017).
3. Wang, L. *et al.* Circulating levels of 25hydroxy-vitamin D and risk of cardiovascular disease: A meta-analysis of prospective studies. *Circ. Cardiovasc. Qual. Outcomes* **5**, 819–829 (2012).
4. Hossein-nezhad, A. & Holick, M. F. Vitamin D for health: A global perspective. *Mayo Clin. Proc.* **88**, 720–755 (2013).
5. Kim, H. A. *et al.* Vitamin D deficiency and the risk of cerebrovascular disease. *Antioxidants* **9**, 327 (2020).
6. Chang, S. W. & Lee, H. C. Vitamin D and health—The missing vitamin in humans. *Pediatr. Neonatol.* **60**, 237–244 (2019).
7. Altieri, B. *et al.* Vitamin D testing: Advantages and limits of the current assays. *Eur. J. Clin. Nutr.* **74**, 231–247 (2020).
8. Datta, P. *et al.* The half-life of 25(OH)D after UVB exposure depends on gender and Vitamin D receptor polymorphism but mainly on the start level. *Photochem. Photobiol. Sci.* **16**, 985–995 (2017).

9. DeLuca, H. F. Overview of general physiologic features and functions of vitamin D. *Am. J. Clin. Nutr.* **80**, 1689S-1696S (2004).
10. Strong, V. J., Grindlay, D., Redrobe, S., Cobb, M. & White, K. A systematic review of the literature relating to captive great apes morbidity and mortality. *J. Zoo Wildl. Med.* **47**, 697–710 (2016).
11. Strong, V. J. *et al.* Idiopathic myocardial fibrosis in captive chimpanzees (*Pan troglodytes*). *Vet. Pathol.* **57**, 183–191 (2020).
12. Gamble, K. C. Pathologic review of the chimpanzee (*Pan troglodytes*): 1990–2003. in *2004 Proceedings AAZV, AAWV, WDA Joint Conference* 561 (AAZV, 2004).
13. Moittié, S. *et al.* Discovery of os cordis in the cardiac skeleton of chimpanzees (*Pan troglodytes*). *Sci. Rep.* **10**, 9417 (2020).
14. Varki, N. *et al.* Heart disease is common in humans and chimpanzees, but is caused by different pathological processes. *Evol. Appl.* **2**, 101–112 (2009).
15. Meredith, A., Boroomand, S., Carthy, J., Luo, Z. & McManus, B. 1,25 Dihydroxyvitamin D3 inhibits TGFβ1-mediated primary human cardiac myofibroblast activation. *PLoS One* **10**, e0128655 (2015).
16. Chen, S. *et al.* Cardiomyocyte-specific deletion of the vitamin D receptor gene results in cardiac hypertrophy. *Circulation* **124**, 1838–1847 (2011).
17. Charytan, D. M., Padera, R. F., Helfand, A. M. & Zeisberg, E. M. Association of activated vitamin D use with myocardial fibrosis and capillary supply: Results of an autopsy study. *Ren. Fail.* **37**, 1067–1069 (2015).
18. Zittermann, A. Vitamin D and disease prevention with special reference to cardiovascular disease. *Prog. Biophys. Mol. Biol.* **92**, 39–48 (2006).
19. Ala-Houhala, M. J. *et al.* Comparison of narrowband ultraviolet B exposure and oral vitamin D substitution on serum 25-hydroxy-vitamin D concentration. *Br. J. Dermatol.* **167**, 160–164 (2012).
20. Bogh, M. K. B., Gullstrand, J., Svensson, A., Ljunggren, B. & Dorkhan, M. Narrowband ultraviolet B three times per week is more effective in treating vitamin D deficiency than 1600 IU oral vitamin D_3 per day: A randomized clinical trial. *Br. J. Dermatol.* **167**, 625–630 (2012).
21. The British Association of Dermatologists *et al.* Consensus Vitamin D position statement. *Consensus Vitamin D Position Statement*. https://www.nhs.uk/livewell/summerhealth/documents/concensus_statement_vitd_dec_2010.pdf (2010).
22. Webb, A. *et al.* Colour counts: Sunlight and skin type as drivers of vitamin D deficiency at UK latitudes. *Nutrients* **10**, 457 (2018).
23. Jablonski, N. G. & Chaplin, G. Human skin pigmentation as an adaptation to UV radiation. *Proc. Natl. Acad. Sci. U.S.A.* **107**, 8962–8968 (2010).
24. Åkeson, P. K., Lind, T., Hernell, O., Silfverdal, S.-A. & Öhlund, I. Serum Vitamin D depends less on latitude than on skin color and dietary intake during early winter in northern Europe. *J. Pediatr. Gastroenterol. Nutr.* **62**, 643–649 (2016).
25. Libon, F., Cavalier, E. & Nikkels, A. F. Skin color is relevant to vitamin D synthesis. *Dermatology* **227**, 250–254 (2013).
26. Ziegler, T. E. *et al.* Comparison of vitamin D metabolites in wild and captive baboons. *Am. J. Primatol.* **80**, e22935 (2018).
27. Jablonski, N. G. & Chaplin, G. The evolution of human skin coloration. *J. Hum. Evol.* **39**, 57–106 (2000).
28. Videan, E. N. *et al.* Relationship between sunlight exposure, housing condition, and serum vitamin D and related physiologic biomarker levels in captive chimpanzees (*Pan troglodytes*). *Comp. Med.* **57**, 402–406 (2007).
29. Junge, R. E., Gannon, F. H., Porton, I., McAlister, W. H. & Whyte, M. P. Management and prevention of vitamin D deficiency rickets in captive-born juvenile chimpanzees (*Pan troglodytes*). *J. Zoo Wildl. Med.* **31**, 361–369 (2000).
30. Crissey, S. D. *et al.* Serum concentrations of lipids, vitamins A and E, vitamin D metabolites, and carotenoids in nine primate species at four zoos. *Zoo Biol.* **18**, 551–564 (1999).
31. Crissey, S., Pribyl, L., Pruett-Jones, M. & Meehan, T. Nutritional management of Old World primates with special consideration for vitamin D. *Int. Zoo Yearb.* **36**, 122–130 (1998).
32. Holmes, E. W., Garbincius, J. & McKenna, K. M. Analytical variability among methods for the measurement of 25-hydroxyvitamin D: Still adding to the noise. *Am. J. Clin. Pathol.* **140**, 550–560 (2013).
33. Ferrari, D., Lombardi, G. & Banfi, G. Concerning the vitamin D reference range: Pre-analytical and analytical variability of vitamin D measurement. *Biochem. Medica* **27**, 030501 (2017).
34. Spiro, A. & Buttriss, J. L. Vitamin D: An overview of vitamin D status and intake in Europe. *Nutr. Bull.* **39**, 322–350 (2014).
35. Moittié, S. *et al.* Comparison of 25-hydroxyvitamin D concentration in chimpanzee dried blood spots and serum. *Vet. Clin. Pathol.* **49**, 299–306 (2020).
36. Alexandridou, A., Schorr, P., Stokes, C. S. & Volmer, D. A. Analysis of vitamin D metabolic markers by mass spectrometry: Recent progress regarding the "gold standard" method and integration into clinical practice. *Mass Spectrom. Rev.* https://doi.org/10.1002/mas.21768 (2021).
37. Holick, M. F. *et al.* Evaluation, treatment, and prevention of vitamin D deficiency: An Endocrine Society clinical practice guideline. *J. Clin. Endocrinol. Metab.* **96**, 1911–1930 (2011).
38. Alberts, S. C. *et al.* Reproductive aging patterns in primates reveal that humans are distinct. *Proc. Natl. Acad. Sci. U.S.A.* **110**, 13440–13445 (2013).
39. Luke, S. G. Evaluating significance in linear mixed-effects models in R. *Behav. Res. Methods* **49**, 1494–1502 (2017).
40. Wielders, J. P. M. & Wijnberg, F. A. Preanalytical stability of 25(OH)-vitamin D3 in human blood or serum at room temperature: Solid as a rock. *Clin. Chem.* **55**, 1584–1585 (2009).
41. Agborsangaya, C. *et al.* The effects of storage time and sampling season on the stability of serum 25-hydroxy vitamin D and androstenedione. *Nutr. Cancer* **62**, 51–57 (2010).
42. Bartlett, S. L. *et al.* Assessment of serum 25-hydroxyvitamin d concentrations in two collections of captive gorillas (*Gorilla gorilla gorilla*). *J. Zoo Wildl. Med.* **48**, 144–151 (2017).
43. Goodroe, A. E. *et al.* Evaluation of vitamin D3 metabolites in *Callithrix jacchus* (common marmoset). *Am. J. Primatol.* **82**, e23131 (2020).
44. Public Health England. *The Scientific Advisory Committee on Nutrition (SACN) vitamin D and health report*. https://assets.publishing.service.gov.uk/government/uploads/system/uploads/attachment_data/file/537616/SACN_Vitamin_D_and_Health_report.pdf (2016).
45. Sempos, C. T. *et al.* Vitamin D assays and the definition of hypovitaminosis D: Results from the first international conference on controversies in vitamin D. *Br. J. Clin. Pharmacol.* **84**, 2194–2207 (2018).
46. Amrein, K. *et al.* Vitamin D deficiency 2.0: An update on the current status worldwide. *Eur. J. Clin. Nutr.* **74**, 1498–1513 (2020).
47. Webb, A. *et al.* Meeting vitamin D requirements in White Caucasians at UK latitudes: Providing a choice. *Nutrients* **10**, 497 (2018).
48. Ross, S. *et al. Chimpanzee (Pan troglodytes) Care Manual* (Association of Zoos and Aquariums, 2010).
49. Towler, D. A. Vitamin D: Cardiovascular effects and vascular calcification. In *Vitamin D* (eds Feldman, D. *et al.*) 1403–1426 (Elsevier, 2011). https://doi.org/10.1016/B978-0-12-381978-9.10073-3.
50. Bouillon, R. *et al.* The health effects of vitamin D supplementation: Evidence from human studies. *Nat. Rev. Endocrinol.* **18**, 96–110 (2022).
51. Mangin, M., Sinha, R. & Fincher, K. Inflammation and vitamin D: The infection connection. *Inflamm. Res.* **63**, 803–819 (2014).
52. Hilger, J. *et al.* A systematic review of vitamin D status in populations worldwide. *Br. J. Nutr.* **111**, 23–45 (2014).
53. Schleicher, R. L. *et al.* National estimates of serum total 25-hydroxyvitamin D and metabolite concentrations measured by liquid chromatography-tandem mass spectrometry in the US population during 2007–2010. *J. Nutr.* **146**, 1051–1061 (2016).
54. Ziegler, T. E., Kapoor, A., Hedman, C. J., Binkley, N. & Kemnitz, J. W. Measurement of 25-hydroxyvitamin D 2&3 and 1,25-dihydroxyvitamin D 2&3 by tandem mass spectrometry: A primate multispecies comparison. *Am. J. Primatol.* **77**, 801–810 (2015).

55. Caccamo, D., Ricca, S., Currò, M. & Ientile, R. Health risks of hypovitaminosis D: A review of new molecular insights. *Int. J. Mol. Sci.* **19**, 892 (2018).
56. Milazzo, V., De Metrio, M., Cosentino, N., Marenzi, G. & Tremoli, E. Vitamin D and acute myocardial infarction. *World J. Cardiol.* **9**, 14–20 (2017).
57. Zittermann, A. The biphasic effect of vitamin D on the musculoskeletal and cardiovascular system. *Int. J. Endocrinol.* **2017**, 3206240 (2017).
58. Wynn, T. A. & Vannella, K. M. Macrophages in tissue repair, regeneration, and fibrosis. *Immunity* **44**, 450–462 (2016).
59. Vannella, K. M. & Wynn, T. A. Mechanisms of organ injury and repair by macrophages. *Annu. Rev. Physiol.* **79**, 593–617 (2017).
60. Henderson, N. C., Rieder, F. & Wynn, T. A. Fibrosis: From mechanisms to medicines. *Nature* **587**, 555–566 (2020).
61. Schafer, S. *et al.* IL-11 is a crucial determinant of cardiovascular fibrosis. *Nature* **552**, 110–115 (2017).
62. Akhurst, R. J. & Hata, A. Targeting the TGFβ signalling pathway in disease. *Nat. Rev. Drug Discov.* **11**, 790–811 (2012).
63. Meems, L. M. G. *et al.* The vitamin D receptor activator paricalcitol prevents fibrosis and diastolic dysfunction in a murine model of pressure overload. *J. Steroid Biochem. Mol. Biol.* **132**, 282–289 (2012).
64. Mehdipoor, M., Damirchi, A., Razavi Tousi, S. M. T. & Babaei, P. Concurrent vitamin D supplementation and exercise training improve cardiac fibrosis via TGF-β/Smad signaling in myocardial infarction model of rats. *J. Physiol. Biochem.* **77**, 75–84 (2021).
65. Unwin, S., Chatterton, J. & Chantrey, J. Management of severe respiratory tract disease caused by human respiratory syncitial virus and *Streptococcus pneumoniae* in captive chimpanzees (*Pan troglodytes*). *J. Zoo Wildl. Med.* **44**, 105–115 (2013).
66. Ianevski, A. *et al.* Low temperature and low UV indexes correlated with peaks of influenza virus activity in northern Europe during 2010–2018. *Viruses* **11**, 207 (2019).
67. Grant, W. *et al.* Evidence that vitamin D supplementation could reduce risk of influenza and COVID-19 infections and deaths. *Nutrients* **12**, 988 (2020).

Acknowledgements

The Ape Heart Project at Twycross Zoo, Sharon Redrobe, Lisa Gillespie, Mike Martin, Paul Fields, the European Association of Zoos and Aquaria (EAZA) Biobank, the EAZA Great Ape TAG, the British and Irish Association of Zoo and Aquaria, and all participating institutions: Zoo delle Star (Aprilia), Aalborg zoo, Africa Alive Zoological Reserve, Zoo African Safari, DierenPark Amersfoort, Zoo Basel, Zoo de Beauval, Blair Drummond Safari Park, Borås Djurpark, Zoo am Meer Bremerhaven, Burgers' Zoo, Copenhagen Zoo, Foundation AAP, Dublin Zoo, Givskud Zoo Zootopia, Zoo Zagreb, Kristiansand Dyreparken, Zoo de La Palmyre, La Vallée des singes, Lisbon zoo, Ölands Djurpark, Pakawi Park, Rio Safari Elche, Safari Ravenna, Schwaben park, Reserve Africaine de Sigean, Bioparco di Sicilia, Twycross Zoo, Zoo Aquarium de Madrid, Zoo Neuwied, Zoobotánico de Jerez, Zoological Society of London. This work was supported by the Biotechnology and Biological Sciences Research Council [grant number 2432081] and the Zebra Foundation for Veterinary Zoological Education.

Author contributions

S.M.: designed the study, collected the data, analysed the results, wrote the manuscript. R.J.: collected the data, wrote and reviewed the manuscript. S. Bandelow: analysed the data, wrote the manuscript. S. Byrne: organised the data, reviewed the manuscript. P.D.: collected samples, reviewed the manuscript. M.G.: reviewed the manuscript. C.R.: analysed the samples, reviewed the manuscript. K.W.: reviewed the manuscript. M.L.: designed the study, wrote and reviewed the manuscript. K.B.: wrote and reviewed the manuscript.

Competing interests

The authors declare no competing interests.

Additional information

Correspondence and requests for materials should be addressed to S.M. or R.J.

Reprints and permissions information is available at www.nature.com/reprints.

Publisher's note Springer Nature remains neutral with regard to jurisdictional claims in published maps and institutional affiliations.